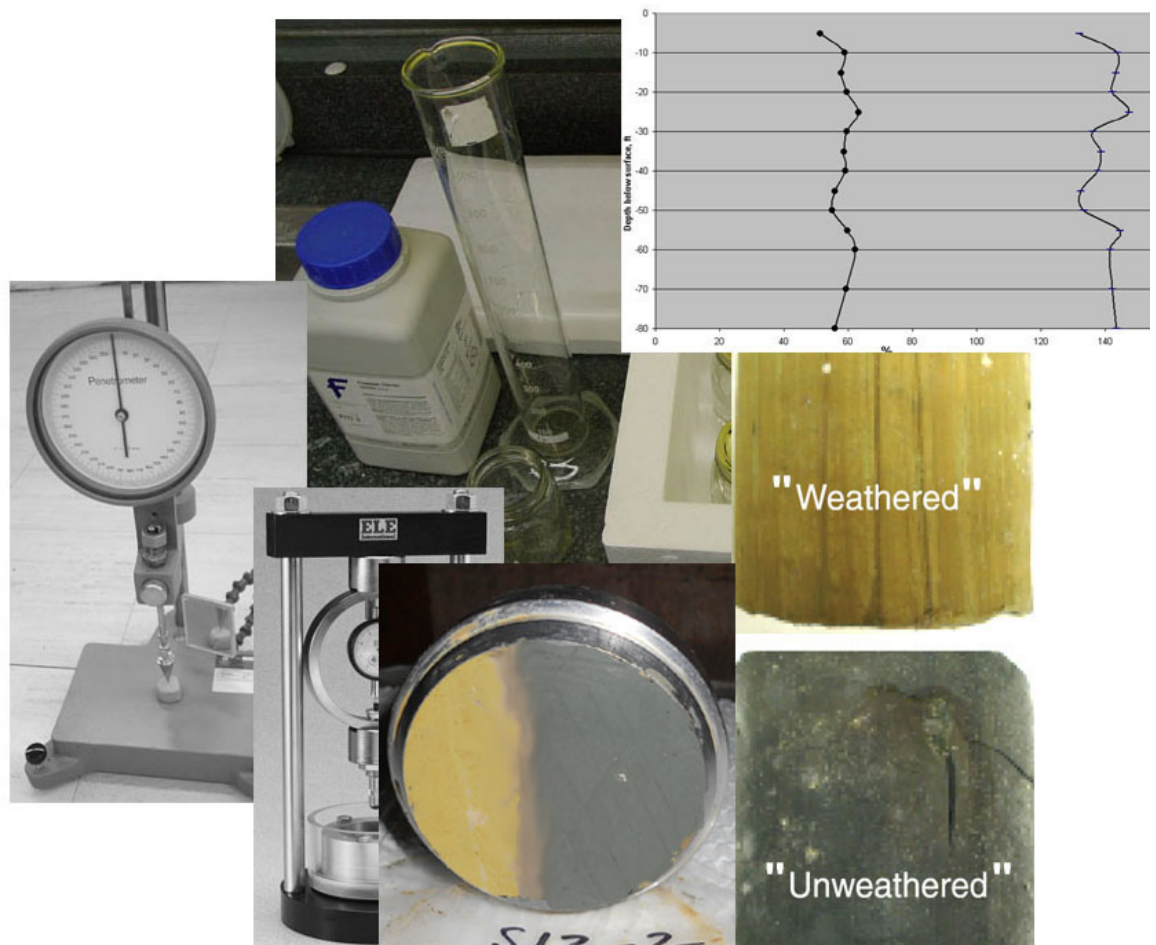




State Study 151 and 236: Yazoo Clay Investigation

Landris T. Lee Jr., P.E.

June 2012



1. Report No. FHWA/MS-DOT-RD-11-236	2. Government Accession No.	3. Recipient's Catalog No.
4. Title and Subtitle State Study 151 and 236: Yazoo Clay Investigation		5. Report Date 1 June 2012
7. Author(s) Landris T. Lee, Jr.		6. Performing Organization Code
9. Performing Organization Name and Address U.S. Army Engineer Research and Development Center, GS-E Geotechnical and Structures Laboratory 3909 Halls Ferry Rd Vicksburg MS 39180		8. Performing Organization Report No. MS-DOT-RD-11-236
12. Sponsoring Agency Name and Address Mississippi Department of Transportation Research Division P O Box 1850 Jackson MS 39215-1850		10. Work Unit No. (TRAIS)
15. Supplementary Notes		11. Contract or Grant No. State Study 236
16. Abstract		13. Type Report and Period Covered Final Report
<p>Mississippi Department of Transportation (MDoT) State Study 236 was assigned to the U.S. Army Engineer Research and Development Center (ERDC) to analyze MDoT-furnished data, perform testing of Yazoo clay soil samples, and provide guidance concerning Yazoo clay identification and characterization. The first tasked portion was to analyze Yazoo clay data previously collected by MDoT researchers in order to finalize an antecedent study (MDoT State Study 151). The second portion was to conduct and document a lab testing program to include descriptions of test methods, analysis of results, conclusions, and recommendations.</p>		14. Sponsoring Agency Code

17. Key Words Expansive, High Volume Change, Shrink, Swell, Heave, Yazoo Clay, Test Methods		18. Distribution Statement Unclassified	
19. Security Classif. (of this report) Unclassified	20. Security Classif. (of this page) Unclassified	21. No. of Pages 256	22. Price

State Study 151 and 236: Yazoo Clay Investigation

Landris T. Lee Jr., P.E.

*Geotechnical and Structures Laboratory
U.S. Army Engineer Research and Development Center
3909 Halls Ferry Rd.
Vicksburg, MS 39180*

Final report

Approved for public release; distribution is unlimited.

Prepared for Mississippi Department of Transportation (MDOT)

Under State Study No. 236- Expansive Soil (Yazoo Clay) Characterization

Monitored by William F. Barstis, P.E., MDoT Research Division
401 North West Street
Jackson, MS 39215-1850

Abstract: Mississippi Department of Transportation (MDOT) State Study 236 was assigned to the U.S. Army Engineer Research and Development Center (ERDC) to analyze MDOT-furnished data, perform testing of Yazoo clay soil samples, and provide guidance concerning Yazoo clay identification and characterization. The first tasked portion was to analyze Yazoo clay data previously collected by MDOT researchers in order to finalize an antecedent study (MDOT State Study 151). The second portion was to conduct and document a lab testing program to include descriptions of test methods, analysis of results, conclusions, and recommendations.

DISCLAIMER: The contents of this report are not to be used for advertising, publication, or promotional purposes. Citation of trade names does not constitute an official endorsement or approval of the use of such commercial products. All product names and trademarks cited are the property of their respective owners. The findings of this report are not to be construed as an official Department of the Army position unless so designated by other authorized documents.

DESTROY THIS REPORT WHEN NO LONGER NEEDED. DO NOT RETURN IT TO THE ORIGINATOR.

Contents

Figures and Tables	4
Preface	11
Unit Conversion Factors	12
1 Yazoo Clay	13
Regional Geology and Mineralogy	13
Regional Yazoo Clay	15
Buried Fossils, Bones and Other Inclusions	20
Clay Mineralogy	22
Engineering Aspects of Yazoo Clay	24
Weathered versus Unweathered Clay	24
Infrastructure Damage	27
Yazoo Clay Investigations	29
MDOT Standard Procedure and Local Design Practice	31
2 Regional Yazoo Clay Investigation (State Study 151)	35
Background	35
MDoT Data Review	36
Mineralogy Tests	36
Analysis	38
Regional Dataset.....	42
Site-specific Data	66
3 Yazoo Clay Sampling and Testing (State Study 236)	84
MDoT Drilling and Testing Program	84
Borehole Sampling.....	84
MDoT Lab Testing	91
ERDC Testing Program	95
Qualitative Classification	96
Quantitative Lab Tests	98
Shrinkage Methods (No-load Tests).....	108
Australian Shrinkage (No-load) and Swell (Load) Tests.....	111
Swell Tests.....	113
Soil Suction.....	119
Clay Chemistry.....	130
4 Site Data and Test Results	138
Clinton Site	138
Lab Results	140
Qualitative Assessment	140
Index Properties	160

<i>Remolded (Blenderized) Tests</i>	162
<i>British Fall Cone Tests</i>	164
<i>Shrink-Swell Vertical Strains</i>	167
<i>Vertical Swell Pressure</i>	176
<i>Australian Shrink-Swell Tests</i>	179
<i>No-load Suction Tests</i>	180
<i>Chemistry Tests</i>	190
<i>Other Tests</i>	192
Analysis of Test Results.....	198
<i>Expansive Soil Indicators</i>	198
<i>Paired Data Correlations</i>	199
<i>Useful Equations</i>	200
5 Conclusions and Recommendations	203
General conclusions.....	203
Specific conclusions.....	203
Recommendations	204
6 References and Expansive Clay Bibliography	206
7 Appendix A: State Study 151 Data	237
8 Appendix B: State Study 236 Data.....	252
Report Documentation Page	

Figures and Tables

Figures

Figure 1. Boundary boxes of the Jackson Formation, including Yazoo clay and its geological equivalents, in Mississippi, Alabama, and Louisiana (after USGS 2010). 14

Figure 2. Major identified geologic structures in the Yazoo clay region (yellow) on the eastern side of the Mississippi Embayment. The Jackson Dome (an extinct volcano structure) lies under the city of Jackson (after Kresse and Fazio 2002). 15

Figure 3. Boundary of the Yazoo clay formation (yellow) in Mississippi (after USGS 2010). 16

Figure 4. Yazoo clay outcrop area (yellow) in central Mississippi under the Jackson metropolitan area and other cities (pink) (after Martin 2007). 17

Figure 5. Yazoo clay samples illustrating color differences for visual degree-of-weathering discrimination. 25

Figure 6. Diagram showing standard MDoT highway cut and fill sections in high volume change soils. 31

Figure 7. Diagram showing a few potential scenarios for poor infrastructure performance on Yazoo clay subgrades or shallow foundations 33

Figure 8. MDoT Yazoo clay mineralogy sample sites (after Taylor 2005 and Martin 2007). 35

Figure 9. Yazoo clay visually-weathered thickness (after Martin 2007). 39

Figure 10. Yazoo clay surface elevations in central Mississippi (after Martin 2007). The natural ground surface generally slopes from about 500 ft msl in Scott County down to about 200 ft msl in Yazoo County, and the top-of-clay elevations also may vary by hundreds of feet. The NW-SE and N-S fence diagrams are shown below. 40

Figure 11. NW-SE fence diagram showing ground surface and top-of-Yazoo clay elevations from MDoT borehole data. The horizontal distance is approximately 50 miles. 40

Figure 12. N-S fence diagram showing ground surface and top-of-Yazoo clay elevations from MDoT borehole data. The horizontal distance is approximately 35 miles. 41

Figure 13. Box plots showing range of depths for visually-classified samples 42

Figure 14. USCS soil classification chart (910 Yazoo clay soil samples). 44

Figure 15. Box plots of 5-county LL data 44

Figure 16. Location of common clay minerals on the plasticity chart (after Holtz and Kovacs 1981). 45

Figure 17. Dry density versus natural water content for all Yazoo clay data in the 5-county area of central Mississippi. 46

Figure 18. Dry density inverse (specific volume, cm³/gram) versus natural water content for Yazoo clay’s typical 15% to 55% natural water content range. Yellow points indicate visually weathered and blue points indicate visually unweathered samples. 47

Figure 19. Ternary diagram of clay-fraction mineralogy results. 49

Figure 20. LL and VC relationships to smectite content in weathered plus unweathered samples. 52

Figure 21. VC% results by county 52

Figure 22. Volume change percent (VC%) values for all Yazoo clay data in the 5-county area of central Mississippi, plotted by elevation above mean sea level (msl).54

Figure 23. Mean shrinkage volume change percent (VC%) values for all (weathered plus unweathered) regional Yazoo clay data, plotted at 5-ft depth intervals.55

Figure 24. Mean shrinkage volume change percent (VC%) values for regional weathered Yazoo clay, plotted at 5-ft depth intervals.55

Figure 25. VC % and PI % correlation for regional weathered plus un-weathered Yazoo clay samples.56

Figure 26. VC % and LL % for regional weathered plus un-weathered Yazoo clay samples.57

Figure 27. Regional weathered plus un-weathered Yazoo clay VC % and Atterberg limit values, averaged by 5-ft depth intervals.57

Figure 28. Regional weathered plus un-weathered Yazoo clay consistency index (Ic) values, averaged by 5-ft depth intervals. Note the Ic values are minimum at the corresponding maximum VC% and LL values (-10, -25, and -55 ft depths).59

Figure 29. LL and VC versus smectite content for weathered and unweathered depth-averaged data. The LL-smectite data provided the better curve fit.64

Figure 30. VC % and LL % for Site 1928, hole 5, weathered plus unweathered Yazoo clay samples.67

Figure 31. Mineralogy of Site 1936, hole 1, weathered plus unweathered Yazoo clay samples.68

Figure 32. VC % , LL % , and PI % for Site 1831, hole 4, Yazoo clay samples.69

Figure 33. Mineralogy of Site 1831, hole 4, Yazoo clay samples.69

Figure 34. VC % , LL % , and PI % for Site 2531, hole 1, weathered plus unweathered Yazoo clay samples.71

Figure 35. Mineralogy for Site 2531, hole 1, weathered plus unweathered Yazoo clay samples.71

Figure 36. VC % , LL % , and PI % for Site 1931, hole 1, weathered plus unweathered Yazoo clay samples.73

Figure 37. Mineralogy of Site 1931, hole 1, weathered plus unweathered Yazoo clay samples.74

Figure 38. VC % , LL % , and PI % for Site 1932, hole 1, weathered plus unweathered Yazoo clay samples.75

Figure 39. Mineralogy of Site 1932, hole 1, weathered plus unweathered Yazoo clay samples.75

Figure 40. VC % , LL % , and PI % for Site 1937, hole 1, weathered plus unweathered Yazoo clay samples.76

Figure 41. Mineralogy of Site 1937, hole 1, weathered plus unweathered Yazoo clay samples.77

Figure 42. VC % , LL % , and PI % for Site 2558, hole 1, weathered plus unweathered Yazoo clay samples.78

Figure 43. Mineralogy of Site 2558, hole 1, weathered plus unweathered Yazoo clay samples.78

Figure 44. Mineralogy of Site 2560, hole 1, weathered plus unweathered Yazoo clay samples.79

Figure 45. Mineralogy of Site 2560, hole 2, weathered plus unweathered Yazoo clay samples.79

Figure 46. Ternary diagram of clay-fraction components at Site 2560, hole 2, labeled by depth, ft (i.e. 5' = 5 ft).....	80
Figure 47. Vicinity location map.....	85
Figure 48. MDoT borehole site next to the original WES Yazoo clay study site.	85
Figure 49. MDoT borehole locations west of existing piezometer P-5.....	86
Figure 50. MDoT borehole site at edge of power line clearing east of the former WES study site. View toward northeast.	87
Figure 51. MDoT rotary drill rig with Shelby tube sampler.....	87
Figure 52. Shelby tube removed from the drill string, ready for core extrusion	88
Figure 53. Hydraulically-extruded core sample from the upper Yazoo clay	88
Figure 54. Extruded core (21- to 24-in long) placed on a shaded flat surface, ready for trimming and waxing.....	89
Figure 55. Trimming an upper sample from a yellow (weathered) clay core prior to waxing.....	90
Figure 56. Diagram of core samples within each 2-ft depth interval preserved for MDoT and ERDC lab testing.....	90
Figure 57. Extruded core sample showing the abrupt boundary between the yellow “weathered” (upper) and the blue “unweathered” (lower) Yazoo clay.....	91
Figure 58. Upper and lower undisturbed sample testing performed at the MDoT lab	93
Figure 59. Approximate dimensions and locations of core slices for each set of ERDC tests conducted on each nominal 2-ft depth interval from Hole 2	99
Figure 60. Fall cone penetrometer. The sample is placed under the tip and the LL and/or PL (shown) may be calculated.	104
Figure 61. Linear shrinkage mold.	108
Figure 62. Syringe with extruded soil paste.....	110
Figure 63. Expansion Index device (courtesy ELE, Inc.).....	113
Figure 64. FHA PVC device (courtesy ELE, Inc.)	115
Figure 65. Consolidation apparatus	118
Figure 66. Direct simple shear apparatus	118
Figure 67. Polymer-capacitance sensors (iButton™ is on the left). U.S. penny shown for scale.....	120
Figure 68. Soil suction-water content sensor calibration. Sensor S1 (measuring RH) and/or S2 (measuring vapor water content) is placed in closed jars with controlled temperature. Headspace vapor equilibrium with the solution is reached and the sensor readings are recorded. The electrolyte solution concentration (molality) is varied from zero (left jar) to very high (right jar) to cover the desired suction range.....	123
Figure 69. Soil total suction determination. Sensor S1 (measuring RH) and/or S2 (measuring water content) is placed above the soil in closed jars with controlled temperature. The soil moisture is varied from high (left jar) to low (right jar).Headspace vapor equilibrium with the soil pore water is reached and the sensor readings are compared to the electrolyte solution calibrations.....	124
Figure 70. Filter paper calibration curves.....	125
Figure 71. iButton™	126
Figure 72. iButton™ calibration curve for each serial numbered device	126
Figure 73. Soil total suction measurement using filter paper and iButton™ (1).....	128

Figure 74. Soil total suction measurement using filter paper and iButton™ (2)	128
Figure 75. Soil total suction measurement using filter paper and iButton™ (3).....	129
Figure 76. Soil total suction measurement using filter paper and iButton™ (4)	129
Figure 77. Soil total suction measurement using filter paper and iButton™ (5)	130
Figure 78. Methylene blue test apparatus	131
Figure 79. Calcium carbonate test apparatus	133
Figure 80. Soil chemistry tests	134
Figure 81. Soil pH test	135
Figure 82. Soil soluble salts (conductivity) test.....	135
Figure 83. From left to right, hand-held pocket penetrometer, GeoTester penetrometer, and Torvane shear devices	136
Figure 84. Surface geology map of the Clinton area showing Yazoo clay (yellow color)	138
Figure 85. Diagram of water content and soil color in Holes 1 and 2. Each horizontal slice represents a 2-ft depth interval below ground surface. Three generalized depth zones (brown, yellow, and blue) are depicted. Transition zone orientations along the transverse axis are unknown due to Shelby tube rotations.....	141
Figure 86. Grab sample containing gravel and limonite ochre nodules from 6 in to 2 ft below ground surface.	145
Figure 87. Upper and lower undisturbed samples at depth interval S1 (2ft – 4ft).....	145
Figure 88. Upper and lower undisturbed samples at depth interval S2 (4ft – 6ft)	146
Figure 89. Upper and lower undisturbed samples at depth interval S3 (6ft – 8ft)	147
Figure 90. Upper and lower undisturbed samples at depth interval S4 (8ft – 10ft).....	148
Figure 91. Upper and lower undisturbed samples at depth interval S5 (10ft – 12ft).....	149
Figure 92. Upper and lower undisturbed samples at depth interval S6 (12ft – 14ft)	150
Figure 93. Upper and lower undisturbed samples at depth interval S7 (14ft – 16ft).....	151
Figure 94. Upper and lower undisturbed samples at depth interval S8 (16ft – 18ft)	152
Figure 95. Upper and lower undisturbed samples at depth interval S9 (18ft – 20ft)	153
Figure 96. Upper and lower undisturbed samples at depth interval S10 (20ft – 22ft).....	154
Figure 97. Upper and lower undisturbed samples at depth interval S11 (22ft – 24ft).....	155
Figure 98. Upper and lower undisturbed samples at depth interval S12 (24ft – 26ft).....	156
Figure 99. Upper and lower undisturbed samples at depth interval S13 (26ft – 28ft). Hole 1 upper sample contained the gypsum crystal shown above.	157
Figure 100. Upper and lower undisturbed samples at depth interval S14 (28ft – 30ft).....	158
Figure 101. Upper and lower undisturbed samples at depth interval S15 (30ft – 32ft).....	159
Figure 102. Upper and lower undisturbed samples at depth interval S16 (32ft – 34ft).....	160
Figure 103. Atterberg Limits (LL and PL) and Volume Change (VC) versus depth	161
Figure 104. Atterberg Limits (Shrinkage Limit and Index) and Volume Change (VC) versus depth	161
Figure 105. LL results from two different sample preparation methods	162
Figure 106. SL results from two different sample preparation methods.....	163
Figure 107. VC results from two different sample preparation methods	163
Figure 108. Blenderized LL and VC results did not correlate.....	164

Figure 109. Undisturbed sample Fall Cone results.	165
Figure 110. Blenderized sample Fall Cone results.	165
Figure 111. LL and PL values picked from the Fall Cone plot.	166
Figure 112. LL values picked from the Fall Cone plot compared to blenderized LL cup values.	166
Figure 113. PL values picked from the Fall Cone plot compared to standard PL values.	167
Figure 114. Sample S7 (depth interval 15 – 17 ft) swell strain versus consolidation load curves. The net swell strain at each load increment is the vertical difference between the pre-wetting compression curve and the inundation wetting curve.	168
Figure 115. Discrete net swell strain and load increment points plotted at each sample interval depth.	169
Figure 116. Regression curve for continuous net swell strain and load function, shown for one sample interval (S7).	170
Figure 117. Regression curves for swell strain as a function of normalized loading. The upper- depth samples S1 thru S6 (at their natural water content) exhibited greater swell when their loadings were less than their in-situ (overburden) stresses.	170
Figure 118. Regression curves for no-load swell strain as a function of water content. The upper-depth samples S1 thru S4 swelled less than lower-depth samples at equal water contents. For all samples, the lower the water content, the higher the swell potential.	171
Figure 119. No-load shrinkage strain measured as a function of water content during air-drying.	172
Figure 120. Regression curves for no-load shrinkage <u>potential</u> strain as a function of water content during air-drying; the higher the initial water content, the higher the probability of shrinkage strain if the soil is dried.	173
Figure 121. Superimposed no-load shrink-swell strain plotted versus water content for sample S7.	175
Figure 122. Combined no-load shrink-swell strain plotted versus water content for sample S7.	175
Figure 123. Low-strain (less than 1%) swell pressures normalized to nominal overburden pressures for each sample interval.	176
Figure 124. Progressively-drier samples exerted exponentially-higher swell pressures after inundation.	177
Figure 125. Sample S7 regression line for normalized swell pressures based on initial water contents.	178
Figure 126. Australian Test Indices.	179
Figure 127. Results of the Alternative Iss Test.	180
Figure 128. Soil total suction results (filter paper tests).	181
Figure 129. Soil total suction results (iButton tests).	182
Figure 130. Regression curves for potential no-load shrinkage strain during air-drying as a function of total suction.	184
Figure 131. Sample S7 no-load shrink-swell curves matched to soil suction results.	186
Figure 132. No-load combined shrink-swell curves matched to iButton™ soil suction results.	187
Figure 133. Sample S7 regression line for low-strain swell pressures based on soil suction results.	189

Figure 134. Soluble sulfate and calcium. Note that the calcium concentration is off the chart (greater than 14000 ppm) below about 7-ft depth, and the sulfate concentration increases at the approximate active zone depth (13 ft)..... 191

Figure 135. Calcium carbonate and pH test results 192

Figure 136. Direct shear test plot for undisturbed sample S16 at natural water content. Overburden load was 4000 psf and handheld Torvane shear was 2000 psf..... 193

Figure 137. Comparison of adjacent borehole data..... 195

Figure 138. Comparison of adjacent test site soil suction data for the 1- to 8-ft depth interval 196

Figure 139. Comparison of adjacent test site soil suction data for the 8- to 24-ft depth interval 197

Figure 140. Comparison of expansive soil data (McKeen 1992) to this study. 198

Figure 141. Comparison of measured and predicted values at other Yazoo clay sites 202

Tables

Table 1. Yazoo clay average index property values.....42

Table 2. Average Yazoo clay volume change percent (VC %) for 5-county area of central Mississippi.....53

Table 3. Correlations of 5-ft interval-averaged values to 5-ft interval depths below ground surface for weathered Yazoo clay samples. Best correlations are highlighted.59

Table 4. Correlations of 5-ft interval-averaged values to sample elevation zone intervals (ft above mean sea level, msl) for weathered Yazoo clay samples. Best correlations are highlighted.....61

Table 5. Elevation zone intervals for the above Table 4.....61

Table 6. Correlations of 5-ft interval-averaged values to 5-ft interval depths below ground surface for unweathered Yazoo clay samples. Best correlations are highlighted.62

Table 7. Correlations of 5-ft interval-averaged values to 5-ft interval depths below ground surface for weathered plus unweathered Yazoo clay samples to 45 ft depth below ground surface. Best correlations are highlighted.....63

Table 8. Correlations of geotechnical data in 5-ft depth intervals at Site 1928, hole 5. The best correlations are highlighted.67

Table 9. Correlation coefficients of site-specific geotechnical property and XRD mineral content percentages for weathered and unweathered Yazoo clay samples. Samples were obtained from relatively shallow depths (less than approximately 50 ft below ground surface) at approximately 5-ft depth intervals. Highest correlations are highlighted.....81

Table 10. Standardized Test Methods.....95

Table 11. Non-standardized Test Methods.....96

Table 12. LI and slake rate comparison (Strohm et al. 1978) 105

Table 13. FHA (1974) PVC Swell Index classification system 115

Table 14. Aqueous solution headspace calibration to total suction at 20 deg C (68 deg F)..... 122

Table 15. Clinton site Yazoo clay values (after Johnson 1973a)..... 139

Table 16. Clinton site Yazoo clay swell values (after Johnson 1973a)..... 139

Table 17. Clinton site Yazoo clay suction values (after Johnson 1973a) 140

Table 18. Sample descriptions141

Table 19. Swell strain versus consolidation load.....	168
Table 20. No-load swell and shrinkage strains versus water content.....	174
Table 21. Swell pressure versus water content	177
Table 22. Soil total suction results.....	182
Table 23. Soil suction-shrinkage strain	184
Table 24. Soil suction-swell strain	186
Table 25. Soil suction-combined shrink-swell strain.....	188
Table 26. Soil total suction results matched to PVC test results	189
Table 27. Disturbed sample test results.....	193
Table 28. Data comparison.....	194
Table 29. Correlation coefficients	199
Table 30. More correlation coefficients	199

Preface

Yazoo clay is the most active shrink-swell (expansive or high volume change) clay found in the state of Mississippi (Teng and Clisby 1975), and is the largest contiguous near-surface expansive clay deposit east of the Mississippi River. Yazoo clay presents an omnipresent challenge to the design, construction, and maintenance of infrastructure due to its notorious shrinkage and swelling behavior. Its presence negatively impacts the engineering design and construction efforts expended on embankments (cuts and fills), shallow foundations, highway subgrades, and deep foundations sited in Mississippi.

The purpose of this report is to document research performed by the U.S. Army Engineer Research and Development Center (ERDC) for the Mississippi Department of Transportation (MDOT). The study was performed at the ERDC Geotechnical and Structures Laboratory (GSL) to explore identification and geotechnical characterization of Yazoo clay based on experimental test results. A previous uncompleted study by MDOT (MDOT State Study 151) was analyzed and completed as part of the tasking for the ERDC study (MDOT State Study 236).

Grateful acknowledgement is given to MDOT personnel for their prompt and efficient assistance in performing drilling, sampling, testing, technical review, and technical assistance during this project. The author especially acknowledges the contributions of William (Bill) Barstis, Sean Ferguson, Mike Stroud, Mike Wright, Caleb Hammons, John Reeves, and Randy Dixon.

Unit Conversion Factors

Multiply	By	To Obtain
atmosphere (standard)	101.325	Kilopascals, kPa
bars	100	Kilopascals, kPa
cubic feet	0.02831685	cubic meters
cubic inches	1.6387064 E-05	cubic meters
cubic yards	0.7645549	cubic meters
degrees Fahrenheit	(F-32)/1.8	degrees Celsius
feet, ft	0.3048	meters
foot-pounds force	1.355818	joules
gallons (U.S. liquid)	3.785412 E-03	cubic meters
inch-pounds (force)	0.1129848	newton meters
microns	1.0 E-06	meters
ounces (mass)	0.02834952	kilograms, kg
ounces (U.S. fluid)	2.957353 E-05	cubic meters
pints (U.S. liquid)	4.73176 E-04	cubic meters
pints (U.S. liquid)	0.473176	liters
pounds (force), lb	4.448222	newtons, N
pounds (force) per foot, plf	14.59390	newtons per meter
pounds (force) per square foot, psf	47.88026	pascals
pounds (force) per square inch, psi	6.894757	kilopascals, kPa
pounds (mass)	0.45359237	kilograms
pounds (mass) per square foot	4.882428	kilograms per square meter
tons (force)	8,896.443	newtons, N
tons (force) per square foot, tsf	95.76052	kilopascals, kPa

1 Yazoo Clay

The presence of Yazoo clay in the vicinity of a highway subgrade or structural foundation in central Mississippi is known to have a negative influence on the infrastructure's life-cycle performance. When its presence is known or suspected, Yazoo clay requires application of unique design procedures. MDoT has codified the design procedure for Yazoo clay and other Mississippi expansive (high volume change) soils. Current MDoT state-of-the-practice for characterizing the expected pavement subgrade or foundation soil behavior at expansive soil sites relies primarily on Atterberg limits and volume change (VC %) test results. The primary purpose of the ERDC research was to identify and evaluate additional useful methods for identifying and characterizing problematic Yazoo clay.

Regional Geology and Mineralogy

Yazoo clay is calcareous and highly-plastic typically with a hard-to-stiff consistency at moisture contents near its plastic limit. Its composition and calcareous nature are attributed to its assumed historical origin and deposition in a marine environment. Its clay-rich structure and smectitic mineralogy have traditionally been blamed for its high volume change (expansive) behavior.

The Yazoo Formation containing Yazoo clay is geologically defined within the Jackson Group that has been identified throughout the southeastern and southwestern United States. The upper stratigraphy of the Jackson Group containing Yazoo clay (or its geological equivalent) outcrops in regional locations across Alabama, Louisiana, and Mississippi (**Figure 1**).

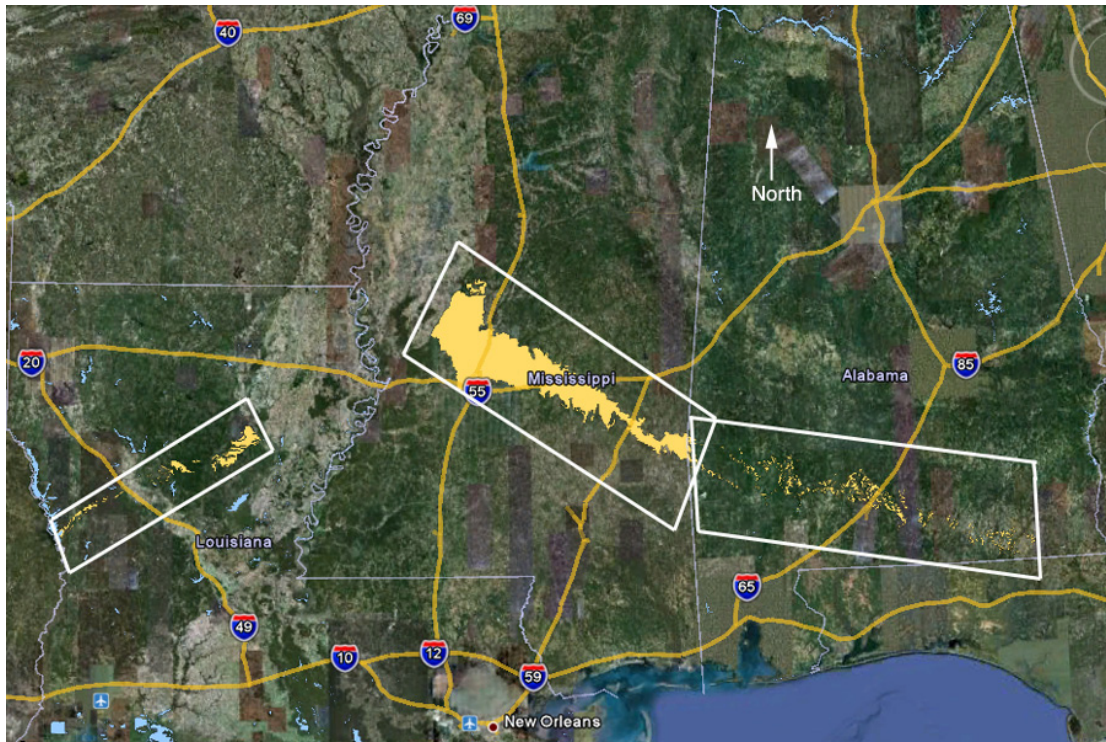


Figure 1. Boundary boxes of the Jackson Formation, including Yazoo clay and its geological equivalents, in Mississippi, Alabama, and Louisiana (after USGS 2010).

The geologic formations of the Jackson Group generally dip toward the modern Gulf of Mexico coastline. The deposits are considered to constitute part of the filling of the Gulf of Mexico Basin by sand, silt and clay carried from the North American continental interior. The sediments are thought to have caused a gradual subsidence of the Earth's crust along the edges of the basin, dipping more steeply toward the Gulf of Mexico than the current land surface (Knox et al. 2007).

Yazoo clay's origin has been postulated as resulting from rapid deposition in a deep water environment (Huff 1960). Discoveries of currently-existing (non-extinct) shallow water micro-fauna buried within the deposit have led to other proposed origins (Dockery and Siesser 1984; Smith and Zumwalt 1987).

In Mississippi, the Yazoo clay outcrops in the central part of the state above geomorphic structures such as the Jackson Dome (an igneous volcanic intrusion about 2000 ft below the Jackson area) and the Pickens-Gilberton fault zone, shown in **Figure 2**. The Jackson Dome has a diameter of 25 miles and is one of the larger structural features in Mississippi

(Harrelson 1981). The base of the Yazoo clay dips downward in all directions from the Jackson Dome's center (near the Belhaven area in Jackson) until its upper contact with the Forest Hill Formation (Dockery et al. 1991). Five-ft diameter tar pods found in the Yazoo clay, assumed to be the residue of escaping hydrocarbons, have also been linked to the extinct volcano structure of the Jackson Dome (Dockery 1985).

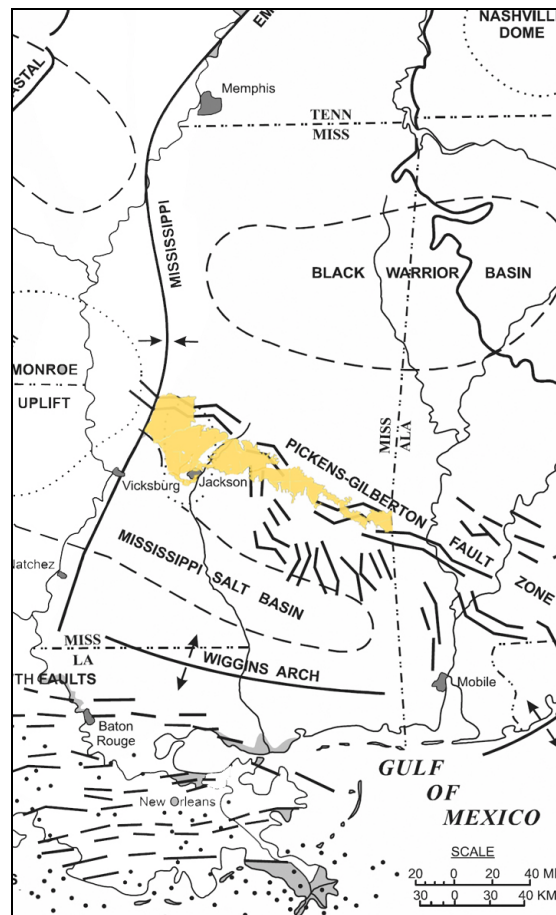


Figure 2. Major identified geologic structures in the Yazoo clay region (yellow) on the eastern side of the Mississippi Embayment. The Jackson Dome (an extinct volcano structure) lies under the city of Jackson (after Kresse and Fazio 2002).

Regional Yazoo Clay

The regional extent of the Yazoo clay lies within the central Mississippi counties of Yazoo, Holmes, Hinds, Rankin, Madison, Scott, Newton, Smith, Jasper, and Wayne (**Figure 3**). The horizontal width of the surface outcrop varies from approximately 35 miles on the west to less than 10

miles on the east. Unfortunately the metropolitan Jackson area is located directly on top of the Yazoo clay. Any overlying non-clay deposits (alluvium, loess, etc.) are generally not thick enough to prevent moisture and water intrusion into the Yazoo clay, and these moisture changes result in expansive, swelling, shrinkage, and otherwise destructive behavior so detrimental to the roads, foundations, and related infrastructure in the central Mississippi region.

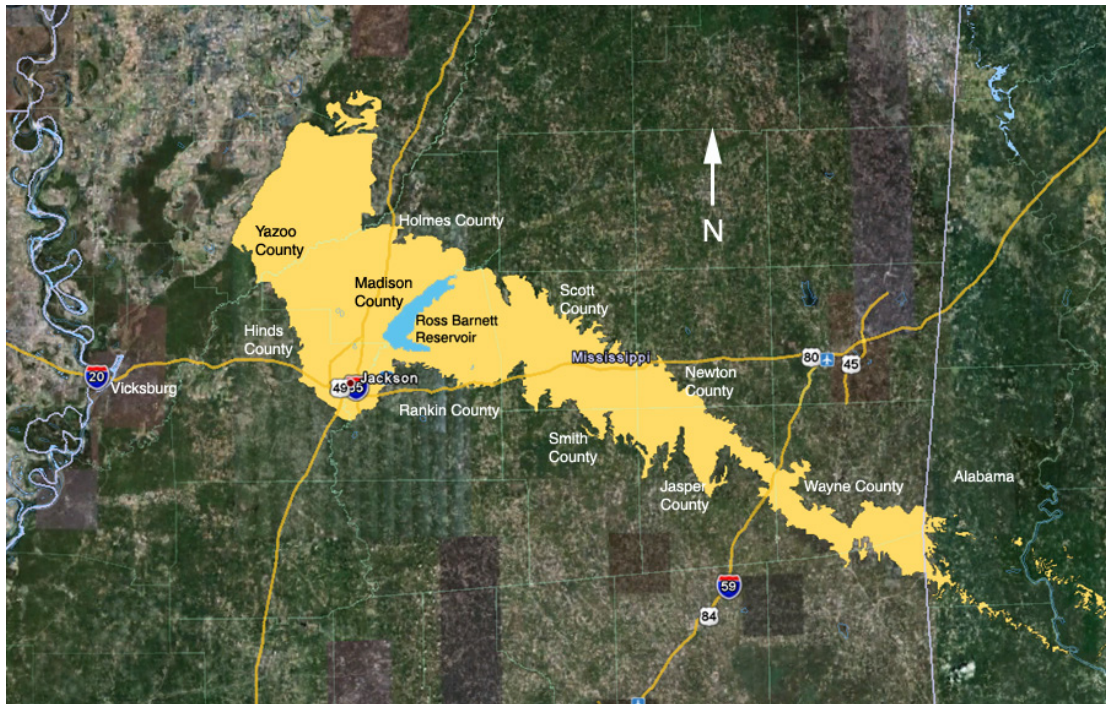


Figure 3. Boundary of the Yazoo clay formation (yellow) in Mississippi (after USGS 2010).

The Yazoo clay soil in the region from Yazoo to Scott Counties (**Figure 4**) is composed of a thick undifferentiated sedimentary deposit geologically classified as the Yazoo Formation on top of the Moody's Branch Formation. The lower Yazoo Formation is a sandy, silty, very glauconitic clay, and its contact with the Moody's Branch is gradational. The Moody's Branch is a fossiliferous, glauconitic sand. The Yazoo-Moody contact is assumed where the glauconite in the Yazoo is not a predominate constituent and the predominance of sand is gradually replaced by clay. Glauconite becomes a minor component above the lower contact (Martin 2007).

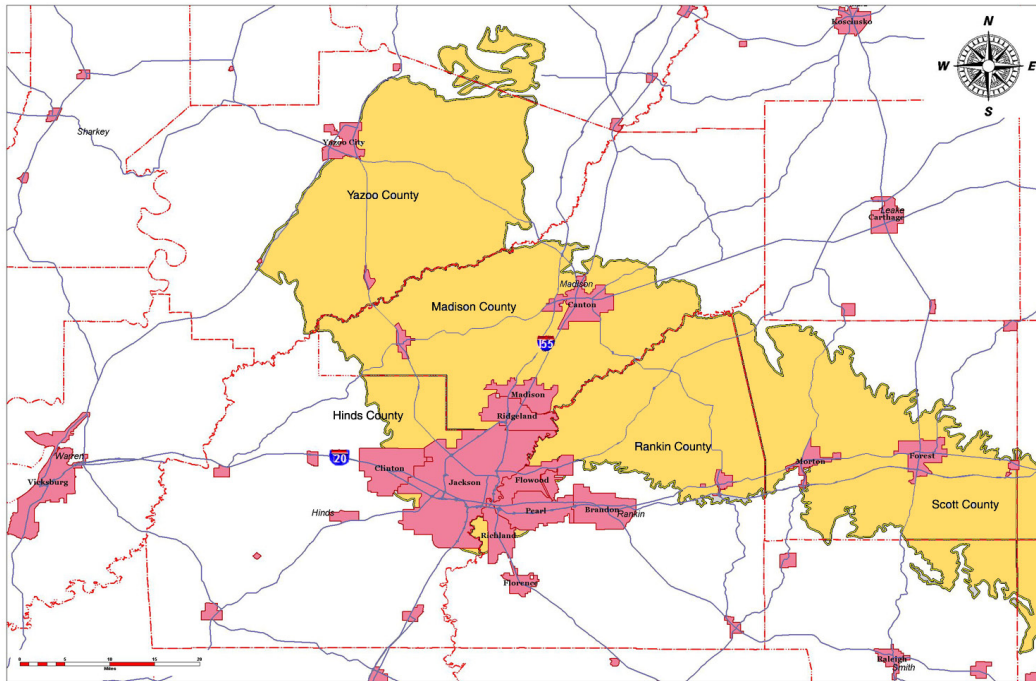


Figure 4. Yazoo clay outcrop area (yellow) in central Mississippi under the Jackson metropolitan area and other cities (pink) (after Martin 2007).

The upper Yazoo Formation contact is generally an unconformity with the Yazoo clay, where it is overlain by Forest Hill sands, lignitic silts, or clays. In certain locations the upper contact has a conformable appearance with an abrupt transition from Yazoo clays to very dark Forest Hill clays with no apparent break. The Yazoo clay shows little evidence of weathering below its Forest Hill contact, and the unweathered clay may be found at shallow depths below ground surface where the overlying Forest Hill layer is thin.

Intermittently-occurring alluvial terrace clays have been confused with the underlying weathered Yazoo clay in the Jackson area. The high-plasticity terrace clays are visually similar to the Yazoo, but are much less expansive. Estimates of expansion (swell) based on tests of the terrace clay layer underestimate the swell potential if the tests are assumed to represent the underlying weathered Yazoo clay. A thin perched water table between the alluvial clay layer and Yazoo clay layer is another anomalous feature intermittently found in the Jackson area (Maxwell 2009a, b).

The Yazoo Formation is up to 480 feet thick in western Hinds County. The Mossy Grove borehole located approximately 4 miles west of the Cynthia

Pit in northwest Hinds County that was drilled by the Mississippi Office of Geology encountered the overlying Forest Hill Formation, then penetrated 462 ft into undifferentiated Yazoo clay (Dockery et al. 1991). In Warren County, west of Hinds County toward the Mississippi River, the top of the Yazoo clay is a minimum of 230 ft below ground surface and does not outcrop in this area (Murphy and Albertson 1996). Toward the southeast in Scott County, (approximately 80 miles distant from the Yazoo River which forms the western outcrop boundary), the Yazoo clay thickness is approximately 100 ft.

The average composition of the Yazoo clay is 28% smectite (probably montmorillonite), 24% kaolinite, 22% quartz, 15% calcite, 8% illite, 2% feldspar, and 1% gypsum based on recent x-ray diffraction results (Taylor 2005). Surface exposures of Yazoo are weathered to a maximum depth of approximately 45 ft below ground surface. Weathered Yazoo clay has a distinctive yellow-brown color while unweathered Yazoo clay is blue-gray.

The environmental geology description (Green and Childress 1974) of the Madison, Ridgeland, Jackson, and Jackson Southeast quadrangle survey area indicates the Yazoo Formation overlies the Moody's Branch Formation, and the unweathered (fresh) Yazoo clay is blue-gray, limy, fossiliferous, and hard. The clay weathers to a tan color and usually will be altered (i.e. weathered) to a depth of 25 or 30 ft below ground surface. The Forest Hill Formation overlying the Yazoo Formation in this area is composed primarily of fine-grained, silty, micaceous sands and silty, carbonaceous clays with a few thin seams of lignite. The sands in the Forest Hill Formation supply fresh water to wells in the areas south, southwest, and southeast of the city of Jackson.

At its western-most outcrop area (in Yazoo County) the lower 350 ft of Yazoo clay is described by Mellon (1940) as a remarkably uniform, homogeneous, silty calcareous, fossiliferous, gummy, plastic, montmorillinitic, and bluish-gray clay. The upper 150 ft is less homogeneous. The clay is less calcareous and contains beds and lamina of silt, silty clay, marl, bentonite and limestone. The Yazoo clay gently dips to the south and south-southwest. Johnson and Clark (1955) described stratigraphy observed in a fresh road cut near Sartartia, the western-most outcrop in Yazoo County. They observed thin (1/8 in to 1 ft) bentonite seams and numerous lenses of fine brown sandstone and siltstone. Fractures had limonitic stains with thin seams of gypsum. Weathered clay had colors of light gray to white.

In Hinds County, Moore et al. (1965) describe the fresh (unweathered) Yazoo clay as fairly homogeneous, blue-green, blue-gray, calcareous, fossiliferous clay with some pyrite. The upper portion is non-calcareous and slightly silty. Locally there are beds of soft white argillaceous (clayey) limestone. The weathered Yazoo clay is yellowish or greenish yellow with limonite and manganese stains along joints. Gypsum is a common mineral in fractures to a depth of 30 or 40 feet.

In Madison County the unweathered (un-oxidized) Yazoo clay is a homogeneous, blue-gray, slightly silty, calcareous (fossiliferous), massively-bedded clay with thin limestones and bentonitic clays in the upper 50 feet (Priddy 1960). It quickly weathers to a dark olive-gray color, then buff, then tan. Weathered Yazoo clay may or may not be calcareous. Caliche (calcium carbonate deposits) and gypsum (calcium sulfate) are common.

In Rankin County, Baughman et al. (1971) describe the Yazoo clay as homogeneous, blue-green, blue-gray, and gray, calcareous (fossiliferous) clay with pyrite. It is limy and slightly sandy near the base and may contain marl and limestone in its upper portions. It weathers to a greenish-yellow-tan with gypsum crystals, limonite stains and manganese stains.

In Scott County, Bergquist and McCutcheon (1942) observed that unweathered Yazoo clay is very fossiliferous, calcareous, greenish-gray clay with locally abundant dark and finely comminuted marcasite streaks. The weathered Yazoo clay is a light tan streaked by gray and iron oxide. The lower Yazoo contains limestone nodules and glauconite. The weathered Yazoo is silty with reddish-brown iron stain. Gypsum crystals are common. Glauconite appears in deposits of greensand, so-called due to its green color. It can also be found in sand or clay formations, or in impure limestone and chalk, world-wide (Hassan and El-Shall 2004; Chang et al. 2008). Glauconite is assumed to develop as a consequence of diagenetic alteration of sedimentary deposits, bio-chemical reduction and subsequent mineralogical changes affecting iron-bearing micas such as biotite. Its development is also assumed to be influenced by the decaying process of organic matter degraded by bacteria in marine animal shells (Wikipedia 2010).

Based on the preceding geological descriptions, Yazoo clay is a heterogeneous material. It contains various structural features and mineralogy, depending on the sampling location and depth. The most common feature

noted is the visual change thought to be caused by the degree of weathering.

Buried Fossils, Bones and Other Inclusions

Yazoo clay is *fossiliferous*, that is, there is a plethora of extinct and non-extinct biological remains preserved within the surrounding clay matrix. The fossils and bones are mostly calcareous (i.e. calcium, calcite, or their various chemical compositions). Hundreds of invertebrate and vertebrate species have been discovered and named. Their taxonomy and location in the geologic column have served as biostratigraphy markers to calibrate the assumed geochronology of the geologic column, and vice versa.

The Jackson Group and Yazoo Formation soils contain abundant evidence of fossils with sizes ranging from whales to foraminifera. For example, scanning electron microscopy (SEM) results (discussed later in this report) have shown a concentration of coccoliths (calcite scales, or plates, covering the surface of microscopic fossil algae cells) in Yazoo clay. Honjo and Berggren (1967) used Yazoo clay planktonic foraminifera specimens to demonstrate the relatively new SEM technology of the 1960's. Blackwell and Powell (1982) described calcareous marine nannoplankton (coccolithophorids, or single-cell algae, usually about the size of a clay particle, 1 micron) found in Yazoo clay deposits in their SEM study. These algae (200 to 300 species) are presently found living in the upper 100 feet or so of warm ocean waters, primarily in the tropics. The algae are known to form calcite plates (coccoliths) from bicarbonate, the principle carbonate source in salt water. Calcareous nannoplanktons are index fossils useful for geochronology calibration to the assumed age and origin of the Yazoo Formation (Dockery and Siesser 1984).

Rogers (1936) examined Yazoo clay samples for the purpose of studying the invertebrate fossils (foraminifera) retained on a "hundred mesh per square inch" sieve after washing. Microscopic examination showed a majority of foraminifera tests (calcareous shells) with some ostracodes, fish bones, pelecypod shells and bryozoans. Over 70 species were identified and their abundance was evidence that the clay was fossiliferous.

The larger fossils (macrofossils) found in Yazoo clay are mostly pelecypods such as oysters (*Ostrea trigonalis*). Smaller fossils (pteropods, or micromollusks) have been found in the Shubuta Member of the Yazoo clay at the Cynthia pit (Dockery and Zumwalt 1986). Microfossils are abun-

dant, and the most common microfossils are coccoliths (single-celled algae, or microflora) and foraminifera (single-celled amoeboid protists, or microfauna). The Yazoo Formation is rich in mollusk shells and contains thin seams of shell hash (Dockery et al. 1991). Echinoids (commonly known as “sand dollars”) have been identified in the Jackson Group layers in Mississippi and other southern States (Zachos and Molineux 2003).

Yazoo clay is rich in cetacean (archaeocete) fossils of extinct whales. Numerous whale bones have been found in the Jackson Group, Yazoo Formation, and Yazoo clay regions across the southeast U.S. (Frazier 1980). The initial discovery of the archaeocete whale *Basilosaurus cetoides* was made in a Yazoo clay deposit exposed by the Ouachita River in Caldwell Parish, Louisiana (Gibbes 1847).

The Mississippi state fossil (the reconstructed *Zygorhiza* whale on display in Mississippi’s Natural Science Museum) and ossified bones from the archaeocete whale (*Basilosaurus*) have been found at various locations and depths in the Yazoo clay. The identification and reconstruction of the state fossil were discussed in Carpenter and Dockery (1985). Starnes and Berry (2010) described excavation of a partial *Zygorhiza* whale found in Yazoo clay near Benton, Mississippi. The whale’s bones were located near the top of the Yazoo clay at the base of an exposed vertical loess bluff.

Dockery and Johnston (1986) describe excavation of whale bones found in Yazoo clay just 10 ft below existing ground surface in the brown (weathered) clay zone, just above a less-weathered brownish gray clay zone. Historically, ossified whale bones were so commonly found near the ground surface and exposed creek banks that local residents used them as fire-place andirons or as foundation supports for cabins.

Dockery et al. (2003) describe excavation of a largely complete whale skeleton found 22 ft below the existing ground surface. The bones rested on top of shell-littered and iron-stained strata. The visual appearance of the bones and their lack of encrusting organisms such as oysters were assumed to indicate the whale’s rapid (i.e. catastrophic) burial. The largely-intact bone structure and its upside-down horizontal position (Starnes and Peyton 2003) were evidence of a rapid burial undisturbed by scavengers.

Other vertebrate fossils found in the Yazoo clay have included great white shark (*Carcharodon* sp.) teeth (Dockery 1981) and an eighteen-ft long sea

snake (*Pterospheus*) (Dockery 1992, 2009b). Remains of deep ocean species of billfish (swordfish) have been found in Yazoo clay (Fierstine and Applegate 1974; Fierstine and Starnes 2005; Fierstine and Stringer 2007). The holotype specimen of the billfish *Xiphiorhynchus kimblalocki* was found in Yazoo clay. Because the bones of the holotype did not show much wear, breakage, or chemical etching, Fierstine and Stringer (2007) postulated that the bones were the remains of an individual that had a deep water burial.

Non-calcareous inclusions have also been found in the Yazoo clay. Byerly et al. (1988) describe tektite micro-spherules that were found in soil samples taken from the “lower part” of the exposed borrow pit wall in the Cynthia (Miss-Lite) Pit. These micro-spherules are silicate glass bodies that are assumed to be of extra-terrestrial origin. The glass is assumed to originate either from outer space or formed as a result of meteor impact. In addition to the innumerable calcareous fossils and mysterious “tar ball” inclusions discovered in Yazoo clay, discovery of the glass micro-spherules add yet another dimension to scientific speculation regarding Yazoo clay origin(s) and geochronology.

Clay Mineralogy

Clays are primarily composed of smectite, illite and kaolinite minerals. Yazoo clay is composed primarily of clays, quartz sand and silt, and calcareous fossils. Minor constituents include pyrite, lignite, gypsum, anhydrite, feldspar, limonite, and hematite. Various authors have identified the major Yazoo clay type to be montmorillonite (Martin 2007). Buck (1956) used the minus 20 μ m portion of unweathered Yazoo clay samples obtained a few miles southwest of Jackson to report their XRD-derived percentages as kaolinite (45%), montmorillonite (30%), illite (15%), and non-clay minerals (10%). The high kaolinite percentage may have been an indicator of unweathered clay. Taylor (2005) found a general trend based on 240 XRD samples indicating that smectite increased as kaolinite decreased in the weathered zone, and smectite decreased as kaolinite increased in the unweathered zone. The trend was highly variable as a function of depth, and the best correlations were found at borehole-specific sites (discussed later in this report).

Yazoo clay contains thin bentonite seams (beds) observed in outcrops or in borehole samples. Johnson and Clark (1955) examined a bentonite seam that was almost a foot thick. Its average refractive index was about 1.5 and

it had a microcrystalline aggregate structure when seen through a petrographic microscope. Its color was buff to tan, and it had a “blocky” structure. Since bentonite beds are thought to originate from volcanic ash deposition, they are useful candidates for obtaining age-related “fingerprints”, or markers, required for calibration to geochronology assumptions. For example, a single sample of sanidine and a single sample of biotite taken from bentonite beds in the Sartartia scarp and the Society Ridge core west of Jackson, respectively, provided the basis for argon radioisotope dating of volcanic ash deposition in the Yazoo Formation (Obradovich et al. 1993).

Hou (1992) performed the first detailed clay mineralogical study of the upper 250 ft of undifferentiated Yazoo clay from a core near the Cynthia Pit northwest of Jackson. Smectite was the most abundant clay mineral (87%), kaolinite had an average abundance of 12%, and illite had an average abundance of 1%. Four bentonite zones were also distinguished, based on the samples having a distinct white color and high smectite percentages.

Taylor (2005) analyzed Yazoo clay samples from central Mississippi to quantify the mineralogy of total clay, quartz, calcite, gypsum, and feldspar fractions in borings to depths of about 70 ft below ground surface. The total clay components were composed of kaolinite, illite, and smectite. Based on 240 x-ray diffraction (XRD) analyses the average composition of Yazoo clay was 28% smectite, 24% kaolinite, 22% quartz, 15% calcite, 8% illite, 2% feldspar and 1% gypsum (Pitalo et al. 2004). Details are discussed later in this report.

Smectite is generally the most abundant clay component in Yazoo clay, and is more abundant in the weathered Yazoo clay than in the unweathered Yazoo clay. Montmorillonite is a type of smectite, and is considered to be the major clay mineral in Yazoo clay as reported by Bergquist and McCutcheon (1942). Kaolinite, which is the clay type that shows the least volume change in wet or dry conditions, is generally more abundant in the unweathered Yazoo than in the weathered section. Illite is generally the least abundant clay type. There is significant lateral and vertical variation in Yazoo clay mineralogy.

Virtually none of the Yazoo clay samples contained gypsum (Martin 2007), which was unusual considering that gypsum is frequently cited as a prom-

inent component of Yazoo clay (Taylor 2005). Mellen (1940) noted that gypsum was not found below the zone of oxidation or in zones of severe weathering, and the presence of gypsum was likely due to pyrite decomposition of calcareous fossils. Monroe (1954) stated that gypsum crystals are not commonly found below depths of 30 ft.

Chemical oxidation of pyrite to form iron sulfate is a known cause of clay swelling (Johnson 1973a). The iron sulfate is a component of limonite commonly found in Yazoo clay. Limonite is responsible for the characteristic greenish-yellow stains commonly observed on the face of fissures toward the bottom of the Yazoo clay weathered zone. The dehydration of limonite to hematite accounts for the reddish stains on the fissures.

Engineering Aspects of Yazoo Clay

Weathered versus Unweathered Clay

Local geologists and engineers describe Yazoo clay as being either “unweathered” or “weathered”, and the visual difference is apparent (**Figure 5**). Unweathered (“fresh” or un-oxidized) clay has a visually distinct blue color that grades into a gray blue and gray, or it may have a green to grayish green color. Silt having a light gray color occurs locally in thin seams and lamina.

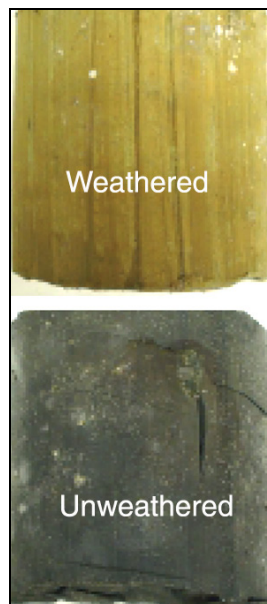


Figure 5. Yazoo clay samples illustrating color differences for visual degree-of-weathering discrimination.

Cycles of exposure to air, wetting and drying tend to cause oxidation and acceleration of clay weathering. Exposure to drying is accompanied by shrinkage and weathering causing mineralogical changes which in turn change the structural and strength characteristics of clay. Many types of clay lose their stability due to drying and tend to “slake” during rewetting (Mitchell 1993). When air-dried Yazoo clay is wetted it quickly slakes, but is affected very little by water if at its natural water content. Detrimental swelling can be expected when Yazoo clay is allowed to dry below the optimum gravimetric water content (~15%) and is then wetted (Redus 1962). As shown later in this report, Yazoo clay can appreciably swell when inundated from its natural water content state.

Boston “blue clay” has a softer consistency but its upper (assumedly weathered) component is a layer of hard yellow clay (Mitchell 1993). Yazoo “blue clay” is unweathered but is typically overlain with visually-distinguishable (assumedly weathered) hard yellow clay. Yazoo clay exhibits weathering effects similar to other high-plasticity clays, in that drying (desiccation) generally increases strength, decreases compressibility, and increases swell potential.

Yazoo clay is remarkably similar to another argillaceous sedimentary expansive soil, London Clay, assumed to originate during the same Eocene era (De Freitas and Mannion 2007). Its upper weathered consistency is soft to firm, with ochre staining due to oxidation of iron compounds. The upper 4 ft or so is the active zone. The lower-depth unweathered clay is blue-gray, firm to very stiff, and highly fissured. London clay is problematic as a shrink-swell material (Kovacevic et al. 2007; Hight et al. 2007; Jones and Terrington 2011), also similar to Yazoo clay.

The unweathered Yazoo clay has structural breaks with slickenside (joints and fissures) features. These slickenside breaks are probably due to unloading after pre-consolidation or from shrinkage cracking during drying. Fissures have been found in normally consolidated clays at water contents well above their shrinkage limit, indicating that neither unloading nor shrinkage were the culprits. One explanation is *syneresis*, which is the mutual attraction of clay particles forming closely knit aggregates with fissures between (similar to that observed in aging gelatine (Mitchell 1993)).

A more recent observable cause of Yazoo clay's joints and fissures may be due to known geologic structure perturbations. As an example, Missouri's New Madrid earthquakes (1811-1812) were known to affect the entire region's geology, causing many fissures, draining water bodies, and causing landslides as far south as Natchez (about 100 miles southwest of Jackson). In 1846, Mr. Charles Lyell, the world-traveled British lawyer-turned-geologist, personally interviewed those who saw such local effects of the earthquake (Bograd 1996). Shaking was felt throughout the mid-continental U.S., and intense liquefaction occurred in a 130- by 50-mile region around the fault zone. Aftershocks were felt for several years afterward (Wheeler and Crone 2001).

The weathered Yazoo clay is generally found in a zone between the ground surface and the deeper unweathered clay. It has a visually-distinct color ranging from a limonite-stained orange to yellow. Near the surface its consistency is usually soft and gummy but it becomes firmer with depth. At the surface, caliche and gypsum crystals are common weathering features, and the clay may or may not be calcareous. At or near the surface most bedding features and fossils weather and become unrecognizable, but with depth these features become gradually distinguishable. Near the surface, the fractured nature of the soft clay allows mixing with surface material, which can include loess silt, alluvial sands, and gravel. Thus the near-surface weathered zone can have a greatly altered structural composition.

Weathered Yazoo clay is marked by numerous fractures. These fractures allow water to penetrate the otherwise low-permeability clay and enhance weathering at depth. At the surface these fractures are of all orientations and can totally disrupt the original fabric of the clay, but below about fifteen feet of depth the dominant fracture orientation is vertical. These fractures have been found at depths of 40 feet. At depth the fractures are lined with limonite coatings. The bottoms of fractures often have very thick (3 to 4 inches) gypsum fill of interlocking crystals that have grown from the fracture sides toward the center. These gypsum crystals serve to keep the fracture open and thus perpetuate the fracture to greater depth (Martin 2007). As noted in a later section, the "gypsum" crystals may indeed be composed of calcite.

Fractures that extend into the unweathered blue clay are limonite stained and discolor the unweathered blue material at the fracture. One unusual, and as yet unexplained, property of the Yazoo clay is that fractures in the

weathered yellow clay are often colored blue in contrast to the yellow clay around the fracture (Martin 2007). As shown later in this report, vertical and horizontal contact zones with abrupt color changes were observed. Fractures between those contacts were visibly absent, thus posing the question of how those colors originated, and if “weathering” caused the color changes.

Green and Childress (1974) indicated that the unweathered clay has shear strength (from triaxial and unconfined compression tests) up to 6000 lbs per sq. ft (psf), and the weathered clay strength is between 1500 to 2500 psf. The clay can undergo high volume changes with changing moisture conditions. Volume change up to 225% and swell pressures up to 25,000 psf were reported.

Infrastructure Damage

Alternate wetting and drying of Yazoo clay exerts powerful forces of shrinkage and expansion which can lift trees, buildings and highways. Some of the earliest literature describing its engineering properties was provided by Johnson and Clark (1955), who gave a good description of slump faulting in a Yazoo County road cut. Mississippi’s research into Yazoo clay’s problematic behavior was initiated in 1956 (Anon 1971), and accurately characterizing the clay’s behavior has remained an enigma ever since.

Another unknown aspect of the clay’s behavior, its possible long-term (time-dependent) loss of shear strength, was inferred by Johnson and Clark (1955) as well as by later authors. This un-researched phenomenon is likely the culprit for causing slumps, slides, and sloughs in otherwise-stable embankments. However, the most publicized culprit is its notorious shrink-swell behavior.

The shrinkage and swelling phenomenon of Yazoo clay has been documented in the public press, especially in the metro Jackson area. Numerous articles in Jackson’s paper, the Clarion Ledger, have been written regarding its damaging effects on foundations and buildings (Clarion Ledger 1990a, b; 1991a, b; 1994). Numerous other articles have been written about its impact on regional construction (Mississippi Business Journal 2001, 2004, 2006a, 2006b, 2008, 2009, 2010, 2011).

Engineers in Mississippi's Yazoo clay region have, over the past decades, developed certain design and construction philosophies (guidelines) to anticipate and circumvent damage to the region's infrastructure. Douglas and Dunlap (2000) detailed some of those philosophies related to shallow foundations under light commercial and residential structures. Visual identification and local geology knowledge are the primary means for detecting Yazoo clay, followed by standard laboratory Atterberg limits tests. Soil suction and swell tests are generally not performed due to their cost.

Maxwell (2011a, b) looked at foundation design and construction issues for 1-, 2- and 3-story buildings in the Jackson area. Under-slab cardboard box forms have not always fared well for single-story buildings, and belled drilled piers (the typical deep-foundation design solution) have not always been adequate for preventing expansive clay damage to multi-story buildings. Failures of commercial drilled pier foundations in central Mississippi are related to underestimating the potential heave and its potential depth (i.e. its active zone). Gently-sloping subsurface Yazoo clay underlying a level ground surface will exacerbate differential foundation settlement.

Maxwell (2011a, b) also noted the intermittent occurrence of alluvial ("terrace") clay above the Yazoo clay that has a perched water table. The terrace clay is not as expansive as the Yazoo clay, but this overlying clay layer has frequently been misidentified as Yazoo clay. This observation is also noted later in this report.

The Eudora Welty house in Jackson's Belhaven area (which lies directly over the extinct Jackson Dome volcano) was built in 1925 on top of a 5-ft thick non-expansive clay layer overlying Yazoo clay. The top of the unweathered (blue) clay averages 27 ft below ground surface. Extensive foundation repairs were needed due to floor tilting and differential settlement. Fourteen-inch-diameter reinforced concrete piers were drilled and cast in place around the foundation perimeter. The pier depth was 3 ft into the unweathered clay, or about 30 ft total depth. The maximum allowable design load for the unweathered Yazoo clay was selected at 6 tons per sq ft (tsf). The foundation piers supported the floor slab's perimeter grade beam, and floor jacking completed the leveling process (Ewing 2010).

Dockery (2005) provided examples of cost overruns caused by engineering geologic failures in Mississippi, including those in Yazoo clay. For example, inadequate surface drainage and low-permeability backfill were

thought to contribute to the slope failure at the newly-constructed Millsaps College football field retaining wall (Galicki 2008; Dockery 2009a).

A slope failure at the Dogwood Festival shopping mall in Rankin County was documented by Dockery (2009c). The steep slope, cut into Yazoo clay, had failed on 2 separate and earlier occasions. The failed slope was over-excavated to the unweathered Yazoo clay at its base and sand was back-filled over a geofabric liner to provide the latest and hopefully lasting repair.

Dockery (2010a) observed slope failures in side slope (embankment) fills along interstate highway I-20 in central Mississippi. It was assumed that the side slope fills were composed of remolded Yazoo clay. The shallow slip-surface slides were observed to occur on slopes that were steeper than 3H:1V, such as bridge abutments and entrance ramps.

Dockery (2010b) noticed repeated slides on the slope behind the Jackson Farmers' Market at the Fairgrounds. The original repair over-excavated the Yazoo clay and backfilled with non-expansive fill dirt. The latest repair was performed using top-down construction of a shotcrete wall anchored by soil nails. The likely culprit causing the repeated slides (a leaky city water pipe) was discovered after the repair was almost complete.

Yazoo Clay Investigations

Mississippi's Yazoo clay has been geologically described and mapped in studies of individual cores or outcrops at various locations by several researchers (Mellen 1940; Bergquist 1942; Priddy 1960; Baughman et al. 1971; Dockery et al. 1991). The MDoT has conducted individual research projects at Jackson's Airport Road and on Interstate Highway I-220 (Teng et al. 1972a, b; Sheffield 1987). These MDoT studies focused on pavement subgrade stabilization issues, and did not address detailed morphological or mineralogical aspects of the Yazoo clay. It was interesting to note that Sheffield (1987) observed that (a) the deeper the undercut below ditch grade, the less the roadway heave and (b) roadway fill sections heaved less than cut sections.

Clark (1956) described engineering problems caused by Yazoo clay. Redus (1962) described Yazoo clay's engineering properties and various case histories around the city of Jackson, Mississippi. Yazoo clay's engineering

properties and behavior aspects were also studied by academia at Mississippi State University in the 1960's (e.g. Springer 1962; Scholtes 1964; Chadwick 1965; Watkins 1965). Each researcher's Yazoo clay samples were typically obtained from a borrow pit northwest of Jackson referred to as the "Cynthia Pit" or the "Miss-Lite" pit.

The Jackson Ready Mix Miss-Lite Aggregate Division's open borrow pit (the Cynthia Pit) was the choice site for Yazoo clay studies over a 34-yr period (1958 – 1992) due to its accessibility and exposed vertical walls revealing a significant depth (~ 130 ft) of exposed Yazoo clay. Numerous studies have been conducted on samples retrieved from different locations in the exposed cuts of the borrow pit. For example, in 1992 a continuous 530-ft borehole core was drilled at that site, and clay mineralogy was analyzed (Yu 1992; Hou 1992). Unfortunately the Miss-Lite plant was closed in 1992. The borrow pit became a pond and vegetation gradually encroached (Dockery 1992).

Yazoo Formation index fossil and lithostratigraphy studies in Mississippi have largely depended on observations made either at the Cynthia Pit or from two boreholes within its 6-mile radius (Mossy Grove and Society Ridge). An exposed creek bank at Thompson Creek, an erosional scarp, and a creek bank at Sartartia are other locations that have revealed evidence enabling assumptions regarding geochronology and biostratigraphy correlations (Blackwell and Dukes 1981; Blackwell and Powell 1982; Dockery and Siesser 1984; Dockery 1985; Dockery et al. 1991; Obradovich et al. 1993).

A field test section located near Clinton, MS was instrumented and analyzed by Waterways Experiment Station (WES) personnel in the late 1960's and early 1970's (Gromko 1969; Johnson 1969; Johnson 1973a, b; Johnson and McAnear 1973; Johnson et al. 1973; Johnson 1974; Johnson and Desai 1975; Johnson and Stroman 1976; Johnson 1977). The 100 ft-square site (described later in this report) was located in Hinds County near the intersection of Clinton's Springridge and McRaven Roads just south of I-20, and its instrumentation provided in-situ measurements for predicting foundation swelling (heave) behavior. The field tests and soil samples enabled some pioneering experimental research for determining expansive soil characterization parameters including pore water pressure and soil suction. Data from that site were included with other expansive clay data around the U.S. to generate numerous reports applicable to

highway subgrade research during the decades of the 1970's and 1980's (Snethen et al. 1975; Snethen et al. 1977a, b; Snethen and Johnson 1977; Johnson and Snethen 1978; Johnson and Snethen 1978; Johnson 1979; Snethen 1979; Snethen 1980; Snethen and Johnson 1980; Snethen 1984).

MDOT Standard Procedure and Local Design Practice

The presence, thickness, and stratigraphy orientations of Yazoo clay (weathered or unweathered) will determine the life-cycle performance of a highway section. Current MDoT state-of-the-practice for characterizing the expected pavement subgrade or foundation soil behavior at expansive (high volume change) soil locations relies on a standard operating procedure using Atterberg limit and VC % results from laboratory testing. The borehole vertical sampling interval typically ranges from 30 inches to 60 inches. The test results dictate the design and construction requirements at the MDoT sites. For example, if the volume change value is greater than 60%, a 3-ft excavation (ditch-to-ditch) is automatically specified per MDoT SOP (TMD-20-14-00-000). Fill sections can not contain any Yazoo clay within the 3-ft zone below the profile. Cut slopes shall be 6H: 1V, and embankment slopes shall be 5H: 1V “to minimize the risk of future slope failure”. **Figure 6** illustrates these specifications for a hypothetical roadway alignment requiring both cut and fill geometry.

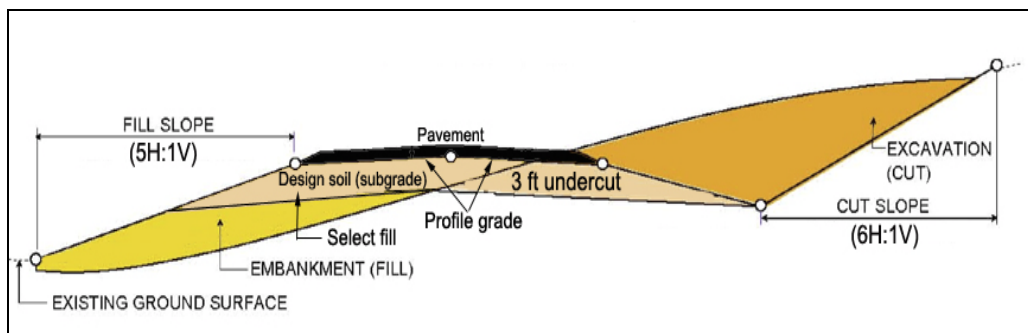


Figure 6. Diagram showing standard MDoT highway cut and fill sections in high volume change soils.

The SOP further defines certain soil types as always having a high volume change. These are the Yazoo, Porters Creek, Zilpha, and Hattiesburg/Pascagoula Formation soils. Excavation to 3 ft below the profile grade and replacement with specified select material is mandatory where

these Formation soils are identified. Lime treatment instead of over-excavation is optional where the Prairie Bluff Chalk, Ripley, Demopolis Chalk, and Mooreville Chalk Formation soils are identified.

AASHTO A-1, A-2-4, A-2-5, or A-3 materials are used in embankments and subgrades, and these classifications are specified in AASHTO M-57. Granular material with a PI of less than 10 generally is acceptable to use as a building material for sub-grades, sub-bases, and embankments. The PI is also used with LL and sieve analysis results to calculate a Group Index for classifying materials of mixed grain size. Generally a PI of 10 or less is required to calculate an acceptable Group Index. Yazoo clay's PI is much greater than 10, so it is unacceptable as an embankment or subgrade material unless it is blended to meet the specified classification.

Design practice for residential and light commercial construction on Yazoo clay in the Jackson area has traditionally been to provide a 5-ft thick non-expansive clayey soil buffer between the structure and the Yazoo clay. Douglas and Dunlap (2000) noted that a buffer of 7- to 10-ft thickness is even better since damage has been observed in shallow foundations having only a 5-ft buffer.

Comparing the MDoT SOP to local design practice illustrates the uncertainties involved when building highways or structures over the Yazoo clay. There are obvious uncertainties inherent in identifying, characterizing the behavior of, designing for, and constructing on Yazoo clay since:

- Highway heave damage has been observed for 3-ft over-excavations.
- Structure heave damage has been observed for 5-ft over-excavations (and buffer fill).
- The moisture-active zone depth is variable, extending to approximate 30-ft depths from top-of-clay.

It has been assumed that the Yazoo clay is primarily composed of montmorillonite clay and this composition (with its undesirable engineering properties) is uniform over central Mississippi. These assumptions have led to under-testing. For example, there is not a single shrinkage volume change percent (VC %) or plasticity index (PI) analysis for the Ya-

zoo clay under Highway 25. In addition, lime-treatment of Yazoo clay subgrades is known to not always be effective, but it is not known why (Martin 2007).

The state-of-the-practice approach has historically yielded mixed results by being either over- or under-conservative with the cut/fill volumes. In addition to reliance on a standardized design approach, another contributing factor is reliance on a limited number of soil test indicators derived from a wide sampling interval.

Figure 7 illustrates three possible field situations contributing to subgrade (or shallow foundation) lifecycle poor performance.

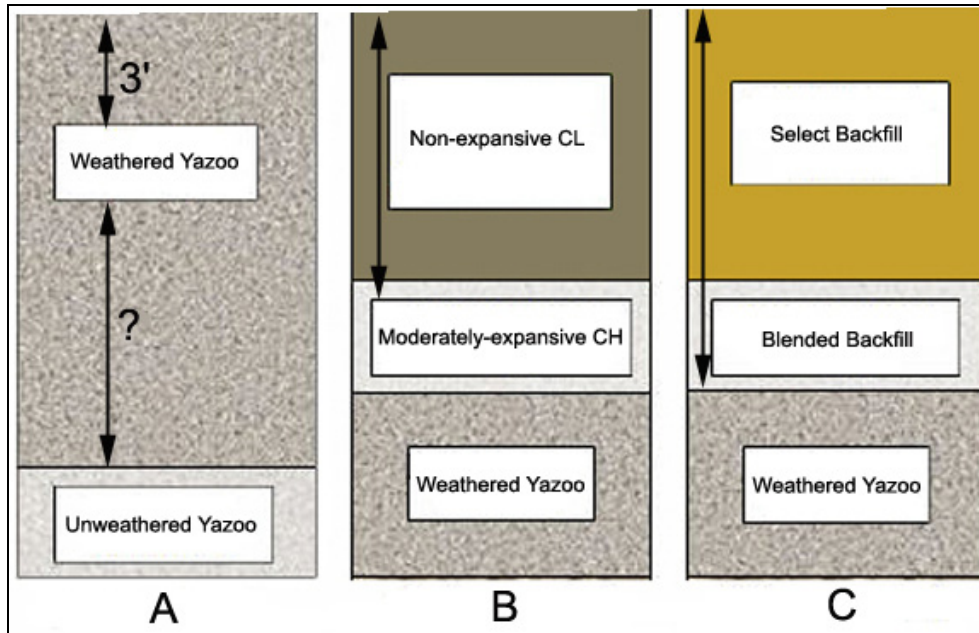


Figure 7. Diagram showing a few potential scenarios for poor infrastructure performance on Yazoo clay subgrades or shallow foundations

- A. A specified 3' undercut and design soil replacement depth may be inadequate for preventing shrink-swell behavior in a weathered clay zone. Knowing the active zone depth is imperative in this case.
- B. A moderately-expansive (non-Yazoo) clay zone may be misidentified as a Yazoo clay zone, thus causing inaccurate expansive behavior prediction/characterization.

- C. During embankment backfill construction, blended borrow materials may inadvertently (or purposely) contain Yazoo clay. Additionally, the SOP-permissible presence of Yazoo Clay 3 ft below profile grade may be detrimental for future roadway performance.

Horizontal soil layering is illustrated in the above **Figure 7**. Actual layering may or may not be horizontal, so the effects of spatial heterogeneity could be important. For example, non-horizontal layers can cause gradual creep. Long term strength reduction (strain softening) is also a definite possibility in such high plasticity clays, and slope stability analyses should include residual or fully softened shear strength parameters (Skempton 1964, 1970; Stark and Eid 1994, 1997; Mesri and Shahien 2003). The SOP slope angles appear to be based on historical performance experience rather than site-specific shear strength parameters.

2 Regional Yazoo Clay Investigation (State Study 151)

Background

Martin (2007) collected data for a previous MDoT study (State Study 151) that addressed mineralogy, mapping, and some engineering properties of Yazoo clay over a 5-county area in central Mississippi. Over thirty boreholes at numerous sites in central Mississippi were drilled to obtain samples for routine geotechnical laboratory testing and specialized mineralogy testing. **Figure 8** shows some of the borehole locations from which 224 samples were analyzed for mineralogical composition using x-ray diffraction (XRD). Eight samples were additionally tested using scanning electron microscopy (SEM). Geotechnical lab test results (density, moisture, Atterberg limits, and shrinkage volume change) were compiled from historical and recent borehole records of approximately 900 individual Yazoo clay soil samples. These data are included in **Appendix A** of this report.

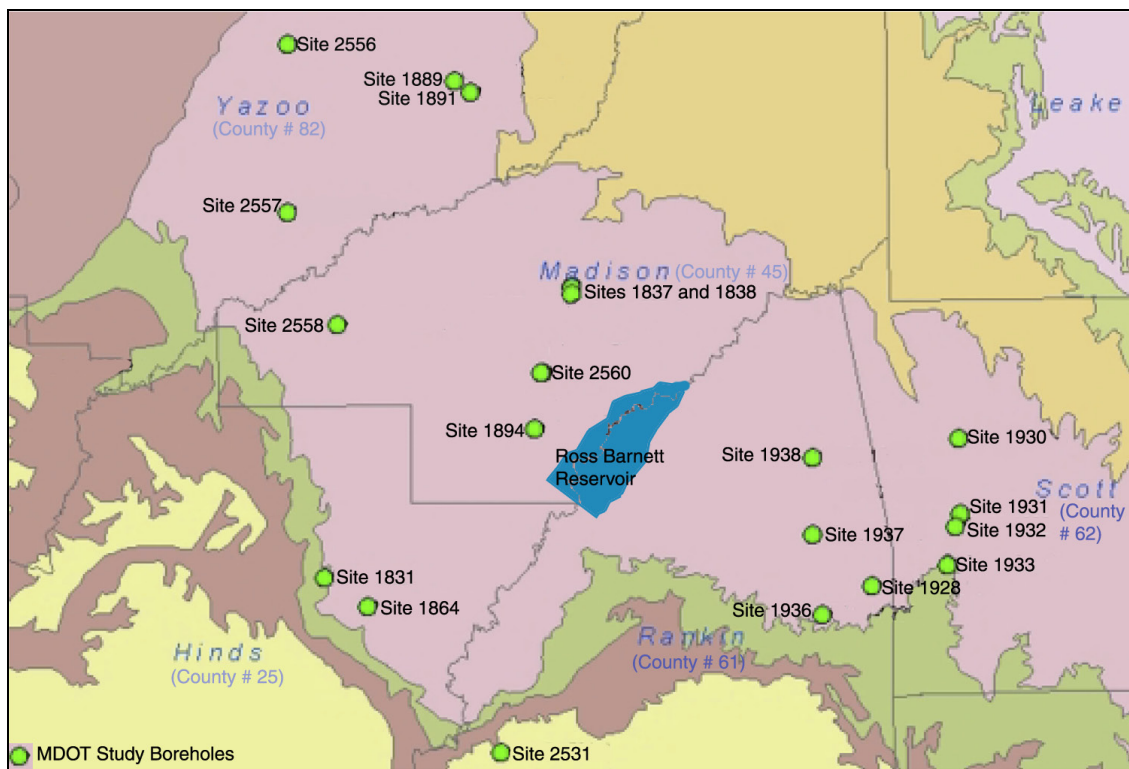


Figure 8. MDoT Yazoo clay mineralogy sample sites (after Taylor 2005 and Martin 2007).

MDoT Data Review

MDoT borehole data files were reviewed and other pertinent information was added to create a computer database and spreadsheet file. A latitude and longitude spatial reference was generated for each of the historical drill holes by locating the hole on a geo-referenced topographic map or aerial photo and recording the location in the computer database. Newer MDoT holes were located using a GPS at the time of drilling. Geographic Information System (GIS) software using kriging technology was utilized to generate maps for top elevations and thicknesses of the Yazoo clay in the central Mississippi area.

In addition to mapping, regression analysis was utilized to correlate the geotechnical parameters with depth below ground surface. An “R” value, also known as a correlation coefficient, was calculated. A value of one (1) implies perfect correlation, and a value of zero (0) implies no correlation.

Plasticity index (PI) and shrinkage volume change percent (VC %) were the two geotechnical parameters statistically analyzed in the antecedent MDoT study effort. The PI is the difference between the Liquid Limit (LL) and the Plastic Limit (PL) as measured using standard geotechnical lab procedures. The PI is a general proxy for volume change and is used as a material quality index to evaluate soil material for various applications in construction.

Mineralogy Tests

Scanning Electron Microscopy

Martin’s (2007) SEM study examined non-clay components in eight samples. Highly fractured Yazoo clay has surface coatings and vein fillings of secondary calcite, gypsum, manganese oxides, and iron oxides. Bedding planes may contain sand and silt seams or fossil layers. The SEM study observed these features.

Eight small samples were selected for SEM examination of mineral components present in clearly visible fracture or bedding planes. Each sample was approximately 1 to 1-1/2 centimeters on a side and 6 to 10 mm thick cut into rectangular pieces with flat undersides for easier mounting. They were mounted at the lab on standard SEM mounts using carbon paint, and coated with 50 angstroms of gold/palladium. The SEM apparatus was

used in high vacuum mode, and one sample at a time was placed in the vacuum chamber. Optimum viewing was obtained with a voltage of 15 V and a spot size of 6.

X-ray Diffraction

Samples were air-dried overnight, powdered by hand with a mortar and pestle, and back-loaded into a sample holder for X-ray diffraction analysis using a Philips X-Pert™ diffractometer with a Philips X'Celerator™. Samples were disaggregated in distilled water using a Branson Sonifier 250 for about 15 seconds to separate the <2- μm fraction. Samples were then cleaned and concentrated by centrifugation in a Sorvall SS-4 Manual Superspeed Centrifuge at 5- 6,000 RPM for 6 minutes. A small amount of sodium pyrophosphate (Calgon™) was added to the clay/water solution as a dispersing agent. The <2- μm size fraction was separated from the clay/water solution and was then siphoned off and concentrated by centrifugation for 1 hour at 6,000 RPM. Oriented clay slides were made from the <2- μm fraction by the modified Millipore® reverse transfer method using Durapore® Membrane Filters. The 47-mm 0.45- μm filters were placed in a high-pressure filtration unit, about 40 ml of clay/water solution were added, and the solution was pressurized to about 90 psig with N₂ gas. The solution was pushed through the filter for about 20 minutes. If, after 20 minutes, the clay concentrated on the filter was of sufficient thickness, the samples were Mg-saturated by passing through a 1-molar MgCl₂ solution and then washing with distilled water. If the clay was not of sufficient thickness, the clay/water solution was gently poured from the filtration unit, stirred, and gently poured back into the unit for further filtration.

The clay and filter were removed and then inverted onto a glass slide to ensure that the clay particles exposed to the X-ray beam were representative of the size fraction in the whole clay-rich sample. The filter, clay, and slide were dried together on a hotplate set on low temperature. Once the slides were dry, the filters were peeled off and the slides were left overnight in a desiccator containing ethylene glycol (C₆H₂O₆). The desiccator was kept in an oven at about 45°C to ensure the glycol completely penetrated the samples. Glycol-solvated slides were X-rayed at a range of 2-40° 2 θ . After the glycol-solvated slides were X-rayed, they were air-dried and X-rayed at a range of 2-30° 2 θ .

The prepared samples were X-rayed in a Philips X-Pert™ diffractometer with a Philips X'Celerator™ using a 1/4° divergence slit and a 1/2°

antiscatter slit. The step size was set at 0.02° and time per step at 150 seconds for the absolute scans using Philips X-Pert™ Data Collector software. The resulting scan speed was about $0.017^\circ/\text{sec}$.

The resulting X-ray diffraction patterns were interpreted for quantitative mineral analysis by comparing the characteristic peaks of gypsum, total clay, quartz, plagioclase feldspar, potassium feldspar, and calcite. Total clay was further analyzed to determine the relative abundance of the clay minerals smectite, illite, and kaolinite (Taylor 2005).

Analysis

MDoT furnished computer spreadsheet Yazoo clay data from the 5-county region in central Mississippi collected within the last decade. Approximately 900 Yazoo clay soil samples were collected, lab-tested, and catalogued by MDoT personnel. The depths and thicknesses of the Yazoo clay in the central Mississippi area were mapped (illustrated in **Figures 9** through **12**), and geotechnical parameters from MDoT laboratory test results were evaluated. Additional analysis of the MDoT data was conducted by ERDC as documented herein.

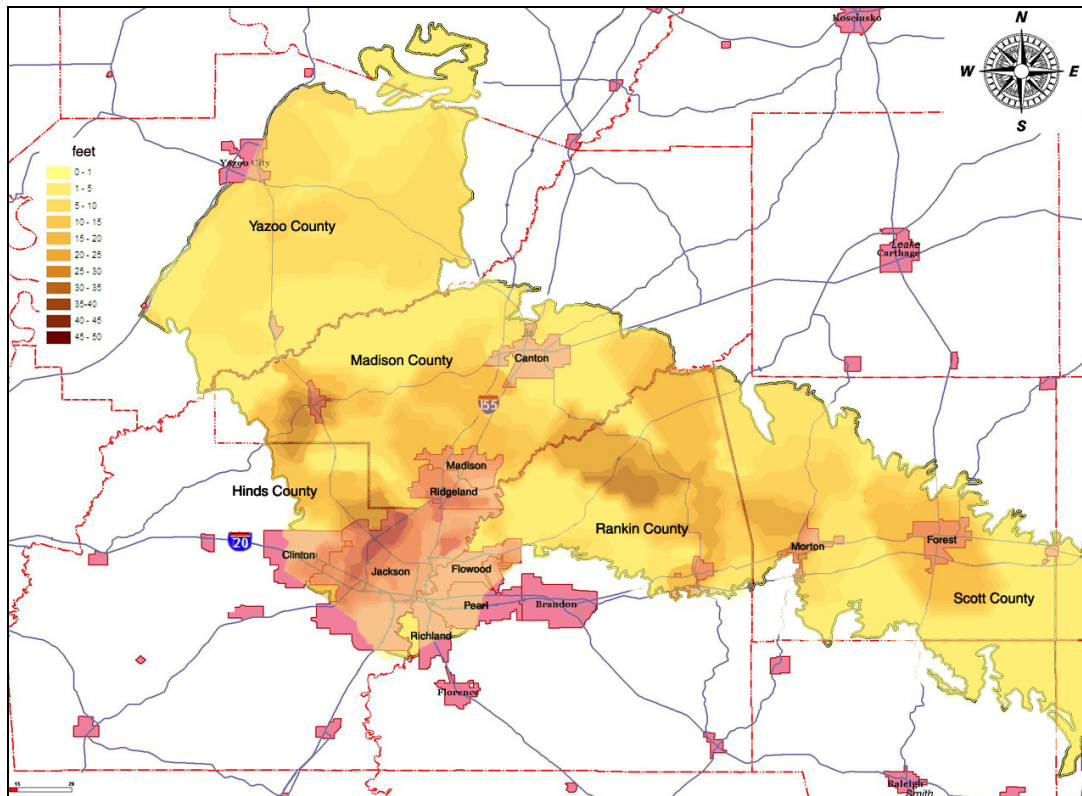


Figure 9. Yazoo clay visually-weathered thickness (after Martin 2007).

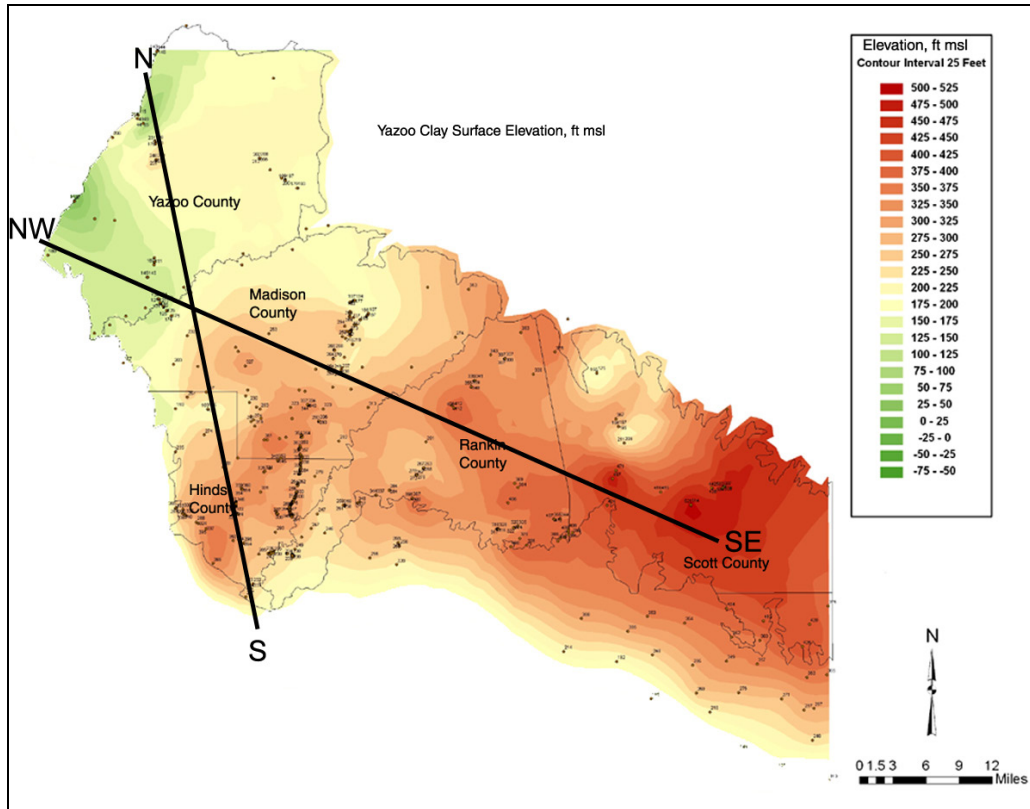


Figure 10. Yazoo clay surface elevations in central Mississippi (after Martin 2007). The natural ground surface generally slopes from about 500 ft msl in Scott County down to about 200 ft msl in Yazoo County, and the top-of-clay elevations also may vary by hundreds of feet. The NW-SE and N-S fence diagrams are shown below.

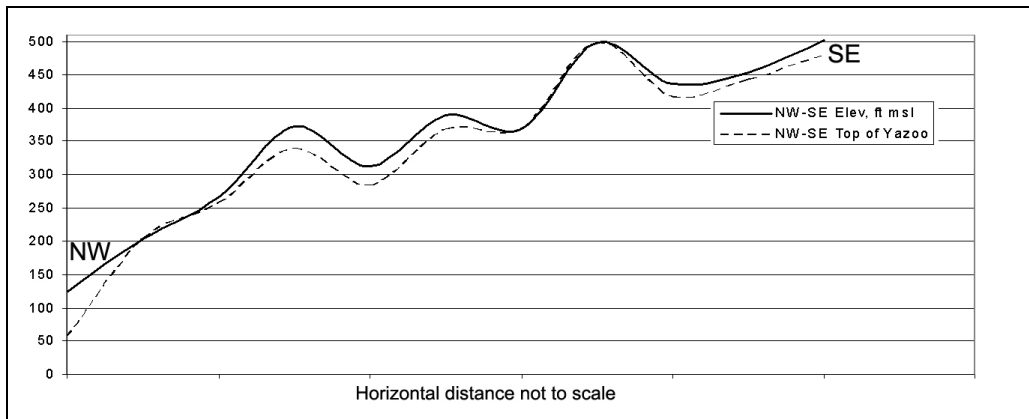


Figure 11. NW-SE fence diagram showing ground surface and top-of-Yazoo clay elevations from MDOT borehole data. The horizontal distance is approximately 50 miles.

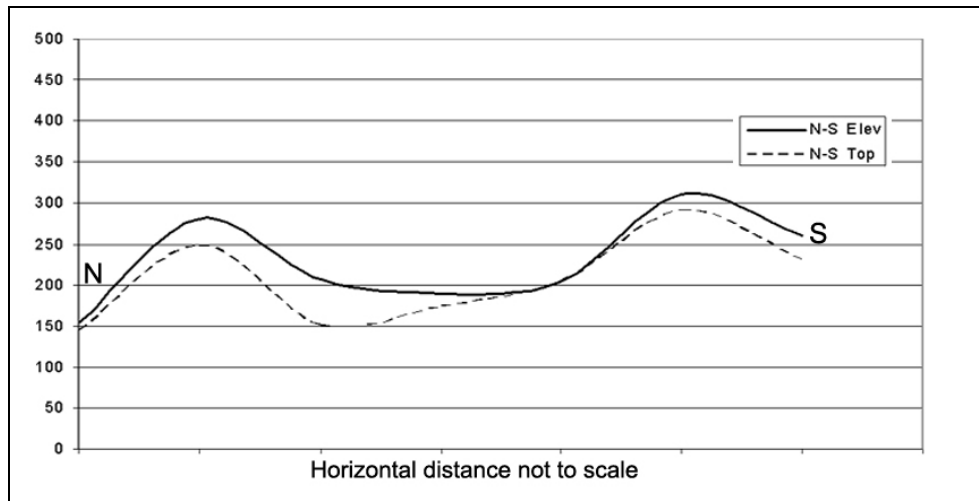


Figure 12. N-S fence diagram showing ground surface and top-of-Yazoo clay elevations from MDoT borehole data. The horizontal distance is approximately 35 miles.

The Yazoo clay surface generally followed the contour of the ground surface. There was more elevation change in the NW-SE direction than in the N-S direction, and this elevation difference might be a primary indicator of Yazoo clay spatial variability.

Figure 13 indicates that the weathered clay generally lies above the unweathered clay. Both were documented at just about any depth below ground surface, and unweathered clay was found above the weathered clay.

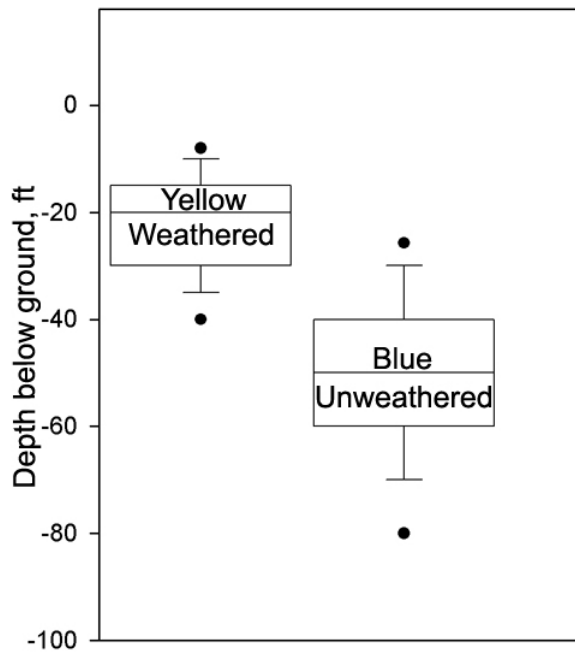


Figure 13. Box plots showing range of depths for visually-classified samples

Regional Dataset

ERDC’s statistical analysis of the MDoT data consisted of evaluating regional and local spatial property variability using Excel[®] spreadsheets and SigmaStat[®] software. Several observations were noted from the regional data statistics, as described below.

Geotechnical Index Properties

Table 1 lists the mean values for all the Yazoo clay soil data visually separated by sample color. The ‘weathered’ samples were yellowish, and the ‘unweathered’ samples had a blue color. Weathered clay was visually identified in samples from the surface to 40 ft depths. Visually-identified unweathered clay was sampled and tested between depths of 25 ft and 80 ft below ground surface.

Table 1. Yazoo clay average index property values

Parameter	Weathered (yellow)		Unweathered (blue)		All	
	Mean	Stan Dev	Mean	Stan Dev	Mean	Stan Dev
γ dry, lbs/cu ft	82	9	82	9	82	9

Parameter	Weathered (yellow)		Unweathered (blue)		All	
	Mean	Stan Dev	Mean	Stan Dev	Mean	Stan Dev
γ wet,, lbs/cu ft	112	10	114	9	113	10
Moisture content %	38	9	39	9	39	9
Field Void Ratio	0.99	0.21	1.03	0.22	1.02	0.22
LL %	94	19	95	16	94	17
PL %	35	8	37	8	36	8
PI %	59	16	58	13	59	14
VC%	140	39	138	38	138	39
*Clay %	53	21	65	14	60	18
*Calcite %	13	16	18	14	16	15
*Smectite %	45	18	48	13	46	15
*Illite %	16	17	11	10	13	14
*Kaolinite %	39	11	42	8	41	10

*XRD data

Figure 14 shows that almost all the samples (maximum n=904) were classified as clay with high plasticity (CH), based on the Unified Soil Classification System (USCS) soil classification chart (U.S. Army Engineer Waterways Experiment Station 1960). A general observation was that the weathered samples exhibited slightly higher LL and PI values.

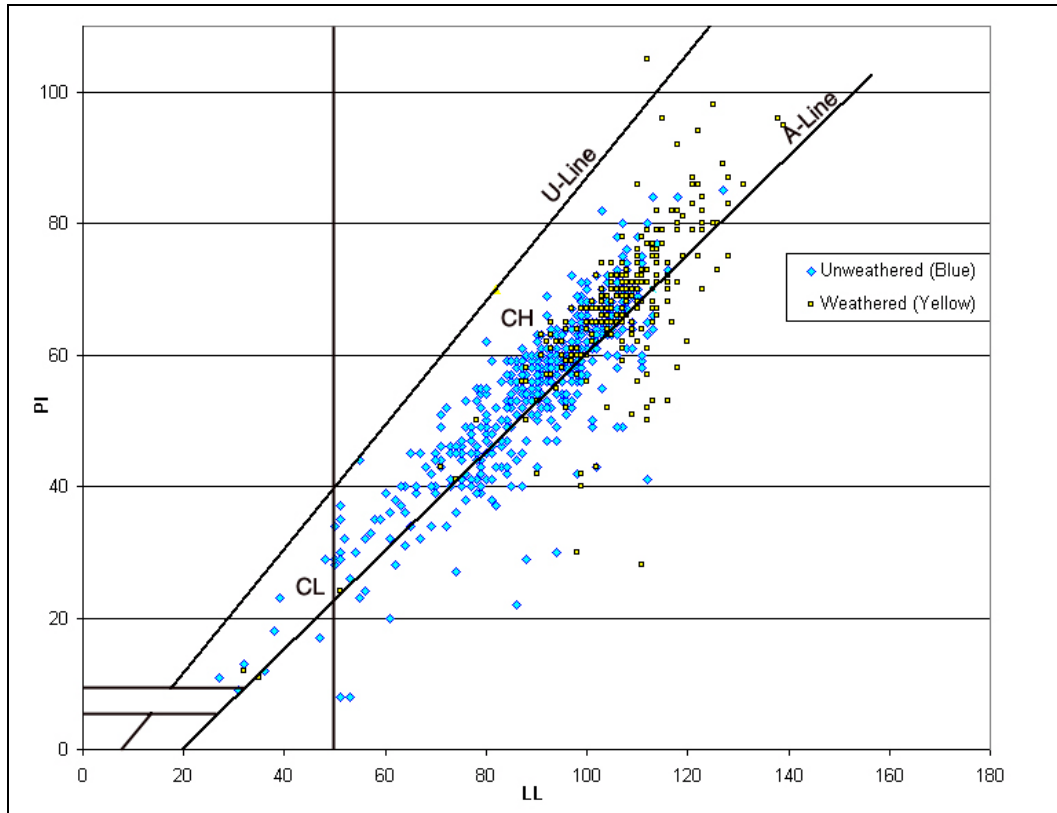


Figure 14. USCS soil classification chart (910 Yazoo clay soil samples).

Figure 15 shows the LL ranges based on the regional data.

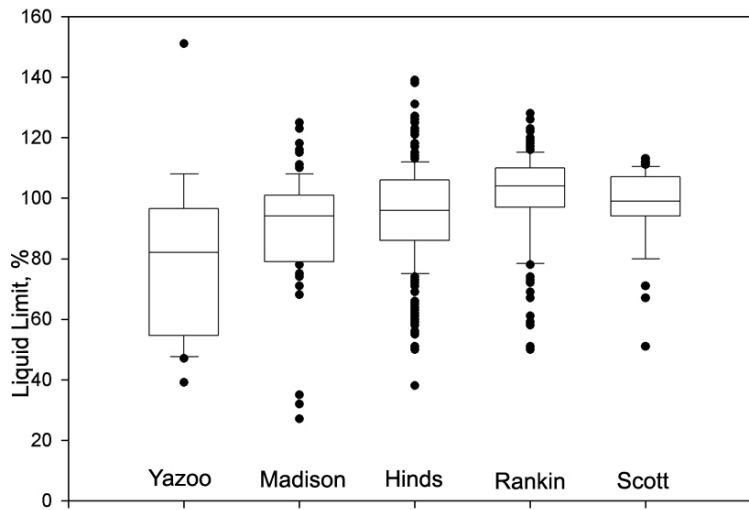


Figure 15. Box plots of 5-county LL data

Figure 16 shows the locations of common clay minerals superimposed on the USCS soil classification chart. Comparing the plasticity charts indicated that the predominate clay minerals should be illite and kaolinite. Mineralogy tests conducted on about 25% of the samples indicated higher percentages of smectite (montmorillonite), discussed later in this section.

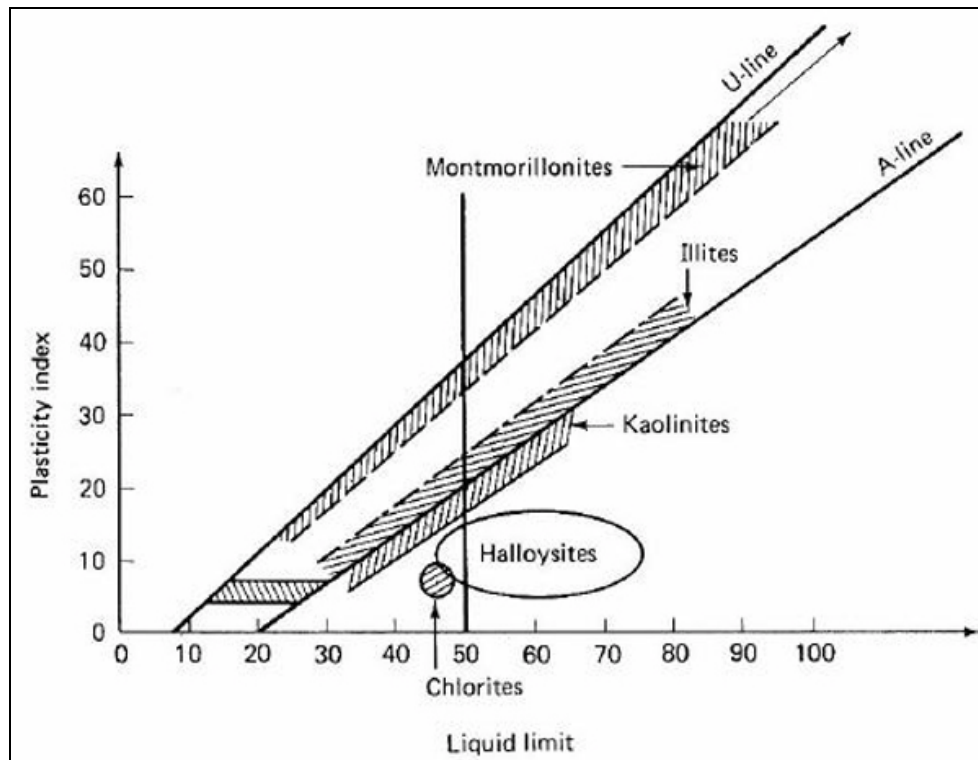


Figure 16. Location of common clay minerals on the plasticity chart (after Holtz and Kovacs 1981).

Correlations between geotechnical index properties for all samples in the regional area were analyzed for their water content percent, dry density, LL percent, PL percent, PI percent, liquidity index LI, consistency index I_c, and shrinkage volume change percent VC parameters. Unless otherwise noted, the percent sign (%) is dropped for brevity (i.e. LL% is noted simply as LL).

The only significant geotechnical index property correlation was between dry density and natural water content (correlation coefficient $R = 0.94$). Sample weathering discrimination was irrelevant for this correlation. The high correlation was noted regardless of the degree of weathering. The best-fit non-linear regression equation (**Figure 17**) was:

$$\text{Dry_density, pcf} = 142.2e^{-0.0143w\%} \quad (1)$$

Where

e = natural log base = 2.718

$w\%$ = water content percent

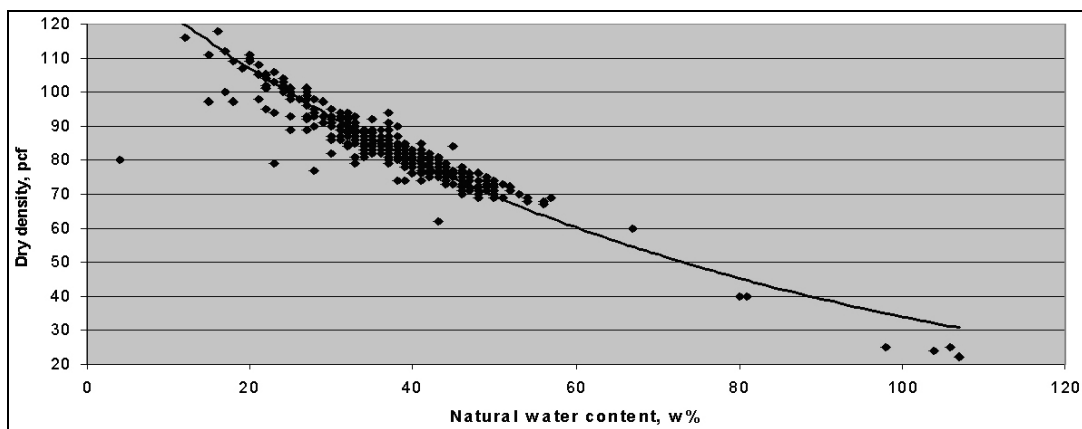


Figure 17. Dry density versus natural water content for all Yazoo clay data in the 5-county area of central Mississippi.

The inverse of dry density is the specific volume (i.e. specimen total volume per dry solid mass). When the specific volume is plotted against the natural water contents it shows the “volumetric compressibility factor” per AASHTO T-273 (Soil Suction). **Figure 18** shows the plot for weathered and unweathered Yazoo clay in the 10% to 55% natural water content range. The regression line ($R^2=0.86$) and slope equation were essentially the same for either visual classification (yellow or blue).

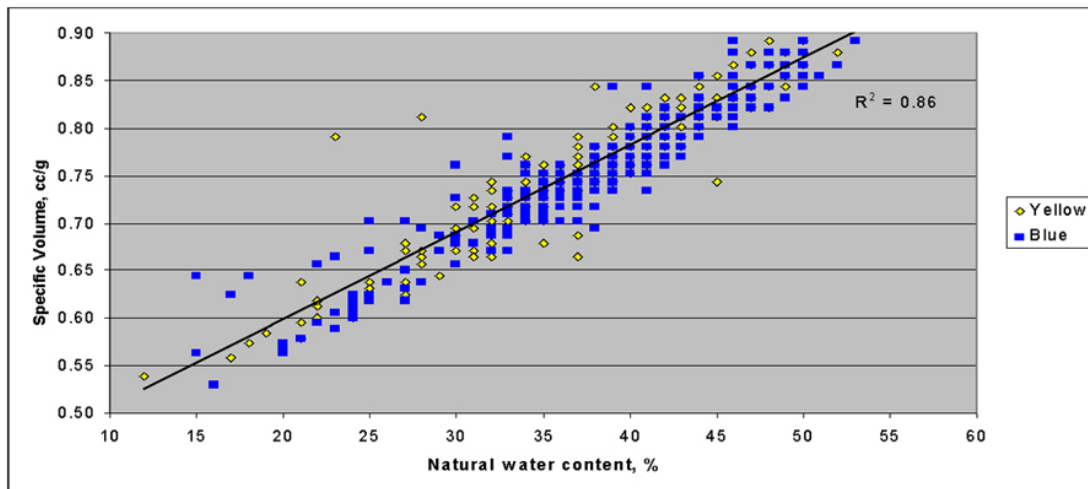


Figure 18. Dry density inverse (specific volume, cm^3/gram) versus natural water content for Yazoo clay's typical 15% to 55% natural water content range. Yellow points indicate visually weathered and blue points indicate visually unweathered samples.

The specific volume equation for weathered or unweathered Yazoo clay was:

$$\text{Specific_Volume, cc/g} = 0.0092(\omega\%) + 0.416 \quad (2)$$

The volumetric compressibility factor, α , was:

$$\alpha = 0.0092(\text{cc/g} / \omega\%) \text{ for dry density measured in grams/cm}^3, \text{ or } (3)$$

$$\alpha = 0.000147(\text{ft}^3 / \text{lb} / \omega\%) \text{ for dry density measured in lb/ft}^3$$

Mineralogical Properties (XRD and SEM)

Correlations between geotechnical properties and available mineralogy data were also analyzed. The mineralogy data included quartz, clay, calcite, smectite, illite, and kaolinite content percentages. Unless otherwise noted, the percent sign (%) was dropped for brevity (i.e. smectite content % was noted simply as smectite).

X-ray diffraction testing yielded results for Yazoo clay mineralogy separated by clay, quartz, smectite, illite, and kaolinite fractions (Taylor 2005; Martin 2007). Calcite and gypsum fractions were also noted. Very minor amounts (1%) of gypsum were found, which was puzzling, since gypsum is

considered to be an omnipresent mineral in Yazoo clay, according to published literature.

Figure 19 is a ternary diagram illustrating the XRD clay fraction component percentages (smectite, illite, and kaolinite). Most data results were clustered in a relatively tight box pattern bounded by 40%-70% smectite (assumed as montmorillonite), 5% to 20% illite, and 20% to 50% kaolinite. There were scattered data points outside this box, but they were primarily at shallow sample depths (5 ft, 10 ft, and 15 ft) where the mineralogy results were interpreted as indicating either a non-Yazoo clay soil type or a true highly-weathered soil having high quartz content.

In the presence of fresh water (i.e. leaching or travel through fissured openings) the smectitic minerals chemically convert to kaolinitic minerals (Sposito 1989). The relatively high smectite contents shown on the ternary diagram are an indication of mineral instability. The weathering process for these Yazoo clay samples has a long way to go before they exhibit mineralogical stability.

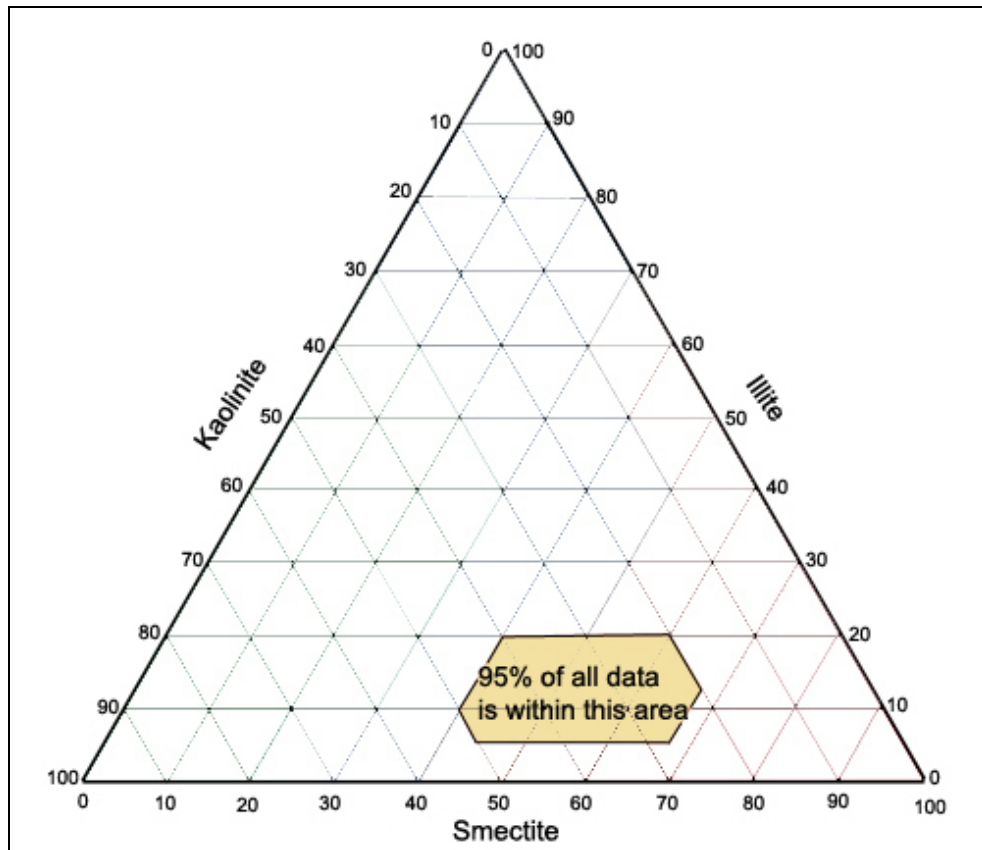


Figure 19. Ternary diagram of clay-fraction mineralogy results

From the SEM study (Martin 2007), iron stain (iron oxide with a dark rust or reddish brown color) commonly found on open fracture surfaces near the ground surface, formed a distinct layer 200 μm to 260 μm thick with very distinct edges. The iron oxide spectrum showed the abundance of iron and oxygen with silica and potassium also present. At right angles the iron stain was 213 to 260 μm thick. The source for the iron is likely the clay. The rust lining forms from oxidation of the iron in the clay as air and water in the fracture come into contact with the clay. The thickness of this layer may be limited by the oxidation layer sealing off the clay. More likely the iron oxide layer is poorly supported on the fracture face and sloughs off as its weight increases, exposing a new surface.

Large, sharply defined calcite crystals had a smooth texture that contrasted with the very small irregular clay texture. The contact on the fracture surface was very sharp, and there was no penetration of the secondary calcite into the clay.

The assumed secondary gypsum fracture lining was discovered to be calcite instead of gypsum. This crystal, typical of near-surface crystals generally visually identified in the field as gypsum, was found to not contain sulfur. The characteristic peaks of calcium, carbon, and oxygen indicated that the crystals were calcite. These crystals also showed fracturing on cleavage plans and bending of these fractured pieces. Manganese oxide was evenly distributed over the sample and was not concentrated along the fracture.

A sample containing a silt seam was mounted so that the silt face was exposed. Silt and fine sand seams were composed of quartz particles, calcite, and fossil fragments. Quartz grains were angular and were typically 30 μm to 60 μm wide. Larger grains were over 100 μm in their largest dimension. Detritus fossil tests were 60 μm to 120 μm wide. Calcite appeared to be detritus with abraded edges having flat blades with long dimensions of 100+ μm and short dimensions of less than 20 μm .

Fossils were found in the weathered and unweathered clay samples. The unweathered clay contained abundant foraminifera and ostracoda microfossils. These were well preserved and generally intact with little or no indication of abrasion or re-crystallization. Microfossils were found individually and in groups. Weathered clay had few microfossils but had common microfossils. These were often broken or poorly preserved from the weathering action. The unweathered samples were calcareous. Abundant microfossils were probably the source of calcite.

Calcite was present on the fracture walls. The source for the calcite was probably the dissolution and re-precipitation of fossil material. It was generally assumed that, in the weathered clay, fossils were dissolved and the calcite was re-precipitated. Microfossils in various stages of deterioration were common in the weathered clay. Calcite crystals may have grown large enough to become interlocking in the fracture for support. Larger crystals showed breaking of the crystal along cleavage surfaces. These surfaces were in places bent, and this bending did not appear to be a result of sample preparation but rather could be the result of the deformations of the clay swelling and shrinking in response to water content changes.

The most prominent discovery was that gypsum was not found. Gypsum, so commonly assumed to be present as a secondary mineral, was not found in either the SEM or the XRD studies.

When comparing regional mineralogy statistics, poor correlations were observed between mineralogy and depth below ground surface (and elevation above mean sea level). Poor correlations were also noted for relationships between mineral fractions. Better correlations were observed for depth interval-averaged values. All these features are discussed in the site-specific section below.

Based on analysis of the available data, it appeared that mineral composition variability was greater in the weathered zone. If visual color discrimination of weathered (yellow) versus unweathered (blue) samples was an accurate indicator, the yellow samples should have had the highest kaolinite content and the unweathered samples should have had the highest smectite content since kaolinite is typically an end product of weathered clays. These data showed an opposing trend. On a regional basis, smectite appeared to be the predominate clay mineral in the visually-weathered zone, and kaolinite predominated in the visually-unweathered zone. This observation indicated that the weathering process may be ongoing since Yazoo clay's expansive smectite behavior is known to predominate over that of its non-expansive kaolinite. The site-specific data shown later in this report illustrates the mineralogy variability within each 5-ft depth interval.

Figure 20 is a plot of LL and VC as functions of the smectite content. The correlations are poor although there appears to be a slight upward trend, especially for LL.

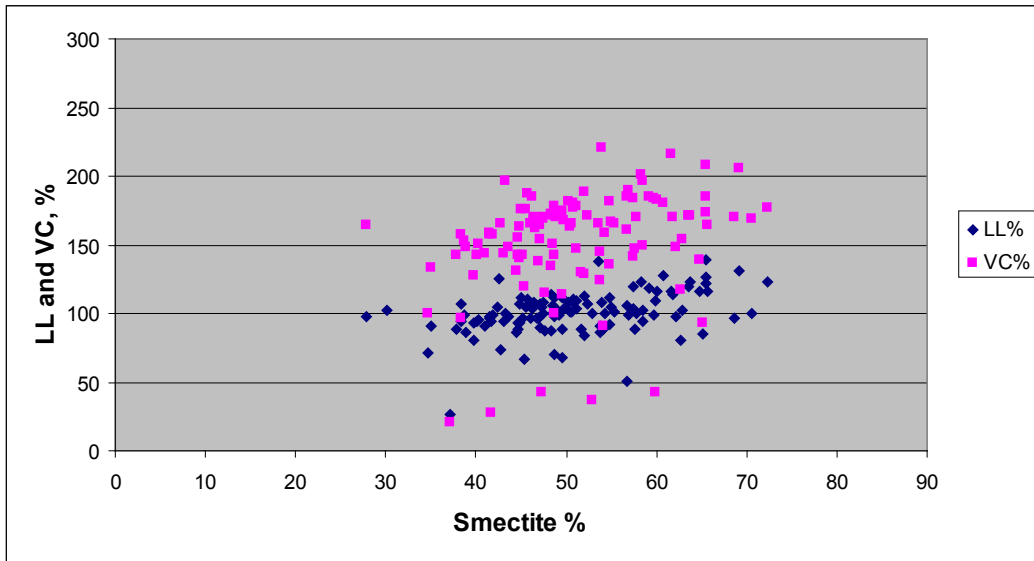


Figure 20. LL and VC relationships to smectite content in weathered plus unweathered samples.

Shrinkage volume change percent (VC %) and depth

Figure 21 shows the VC% ranges by county.

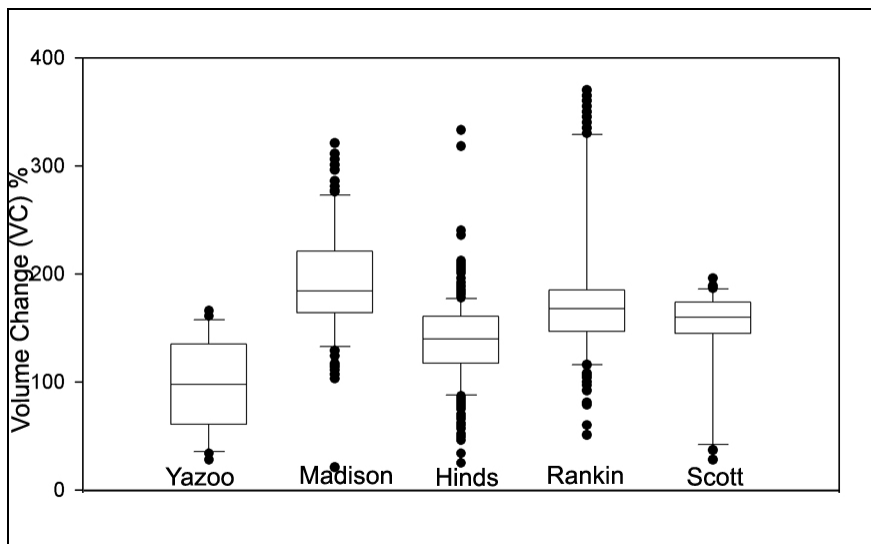


Figure 21. VC% results by county

Table 2 shows little distinction between regional VC values averaged over depth intervals in the upper 80 ft of the Yazoo Formation. The average regional VC value in the weathered Yazoo was 141%, ranging from 131% to 145% in the near-surface (above 40-ft depth). The average regional VC

value in the unweathered clay was 138%, with average values ranging from 128% at 80-ft depth to 161% at 25-ft depth. The presence of near-surface unweathered clay is likely due to either a shallow overlying weathered clay layer or a shallow overlying cover such as alluvium (Martin 2007).

Table 2. Average Yazoo clay volume change percent (VC %) for 5-county area of central Mississippi

Depth Zone	Average VC %
Weathered plus un-weathered, 0 – 80 ft	139
Weathered (yellow) only (above ~ 40 ft)	141
Un-weathered (Blue) only (below ~ 40 ft)	138
Yazoo Formation (~ 400 ft depth): Upper 100 ft	150
Yazoo Formation (~ 400 ft depth): Middle (varies)	141
Yazoo Formation (~ 400 ft depth): Bottom 100 ft	109

There was little correlation between sample depth (or elevation above mean sea level as shown in **Figure 22**) and regional VC. There also appeared to be little correlation between regional VC and visual color identification of weathering as a function of depth (or elevation). Using visual color identification (yellow or blue) as the primary method to discriminate between weathered and unweathered clay may not be a reliable indicator for regional VC.

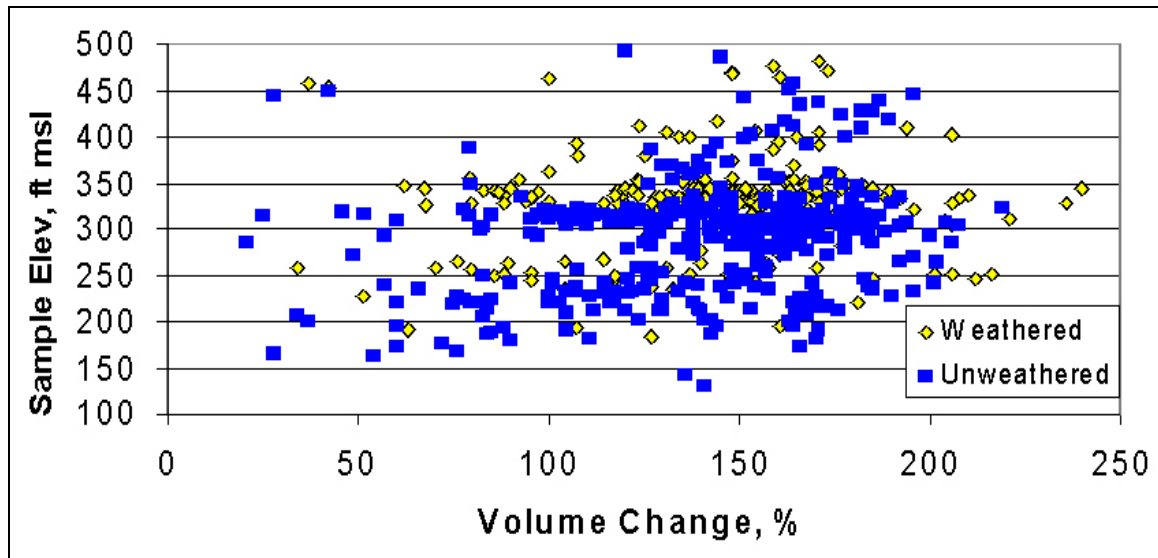


Figure 22. Volume change percent (VC%) values for all Yazoo clay data in the 5-county area of central Mississippi, plotted by elevation above mean sea level (msl).

Regression analysis indicated almost no correlation between the averaged VC values as a function of depth. Averaged VC values did exhibit an observable pattern when grouped by depth intervals. **Figure 23** shows there may be an identifiable pattern if the regional VC weathered and unweathered values are lumped together and averaged over incremental (~ 5 ft) depths. A similar pattern emerged when the regional weathered-only VC values were averaged over incremental 5 ft depths as shown in **Figure 24**. For example, peak average weathered VC values were found in the 5-ft intervals around 10-ft and 25-ft depths below ground surface.

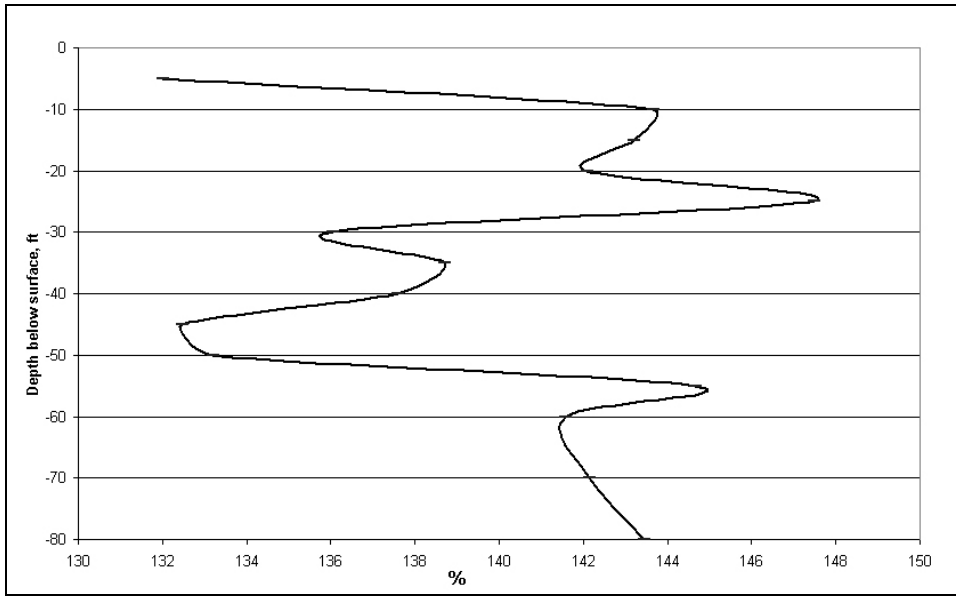


Figure 23. Mean shrinkage volume change percent (VC%) values for all (weathered plus unweathered) regional Yazoo clay data, plotted at 5-ft depth intervals.

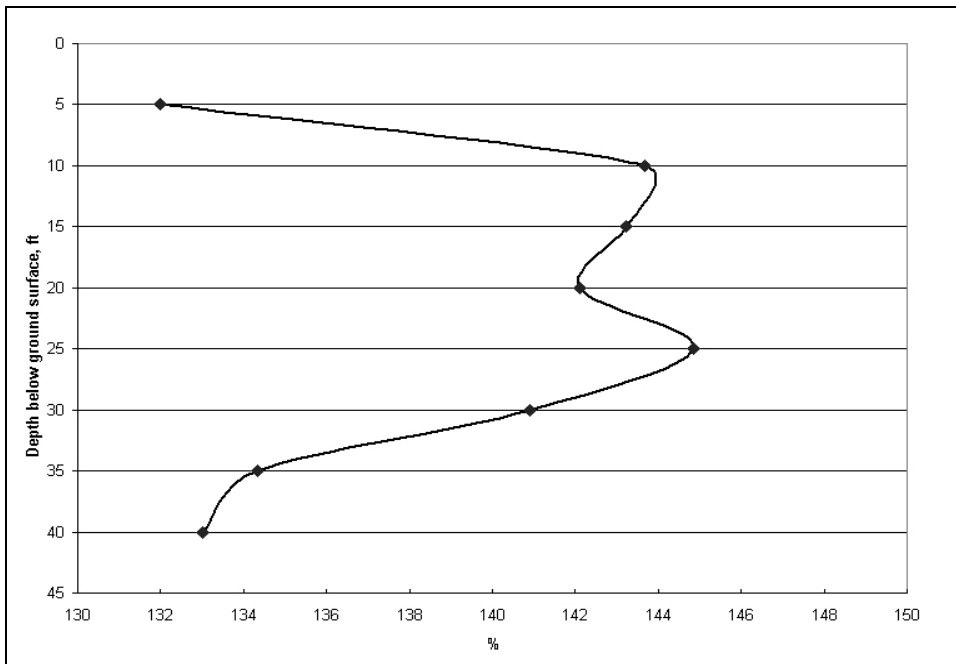


Figure 24. Mean shrinkage volume change percent (VC%) values for regional weathered Yazoo clay, plotted at 5-ft depth intervals.

Atterberg Limits and VC %

High volume change in expansive clay is traditionally associated with high PI values. The data were statistically analyzed to explore correlations be-

tween Yazoo clay VC and Atterberg limits (LL, PL, and PI). Since $PI = LL - PL$, the dependence of any correlation to PI relies on the LL, the PL, or both.

Results of the regression analysis for all sample data (weathered and un-weathered) from the central Mississippi region are shown in **Figure 25**. It is apparent that very poor correlation exists ($R^2=0.39$) for regional Yazoo clay. Similar analyses of PI as a function of depth also indicated non-correlation with depth (or elevation).

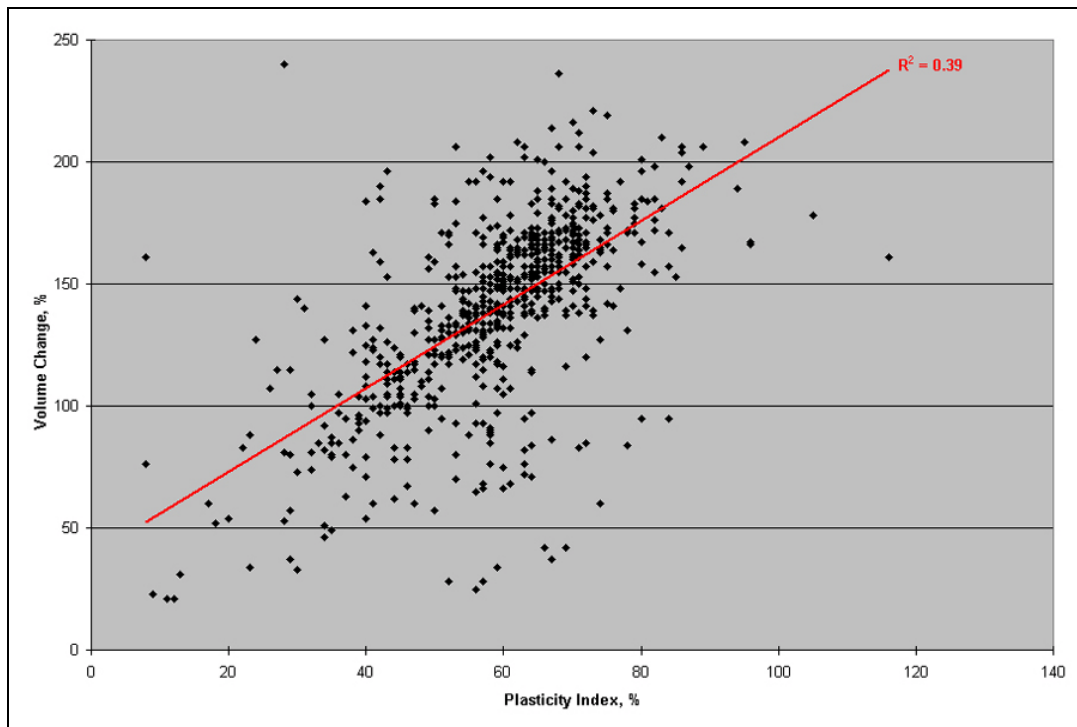


Figure 25. VC % and PI % correlation for regional weathered plus un-weathered Yazoo clay samples.

Comparing VC to LL (**Figure 26**) showed a closer relationship ($R^2=0.52$) than VC to PI, thus hinting that LL may be a more useful value than PI for Yazoo clay volume change correlations. Similar analysis comparing averaged values of VC, LL, PL, and PI by 5-ft depth intervals (**Figure 27**) also indicated that the LL may be the dominating Atterberg limits parameter for predicting volume change (VC%).

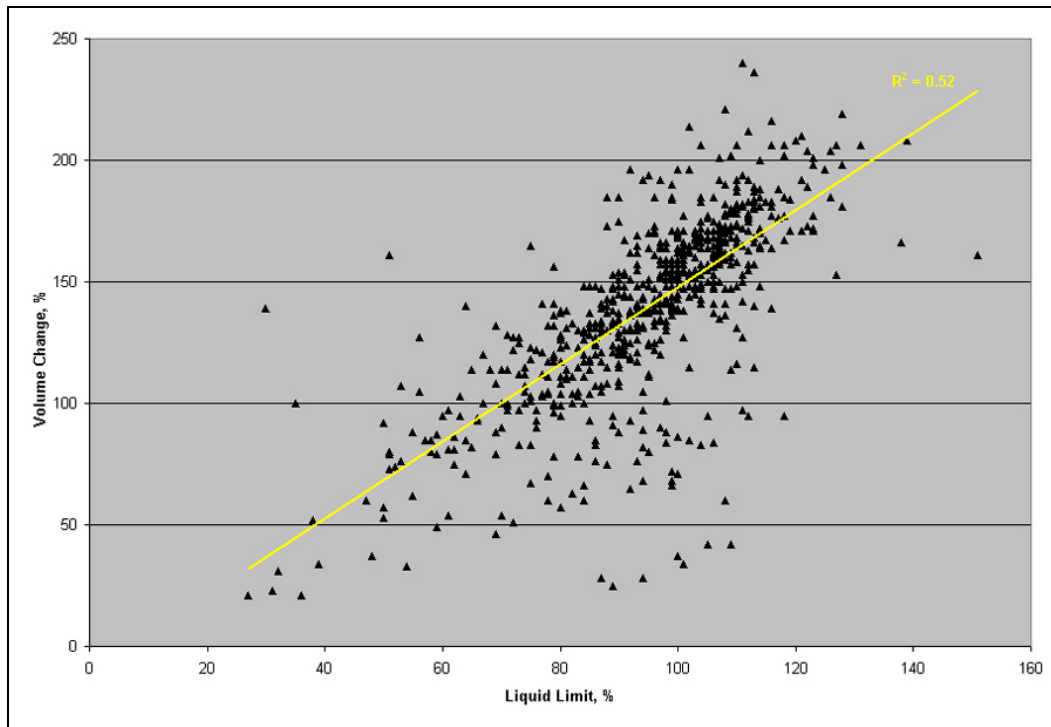


Figure 26. VC % and LL % for regional weathered plus un-weathered Yazoo clay samples.

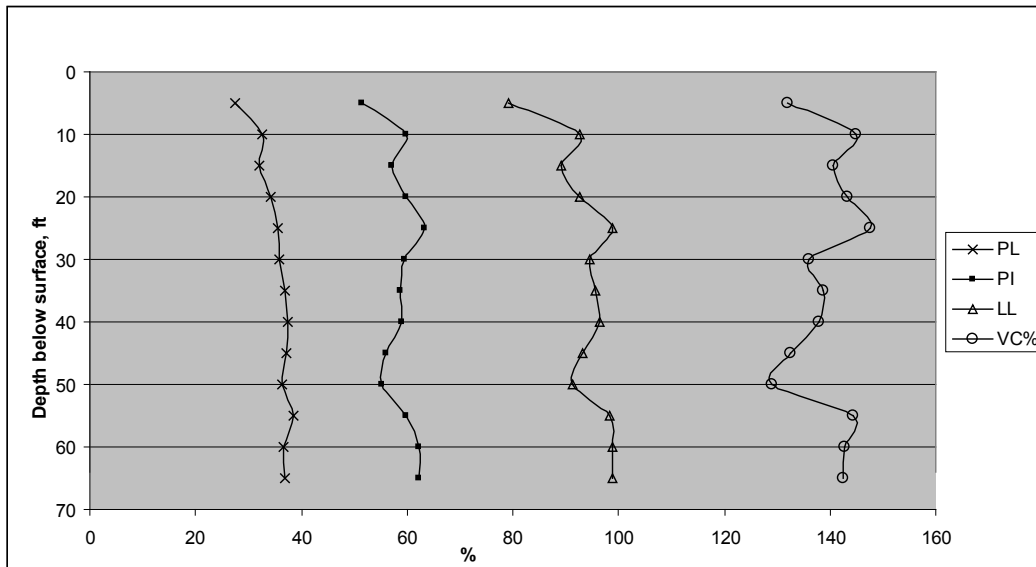


Figure 27. Regional weathered plus un-weathered Yazoo clay VC % and Atterberg limit values, averaged by 5-ft depth intervals.

The above **Figure 27** shows that the PL values did not vary much by depth, but the LL (and thus the PI) values varied in concert with the VC% values. Although these data are regional, the following trends were noted:

- Average VC% and LL values were lowest above -10 ft and around -50 ft.
- Average VC% and LL values were highest around -10 ft, -25 ft, and -55 ft.

These regional data indicated non-uniformity of Atterberg limits and expansive behavior patterns with depth.

Correlations of depth interval-averaged values

Lackcluster correlations of single-point data values in a given borehole sample depth interval were found to improve if the interval-averaged data values were also analyzed. Correlation matrices were developed to further explore regional relationships between geotechnical properties, mineralogy, depth, and elevation for weathered and un-weathered samples. Highest positive correlation between any two variables was indicated by a value of one (1). Highest inverse correlation was indicated by a value of negative one (-1). The closer the value to 1 (or -1), the higher was the correlation.

Analyzing the liquidity index (LI) and consistency index (Ic) showed that both were somewhat related to the VC% maximums shown in the above **Figure 27**. That is, LI and Ic indicated maximum changes also at -10, -25, and -55 ft depths. Since LI may contain negative values that may cause numerical ranking difficulty, the Ic was considered as the better indicator. **Figure 28** shows the Ic versus depth plot for the 5-ft depth interval-averaged values.

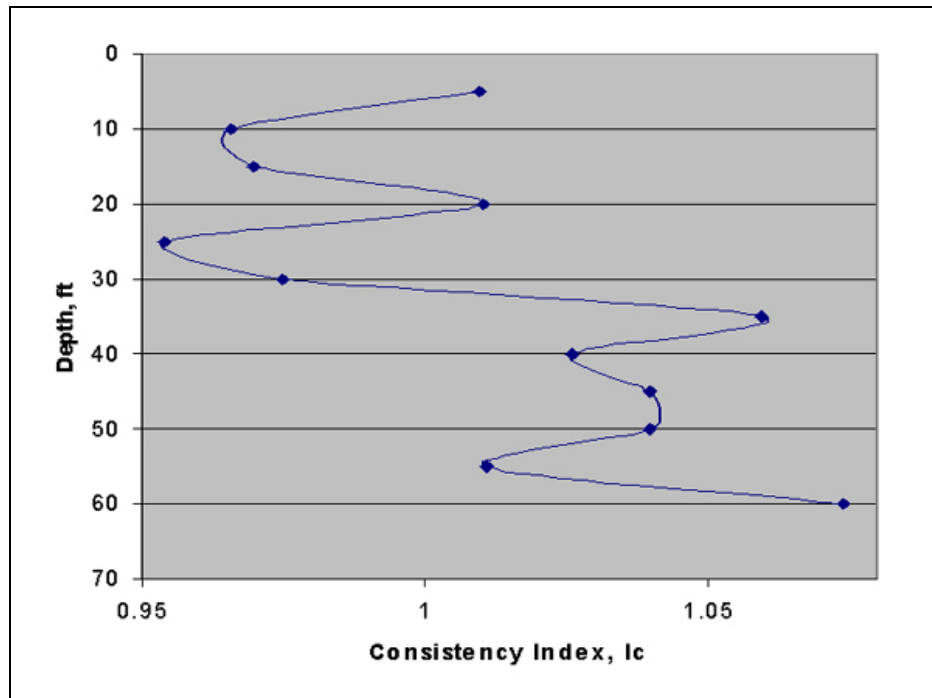


Figure 28. Regional weathered plus un-weathered Yazoo clay consistency index (Ic) values, averaged by 5-ft depth intervals. Note the Ic values are minimum at the corresponding maximum VC% and LL values (-10, -25, and -55 ft depths).

Table 3 lists correlations of 5-ft sample interval averaged values grouped by 5-ft sample depth intervals for weathered Yazoo clay samples. Samples were distinguished by visual discrimination of weathering (i.e. yellow color indicated a weathered sample). Maximum weathered sample depth was 45 ft below ground surface.

Table 3. Correlations of 5-ft interval-averaged values to 5-ft interval depths below ground surface for weathered Yazoo clay samples. Best correlations are highlighted.

Increasing depth below surface, ft	γ dry	γ wet	ω %	LL	PL	PI	VC%	Clay*	Calcite*	Smectite*	Illite*	Kaolinite*
	-0.22	-0.24	0.45	0.49	0.66	0.42	-0.14	0.89	0.39	0.58	-0.83	0.65
γ dry	1.00											
γ wet	0.89	1.00										
Nat ω %	-0.96	-0.89	1.00									
LL	-0.89	-0.69	0.93	1.00								
PL	-0.80	-0.78	0.92	0.89	1.00							
PI	-0.84	-0.56	0.85	0.97	0.80	1.00						
VC%	-0.39	0.01	0.30	0.55	0.23	0.69	1.00					
Clay %	-0.59	-0.61	0.76	0.71	0.86	0.63	-0.07	1.00				
Calcite %	-0.70	-0.59	0.70	0.69	0.65	0.73	0.33	0.64	1.00			

Increasing depth below surface, ft	γ dry	γ wet	ω %	LL	PL	PI	VC%	Clay*	Calcite*	Smectite*	Illite*	Kaolinite*
	-0.22	-0.24	0.45	0.49	0.66	0.42	-0.14	0.89	0.39	0.58	-0.83	0.65
Smectite%	-0.52	-0.19	0.57	0.79	0.59	0.84	0.55	0.61	0.56	1.00		
Illite%	0.54	0.46	-0.66	-0.70	-0.74	-0.68	-0.08	-0.91	-0.79	-0.76	1.00	
Kaolinite%	-0.38	-0.60	0.51	0.34	0.63	0.26	-0.33	0.78	0.65	0.11	-0.71	1.00

* indicates percentages derived from x-ray diffraction testing

Some observations noted from the above **Table 3** for weathered Yazoo clay were:

- Average natural water content and average dry density correlated very well ($R=-0.96$), i.e. dry density and water content were inversely proportional. Wet density also correlated well with water content, but that was expected since the wet and dry density difference in any given soil sample relies solely on its water content value.
- Average natural water content and average LL correlated very well ($R=0.93$). These two parameters are not typically directly related, but may be so for weathered Yazoo clay. Additionally, knowing the average LL implied a knowledge of the PL value ($R=0.89$). These two parameters were also not necessarily directly related to each other, but may be so for weathered Yazoo clay.
- The average mineralogical clay content (measured by x-ray diffraction) of weathered Yazoo clay increased with depth ($R=0.89$). No similar pattern seemed to exist for the other mineralogical entities (calcite, etc.) although clay and illite contents were inversely related ($R=-0.91$).
- There appeared to be no correlation between average VC and depth. The closest correlation was between VC and PI ($R=0.69$), which was not a good correlation.

Table 4 lists correlations of 5-ft interval averaged values to sample elevation zone intervals (ft above mean sea level, msl) for weathered Yazoo clay samples. Samples were distinguished by visual interpretation of weathering (i.e. yellow color indicated a weathered sample). Maximum weathered

sample depth was 45 ft below ground surface. **Table 5** lists the elevation zone intervals.

Table 4. Correlations of 5-ft interval-averaged values to sample elevation zone intervals (ft above mean sea level, msl) for weathered Yazoo clay samples. Best correlations are highlighted.

Decreasing elevation zone	γ dry	γ wet	ω %	LL	PL	PI	VC%	Clay*	Calcite*	Smectite*	Illite*	Kaolinite*
	-0.27	-0.22	0.03	0.16	0.10	0.13	0.48	0.71	0.20	0.36	-0.81	0.11
γ dry	1.00											
γ wet	0.91	1.00										
Nat ω %	-0.91	-0.84	1.00									
LL	-0.33	-0.21	0.52	1.00								
PL	-0.77	-0.76	0.81	0.58	1.00							
PI	-0.05	0.07	0.24	0.95	0.34	1.00						
VC%	-0.33	-0.12	0.43	0.81	0.47	0.75	1.00					
Clay %	-0.21	0.00	0.20	0.51	-0.04	0.52	0.73	1.00				
Calcite %	-0.20	-0.23	-0.05	-0.18	0.11	-0.21	0.10	-0.13	1.00			
Smectite%	0.16	0.11	-0.01	0.21	-0.18	0.22	0.24	0.55	-0.58	1.00		
Illite%	0.16	0.09	-0.08	-0.31	0.02	-0.31	-0.62	-0.82	-0.10	-0.54	1.00	
Kaolinite%	-0.42	-0.28	0.17	0.07	0.36	0.02	0.23	-0.13	0.81	-0.81	0.05	1.00

* indicates percentages derived from x-ray diffraction testing

Table 5. Elevation zone intervals for the above Table 4.

Zone	1	2	3	4	5	6	7	8	9	10	11
Elevation interval, ft msl	482-454	417-400	400-350	350-340	340-330	330-320	320-300	300-250	250-220	220-200	200-150

Illite content was the only parameter influenced by elevation zone ($R=-0.81$), in that illite content decreased as the sample elevation above mean sea level decreased (or the zone number increased). VC and LL were related at each elevation zone ($R=0.81$), as were calcite to kaolinite, smectite to kaolinite, and clay to illite.

Table 6 lists correlations of 5-ft sample interval averaged values to 5-ft sample depth intervals for unweathered Yazoo clay samples. Samples were distinguished by visual interpretation of weathering (i.e. blue color indicated an unweathered sample). Maximum unweathered sample depth was 80 ft below ground surface.

Table 6. Correlations of 5-ft interval-averaged values to 5-ft interval depths below ground surface for unweathered Yazoo clay samples. Best correlations are highlighted.

Increasing depth below surface, ft	γ dry	γ wet	ω %	LL	PL	PI	VC%	Clay*	Calcite*	Smectite*	Illite*	Kaolinite*
	0.09	0.22	-0.03	0.07	0.46	-0.39	-0.20	0.44	-0.29	-0.08	-0.42	0.09
γ dry	1.00											
γ wet	0.86	1.00										
Nat ω %	-0.97	-0.76	1.00									
LL	-0.89	-0.65	0.92	1.00								
PL	-0.71	-0.48	0.78	0.75	1.00							
PI	-0.58	-0.48	0.55	0.71	0.07	1.00						
VC%	-0.73	-0.42	0.82	0.84	0.66	0.72	1.00					
Clay %	0.66	0.37	-0.77	-0.70	-0.52	-0.62	-0.94	1.00				
Calcite %	-0.56	-0.66	0.61	0.59	0.36	0.56	0.69	-0.90	1.00			
Smectite%	0.37	0.49	-0.44	-0.28	-0.51	0.01	-0.24	0.43	-0.56	1.00		
Illite%	-0.66	-0.33	0.76	0.67	0.53	0.57	0.92	-0.99	0.71	-0.37	1.00	
Kaolinite%	0.12	-0.09	-0.07	-0.15	0.13	-0.35	-0.17	0.06	0.27	-0.87	-0.11	1.00

* indicates percentages derived from x-ray diffraction testing

Some observations noted from the above **Table 6** for unweathered Yazoo clay were:

- There were close relationships between water content, LL and dry density.
- Calcite and illite had strong inverse correlations to clay content but did not appear to be a function of depth.
- VC and clay content were strongly inversely related ($R=-0.94$) in that VC decreased as clay content increased. Smectite and kaolinite were inversely related ($R=-0.87$) but did not appear to be related to depth.
- There appeared to be no correlation between average VC and depth. VC was more closely related to LL ($R=0.84$) than any other index property. The correlation between VC and PI ($R=0.72$) was not very strong.

Table 7 lists correlations of 5-ft sample interval averaged values to 5-ft sample depth intervals below ground surface for all Yazoo clay samples to 45 ft depth below ground surface. Samples were undistinguished by visual

interpretation of weathering, that is, the samples were not grouped as yellow or blue.

Table 7. Correlations of 5-ft interval-averaged values to 5-ft interval depths below ground surface for weathered plus unweathered Yazoo clay samples to 45 ft depth below ground surface. Best correlations are highlighted.

Increasing depth below surface, ft	γ dry	γ wet	ω %	LL	PL	PI	VC%	Clay*	Calcite*	Smectite*	Illite*	Kaolinite*
	-0.63	-0.51	0.75	0.61	0.90	0.37	-0.40	0.96	0.46	0.61	-0.84	0.85
γ dry	1.00											
γ wet	0.95	1.00										
Nat ω %	-0.98	-0.92	1.00									
LL	-0.91	-0.85	0.94	1.00								
PL	-0.82	-0.70	0.91	0.87	1.00							
PI	-0.85	-0.81	0.84	0.93	0.72	1.00						
VC%	-0.32	-0.30	0.21	0.42	0.00	0.62	1.00					
Clay %	-0.72	-0.63	0.83	0.70	0.95	0.54	-0.27	1.00				
Calcite %	-0.75	-0.73	0.77	0.79	0.68	0.83	0.41	0.60	1.00			
Smectite%	-0.95	-0.91	0.94	0.93	0.85	0.91	0.34	0.75	0.77	1.00		
Illite%	0.81	0.75	-0.87	-0.80	-0.90	-0.69	0.04	-0.92	-0.84	-0.84	1.00	
Kaolinite%	-0.54	-0.46	0.65	0.55	0.79	0.40	-0.26	0.87	0.72	0.55	-0.90	1.00

* indicates percentages derived from x-ray diffraction testing

Figure 29 is a plot of LL and VC as functions of smectite content for 5 ft interval depth-averaged data. The plot shows that LL and smectite were correlated well as seen in the above Table. The VC-smectite trend was not as good.

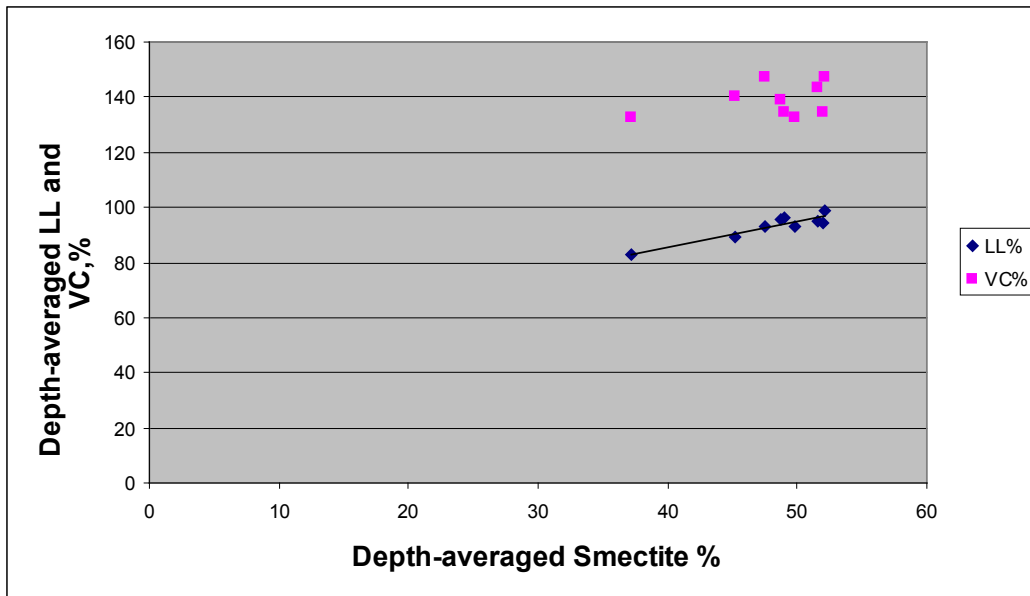


Figure 29. LL and VC versus smectite content for weathered and unweathered depth-averaged data. The LL-smectite data provided the better curve fit.

Some observations noted from above **Table 7** for visually non-discriminated samples (to -45 ft depth) whose data were averaged by 5-ft depth intervals were:

- There were more positive correlations compared to the preceding tables for visually-discriminated samples.
- There were more positive depth-related correlations.
- The geotechnical index properties were good indicators of smectite content. The smectite to VC correlation improved, but was a very low value (0.34).
- PI provided the better correlation to VC% than did LL which was an opposite trend for the un-averaged data.

Synopsis of Regional Observations

For all the above correlation matrices constructed from regional soil test data averaged by 5-ft depth intervals, the following observations were made for weathered, unweathered, and visually non-discriminated Yazoo clay samples:

- Strong relationships existed between average natural water content, LL, PL, and dry density. For example, knowing the natural water content averaged over any 5-ft depth interval for a Yazoo clay sample retrieved from less than 45 ft below ground surface enabled estimates such as:

$$LL\% = 15.17(w\%)^{0.49} \quad (R=0.90) \quad (4)$$

$$PL\% = 1.36(w\%)^{0.89} \quad (R=0.91) \quad (5)$$

$$\text{Drydensity, pcf} = 296.6(w\%)^{-0.35} \quad (R=0.95) \quad (6)$$

$$\text{Wetdensity, pcf} = 188.1(w\%)^{-0.14} \quad (R=0.80) \quad (7)$$

For non-discriminated samples (i.e. those not separated by visual degree-of-weathering), averaged PL and clay content percent were strongly related to depth. They were also strongly related to averaged smectite, illite, and kaolinite percentages. For example, knowing the Yazoo clay sample depth (less than 45 ft below ground surface) enabled estimates of interval-averaged values such as:

$$PL\% = 24.63(\text{Depth, ft})^{0.11} \quad (R=0.94) \quad (8)$$

$$\text{Clay}\% = -33.5 + 0.31(\text{Depth, ft}) + 2.33(PL\%) \quad (R=0.97) \quad (9)$$

$$\text{Smectite}\% = -21.94 - 0.21(\text{Depth, ft}) + 2.18(PL\%) \quad (R=0.91) \quad (10)$$

- VC was poorly related to any of the index or mineralogy properties.
- The regional data yielded poor correlations for Yazoo clay behavior (i.e. volume change percent) to geotechnical index or mineralogical properties, with the one exception being the dry density-natural water content relationship previously shown.
- The regional data yielded poor correlations between geotechnical index or mineralogical properties related to depth below ground surface, unless those values were depth-averaged in 5-ft intervals. Poor regional correlations to elevation above msl were also noted.

Site-specific Data

The regional Yazoo clay data were composed of 904 samples taken at 41 MDoT sites in five central Mississippi counties surrounding the Jackson metropolitan area. Each site had up to 40 boreholes laterally spaced over hundreds of feet, although typically at each site there were 2 to 4 boreholes with variable lateral and vertical spacing. Most borehole samples were visually discriminated by color (yellow for weathered versus blue for unweathered) and the lab test results were recorded on approximate 5-ft depth intervals. Although the site-specific data points were limited compared to the larger regional dataset, there were observable correlation patterns in the site-specific data.

Data were plotted from sites that were selected using the following criteria:

- Availability of both geotechnical and XRD data
- Availability of both weathered and unweathered sample data
- Availability of at least 4 or 5 samples per borehole

Site 1928

This site's geotechnical data were plotted to illustrate the index property variation with depth that was so typical for both regional and site-specific results. Plotted data from hole 5 indicated that LL and VC were closely correlated by depth interval (**Figure 30**). Both LL and VC reach peak values at 30-ft depth and minimum values at 40-ft depth. **Table 8** lists the correlations between index properties and depth.

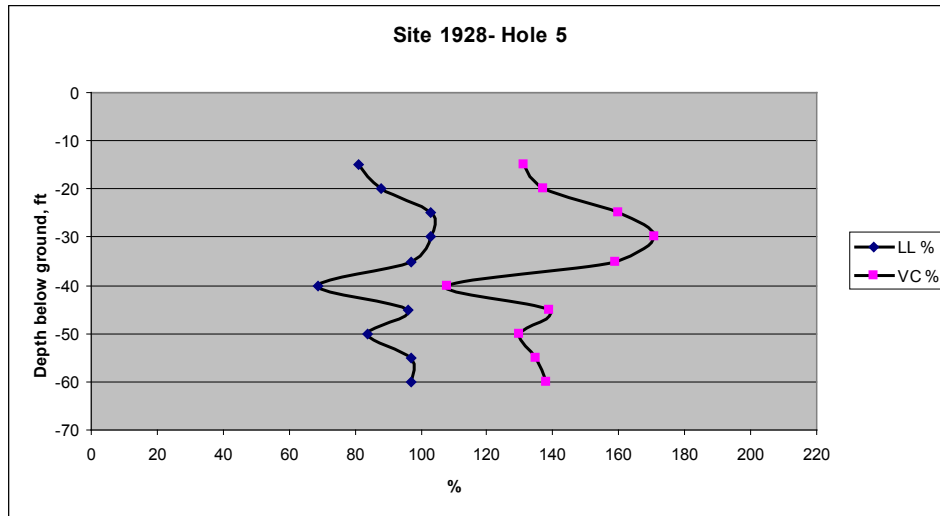


Figure 30. VC % and LL % for Site 1928, hole 5, weathered plus unweathered Yazoo clay samples.

Table 8. Correlations of geotechnical data in 5-ft depth intervals at Site 1928, hole 5. The best correlations are highlighted.

Increasing depth below surface, ft	γ dry	Nat ω %	LL	PL	PI	VC %
	0.64	-0.70	0.11	-0.61	-0.14	-0.25
γ dry	1.00					
Nat ω %	-0.81	1.00				
LL	0.32	0.17	1.00			
PL	-0.41	0.55	0.48	1.00		
PI	-0.15	0.36	0.94	0.49	1.00	
VC %	0.06	0.28	0.87	0.46	0.80	1.00

Poor correlations existed between geotechnical index properties as functions of increasing depths below ground surface, but high correlations were noted for some index properties when grouped by 5-ft depth intervals. Natural water content was a fairly good inverse indicator of dry density ($R = -0.81$) and LL was the best indicator for VC ($R = 0.87$) when grouped by increasing depth. For example, the non-linear regression equation ($R^2 = 0.90$) predicting VC as a function of LL and depth below ground surface at Site 1928, hole 5 was:

$$VC\% = 17.22 - 0.42(\text{Depth, ft}) + 1.52(LL\%) \quad (11)$$

Or, knowing the LL% enabled estimation of the VC% at this borehole as:

$$VC\% = -5.19 + 1.63(LL\%) \quad (R^2 = 0.91) \quad (12)$$

Site 1936

This site's hole 1 data included XRD mineralogy only (i.e. no geotechnical test results), as shown in **Figure 31**.

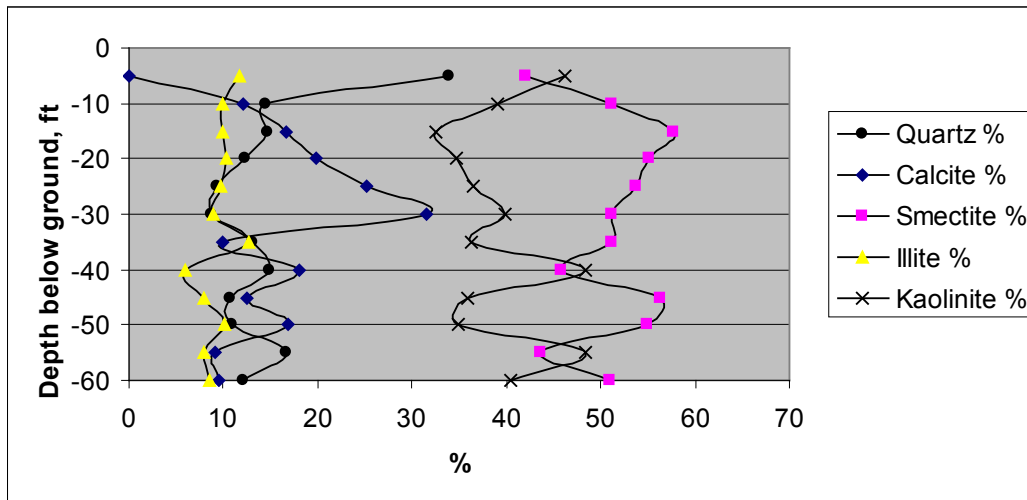


Figure 31. Mineralogy of Site 1936, hole 1, weathered plus unweathered Yazoo clay samples.

Some observations from these results were:

- Non-Yazoo clay soil was noted above -10 ft based on the high quartz content. Below that depth the smectite content increased inversely with the kaolinite content.
- High-calcite content was seen at -30 ft.
- Mineralogical weathering based on kaolinite content was indicated at -40 ft and -55 ft, but visual classification indicated unweathered samples only below 35 ft.

Site 1831

This site's hole 4 data are plotted in **Figures 32** and **33**. Samples were collected between the depths of 30 ft to 50 ft below ground surface, primarily in the visually unweathered (blue clay) zone. The -45 ft sample was visually identified as weathered (yellow).

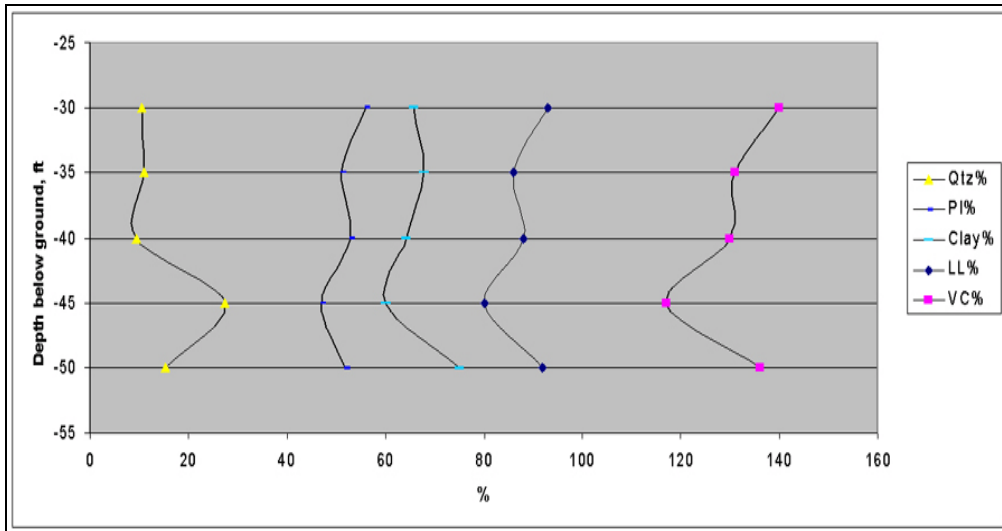


Figure 32. VC % , LL % , and PI % for Site 1831, hole 4, Yazoo clay samples.

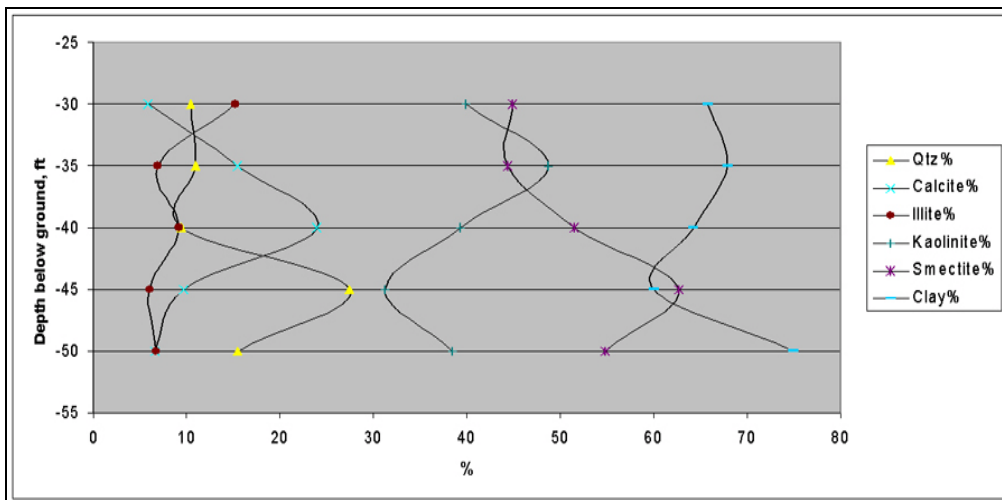


Figure 33. Mineralogy of Site 1831, hole 4, Yazoo clay samples.

Some observations from Site 1831, hole 4 results were:

- The parameters were not consistent with respect to depth below ground surface. There were very poor correlations to depth. There were variations exhibited at different depth intervals, such as those seen at 35 and 45 ft below ground surface. The depths above 30 ft probably contain the most relevant information, but sample data was not available in that region.

- Liquid Limit (LL) and volume change percentage (VC) were the two most closely-related parameters (correlation coefficient $R = 0.97$). Plasticity Index (PI) and VC were slightly less ($R = 0.92$).
- Quartz content and VC were inversely related ($R = -0.80$).
- Smectite content and VC were inversely related ($R = -0.76$).
- Smectite and kaolinite were closely inversely related ($R = -0.87$). Smectite increased with depth in the unweathered zone, as kaolinite decreased.
- The yellow sample at -45 ft had the highest smectite, lowest kaolinite, and lowest VC compared to the blue samples. The low VC value should be suspect, but the quartz content was unusually high (28%) at that depth, indicating a sandy-clay layer. A sandy material would have the lower VC value.

The non-linear regression equation ($R^2 = 0.98$) predicting VC as a function of LL and depth below ground surface at Site 1831, hole 4 was:

$$VC\% = 1.95 + 0.19(\text{Depth, ft}) + 1.55(LL\%) \quad (13)$$

Or, knowing only the LL enabled estimation of the VC at this borehole as:

$$VC\% = -11.88 + 1.63(LL\%) \quad (R^2 = 0.95) \quad (14)$$

Site 2531

This site's hole 1 data is plotted in **Figures 34** and **35**. Samples were collected between the depths of 10 ft to 60 ft below ground surface.

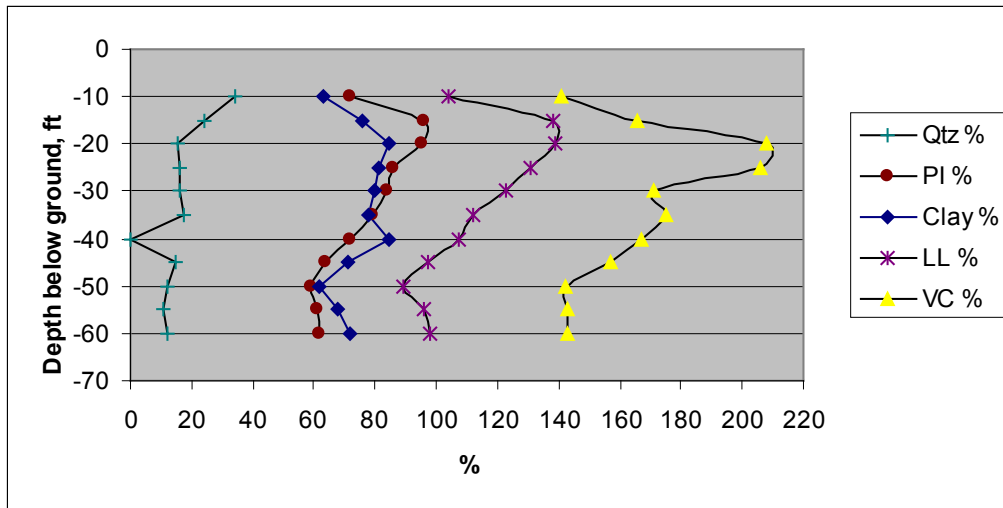


Figure 34. VC %, LL %, and PI % for Site 2531, hole 1, weathered plus unweathered Yazoo clay samples.

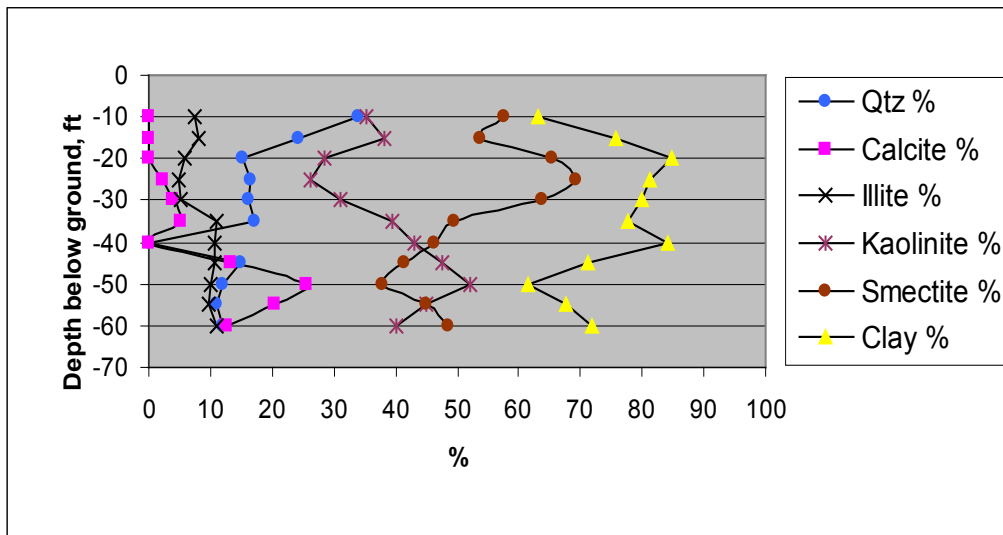


Figure 35. Mineralogy for Site 2531, hole 1, weathered plus unweathered Yazoo clay samples.

Some observations from Site 2531, hole 1 results were:

- The parameters were not consistent with respect to depth below ground surface. There were very poor correlations to depth, but there were variations exhibited at different depth intervals, such as those seen at 20, 40, and 50 ft below ground surface. The highest

VC was found at the 20-25 ft depth, where the highest smectite content was also found.

- Liquid Limit (LL) and shrinkage volume change percentage (VC) were the two most closely-related parameters (correlation coefficient $R = 0.82$). Plasticity Index (PI) and VC were slightly less ($R = 0.78$).
- No mineralogy constituents correlated well, except for smectite and kaolinite which were closely inversely related ($R = -0.99$). If their relative proportions are indicative of weathering, then it appears the unweathered zone is about 40 ft to 45 ft below ground surface. These data question the validity of visual identification of weathering since the visually-weathered (yellow) samples had much higher smectite percentages than the visually-unweathered (blue) samples. These data show that, although the most expansive upper zone contains higher amounts of smectite, it is actually less weathered from a mineralogy perspective. Non-expansive kaolinite is usually the end product of mineralogical weathering.

The non-linear regression equation ($R^2 = 0.70$) predicting VC as a function of LL and depth below ground surface at Site 2531, hole 1 was:

$$VC\% = -0.5 - 0.37(\text{Depth, ft}) + 1.36(LL\%) \quad (15)$$

Or, knowing the LL enabled estimation of the VC at this borehole as:

$$VC\% = 41.17 + 1.1(LL\%) \quad (R^2 = 0.67) \quad (16)$$

Site 1931

This site's hole 1 data is plotted in **Figures 36** and **37**. Samples were collected between depths of 5 ft to 70 ft below ground surface. Some observations from Site 1931, hole 1 were:

- The parameters were not consistent with respect to depth below ground surface. There were very poor correlations to depth, but there were variations exhibited at different depth intervals, such as those seen at 15, 20, 30 and 35 ft below ground surface. Below 40 ft the data points were more uniform. The highest VC was found at

the 40 ft depth, but the highest smectite contents were found at -15 ft and -30 ft.

- Liquid Limit (LL) and shrinkage volume change percentage (VC) were the two most closely-related parameters (correlation coefficient $R = 0.82$). Plasticity Index (PI) and VC were slightly less ($R = 0.78$).
- No mineralogy constituents correlated well, except for smectite and kaolinite which were closely inversely related ($R = -0.97$). Yellow samples were observed above 30 ft and below that depth the samples were visually unweathered (blue). The true weathered zone appeared to be above -15 ft, where kaolinite predominated. The high quartz content in this zone also indicated true weathering, or else the presence of a non-Yazoo clay layer.

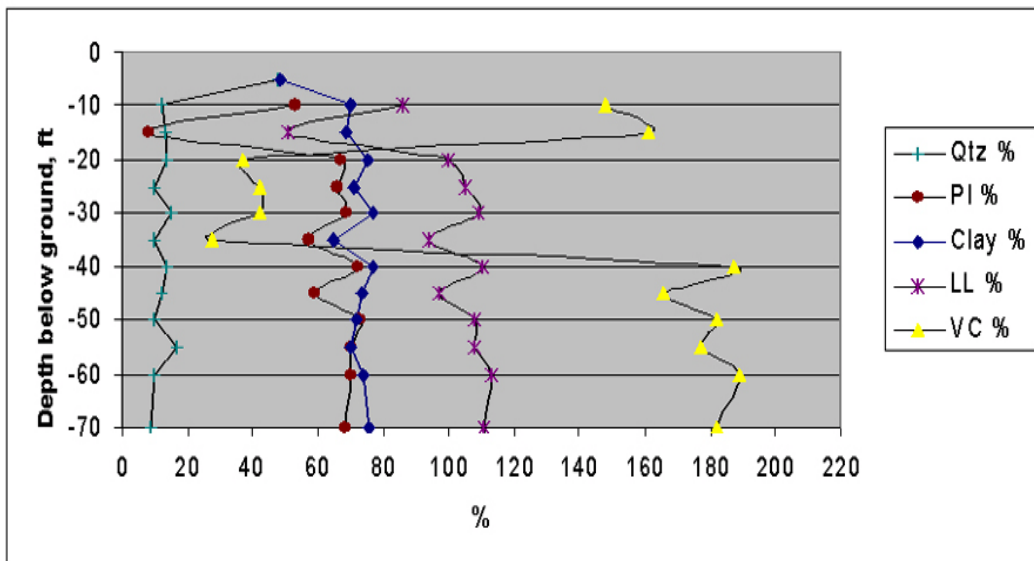


Figure 36. VC % , LL % , and PI % for Site 1931, hole 1, weathered plus unweathered Yazoo clay samples.

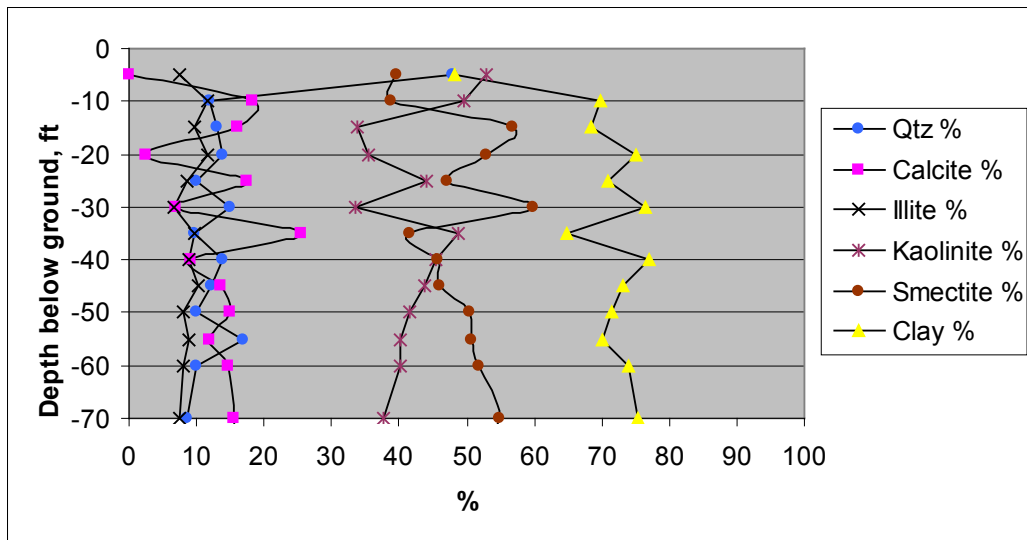


Figure 37. Mineralogy of Site 1931, hole 1, weathered plus unweathered Yazoo clay samples.

Site 1932

This site's hole 1 data is plotted in **Figures 38** and **39**. Samples were collected between depths of 5 ft to 70 ft below ground surface.

Some observations from Site 1932, hole 1 were:

- The parameters were not consistent with respect to depth below ground surface. There were very poor correlations to depth, but there were similar patterns exhibited at different depth intervals, such as those seen at 15, 20, 25, 35, and 50 ft below ground surface. The highest VC was found at the 50 ft depth; the highest smectite content was found at -20 ft.
- Liquid Limit (LL) and shrinkage volume change percentage (VC) are the two most closely-related parameters (correlation coefficient $R = 0.79$). Plasticity Index (PI) and VC are slightly less ($R = 0.78$).
- No mineralogy constituents correlate well, except for smectite and kaolinite which are closely inversely related ($R = -0.98$). If their proportions were indicative of weathering, then it appeared the unweathered zones were about 5 ft and 30-40 ft below ground surface. Yellow samples were taken in the depths above -35 ft.

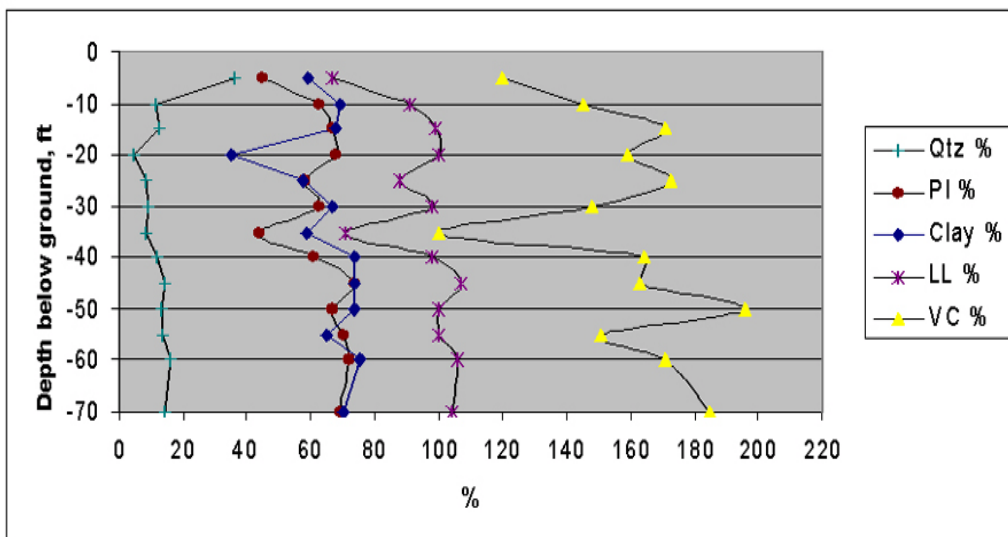


Figure 38. VC %, LL %, and PI % for Site 1932, hole 1, weathered plus unweathered Yazoo clay samples.

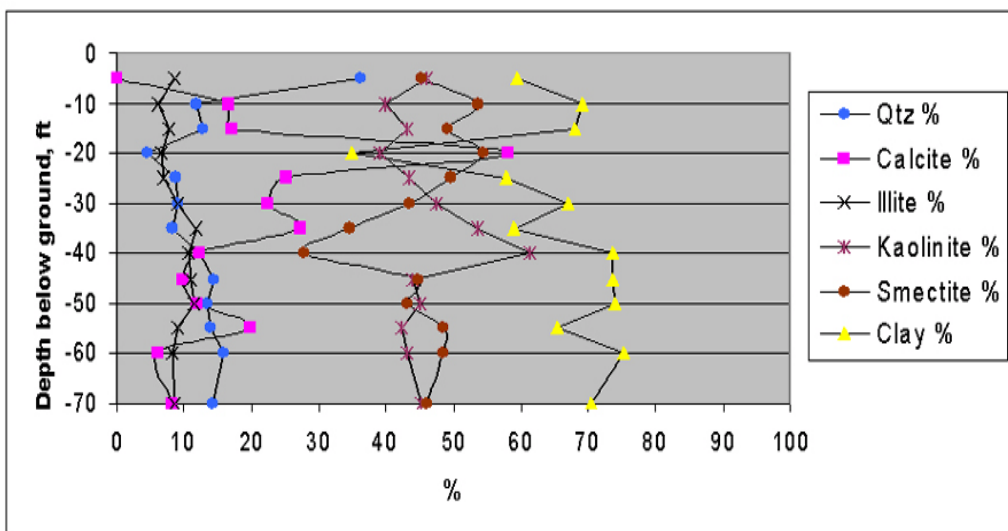


Figure 39. Mineralogy of Site 1932, hole 1, weathered plus unweathered Yazoo clay samples.

Site 1937

This site’s hole 1 data also included XRD results (**Figures 40 and 41**). Samples were collected between depths of 10 ft to 70 ft below ground surface.

Some observations from Site 1937, hole 1 were:

- The parameters were not consistent with respect to depth below ground surface, but were more uniform compared to other sites. There were very poor correlations to depth, but there were variations exhibited at different depth intervals, such as those seen at 40 ft below ground surface. The lowest VC was found at the 40 ft depth, where the smectite content was very high.
- There were poor correlations between LL, PL, PI and VC.
- No mineralogy constituents correlated well, except for smectite and kaolinite which were closely inversely related ($R = -0.97$). If their proportions are indicative of weathering, then it appeared the unweathered zone extended to -12 ft. Below that depth the smectite content was much higher than that of kaolinite.

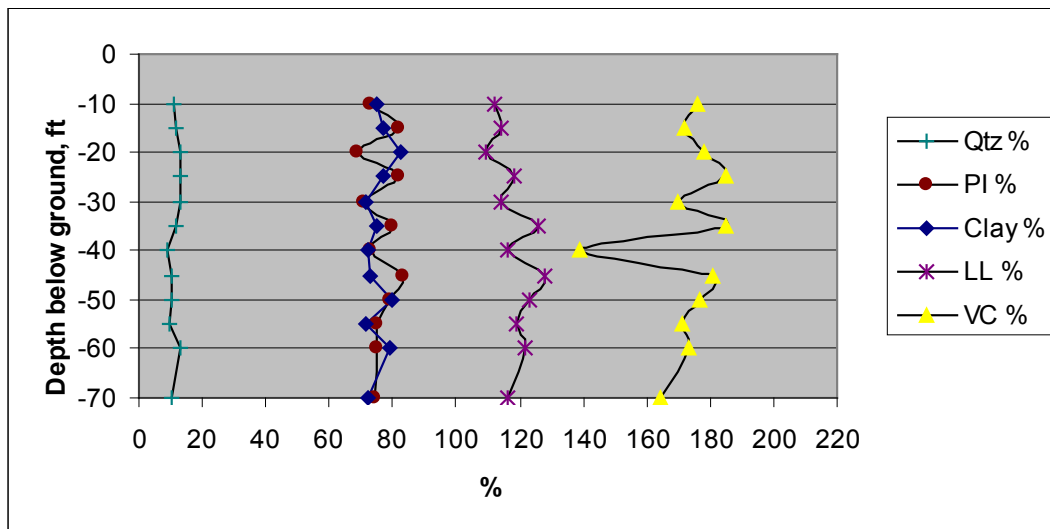


Figure 40. VC % , LL % , and PI % for Site 1937, hole 1, weathered plus unweathered Yazoo clay samples.

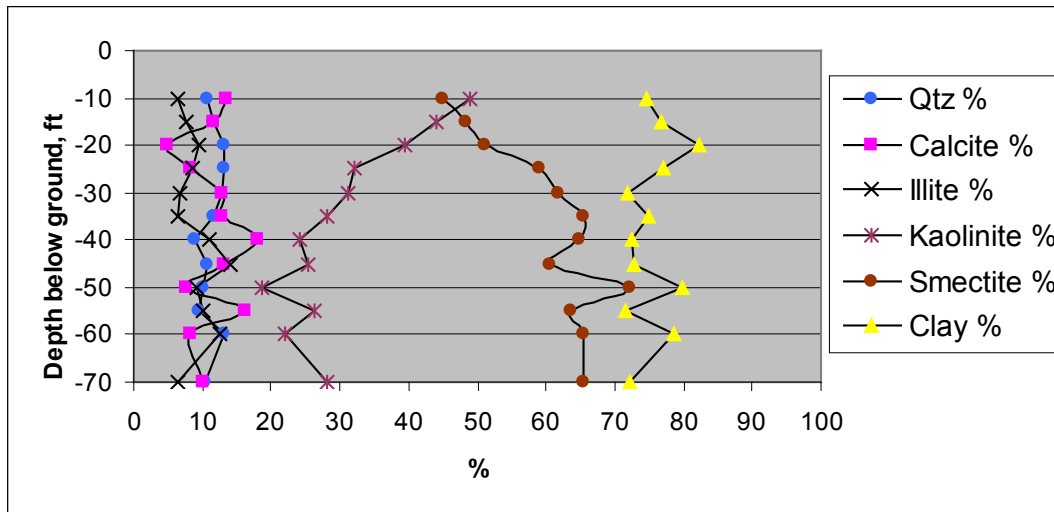


Figure 41. Mineralogy of Site 1937, hole 1, weathered plus unweathered Yazoo clay samples.

Site 2558

This site's hole 1 data also included XRD results (**Figures 42 and 43**). Samples were collected between depths of 5 ft to 70 ft below ground surface.

Some observations from Site 2558, hole 1 were:

- The parameters were not consistent with respect to depth below ground surface. There were very poor correlations to depth, but there were variations exhibited at different depth intervals, such as those above -30 ft. The highest VC was found at the 30 ft depth and the highest smectite content was found at the 25 ft depth.
- Liquid Limit (LL) and shrinkage volume change percentage (VC) were exceptionally correlated (correlation coefficient $R = 1$). Plasticity Index (PI) and VC were slightly less ($R = 0.98$).
- Smectite and kaolinite were closely inversely related ($R = -0.87$). If their proportions were indicative of weathering, then it appeared the unweathered zone extended to -20 ft. Below that depth the smectite content was higher (except at -40 ft where they equaled each other). The high quartz content above -20 ft indicated true weathering, presence of a non-Yazoo layer, or both.

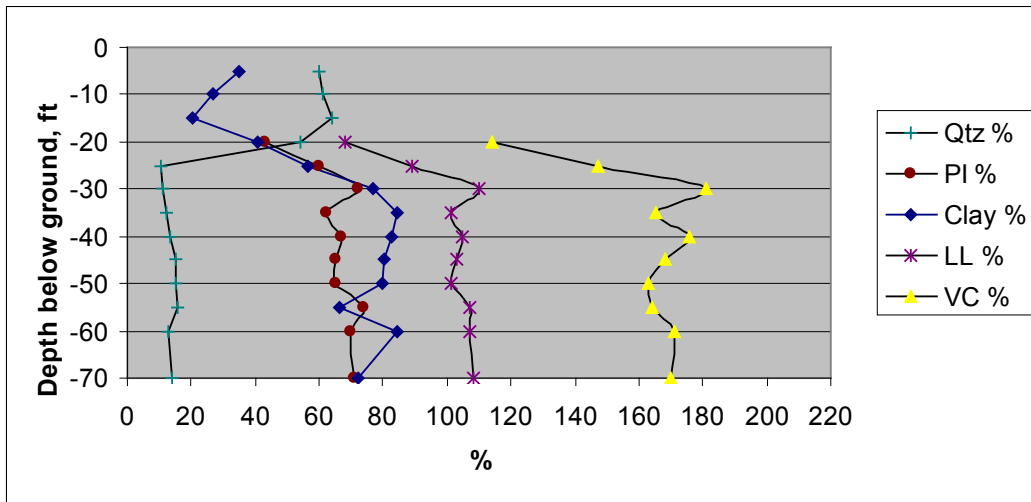


Figure 42. VC % , LL % , and PI % for Site 2558, hole 1, weathered plus unweathered Yazoo clay samples.

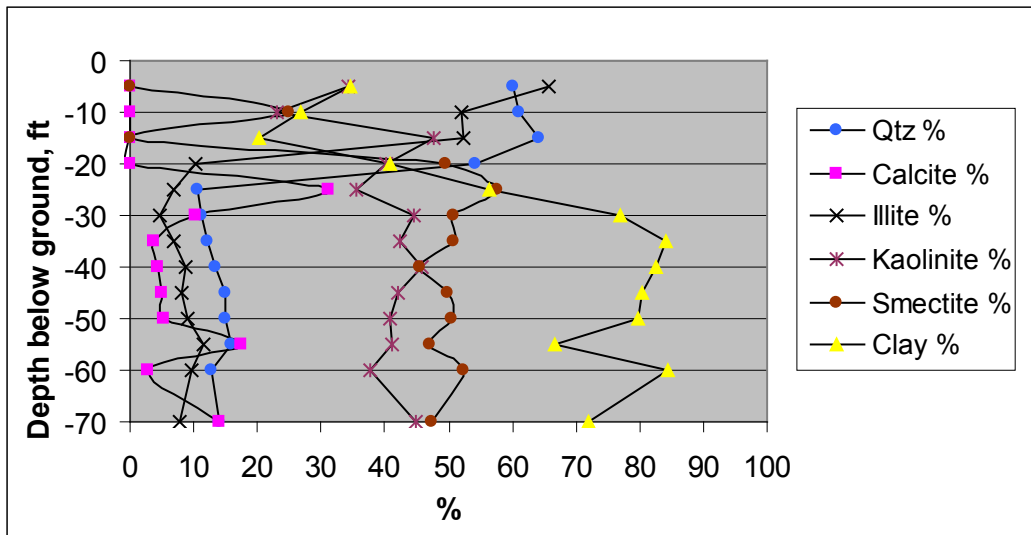


Figure 43. Mineralogy of Site 2558, hole 1, weathered plus unweathered Yazoo clay samples.

Site 2560

This site's hole 1 data are plotted in **Figure 44**. The hole 2 data are shown in **Figure 45**. XRD tests were run on samples from -5 to -70 ft, but geotechnical data were available only for depths below about -25 ft.

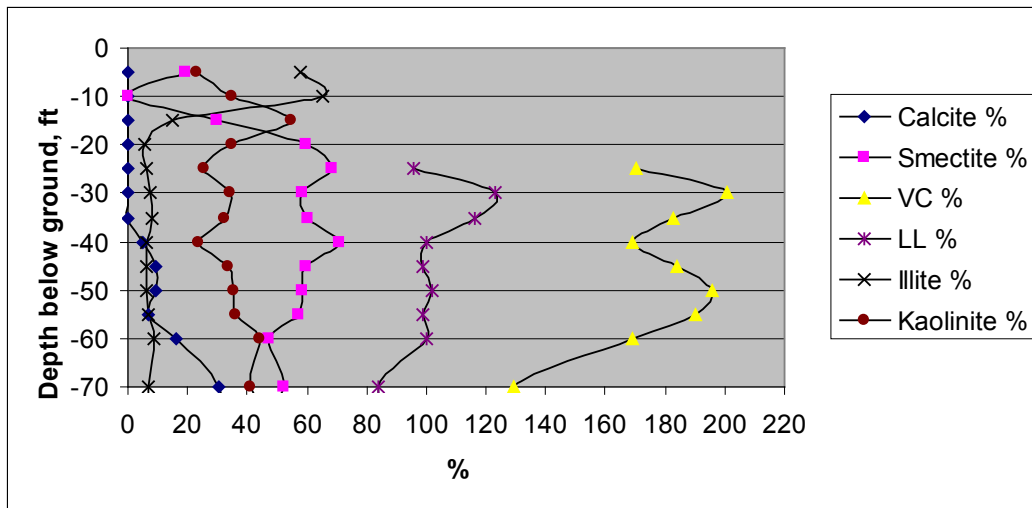


Figure 44. Mineralogy of Site 2560, hole 1, weathered plus unweathered Yazoo clay samples.

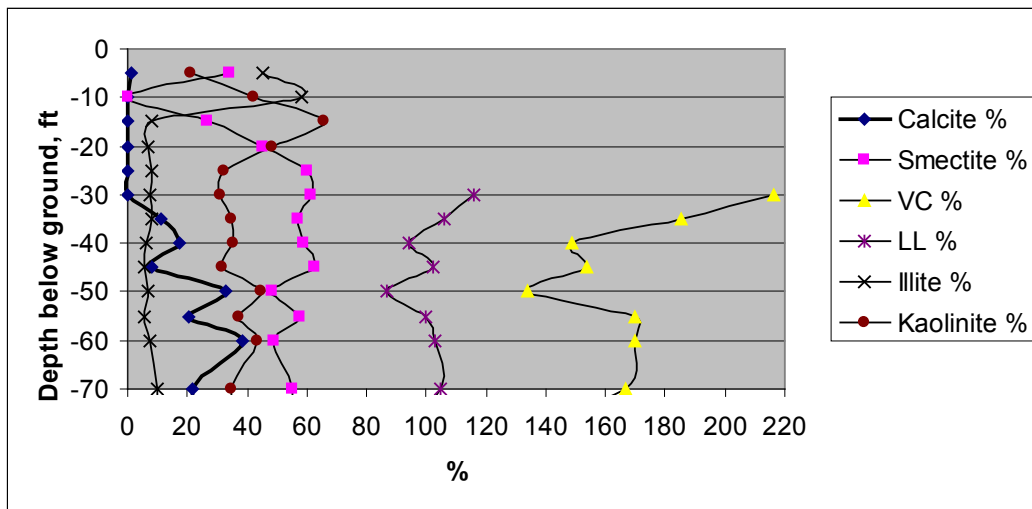


Figure 45. Mineralogy of Site 2560, hole 2, weathered plus unweathered Yazoo clay samples.

Some observations from Site 2560, holes 1 and 2, were:

- Typical non-uniformity of parameters with depth, and poor correlations to depth. Although both holes were at the same site (approximately 100 ft apart at the same ground elevation), their sampled properties varied quite a bit. Both holes exhibited a notable mineralogy change at approximately 15 – 20 ft depth.
- Geotechnical data for hole 1 correlated poorly. Hole 2 data correlated much better; the best correlation was LL to VC (R=0.96).

- Although both holes were at approximately equal surface elevations, visually-weathered samples were observed to -30 ft in hole 1 and -35 ft in hole 2. The smectite-kaolinite crossover point occurred at -15 ft in hole 1 and -20 ft in hole 2. The mineralogy changes to -20 ft are also observed from the ternary plot, **Figure 46**. These depth differences indicated non-horizontal soil layering from hole 1 to hole 2. The mineralogy differences illustrated the discrepancy between visual and mineralogy classifications when characterizing soil weathering.

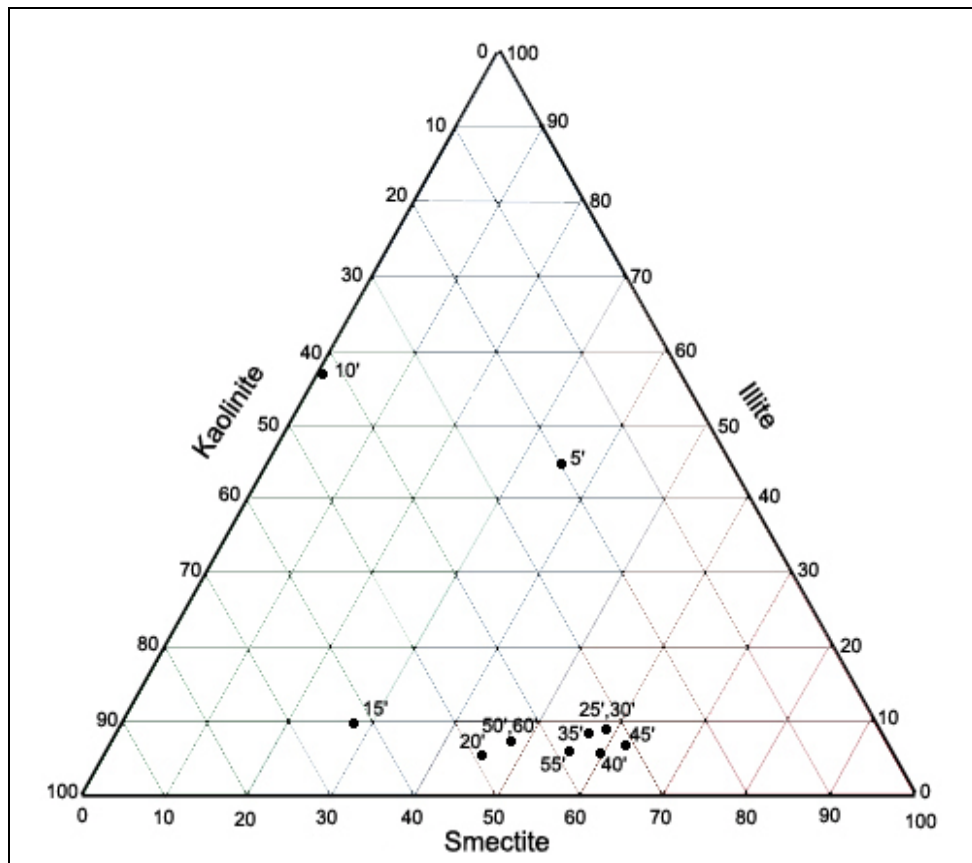


Figure 46. Ternary diagram of clay-fraction components at Site 2560, hole 2, labeled by depth, ft (i.e. 5' = 5 ft).

Synopsis of Site-specific correlations

Mineralogy XRD results in addition to geotechnical properties were obtained at the sites listed in **Table 9**. Data were collected between the depths of -5 ft to -80 ft, but the correlations are shown only for data from

depths to approximately 50 ft below ground surface to capture any useful near-surface correlations. The correlations differ from those listed in the site-specific data due to truncating at the 50 ft depth. The data resolution was based on 5-ft depth intervals and a limited number of tests (i.e. sample sizes of four to five per hole), but some general observations were noted.

Table 9. Correlation coefficients of site-specific geotechnical property and XRD mineral content percentages for weathered and unweathered Yazoo clay samples. Samples were obtained from relatively shallow depths (less than approximately 50 ft below ground surface) at approximately 5-ft depth intervals. Highest correlations are highlighted.

Site (Hole)	Clay % to LL	LL to VC	PI to VC	Smectite to VC	Smectite to PI	Smectite to LL	Smectite to PL	Quartz to VC	Calcite to VC	Clay to VC	Kaolinite to VC	Smectite to Kaolinite
1831 (4)	0.69	0.97	0.92	-0.76	-0.76	-0.60	-0.25	-0.80	-0.23	0.67	0.53	-0.87
1889 (1)	0.99	0.84	0.76	-0.38	-0.87	-0.82	-0.20	0.96	-0.99	0.97	0.25	-0.99
1931 (1)	0.55	-0.22	-0.21	-0.16	-0.20	-0.12	0.51	0.02	0.03	0.13	0.16	-0.97
1932 (1)	0.33	0.79	0.78	0.21	0.35	0.16	-0.30	-0.29	0.01	0.26	-0.24	-0.98
1933 (1)	0.62	0.74	0.36	0.46	-0.18	-0.05	0.17	0.11	-0.78	-0.12	-0.66	-0.90
1937 (1)	0.00	0.30	0.42	-0.13	0.21	0.66	0.70	0.63	-0.64	0.38	0.17	-0.97
2531 (1)	0.69	0.78	0.72	0.72	0.72	0.80	0.81	-0.22	-0.48	0.83	-0.74	-0.99
2556 (1)	0.91	-0.36	-0.17	0.10	0.14	0.50	0.29	0.27	-0.18	-0.05	-0.12	-1.00
2558 (1)	0.86	1.00	0.98	-0.26	-0.10	-0.22	-0.41	-0.87	0.00	0.92	0.60	-0.87
2560 (1)	0.00	0.57	0.13	-0.89	0.08	-0.41	-0.65	-0.01	0.17	-0.09	0.88	-0.99
2560 (2)	0.95	0.96	0.96	0.53	0.74	0.72	0.70	0.91	-0.84	0.83	-0.66	-0.98
Mean R=	0.60	0.58	0.51	-0.05	0.01	0.06	0.12	0.06	-0.36	0.43	0.01	-0.96

Some observations were:

- The only consistent correlation for all sites was that the kaolinite content decreased as the smectite content increased, i.e. there was a very strong inverse relationship between smectite and kaolinite percentages. Typically the highest kaolinite contents were found above an approximate -10 ft to -15 ft depth, coinciding with higher quartz and lower VC percentages.

- LL, instead of PI, was better correlated to VC. This implied that the simpler LL test may be more useful for predicting VC, without performing the follow-on PL test and obtaining a PI value.
- The Atterberg Limits were positively related to the mineralogy (clay % and smectite %), but their relative correlations varied quite a bit and were site-specific.
- There was a discrepancy between visual and mineralogical indicators of weathering. The near-surface zone (to about -15 ft depth) appeared to be more weathered based on its high quartz content, high kaolinite content, and low VC. Otherwise the near-surface zone could be considered to be composed of different soil types such as alluvium or colluvium. Visual descriptors of “weathering” are not synonymous with “mineralogical stability”; as clay weathers it assumedly becomes more kaolinitic, less expansive, and thus more stable. Based on these data, the weathering process is not limited to the near-surface zone. Deep fissures, joints, or cracks may serve as preferential flow paths for ground- or surface-water. To compound the complexity and mystery of these observations, diagenetic (mineral transformation) processes may be occurring at different depths.
- Due to the high parameter variability with depth, analyzing 5-ft depth interval data points did not provide many statistically-robust answers. Site-specific data should be obtained if a high degree of confidence in either the geotechnical or mineralogy parameters is desired. Numerous non-uniform soil parameters were noted, indicating that Yazoo clay is not a uniformly identified or characterized soil.

3 Yazoo Clay Sampling and Testing (State Study 236)

MDoT Drilling and Testing Program

MDoT provided Yazoo clay samples for the laboratory testing tasked in State Study 236. Per the Memorandum of Understanding between MDoT and ERDC, two immediately-adjacent boreholes were drilled. Continuous-core soil samples from the respective boreholes were retrieved, sealed, and transported to the MDoT and ERDC soils labs for testing.

Borehole Sampling

The WES test site was re-discovered during preparation for this study, and it was selected as the location for the soil borings conducted by MDoT for this study. The site, located within a 600-acre property donated by WES to Mississippi College in the 1970's (**Figures 47 and 48**), was characterized and extensively instrumented in 1968. It was then abandoned and became overgrown with pine trees and upland hardwood vegetation. Much of the instrumentation (piezometers, heave plugs, access tubes, and a permanent benchmark) has survived, and the borehole data are referenced in this study.

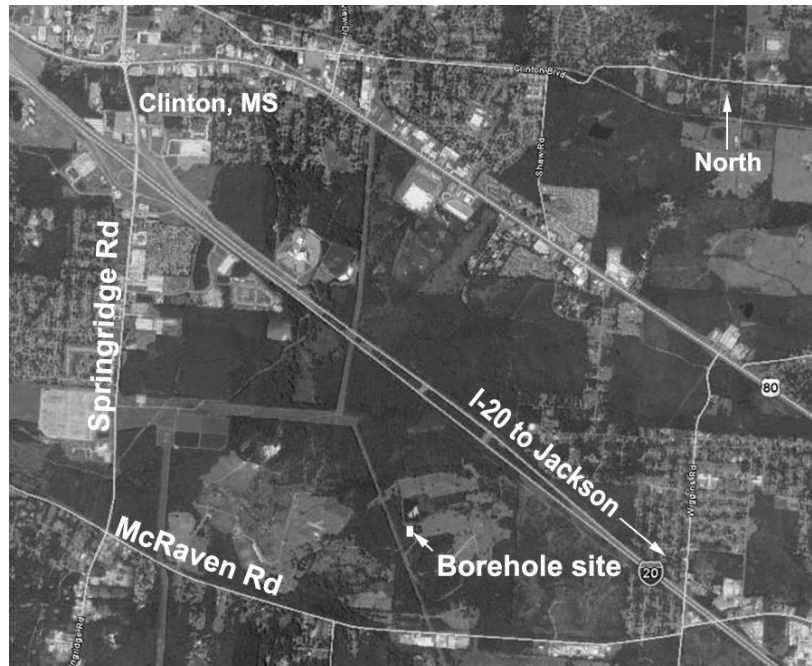


Figure 47. Vicinity location map



Figure 48. MDot borehole site next to the original WES Yazoo clay study site.

The 2 adjacent boreholes (6-ft lateral spacing) were located as closely as possible to the former WES study site. The selected location is shown in **Figure 49**.

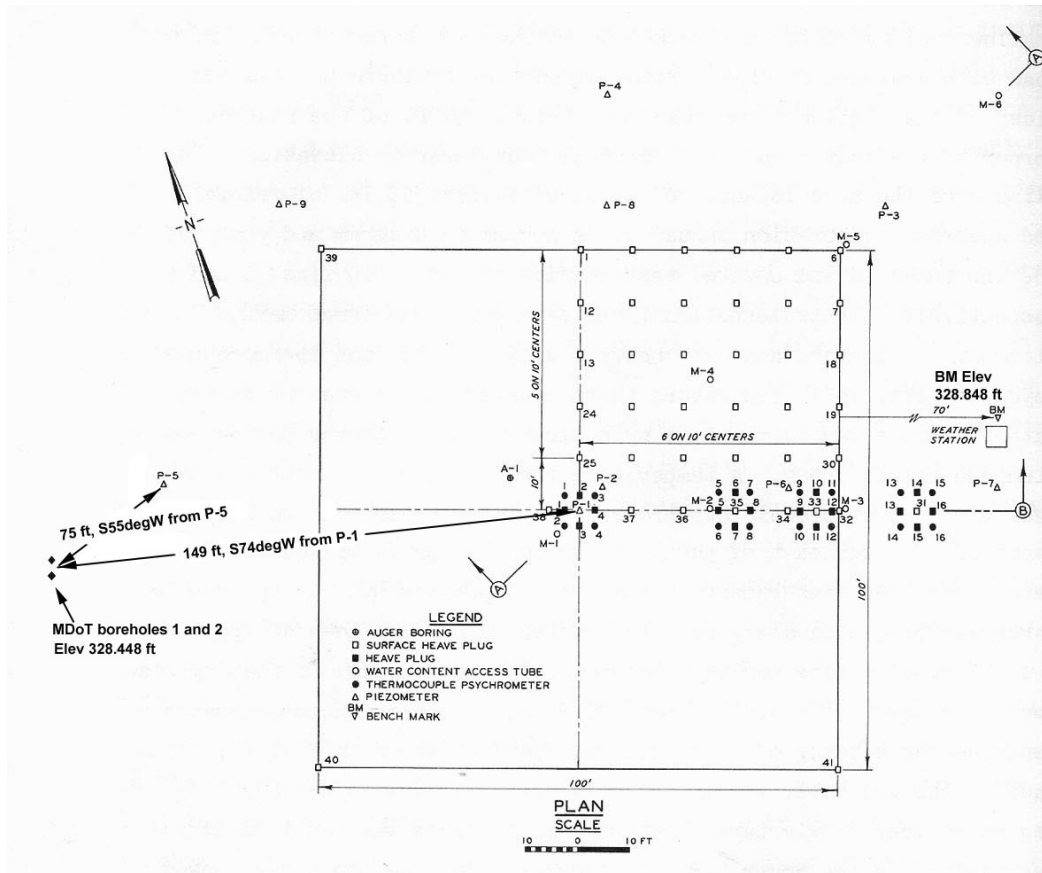


Figure 49. MDoT borehole locations west of existing piezometer P-5

The MDoT rotary drill rig set up at the site and performed continuous Shelby-tube sampling per their well-established procedures. After Hole 1 was drilled and sealed, the rig moved 6 feet and drilled Hole 2. The intent was to obtain borehole samples that were as identical as possible to each other, to include the entire soil profile from the weathered zone (yellow clay) into the unweathered zone (blue clay). The drill bit and recirculation mud reamed out the borehole prior to advancing the 2-ft long Shelby tube sampler. The sampler retrieved continuous “undisturbed” soil samples in the interval between about 3 ft to 33 ft below ground surface. **Figures 50** through **53** show the drill rig setup and operation.

The first borehole (Hole 1) yielded undisturbed soil samples that were initially sent to the MDoT soils lab. Hole 2 samples were tested in the ERDC

soils research lab located on the first floor of the Geotechnical and Structures building 3396.



Figure 50. MDot borehole site at edge of power line clearing east of the former WES study site. View toward northeast.



Figure 51. MDot rotary drill rig with Shelby tube sampler



Figure 52. Shelby tube removed from the drill string, ready for core extrusion



Figure 53. Hydraulically-extruded core sample from the upper Yazoo clay

After the core sample was hydraulically extruded, it was carried to the sample preparation area where it was logged and trimmed into sections (**Figures 54** and **55**). The retrieved core length varied, but was typically around 21 inches. The upper 3 inches or so was trimmed and placed in a sealed glass jar, and the remainder of the core was trimmed into two 6-in lengths and placed in separate waxed mold cylinders. Thus a jar sample, an upper 6-in sample, and a lower 6-in sample were preserved from each logged 2-ft Shelby tube depth interval, as diagrammed in **Figure 56**.



Figure 54. Extruded core (21- to 24-in long) placed on a shaded flat surface, ready for trimming and waxing



Figure 55. Trimming an upper sample from a yellow (weathered) clay core prior to waxing

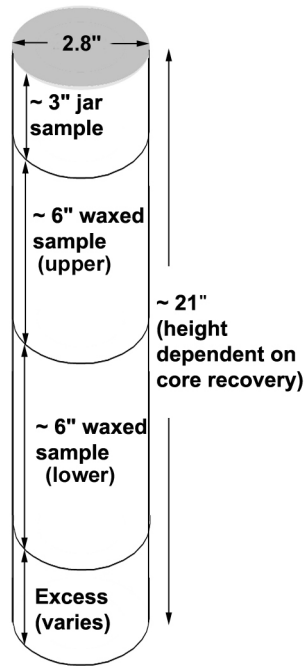


Figure 56. Diagram of core samples within each 2-ft depth interval preserved for MDoT and ERDC lab testing

Although the two boreholes were laterally spaced 6ft apart, the core samples retrieved from the same depth intervals between boreholes were not always visually the same. For example, the first borehole at 28 ft-depth advanced through blue clay while the second borehole advanced through blue clay at 23 ft-depth. This 5-ft elevation difference illustrated the lateral variability of Yazoo clay. The abrupt visual difference between yellow and blue clay was easily distinguished, as seen in **Figure 57**. Other visual heterogeneity (anomalies) occurred in the lower depths, as shown and discussed later in this report.



Figure 57. Extruded core sample showing the abrupt boundary between the yellow “weathered” (upper) and the blue “unweathered” (lower) Yazoo clay

MDot Lab Testing

MDot sampling and testing procedures for expansive soils are based on the following AASHTO standards:

- T-11 (Materials finer than 75um (No. 200) sieve in mineral aggregates by washing)
- T-27 (Sieve analysis of fine and coarse aggregates)

- T-87 (Dry preparation of disturbed soil and soil aggregate samples for testing)
- T-88 (Particle size analysis of soils (with MT-23 Methods for Testing Soils))
- T-89 (Determination of the liquid limit of soils)
- T-90 (Determining the Plastic Limit and Plasticity Index of soils)
- T-92 (Determining the shrinkage factor of soils)

MDoT uses AASHTO Designation T-89 and T-90 as its test standards for LL and PI, respectively. These standards are essentially the same as the ASTM D4318 standard for Atterberg limits. AASHTO T-92 is essentially the same as ASTM D427, Mercury Method, although the Mercury Method was recently removed as a standard. It was replaced with ASTM D4943, Wax Method.

Laboratory Sample Preparation

The waxed cylinders from Hole 1 were brought to the MDoT Soils Lab for testing. Each cylinder was unwrapped, weighed, and its soil volume was measured with a digital caliper to obtain the wet density. The core was cut in two and a moisture content sample was scooped from the center. The remainder was placed in a sealed plastic bag and a sealed glass jar.

The jar sample (at its natural water content) was shaved with a rotary cheese grater and distilled water was added to bring it to near its estimated LL. The LL and PL tests were then conducted. The remaining LL paste was placed into a tare for the shrinkage limit (SL) and volume change (VC) test. For blended-soil mix testing (i.e. for road sub-base courses and pavement projects) the jar sample is normally air-dried, shaved, and passed through the #40 sieve. A portion of the air-dried sample then goes to the Atterberg tests and the remainder goes to the VC test. The LL and PL samples were not air-dried for this study. The samples were tested from their natural water content state. The samples for the specific gravity and hydrometer tests were oven-dried. Those tests were conducted using the standard methods. **Figure 58** illustrates the tests performed on the MDoT samples.

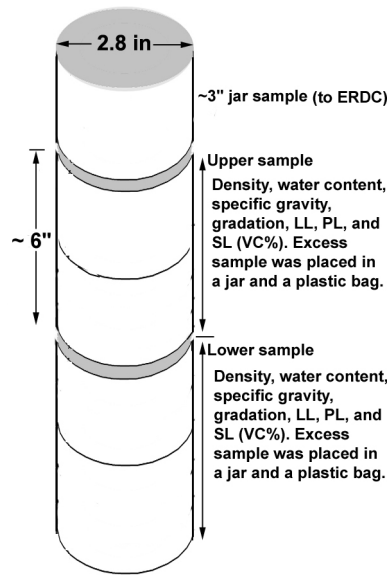


Figure 58. Upper and lower undisturbed sample testing performed at the MDoT lab

Shrinkage and Volume Change

MDoT's test method defining volume change percent (VC %) follows AASHTO T-92 (ASTM D427/D4943) which is the standard method for determining the Atterberg shrinkage limit. The ASTM D427 mercury method is no longer an ASTM standard. It was replaced with ASTM D4943 (Wax Method) in 2008, due to the hazardous nature of working with mercury.

Either the hot-dip wax or an aerosol spray wax (manufactured by Interflon B.V.) coated the oven-dried VC% specimen, prior to water bath immersion to determine its buoyant weight. Lab VC% results have been observed to indicate an approximate difference of +15% for either wax method, compared to the old mercury method. MDoT is gathering data to investigate this difference between the old mercury method, the new wax method, and the modified (spray wax) method.

AASHTO T-92 defines the SL as "the maximum calculated water content at which a reduction in water content will not cause a decrease in the soil volume", and it is calculated as:

$$SL = (V_w - \Delta V) \div W_s \quad (17)$$

Where

SL = shrinkage limit (multiply by 100 to obtain percentage, %)

V_w = volume of water in wet soil (assumed to equal the weight of water in wet soil)

ΔV = change in volume from the wet- to oven-dried soil

W_s = weight of oven-dried soil

Or,

$$SL = \omega - (\Delta V \div W_s) \times 100 \quad (18)$$

Where

SL = shrinkage limit, %

ω = water content of wet soil, in percentage of oven-dried soil weight. Per the test standard, the initial wet soil water content is at or within 10% of its LL.

The VC % (or volumetric shrinkage percentage) is determined using the calculated SL as:

$$VC = (\omega - SL)R \quad (19)$$

Where

ω = a given gravimetric water content, %. Per the test standard, the initial wet soil water content is at or within 10% of its LL.

SL = shrinkage limit % calculated from the test results

R = shrinkage ratio calculated from the test results, or

$$R = M_s / (V_s)(1g / cc) \quad (20)$$

Or

$$VC = ((V_w + \Delta V) \div V_s) \times 100 \quad (21)$$

Where

VC = volumetric shrinkage percentage, or volumetric change percentage

V_s = volume of oven-dried soil

Thus the SL and VC use the oven-dried soil weight and volume, respectively, as their denominator (i.e. they are relative to the final oven-dried soil instead of the initial wet soil weight and volume).

ERDC Testing Program

Tables 10 and **11** list the standardized and non-standardized test methods, respectively, initially considered for inclusion in the ERDC testing program.

Table 10. Standardized Test Methods.

Test	Standard
Atterberg limits	ASTM D4318, AASHTO T-87 thru T-92
Dis-aggregated Liquid Limits	USACE EM-1906, TxDot 101-E
Calcium carbonate	ASTM D4373
Emerson Crumb test	ASTM D6572
Swell tests (oedometer)	ASTM D4546, AASHTO T-258
Shrinkage test (wax method)	ASTM D4943
Expansion Index	ASTM D4829
Clod Test	ASTM D7263
Methylene Blue Index	ASTM C837, AASHTO T-330-07
Sulfates	ASTM D1580, AASHTO T-290, TxDot 145-E
Chlorides	AASHTO T-291-94
Suction (filter paper)	ASTM D5298, AASHTO T-273
Shrinkage Volume Change	AASHTO T-92
Field moisture equivalent	AASHTO T-93
Slake time	TxDot 102-E
COLE	USDA-NRCS NSSH Part 618
Linear shrinkage	TxDot 107-E, BS 1377 Part 2

Test	Standard
Potential Volume Change (PVC)	FHA 4075.15
Free Swell Index	Indian Standard Code IS:2720 Part 40
Fall cone LL	British Standard BS 1377 Part 2, ISO TS 17892-12
Australian Soil Reactivity Tests	AS 1289, Methods 7.1.1, 7.1.2, and 7.1.3

Table 11. Non-standardized Test Methods.

Test (Published Reference)
Qualitative tests (color, consistency, dry strength, structure, slaking) (Heley and MacIver 1971)
Fall cone PL (Lee and Freeman 2009)
Free Swell Test (Holtz and Gibbs 1954)
Modified Free Swell (Sivapullaiah et al. 1987)
Ring Shrinkage (Hanafy 1998)
iButton suction (Albrecht, Benson, and Beuermann 2003)
W 24/72 (Erguler and Ulusay 2003a)
Clod shrinkage (Krosley et al. 2003)
Equilibrium water content (SAMC) (Yao et al. 2004)
Saturation water content (Kariuki and van der Meer 2004)

Qualitative Classification

The first step in examining and testing the intact soil samples was to qualitatively describe the soil without using specialized equipment.

Color and Consistency

The visual color at its natural water content was described for the continuous portions of the sample, using the Munsell soil color chart. The consistency was determined by hand or with a pocket penetrometer for:

- An intact piece at its natural water content
- The same piece after thorough remolding without reducing its water content

Comparing these values was a measure of the material's sensitivity. Textbook descriptors of consistency (i.e. soft to very hard) were used.

Dry Strength

The crushing strength of a piece of material after it has been remolded to near its liquid limit and then air-dried is indicative of the quantity and type of clay-sized particles in the material. A high dry strength is indicative of high plasticity caused by the presence of active clay minerals (Heley and MacIver 1971). The dry strength was determined by hand-crushing the materials as follows:

- An intact piece (about 1 cc volume) at its natural water content
- A cube or ball (about 1 cc volume) remolded with distilled water to near its liquid limit
- Air-drying both materials and tested by crushing between the thumb and fingers

Comparing these values was based on using textbook descriptors for crushing strength (i.e. very low to very high).

Emerson Crumb Test

ASTM (2005) D6572 is a method to determine the dispersive characteristics of clay samples. It is an indirect method to indicate sodium cation absorptive capacity, and although not an expansive soil test, it may be useful. A natural soil clod or remolded cube (about the size of dice) is placed in a white porcelain dish filled with distilled water. The size of the deflocculated (dispersed) soil's colloidal suspension and the water turbidity are identified as one of 4 visual grades. Grade 1 is "non-dispersive", grade 2 is "intermediate", grade 3 is "dispersive", and grade 4 is "highly dispersive".

Slaking Behavior

Similar to the Emerson test, the disintegration of an intact piece upon immersion in water reflects the type of clay minerals present, the fabric of the material, and the character of the inter-particle bonds. *Slaking* is the crumbling and disintegration of clay when exposed to air or moisture.

When dried clay is water-saturated it breaks down due to progressive swelling and sloughing off of its outer layers (Heley and MacIver 1971).

Slaking behavior was indexed using the following tests:

- An intact piece (about 1cc volume) was immersed at natural water content in distilled water
- An intact piece (about 1cc volume) of air-dried material was immersed in distilled water
- The approximate volume of material which became completely disaggregated and the slaking rate were noted.

Acid Reaction

A drop of weak hydrochloric acid on air-dried samples indicated the relative presence of calcareous material. Calcareous soil will react to acid. This test also aided identification of calcite and gypsum crystals in the sample.

Quantitative Lab Tests

Hole 2 waxed cylinders and jar samples were transported from the drill site to the ERDC soil research lab for testing. The leftover MDoT lab bag and jar samples from Hole 1 were also tested at ERDC.

Test Design

Thirty-two (32) undisturbed core samples consisting of an upper 6-in and a lower 6-in sample from each 2-ft interval were retrieved for ERDC testing. Due to the number of desired tests and limited soil availability, it was necessary to treat the upper and lower 6-in samples as a one foot-long test sample (16 ea) instead of performing tests on each of the 32 separate samples. Since the 6-in samples were trimmed adjacent to each other instead of at opposing ends of the 2-ft Shelby tube core, they more accurately represented a foot-long sample taken from the center of the Shelby tube. Thus the 16 sets of tests were performed at depth intervals more closely representing nominal 2-ft spacing rather than nominal 1-ft spacing.

Figure 59 shows the approximate undisturbed core slice layout for each set of tests.

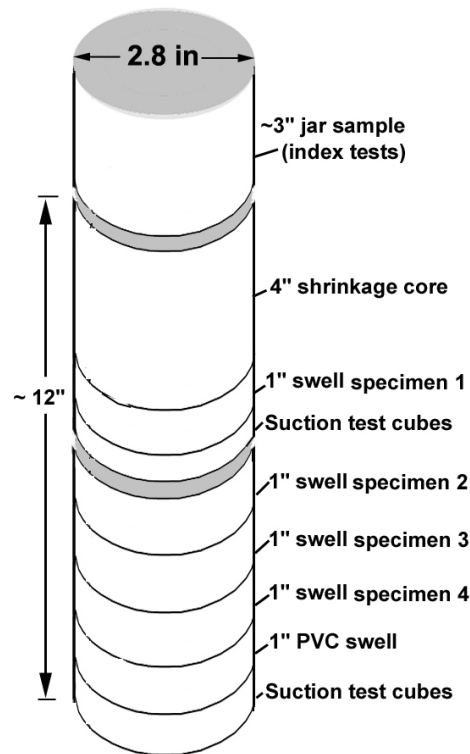


Figure 59. Approximate dimensions and locations of core slices for each set of ERDC tests conducted on each nominal 2-ft depth interval from Hole 2

Sample Storage, Handling, and Preparation

The unopened samples were stored in a controlled high-humidity room at ERDC. After peeling off the waxed cylinder mold, each sample was placed in a heat-sealed airtight plastic bag inside the controlled high-humidity room. Every effort was made to control any moisture loss from the samples' natural water content state prior to and during testing.

The majority of tests were conducted within a separate controlled temperature room which was kept at 20 deg C (68 deg F) for the duration of testing. Every effort was made to maintain a standard temperature and a constant relative humidity in order to eliminate those test variables.

Remolded Sample (Atterberg Limits) Preparation

State DoTs, AASHTO, ASTM, and USACE have different test preparation protocols. USACE (1970) describes alternative preparation methods for clay shale-derived materials, including expansive clays. Instead of using the ASTM D4318 method for preparing the sample, USACE (1970) and

TxDOT (2010) specify using a mechanical malt mixer to ‘blenderize’ (disaggregate) the soil into slurry prior to Atterberg limits testing. The intent is to allow the clay to achieve a thoroughly-dispersed particle orientation that assumedly neutralizes its past history and over-consolidated stress state. By mimicking its normally-consolidated stress state, the soil’s ‘fully-softened’ shear strength at failure is more accurately obtained (Stephens et al. 2011). It has also been shown that sample preparation methods utilizing ‘blenderizing’ can markedly change the LL (but not the PL) results in expansive clays (Dept. of Army 1971). Studies by Heley and MacIver (1971) and Townsend and Gilbert (1974) indicate that sample preparation matters when determining soil classification based on LL. The higher the LL results from the standard method, the higher the difference from the blenderized slurry method.

The USACE sample preparation procedure:

- Shave or shred material at essentially natural water content and air-dry to a constant weight in an atmosphere with a temperature less than 50 degrees C and a relative humidity less than 30 percent. After a constant weight is attained (and after a drying period of at least 48 hr), soak the material in distilled water for at least 48 hr.
- Place about 500 ml of the slurry in the 1000-ml container of a single-speed blender (available from any laboratory supply company). Make the initial water content of the slurry above 300 percent or more than twice the estimated liquid limit (blenderized) whichever is greater. Typically, the weight of dry soil in the blender at any one time should not exceed 150 g.
- Blenderize the slurry without interruption for 10 min and then wash through a 425-um (No. 40) sieve. Remove excess water using a plaster of Paris dish lined with filter paper. Work material at a water content above the liquid limit in a thin layer on a glass plate with a steel spatula until no further reduction in the size of lumps can be achieved.
- Conduct LL and PL tests per ASTM D4318.

AASHTO T-87 and T-146 (Dry and Wet Preparation of Disturbed Soil Samples for Testing, respectively) also differ. The Dry Preparation method

(the MDoT method, per SOP TMD-20-14-00-000) specifies sample drying in air or an oven at less than 60 deg C (140 deg F), then pulverizing and dry-sieving:

- The sample is either thoroughly air-dried or oven-dried (at ≤ 60 deg C).
- The sample is then sieved through the #40 sieve.

The T-146 Wet Preparation method is more detailed:

- Method A (preferred) dries the sample to ≤ 60 deg C, pulverizes, and then dry sieves it. The sieving and mixing details are omitted here, but the sample is soaked for less than 24 hrs, wet-sieved through the #40 sieve, and again dried to ≤ 60 deg C.
- Method B soaks the undried natural sample until it is “soft”, wet-sieves through the #40 sieve (with option to use a “mechanical stirrer” if needed), decanted and filtered until its water content is above (“never below”) the approximate LL.

ASTM D4318 prefers the wet preparation method instead of the dry preparation method:

- The undried natural sample is either dry-sieved or wet-sieved through the #40 sieve. The dry preparation method takes the air-dried sample, pulverizes it and then dry- or wet-sieves it.
- Water is then added to the sample produced by either method to achieve the desired consistency for the LL test.

Texas Dept of Transportation (TxDOT 2010) specifies their preferred Method A:

- Oven-dry the sample to 60 deg C, slake it by soaking for 12 hours, wet-sieve through the #40 sieve, and decant the excess water. Then oven-dry it to 60 deg C and pulverize (mortar and pestle) to achieve a uniform sample. The dry sample is then mixed with distilled water and spatula for the LL test.

- Method B soaks the undried natural sample ≤ 12 hours, wet-sieves it through a #10 sieve, slurries it for 3 to 5 minutes using a “malt mixer and dispersion cup”, wet-sieves the slurry through the #40 sieve, and decants/evaporates the slurry to below the approximate LL. Then it is placed into the LL cup for testing.

The USACE sample preparation method (48 hr air dried, soaked, and then blenderized) and the TxDOT Method B (natural water content, soaked, then blenderized) were followed in this study. Hole 1 surplus undisturbed material at its natural water content was used in both methods. The results were compared to the standard LL method results.

Liquid Limit Testing

The percussion (Casagrande cup) methods (ASTM D4318 and AASHTO T-89) and the fall cone method, originally called the Swedish cone from 1915 (Hansbo 1957), have been the two prominent methods for determining the LL. Geotechnical literature suggests the increasing popularity of the fall cone method in the international community of practice, but the ASTM method is used almost exclusively in the United States. Other methods to determine LL have included soil moisture tension, a rheological procedure, extrusion, equilibrium sediment volume (Prakash and Sridharan 2002) and the cylinder slump test (Lee 2004), but these esoteric methods were not utilized in this study.

The ASTM/AASHTO LL test basically consists of smearing a remolded soil sample into a brass cup, grooving it into two sections, and then dropping the cup a number of times until the groove closes 1/2 inch. The soil deformation is induced in part by the soil's weight. Method A (the multi-point method) uses at least three trials over a range of water contents, and the trial data forms the relationship for determining the LL. Method B (the one-point method) uses data from two trials at the same water content multiplied by a correction factor to determine the LL. The ASTM and AASHTO tests use different grooving tool types.

Since the PL standard (rolling thread method) is universal, it has no substitute. However, the fall cone can also determine the PL but it is not a standard procedure (Harison 1988; Feng 2004). Of all the international standards specifying the fall cone for LL, only one specifies using the fall cone to determine both LL and PL (Koester 1992). The People's Republic of China specifies that the PL be determined by extrapolating LL results

down to the 2mm penetration. No actual penetration is attempted at water contents near the PL, so a single fall cone test for LL also determines PL and PI. Unfortunately this extrapolation does not compare well with the ASTM PL values. Lee and Freeman (2009) showed how to modify the fall cone methodology to achieve congruence with ASTM PL results, but did not explore its applicability to expansive clay PL testing.

British Fall Cone Liquid and Plastic Limit Test

An advantage of the fall cone method is both intact (undisturbed) and remolded soil samples may be tested. The ASTM method (Casagrande cup) only allows for remolded sample testing. The fall cone LL method is popular outside the United States. Its use is standardized with the Intl Organization for Standards (ISO 2004) as TS 17892-12:2004. A metal cone of a given weight and apex angle is vertically suspended over a remolded soil sample (**Figure 60**). The cone falls by gravity and penetrates the sample. The penetration distance is correlated to the LL. There are over half a dozen variations of this device (cone angle and cone mass differences) used in numerous countries. The most common fall cones are the Swedish cone (60 degree angle and 60g mass) and the British / French cones (30 degree angle and 80 g mass) (Leroueil and Bihan 1996).



Figure 60. Fall cone penetrometer. The sample is placed under the tip and the LL and/or PL (shown) may be calculated.

Using a standard 30-deg, 80g mass (British Standards Institution 1990) fall cone with the capability for rapidly changing the cone weights without removing the cone tip during the test sequence, the dual-weight fall cone procedure used for remolded samples is as follows:

- Divide the given soil sample into a test sequence having a minimum of four subsamples to be used for testing at different water contents. Higher accuracy is achieved with more subsamples. To achieve a wide range of water contents (encompassing the LL and PL range), add distilled water to increase the water contents and air dry to decrease the water contents of the test sequence. The subsamples' water contents should range from high values near the LL to low values near the PL. The greater the plasticity, the wider the range of water contents. The driest subsamples are allowed to dry while unconfined. Integral samples should exhibit uniform level top and bottom surfaces without hairline cracks or inclusions.
- Separately penetrate each subsample. Use the 80g mass in at least two subsamples exhibiting penetration depths greater than 14mm, and add an approximately doubled cone mass (152g in this set of

experiments) to penetrate the remaining subsamples (penetration depths less than 14mm).

- Plot the water content versus square root of penetration for each subsample. Perform a linear regression or best-fit to obtain a single regression line through all the data points of all subsamples.
- The LL and PL values for the soil are picked off the regression line. The water contents at the regression line intercepts of $2^{\wedge} 0.5 \text{ mm} = 1.41$, and $20^{\wedge} 0.5 \text{ mm} = 4.47$, represent the PL and LL, respectively, following the traditional assertion that there is a given decrease in undrained shear strength between the PL and LL (Skempton and Northey 1953; Wood and Wroth 1978).

Liquidity Index Change

The change in liquidity index (LI) is related to the rate of slaking according to Strohm et al. (1978), as shown in **Table 12**. An oven-dried 1-in. sample was soaked in distilled water for two hours, and then drained in a funnel with filter paper to prevent loss of fines. The LI change (ΔLI) was calculated as the difference between the soaked water content and the natural water content, divided by the PI.

Table 12. LI and slake rate comparison (Strohm et al. 1978)

ΔLI	Slake rate
< 0.75	Slow
0.75 - 1.25	Fast
> 1.25	Very fast

Field Moisture Equivalent

Per AASHTO T-93, the field moisture equivalent (FME) is the minimum water content at which a drop of water placed on a smoothed surface of the soil will not be completely absorbed in 30 seconds, but will spread out over the surface leaving a thin film of moisture.

The FME is a measure of the largest water content that an unloaded soil would normally attain in the field, and usually lies somewhere between the PL and LL. Lightly-loaded soils might have a water content approaching 75% of the FME. Lambe (1960) also noted that the water content of “ini-

tially moist” samples (after swelling under a 200 psf load) averaged about 93% of the samples’ FME values.

About 50 g of a dry sample passing the No. 40 sieve is placed in a mixing dish, water is added, and a spatula motion forms clay balls. Their surface is smoothed with the spatula, and a drop of water is added to a formed slight depression on the surface. The water content at which adding a drop of water will not show complete absorption in 30 seconds is the FME. Limited FME testing was accomplished in this study since the test has little relationship to MDoT requirements.

Free Swell Test

Holtz and Gibbs (1954) proposed a simple identification test for expansive clays, called the *Free Swell Test*. The test is performed by slowly pouring 10 cu cm of dry soil passing the No. 40 sieve into a 100-cu cm graduated cylinder filled with water and noting the swelled volume of the soil after it comes to rest at the bottom. Although the type of water was not noted, it is assumed to be distilled. The free swell (FS %) value in percentage is determined by:

$$FS\% = 100(\text{final_volume} - \text{initial_volume}) / \text{initial_volume} \quad (22)$$

Commercial-grade bentonite will have a FS% ranging from 1200% to 2000%. Soils having FS% as low as 100% may exhibit considerable volume change when wetted under light loadings. Soils having FS% below 50% seldom have appreciable volume changes, even under very light loadings. These data were based on western U.S. soils primarily from California, Arizona, and Colorado.

Modified Free Swell Test (MFSI)

Sivapullaiah et al. (1987) MFSI procedure is as follows:

- Take 10 g of oven-dried soil passing a 425- μm (#40) sieve, and mix it with distilled water thoroughly to form a soil-water suspension of initial volume of 100 ml in a 100-ml graduated jar. Allow the soil-water suspension to equilibrate for 24 h. Note the swelled volume of the soil (V). Calculate the dry soil volume (V_s) as $W_s / (G_s \gamma_w)$, where $W_s = 10$ g. The MFSI is $(V - V_s) / V_s$.

Prakash and Sridharan (2004) noted that the MFSI value equals $V/10$, which is an easier calculation than the one above. They also noted that the MFSI procedure may yield erroneous results for kaolinitic soils.

Free Swell Index (FSI) and Ratio (FSR)

Prakash and Sridharan (2004) recommended an alternate procedure using a non-polar solvent (kerosene) and distilled water as follows:

- Take 10 g of oven-dried soil passing a 425- μm (#40) sieve, and mix it with distilled water thoroughly to form a soil-water suspension of initial volume of 100 ml in a 100-ml graduated jar. Allow the soil-water suspension to equilibrate, the normal equilibrium period for natural soils being 24 h. Note the equilibrium (swelled) sediment volume of the soil (Vd).
- Take 10 g of oven-dried soil passing a 425- μm sieve, and mix it with carbon tetra chloride or kerosene thoroughly to form a soil-liquid suspension of initial volume 100 ml in a 100-ml graduated jar. Allow the soil-liquid suspension to equilibrate. Note the equilibrium (swelled) sediment volume of the soil (Vk) after 24 h. The non-polar liquid carbon tetrachloride was proposed for the free swell index test (Sridharan et al. 1986a), but according to Sridharan et al. (1990), the equilibrium sediment volume of soil in kerosene and that in carbon tetrachloride are essentially the same. The non-polar liquid kerosene is more readily available and not as hazardous as carbon tetrachloride.
- Calculate the free swell index (FSI) as:

$$FSI = \frac{(Vd - Vk) \times 100}{Vk} \quad (23)$$

- Calculate the free swell ratio (FSR) as:

$$FSR = \frac{Vd}{Vk} \quad (24)$$

- Identify the soil as kaolinite if FSR is less than unity or as montmorillonite if FSR is more than 1.5.

- If FSR is in between 1.0 and 1.5, the soil under consideration is of mixed clay mineral type (i.e., mixture of kaolinite and montmorillonite).

Shrinkage Methods (No-load Tests)

Shrinkage Volume-Water Content Determination

AASHTO T-92, in addition to determining the shrinkage limit (SL) and volumetric shrinkage (VC %), also includes a calculation for “lineal” shrinkage percent (LS %). The AASHTO T-92 equation is:

$$LS\% = 100 \times \left(1 - \sqrt[3]{100 \div (VC + 100)}\right) \quad (25)$$

Where

VC = volumetric change percent, as defined by AASHTO T-92

(Bar) Linear Shrinkage

The linear shrinkage method (BSI 1990) is a measurement of length change after a soil sample dries inside a mold or “bar” (**Figure 61**). It is reported as a percentage, and is a common test outside the U.S. in countries such as Australia, New Zealand, Kenya, and South Africa. It is used in the U.S. to characterize soil binder materials (TexDOT 2005). When the linear shrinkage percentage (Ls) is multiplied by the percentage of dried sample passing the #40 (0.425mm) sieve, it becomes the Shrinkage Product (Sp). The Sp is useful for assessing soils to be used on unpaved roads (IFG 2005).



Figure 61. Linear shrinkage mold.

Clod Test

The Clod test for determining the unit weight of wax-coated irregularly-shaped soil specimens (i.e. clods) was modified per Krosley et al. (2003). Instead of wax, Elmer's glue was used. One specimen was coated with glue and allowed to dry for different time intervals. The specimen was then weighed in a water bath and oven-dried to determine the shrinkage volume – water content relationship. This test was conducted to observe the viability of a glue coating that allows moisture to escape from the soil without allowing the water bath to infiltrate the specimen. Although the limited testing successfully showed the viability of conducting a glue-coated Clod test, it probably has little applicability to MDoT needs.

COLE (rod) Test

The COLE (rod) value was determined according to the method of Schafer and Singer (1976). Previously air-dried, ground, and sieved (minus 2 mm) soil samples were used for COLE (rod) measurement. For each sample, approximately 100 g of soil were added to small plastic cups, and enough distilled water was added to make a saturated paste. The soil paste was covered and left to equilibrate for 24 h. A disposable plastic syringe was modified using a drill so its orifice was smooth with a uniform 1.0-cm diameter. The syringe was filled with paste using a spatula. Three 60- to 100-mm long soil rods were slowly extruded onto a waxed paper sheet (**Figure 62**). Samples with higher clay contents were extruded to a length of 60 to 70 mm to decrease the likelihood of cracking on drying. A spatula was used to trim the ends of the rods for measurement with a digital caliper. The rods were dried in an oven for 2.5 h at 105 deg C. COLE (rod) was determined by the equation:

$$\text{COLE (rod)} = (l_m - l_d)/l_d \quad (26)$$

Where l_m is the moist-rod length and l_d is the dry-rod length; thus COLE (rod) values are unit-less.



Figure 62. Syringe with extruded soil paste

Standard Absorption Moisture Content (SAMC)

Yao et al. (2004) proposed the standard absorption moisture content (SAMC) test that, along with the PI and the Holtz and Gibbs (1954) free swell test results, has been adopted as the Chinese swelling potential rating system (Zheng et al. 2008). Although the method has not been directly compared to undisturbed sample swell tests, the SAMC method uses slices from undisturbed samples.

The SAMC is the equilibrium water content when the undisturbed soil slice is dried from its natural water content to that in a 60% relative humidity desiccator at 25-deg C temperature. Slight modifications yielding comparable results were conducted during this study.

$\omega_{24/72}$ Method

The $\omega_{24/72}$ method proposed by Erguler and Ulusay (2003a) simply measured the remolded slurry (near its LL) water contents after sitting for 24 and 72 hrs, respectively. Excellent correlations were found between the 24-hr water contents, LL, dry density, methylene blue value, swelling pressure, and swell percent. Their simple empirical predictive model, developed using multiple regression, applied to Ankara (Turkey) clay.

Russian Method

Nikol'skii (1959) pushed the soil sample into a metal cylinder of known weight and volume, weighed it, and let it air-dry for several days. Then it was oven-dried at 105 deg C until it attained a constant weight. The shrunken sample's diameter and volume were measured. The shrinkage percentage was calculated as the change in sample volume divided by its original volume. Due to limited availability of undisturbed sample lengths, this test was not conducted for this study. Comparable results were obtained from alternate shrinkage test methods discussed later in this report.

Ring Shrinkage Tests

Hanafy's (1998) ring shrinkage test for expansive clays requires an undisturbed sample and standard consolidation (oedometer) rings. For each test, 2 specimens at 90-deg orientations from the same undisturbed sample are trimmed to fit inside separate oedometer rings. As the specimens are allowed to air-dry, water content and dimensions are measured and averaged. Vertical, lateral, and volumetric shrinkage values are noted. Due to limited availability of undisturbed sample lengths, these tests were not conducted for this study. Comparable results were obtained from alternate shrinkage test methods discussed later in this report.

Australian Shrinkage (No-load) and Swell (Load) Tests

Australian Core Shrinkage Tests and Shrink-Swell Tests measure the linear strain-water content relationship and swell strain using undisturbed samples. The Instability Index is calculated when the Core Shrinkage results are combined with the suction-water content curve results for the given soil sample. The estimated surface heave can be calculated if the Instability Index is known.

There are three different Australian shrink and/or swell test methods. The Shrink-Swell Index (Iss) requires measurement of 4-inch long core length change (strain) upon air- and oven-drying, and is conducted per Australian Standard (2003) Test Method 7.1.1. Method 7.1.2 requires a special shrinkage cell device to determine the Loaded Shrinkage Index (Ils). Method 7.1.3 requires the same type of measurement as the Iss test, but adds a vacuum desiccator for obtaining the moisture characteristic. The desiccator holds super-saturated ammonium chloride, whose headspace

relative humidity theoretically equilibrates to an equivalent total suction of 5.5 pF.

This study used the AS 1289-7.1.1 shrink-swell test method, which required an undisturbed sample split for two separate tests (no-load core shrinkage and 525 psf swell). The shrinkage strain and the swelling strain were separately measured, then combined to yield the shrink-swell index, I_{ss} :

$$I_{ss} = (\varepsilon_{shrink} \times \varepsilon_{swell} / 2) / 1.8 \quad (27)$$

Where

ε_{shrink} and ε_{swell} = shrinkage and swelling strains, respectively

Instability Index

The Australian Standards (2003) Instability Index (I_{pt}) is defined as “the percent vertical strain per unit change in suction (pF), taking into account the expected design values of applied stress, lateral restraint, and suction range.” It is equivalent to the “suction index” (Johnson 1979, Snethen 1980) and the “suction compression index” (McKeen and Hamburg 1981). It is calculated based on results from the AS 1289-7 test methods for soil reactivity, and is useful for either identifying expansive soils or estimating their potential expansion.

Mitchell and Avalue (1984) linked the I_{pt} to the AS 1289 Core Shrinkage Test and the suction-water content curve (i.e. the soil water characteristic curve) for no-load undisturbed expansive soil samples. The Instability Index is calculated as:

$$\text{Instability Index, } I_{pt} = \frac{\varepsilon}{\Delta\omega} \times \frac{\Delta\omega}{\Delta u} \quad (28)$$

Where

$\varepsilon / \Delta\omega$ = Core Shrinkage Test linear slope

$\Delta\omega / \Delta u$ = water content-suction curve (i.e. soil water characteristic curve) linear slope

Field measurements of surface heave and modeled surface heave (using above relationships) agreed closely for Australian soils in the Adelaide area (Mitchell and Avalue 1984).

Swell Tests

Expansion Index

The soil sample is air-dried, sieved, compacted via standard Proctor method to 50% saturation water content, loaded with a 1 psi surcharge, inundated with distilled water, and allowed to swell. The EI is calculated from the height change due to swelling. The exact test procedure is detailed in ASTM (2008c) D4829. **Figure 63** shows the test apparatus.



Figure 63. Expansion Index device (courtesy ELE, Inc.)

The Expansion Index Test (EI) was developed in the late 1960s predominantly in the Southern California counties and in the western United States where expansive soils are abundant (Anderson and Lade 1981). It was developed based on experience with expansive soils in Southern California having $LL < 60$. It is prescribed in California's building code and is sometimes referred to as the "UBC" test method for determining the expansive potential of compacted soils upon inundation with water.

The EI was developed to measure a basic index property of the soil, and thus be comparable to other soil indices such as the Atterberg limits. The test procedure does not duplicate any particular field conditions such as soil density, moisture content, or loading, thus the test consequently has little direct design application.

The compacted specimen is placed in a consolidometer (oedometer) with porous stones at the top and bottom. A pressure of 6.9 kPa (1 psi) is applied to the specimen, which is then flooded with distilled water. The one-dimensional expansion of the specimen is determined after 24 h or after the rate of expansion decreases to 0.005 mm per hour (0.0002 in. per hour).

The EI test was initially considered for this study. Due to the requirement for testing remolded (compacted) soil at a given saturation value, any information gained would not be appropriate for field application. Utilizing compacted or remolded Yazoo clay in or under a structure is not recommended.

FHA PVC Test

The FHA's potential volume change (PVC) swell index device (**Figure 64**) is useful for field application when undisturbed samples are utilized instead of using remolded (compacted) samples. The method was originally developed for compacted samples where the un-sieved soil sample is air-dried, placed in 3 layers and compacted in the apparatus (Lambe 1960; FHA 1974). Water is added and the specimen expands for a maximum of 2 hrs.

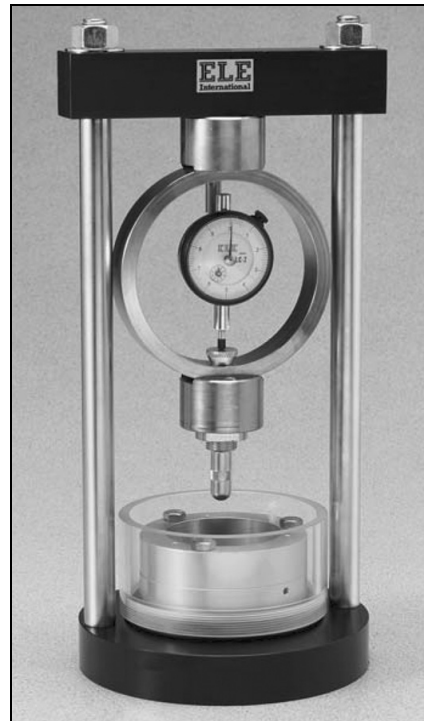


Figure 64. FHA PVC device (courtesy ELE, Inc.)

The test is essentially a measurement of the pressure exerted by a soil sample when it swells against a dial-gauged proving ring after being wetted for a maximum of 2 hrs. The PVC Swell Index value is correlated from the dial gauge reading, and the corresponding pressure (lb/sq ft) is read from a calibration chart. The estimated PI may also be read from a chart. **Table 13** shows the PVC Swell Index and corresponding soil categories.

Table 13. FHA (1974) PVC Swell Index classification system

PVC rating	Expansion potential category
< 2	Non-critical
2 - 4	Marginal
4 - 6	Critical
> 6	Very critical

The PVC classification system was originally developed from ten (10) soil samples ranging from plastic silts to high-plasticity clays. The highest LL was 81%, and the soils were tested at only three “relative water contents”: “dry” (air-dried condition), “moist” (somewhere between “dry” and “wet”), and “wet” (water content somewhere near the soil’s plastic limit). If a soil

is tested at some other water content, the PVC rating may be off by a factor of 2 (Lambe 1960). The FHA later expanded the PVC ratings database. One hundred fifty two (152) soil samples from locations around the U.S. were tested to create the FHA (1974) PVC classification system. Eighty six of those were from Texas, and only one was from Mississippi.

The Mississippi sample was Yazoo clay, and its expansion potential was classified as “very critical”. Its PVC swell pressure was 9500 lb/sq ft and its estimated PI was 68 from the FHA charts. Easson et al. (2005) tested Mississippi less-expansive clay, Porters Creek, using the PVC test. The Porters Creek clay also fell into the “very critical” expansion potential category.

Undisturbed samples were trimmed and placed in the PVC device during this study. Remolded or compacted specimens were not tested, since any information gained would not be appropriate for field application. Placing compacted or remolded Yazoo clay in or under a structure is not recommended.

Oedometer (Consolidation) Tests

ASTM D4546 (ASTM 2008a), AASHTO T-258 (AASHTO 2008b), and EM 1100-2-1906 (U.S. Army Corps of Engineers 1970), Appendix VIIIa, detail the requirements for conducting one-dimension swell (consolidation) tests. These methods produce results that show the potential swell %, the swell pressure, or both. For example, ASTM D4546 lists three different test methods (A, B, and C). Method A requires four or more identical specimens assembled in consolidometer cells with a different load applied to each cell. The cells are then inundated with distilled water and allowed to swell. The resulting strains are measured to interpret the minimum vertical stress required to prevent swell (i.e. the “swell pressure”) and the magnitude of free swell (i.e. the swell strain at near-zero vertical stress). Such swell tests represent the maximum swell scenario since a subsurface soil layer will not likely be totally inundated with water.

A goal of this study was to prevent duplication of effort and fully utilize the limited number of available undisturbed samples by merging components of several test methods into one overall method. Using this approach did not violate the requirements of any one method but maximized the amount of data collected given the available core samples. The process met the requirements detailed in ASTM D4546 Method A, AASHTO T-

258, and EM 1100-2-1906. Each 2-ft interval core sample from Hole 2 was divided into four 1-in high oedometer specimens (meeting ASTM D4546 Method A and other specified methods) as follows:

Specimen 1: This specimen slice was taken immediately below the AS 1289.7.1.1 shrinkage core sample in order to meet the swell test requirements of that Australian standard. After placing the consolidation cell into the loading device (GeoTac Sigma-1 Automated Load Test System, **Figure 65**), a seating pressure of 5 kPa (105 psf) was applied and the dial gauge was zeroed. The load was increased to 25 +/- 1 kPa (525 psf) for up to 30 minutes. The specimen was then inundated with distilled water and allowed to swell for a minimum of 24 hr. The magnitude of the swelling strain in percent (ϵ_{swell}) was noted.

Specimen 2: This specimen slice was taken as closely as possible to the other 3 specimen slices, and loading was performed to meet the requirements of AASHTO T-258, Method I. After a seating load of 1 kPa (20 psf) was applied (specified in ASTM but not AASHTO), the load was incrementally increased to the in-situ overburden pressure. After equilibrium was reached, the sample was inundated with distilled water and allowed to swell until equilibrium was again reached. The sample was then incrementally unloaded to an arbitrary pressure (1 kPa or 20 psf). A follow-on normal consolidation –rebound test was not conducted because the data points were not needed in this study.

Specimen 3: This slice had seating load of 1 kPa (20 psf) per ASTM D4546 and was then loaded to an arbitrary 1 psi (6.8 kPa or 144 psf), after which it was inundated with distilled water and allowed to swell to equilibrium. This test met the requirements for the third wetting specimen per ASTM D4546.

Specimen 4: This slice had a seating load of 1 kPa (20 psf) per ASTM D4546, was inundated with distilled water, and then allowed to swell to equilibrium. This specimen also met the requirement for the ASTM Method B free-swell strain (single-point wetting-after-loading test).

The ASTM D4546 deformation-vertical stress curve was generated using the data obtained from the above tests on specimens 1 through 4.

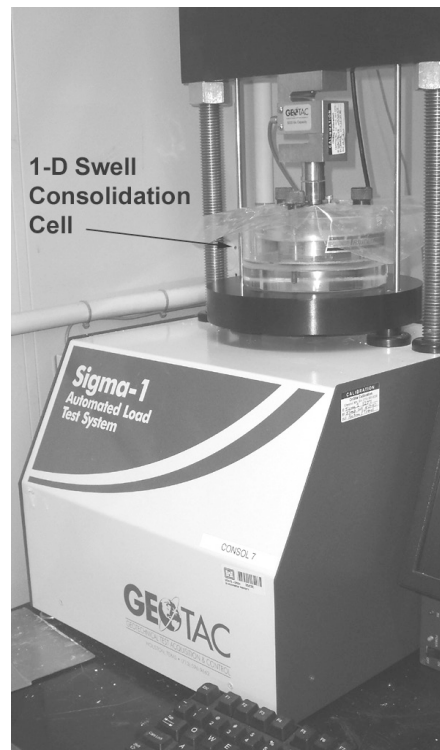


Figure 65. Consolidation apparatus

Simple Direct Shear

One undisturbed sample slice was tested in direct shear (**Figure 66**). After loading to the normal overburden stress, the sample was loaded to shear failure.



Figure 66. Direct simple shear apparatus

Soil Suction

AASHTO T-273 (AASHTO 2008a) specifies thermocouple psychrometers and ASTM D5298 (ASTM 2010) specifies filter paper for conducting unsaturated soil suction tests. Filter paper and a non-standard method (polymer capacitance sensors) were utilized in this study to determine total suction values.

Standard Filter Paper Method

Several methods besides the standard filter paper method are available for measuring soil total suction. These methods use devices that vary widely in terms of range of measurement, accuracy, precision, and reliability. Decagon's WP4 Dewpoint Potentiometer chilled-mirror technique and Wescor Inc. thermocouple psychrometers connected to a microvolt data logger were originally considered for this study but were not selected. Patrick et al. (2007) compared the WP4 to filter paper and determined that the results were essentially the same when adequate equilibrium times were followed. The WP4 results were obtained in about 30 minutes each while the filter paper results were obtained in about a week each, but the cost of the WP4 was about 6000 times higher than the cost of filter paper.

Mabirizi and Bulut (2009) compared the performance of filter papers, thermocouple psychrometers and chilled-mirror psychrometers for measuring the total suction of various high plasticity clay samples taken directly from Shelby tubes. The difference in suction readings was negligible at higher suction ranges. The filter paper technique cost less and reliably measured almost the entire range of total suction. If good laboratory protocol is established it provides very reliable total suction estimates compared to the thermocouple and chilled-mirror psychrometers. Other studies of the filter paper method (Houston et al. 1994, Leong et al. 2002, Bulut and Wray 2005) demonstrated that if a consistent and well-maintained laboratory testing protocol is followed, the filter paper technique is a very reliable method.

Capacitive Polymer-based Sensors

Polymer sensors measure relative humidity (RH) over an extremely wide range (near 0% to near 100%) and contain two electrodes separated by a polymer film that absorbs or releases water as the RH of the surrounding air changes. Measurements of capacitance (or resistance) of the polymer

film are used along with a calibration curve to determine the RH. The electrodes and polymer film are enclosed in a porous body. Polymer sensors respond rapidly, can measure RH from near 0% to near 100%, and exhibit little to no drift. Polymer capacitance sensors (illustrated in **Figure 67**) typically exhibit a more linear calibration curve and are less sensitive to temperature in comparison to polymer resistance sensors. Capacitance sensors are also essentially unaffected by most contaminants (except organic solvents) and are not damaged by freezing or inundation by water.

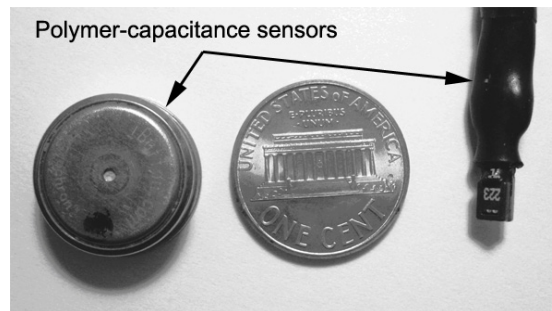


Figure 67. Polymer-capacitance sensors (iButton™ is on the left). U.S. penny shown for scale.

The iButton™ DS1923 was selected for this study based on past research at ERDC (Berney and Lee 2010) and elsewhere (Albrecht, Benson and Beuermann 2003). The iButton™ DS1923 is a miniature polymer capacitive sensor that measures RH and temperature. The autonomous iButton™ sensor is powered by an internal battery and does not require wired connections. External dimensions are 17mm in diameter x 5mm in height. The iButton comes with a fine fabric filter covering the sensor opening, allowing only water vapor to pass and restricting soil or water beads.

For this study, each iButton™ was programmed to record RH and temperature at a high (0.04%) resolution, which allowed approximately 2000 data points before filling the onboard memory. Each iButton™ was placed in the headspace of the salt solution and soil sample jars together with the filter paper (illustrated as device S1 in the above figures), so the vapor pressure (RH) and temperature environment was the same for both.

After retrieving the iButton™ at the end of each test, the RH and temperature data were downloaded via a data logger connected to a computer. The data were analyzed using iButton™ software and suction-RH calibration curve determined the total suction value for the specimen.

Calibration to Theoretical Relative Humidity

Calibrations were required for determining accurate relationships between polymer capacitance sensor readings, filter paper moisture content, headspace relative humidity (RH) and soil suction values. The first step was to create electrolyte aqueous solutions with known (theoretical) headspace RH. The value of the headspace (enclosed air volume) RH depends on the concentration of the electrolyte solution. The concentration is a function of the electrolyte or salt compound and its gram-formula weight. In general, the higher the gram-formula weight, the lower the achievable headspace RH.

Textbook equations relate solute concentration and temperature in an aqueous salt (i.e. potassium chloride, KCl, or sodium chloride, NaCl) electrolyte solution to the vapor pressure in the headspace above the solution. The thermodynamic principles are similar for liquid and vapor phase relationships. The partial vapor pressure (a component of RH) in the headspace above an aqueous salt solution decreases as the solution molality increases, based on the formula (Frazer et al. 1928):

$$(p / p_0)100 = RH\% = [100 - (100R)(m)] \quad (29)$$

Where

p = partial vapor pressure of the solvent from the solution

p_0 = vapor pressure in pure state at the same temperature

RH% = relative humidity

m = molality (gram-formula weight of solute per 1000 ml solvent, water)

$100R$ = values obtained from aqueous chemistry tables, i.e. Frazer et al. (1928)

Molality (moles per liter) is based on a constant solvent (water) volume. For example, one mole of pure sodium chloride (NaCl) is 58.44 grams, and one mole per liter is 58.44 grams dissolved in one kilogram (or 1000 ml) of water. The lowest RH achievable in the headspace of a saturated NaCl aqueous solution is about 75%.

CaCl-2H₂O (calcium chloride dihydrate) was also mixed in an aqueous solution at 20 to 25 deg C. One mole is 129 grams, and one mole per liter is 129 grams dissolved in 1000 ml of water.

The second step (after creating aqueous solutions with known RH) was to convert the RH values to total suction values. Total suction as a function of RH and temperature was calculated using the following equation derived from the Ideal Gas Law:

$$Total_suction, kPa = -460.573 \times (273.16 + ^\circ C) \times \ln(RH) \quad (30)$$

Where

RH = relative humidity = partial vapor pressure / pure state vapor pressure, as a decimal fraction instead of a percentage

Table 14 shows the NaCl and CaCl-2H₂O solutions used in this study. The theoretical headspace RH% was calculated using the partial vapor pressure equation above and chemistry tables for NaCl and CaCl-2H₂O aqueous solution molalities. The total suction values were calculated from the Ideal Gas Law equation above.

Table 14. Aqueous solution headspace calibration to total suction at 20 deg C (68 deg F)

Grams NaCl per 100 ml distilled water*	Grams CaCl-2H ₂ O per 100 ml distilled water*	Theoretical headspace RH*	Theoretical total suction, MPa
0.042	-	99.8%	0.033
0.584	-	99.7%	0.405
5.84	-	97%	4.531
16.36	-	90%	14.076
23.37	-	85%	21.943
29.22	-	80%	29.12
36.0	-	75%	38.84
-	62.5	73%	42.49
-	88.2	58%	73.55
-	106.6	47%	101.94
-	161.7	35%	141.75

* Data from Frazer et al. (1928).

The third step required placing polymer capacitance sensors and filter papers into the enclosed headspace above the aqueous solutions. **Figure 68** illustrates the process where the total suction was measured using a procedure after sensor devices measuring RH and filter paper water content were calibrated to known electrolyte solution molalities and RH.

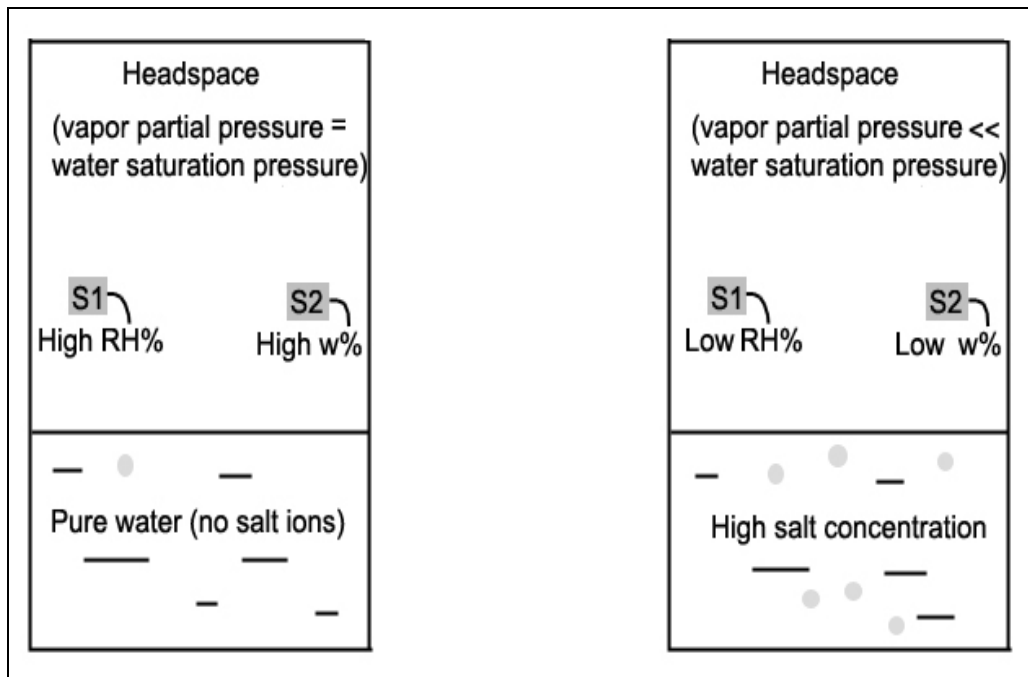


Figure 68. Soil suction-water content sensor calibration. Sensor S1 (measuring RH) and/or S2 (measuring vapor water content) is placed in closed jars with controlled temperature. Headspace vapor equilibrium with the solution is reached and the sensor readings are recorded. The electrolyte solution concentration (molality) is varied from zero (left jar) to very high (right jar) to cover the desired suction range.

Measurements to Obtain Soil Suction Values

After the calibration process was completed, the soil suction values and soil water characteristic curves (SWCC) upon drying were determined using the RH and water content proxy measurements. The soil samples at varying water contents and the sensors were placed in sealed jars in a controlled-temperature environment. The sensor readings after headspace vapor equilibrium were then matched to their respective calibration curves to determine the soil pore water content and /or vapor RH. **Figure 69** illustrates the process where the soil's total suction was determined by proxy measurement of the sensor RH (or water content).

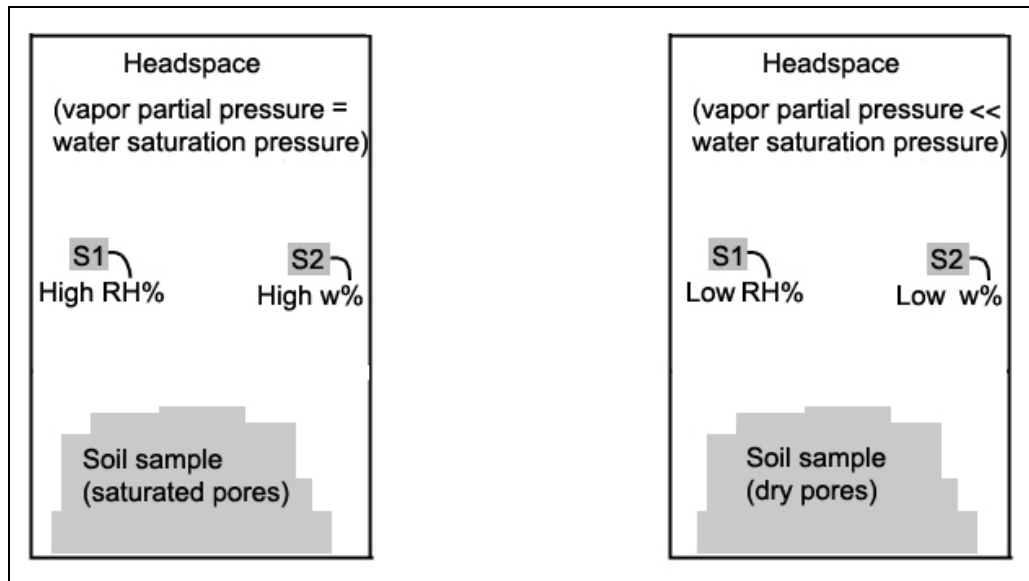


Figure 69. Soil total suction determination. Sensor S1 (measuring RH) and/or S2 (measuring water content) is placed above the soil in closed jars with controlled temperature. The soil moisture is varied from high (left jar) to low (right jar). Headspace vapor equilibrium with the soil pore water is reached and the sensor readings are compared to the electrolyte solution calibrations.

Filter Paper and iButton™ Calibration

Filter paper (represented by S2 in the above figures) only gains or loses moisture (water content) in response to headspace vapor pressure. Whatman No. 42 filter paper discs were selected due to their predominance in published soil suction literature. The non-contact filter paper technique was used to measure total suction since the filter papers came to water vapor (head space) equilibrium with the soil moisture without contacting the specimen. Calibrations for osmotic (pore fluid-induced) and matric suction (contact technique) were not used since no technique used in this study was in direct contact with soil or pore fluid, and at higher suction values the matric suction value essentially becomes the total suction value (Bulut and Leong 2008).

To obtain a calibration curve, filter papers were air-dried in a controlled humidity/temperature room, where the RH was within a relatively dry 43% to 48% range, and the temperature was 20 deg C, ± 1 deg. The initial water content of the low-humidity air-dried filter papers was measured by weighing them on a 0.001g-resolution balance scale. The air-dried filter papers were then suspended over known concentrations of NaCl or CaCl-

2H₂O solutions in sealed glass jars during a nominal two-week equilibrium period.

The equilibrium water content of the filter paper was measured and plotted against total suction for each salt concentration to define the calibration curve. **Figure 70** shows the calibration results of the Whatman #42 filters used in this study compared to the standard ASTM D5298 curve for Whatman #42 filters.

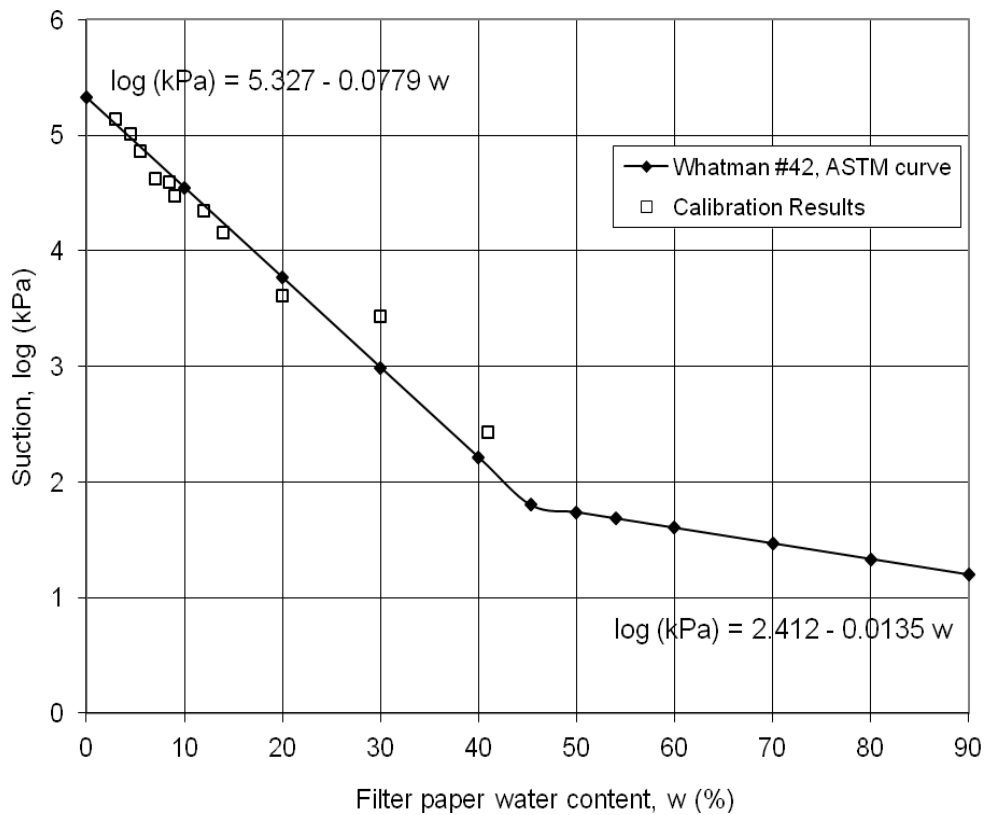


Figure 70. Filter paper calibration curves

The iButton™ calibration was performed in an identical fashion to the filter paper calibration. Instead of using a scale balance, the iButton™ (**Figure 71**) was connected to the computer and the RH values were displayed. **Figure 72** shows the iButton™ calibration plot for each serial-numbered sensor used in this study.

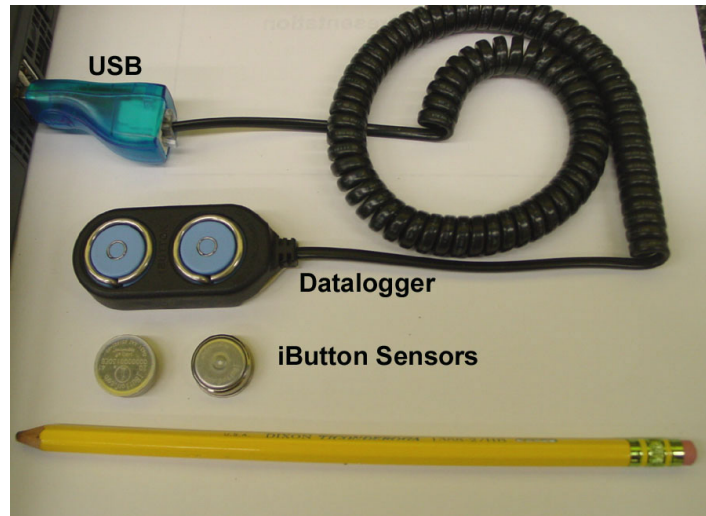


Figure 71. iButton™

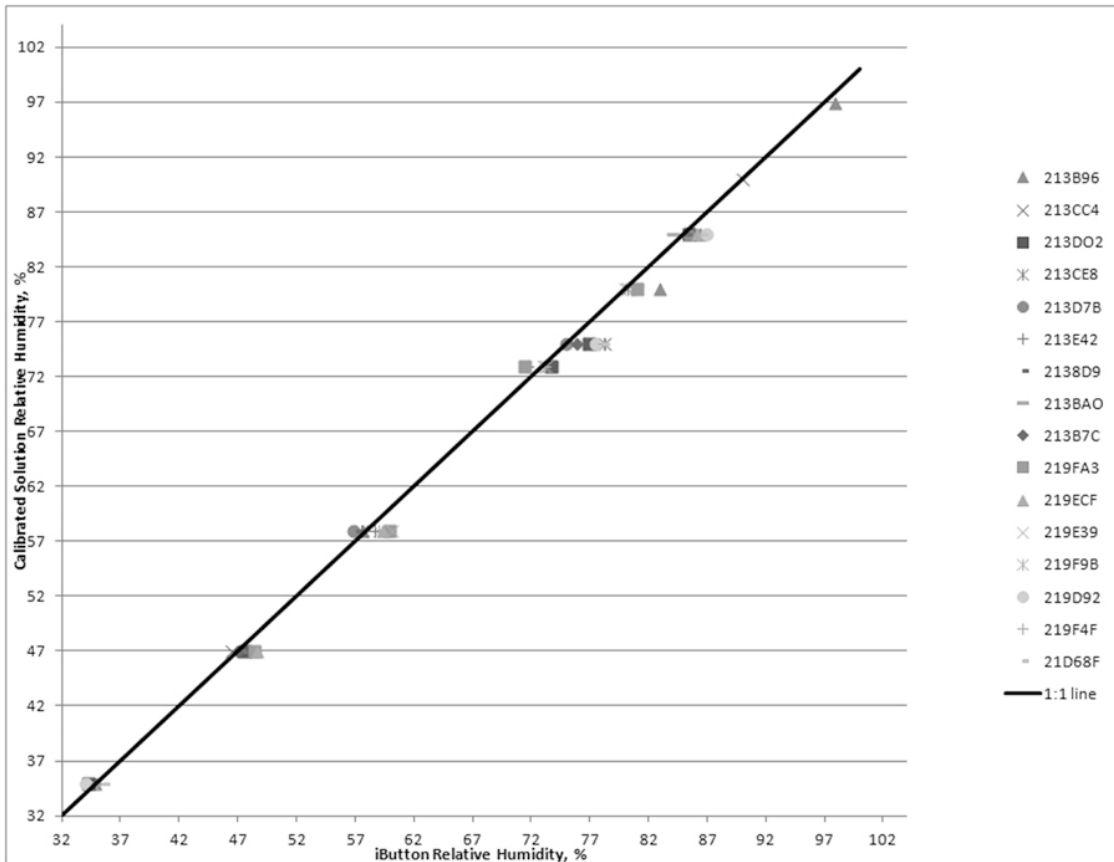


Figure 72. iButton™ calibration curve for each serial numbered device

Filter Paper and iButton™ DS1923 Test Procedure

ASTM (2010) D5298 was the followed standard for measuring soil suction using filter paper. Undisturbed core soil samples at their natural water contents were sliced and sub-divided into 9 approximately one-inch specimens having a state of water content as follows:

- Specimen 1: slightly wetter than natural water content; taken from post-swell consolidation sample
- Specimen 2: natural water content
- Specimen 3: air-dried overnight in a high-humidity environment (90% RH)
- Specimen 4: air-dried overnight in a low-humidity environment (50% RH)
- Specimen 5: air-dried overnight in a low-humidity environment (~40% RH)
- Specimen 6: oven-dried in a 60 deg C oven for 1 hour
- Specimen 7: oven-dried in a 60 deg C oven for 10 to 16 hours
- Specimen 8: oven-dried in a 60 deg C oven overnight
- Specimen 9: oven-dried in a 110 deg C oven overnight

Each specimen was then placed in a sealed jar and taken to a controlled-temperature environment for the test duration.

A filter paper and an iButton™ DS1923 were suspended above each soil specimen in the sealed jar during the elapsed time for headspace water vapor equilibrium. After achieving an equilibrium moisture state, the filter paper was first removed and its wet water content was determined as quickly as possible (within one minute). Then the iButton™ DS1923 was removed and logged. After oven-drying the filter paper and retrieving the iButton™ DS1923 data, the respective calibration curves were then used to plot the total suction values for each specimen.

Figures 73 through **77** illustrate the test procedure. The filter paper was placed over, but not touching, the soil sample. One iButton™ DS1923 polymer capacitance sensor was also placed in the jar to capture the head-space vapor pressure without touching either the soil sample or the filter paper.



Figure 73. Soil total suction measurement using filter paper and iButton™ (1)

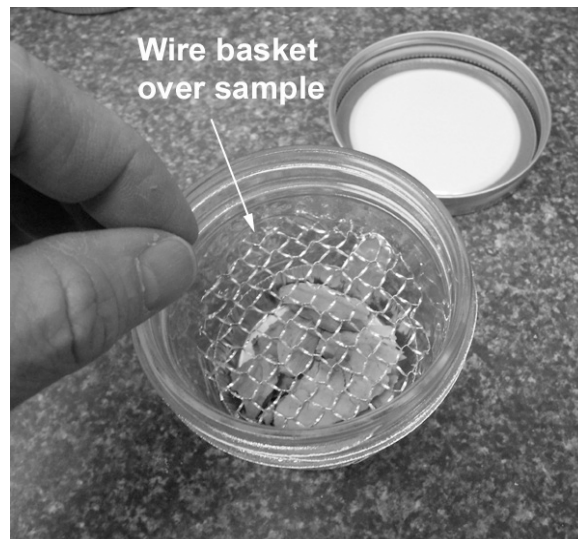


Figure 74. Soil total suction measurement using filter paper and iButton™ (2)

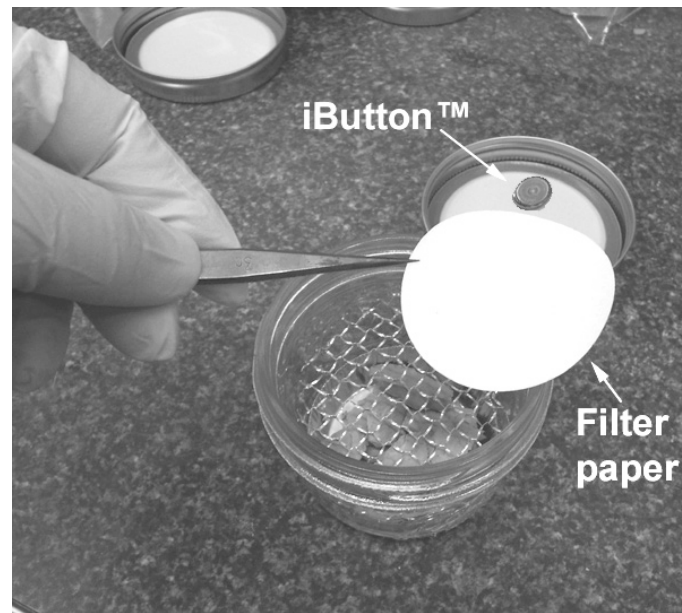


Figure 75. Soil total suction measurement using filter paper and iButton™ (3)



Figure 76. Soil total suction measurement using filter paper and iButton™ (4)



Figure 77. Soil total suction measurement using filter paper and iButton™ (5)

Clay Chemistry

Cation Exchange Capacity (CEC)

A straight-line relationship exists between CEC and the methylene blue index (MBI). ASTM C837 (ASTM 2009a) test method covers the measurement of the adsorption of methylene blue dye by a clay from which the MBI is calculated. **Figure 78** shows the apparatus used in this study.



Figure 78. Methylene blue test apparatus

The procedure is as follows:

- Weigh out 10 g of properly dried clay and place in a 600-mL beaker. If the clay cannot be tested immediately after drying, store it in a desiccator.
- Add 300-mL of distilled water to the beaker and stir with a mixer until the clay is uniformly dispersed. With the slurry still being agitated, fill a burette with the methylene blue solution, add 5 ml of the solution to the slurry, and stir for 1 to 2 min. Remove a drop of the slurry, using the dropper or the glass stirring rod, and place on the edge of filter paper.
- Observe the appearance of the drop on the filter paper. The end point is indicated by the formation of a light blue halo around the drop. Continue adding the methylene blue solution to the slurry in

1.0-mL increments with 1 to 2 min of stirring after each addition, then testing, until the end point is reached. Allow 1 to 2 min of stirring after each 5-mL increment. After the end point is reached, continue stirring for 2 min and retest.

- Perform calculations per standard, and record the MBI for the clay.

Calcium Carbonate Content

Since calcite (CaCO_3) is a known component of Yazoo clay, lab test methods to evaluate the presence and content of calcite were reviewed. Chaney et al. (1982) did a comprehensive survey on calcium carbonate determination from a geotechnical engineering viewpoint. They evaluated ten different lab test methods and found that the pressure calcimeter test is best suited for geotechnical engineering applications. The pressure calcimeter (also known as the “Karbonat-Bombe”) test is standardized as ASTM D4373 (ASTM 1996). The test procedure converts the clay’s CaCO_3 to CO_2 in a closed cylinder of known volume. The CO_2 pressure is gauged and pre-calibrated to the CaCO_3 content. **Figure 79** shows the apparatus used in this study.



Figure 79. Calcium carbonate test apparatus

The test procedure is:

- Place a known weight of dry soil powder in the cylinder.
- Place hydrochloric acid (HCl) inside a hanging basket in the cylinder and close the lid.
- Shake the vessel to combine the soil and HCl, which generates the CO₂ gas.
- Read the pressure gauge after the reaction has completed. The CaCO₃ content is determined by matching the gauge reading to the calibration standard.

Water-soluble Sulfate Ion

Gypsum (calcium sulfate) is a commonly-reported component in Yazoo clay, although its presence was generally not observed in the MDoT data

analyses detailed elsewhere in this report. Sulfates in soils and aggregates are known to have deleterious effects on concrete, and crystalline growth of the expansive minerals is known to result from the combination of lime, soluble sulfates, and clay minerals in the subgrade (Lytton et al. 2005). The effect of sulfate swelling is not addressed in MDoT's design procedure for Yazoo clay.

ASTM (2009c) C1580 details the standard test method for determining the water-soluble sulfate ion content of soils. Colorado Dept. of Transportation (CDOT 2011) details the method with slight revisions. A commercially-available soil chemistry test kit (LaMotte, Inc) was used in this study (**Figure 80**).



Figure 80. Soil chemistry tests

Other Tests

pH and soluble salt (conductivity) tests were conducted using commercially-available test devices and methods (**Figures 81 and 82**). Soluble calcium, available iron, soluble manganese and magnesium values were obtained using the LaMotte soil test kit.

Estimates of shear strength were determined using the pocket penetrometer, the GeoTester penetrometer, and the Torvane shear devices (**Figure 83**).



Figure 81. Soil pH test



Figure 82. Soil soluble salts (conductivity) test



Figure 83. From left to right, hand-held pocket penetrometer, GeoTester penetrometer, and Torvane shear devices

4 Site Data and Test Results

Clinton Site

The Clinton field test section located adjacent to this study site was researched by former Waterways Experiment Station personnel in the late 1960's and early 1970's (Gromko 1969; Johnson 1973a; Johnson and Desai 1975). The 100 ft-square site, located 150 ft from this study site provided in-situ measurements for predicting foundation swelling (heave) behavior. **Figure 84** shows the surface geology at the site is composed of Yazoo clay.

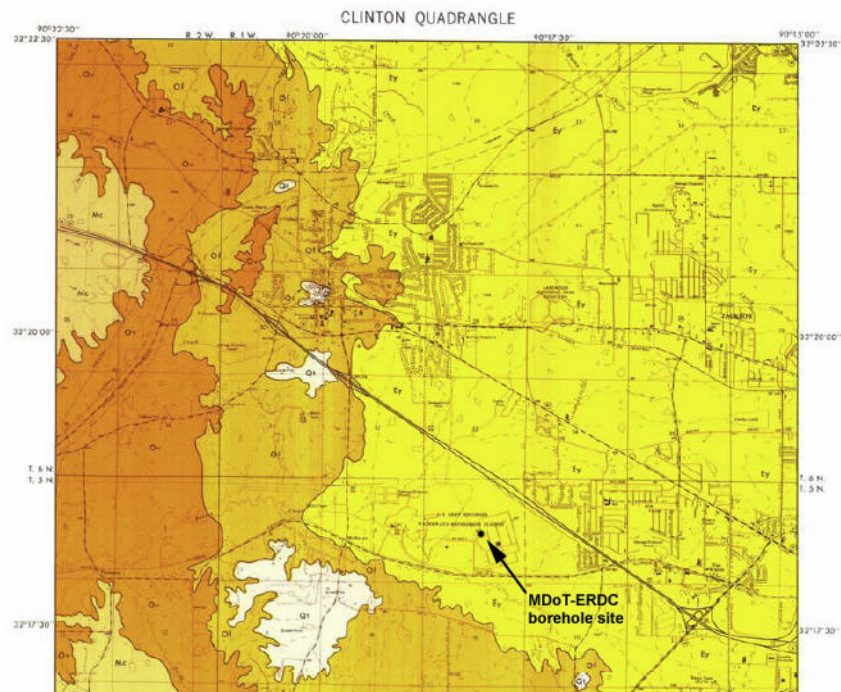


Figure 84. Surface geology map of the Clinton area showing Yazoo clay (yellow color)

Per Johnson (1973a), the Yazoo clay at that site is overlain by about 8 ft of lean clay (CL), and a 1-psi surcharge load was placed on the 100 ft-square ground surface. Soil borings, piezometers, in-situ thermocouple psychrometers, heave plugs, and a weather station were located at the site. Instrument readings were collected over a 4-yr span for the purpose of modeling heave behavior under the weather-protected surcharge layer. **Table 15** shows the test site soil data. The weathered Yazoo clay lies between

8 ft to 26 ft, and the un-weathered (blue) Yazoo clay lies below 26 ft. The soil boring logs indicate the presence of gypsum between 20 and 30 ft.

The natural water contents in the uppermost (non-Yazoo clay) layer are nearly equal to the plastic limits (PL). The natural water contents of the Yazoo clay layers are greater than the PL. Also interesting is the shrinkage limit (SL) of the CL layer is close to the SL of the weathered Yazoo clay layer immediately below it. The LL and Liquidity Index (LI) appear to provide the best markers separating the non-Yazoo from the Yazoo clay.

Table 15. Clinton site Yazoo clay values (after Johnson 1973a)

Depth, ft	USCS Class	Spec. Gravity	Average Dry Dens, pcf	LL, %	PL, %	SL, %	PI, %	Natural water content, %	Liquidity Index, LI	Clay content (< 2 um), %	Activity A
0 - 4	CH	2.68	97	50 - 58	20 - 26	-	28 - 34	20 - 25	< 0.01	22	1.6 - 1.9
4 - 8	CL	2.71	104	35 - 50	15 - 20	19	17 - 32	25 - 35	0.01 - 0.16	19	1.2 - 2.0
8 - 26	CH	2.73 - 2.75	76	60 - 117	17 - 28	15	43 - 89	35 - 50	0.2 - 0.26	67 - 72	0.7 - 1.4
> 26	CH	2.71	83	91 - 101	28 - 32	-	59 - 73	37 - 48	0.1 - 0.2	-	~ 1

Table 16 shows the degree of expansion converted to total volume expansion and swell potential for the Jackson site soil layers with an overburden load of 1 psi.

Table 16. Clinton site Yazoo clay swell values (after Johnson 1973a)

Depth, ft	Degree of expansion	Volume expansion, air-dry to saturation for a 1-psi load, %
0 - 4	High (critical)	20 - 30
4 - 8	Medium-low (marginal)	10 - 20
8 - 26	Very high (critical)	> 30
> 26	Very high (critical)	> 30

Table 17 shows averaged suction values of undisturbed samples from one boring location at the Clinton site. Thermocouple psychrometers measured the total suction values as the samples air-dried at lab room temperature. The total suction values are small (~ 1 ton/ sq ft) at natural water content and based on comparisons with swell pressure data, Johnson (1973a) concluded that the osmotic suction is negligible due to soil leach-

ing in the humid climate. Hence the total suction values are equivalent to the matric suction values.

Table 17. Clinton site Yazoo clay suction values (after Johnson 1973a)

Depth, ft	Drying time, hr	Water content , %	Total suction, tons/sq ft
4.3 - 4.5	44	24.3 (initial)– 5.9 (final)	0.75 (initial) – 85 (final)
7.2 - 7.4	48	35.4 (initial) – 20 (final)	1(initial) – 75 (final)
18.5 - 18.6	30	49.2 (initial) – 19.3 (final)	1.75 (initial) – 73 (final)
31 - 31.1	31	45.8 (initial)– 26.8 (final)	1.25 (initial)- 59 (final)

Lab Results

Tabulated test results are shown in **Appendix B**. Plotted data results are shown in this section.

Qualitative Assessment

The borehole cores were not identical even though Holes 1 and 2 were only 6 ft apart, as illustrated in **Figure 85**. The cores were generally visually similar to a depth of about 24 ft below ground surface. There were distinct color differences below that depth, with abrupt transitions occurring vertically and laterally in the lower depth intervals.

All samples below 6-in depth were classified as high-plasticity clay (CH), with color changing from brown (10YR/ 5/3) to dark grayish brown (10YR /4/2) to a light yellowish brown (2.5Y/6/3) in the upper 24 ft. Below 24 ft or so, the “unweathered blue” (dark greenish gray 4/5GY Gley 1) zone began to predominate in Hole 2 but did not appear in Hole 1 until about 28 ft.

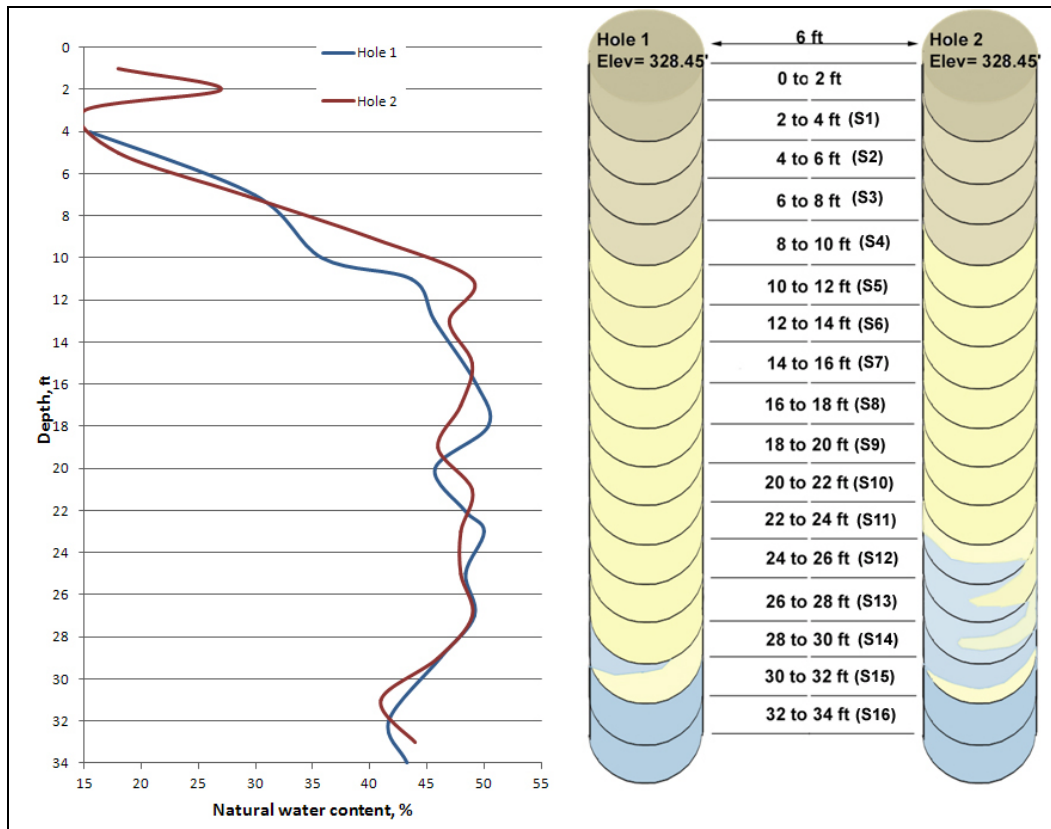


Figure 85. Diagram of water content and soil color in Holes 1 and 2. Each horizontal slice represents a 2-ft depth interval below ground surface. Three generalized depth zones (brown, yellow, and blue) are depicted. Transition zone orientations along the transverse axis are unknown due to Shelby tube rotations.

Table 18 lists general qualitative descriptions of each sampled interval.

Table 18. Sample descriptions

Sample Number (depth interval, ft below surface)	Color, Consistency, and other features	Strength (penetration, tsf)	Crumb Test	Slake Time, minutes	Acid Reaction (Oven-dry sample)
S1 (2-4)	10YR 5/3 (brown) with < 0.3in diameter ochre (7.5R 2.5/1 reddish brown) limonite nodules	Stiff (1.5)	Grade 1 (non-dispersive)	2 - 3	None

Sample Number (depth interval, ft below surface)	Color, Consistency, and other features	Strength (penetration, tsf)	Crumb Test	Slake Time, minutes	Acid Reaction (Oven-dry sample)
S2(4-6)	10YR 4/3 (brown) with < 0.3in diameter ochre (7.5R 2.5/1 reddish brown) limonite nodules; calcium concretions	Stiff(1.5)	Grade 1 (non-dispersive)	6 - 13	None
S3(6-8)	10YR 4/2 (dark grayish brown) with calcium concretions and limonite nodules	Hard (4)	Grade 1 (non-dispersive)	4 - 13	Weak
S4(8-10)	2.5Y 6/3 (light yellowish brown) with calcium concretions and limonite nodules	Stiff (1.3)	Grade 1 (non-dispersive)	4 - 10	Very strong
S5(10-12)	2.5Y 6/3 (light yellowish brown) with multi-fissured <0.125in-wide seams (5Y 6/2, light olive gray)	Stiff (1.7)	Grade 1 (non-dispersive)	4 - 10	Strong
S6(12-14)	2.5Y 6/3 (light yellowish brown) with multi-fissured <0.125in-wide seams (5Y 6/2, light olive gray); oxidized in lab when exposed for several months (10YR 5/6 limonitic stains)	Stiff (1.3)	Grade 1 (non-dispersive)	3 - 7	Very strong
S7(14-16)	2.5Y 6/3 (light yellowish brown) with multi-fissured <0.125in-wide seams (5Y 6/2, light olive gray); oxidized in lab when exposed for several months (10YR 5/6 limonitic stains)	Stiff (1.9)	Grade 1 (non-dispersive)	3 - 7	Strong

Sample Number (depth interval, ft below surface)	Color, Consistency, and other features	Strength (penetration, tsf)	Crumb Test	Slake Time, minutes	Acid Reaction (Oven-dry sample)
S8(16-18)	2.5Y 6/3 (light yellowish brown) with multi-fissured <0.125in-wide seams (5Y 6/2, light olive gray); < 0.25in-long gypsum crystal inclusions	Stiff (1.9)	Grade 1 (non-dispersive)	3 - 8	Strong
S9(18-20)	2.5Y 6/3 (light yellowish brown) with multi-fissured <0.125in-wide seams (5Y 6/2, light olive gray); small gypsum crystals	Very stiff (2.3)	Grade 1 (non-dispersive)	8 - 10	Strong
S10(20-22)	2.5Y 6/3 (light yellowish brown) to 2.5Y 6/4 with multi-fissured <0.125in- wide seams (5Y 6/2, light olive gray)	Very stiff (2.6)	Grade 1 (non-dispersive)	3 - 10	Very strong
S11(22-24)	2.5Y 6/3 (light yellowish brown) with multi-fissured <0.125in-wide seams (5Y 6/2, light olive gray); Hole 2 sample had abrupt transition to 4/5 GY (Gley 1, dark greenish gray)	Very stiff (3.5)	Grade 1 (non-dispersive)	4 - 10	Very strong
S12(24-26)	2.5Y 6/3 (light yellowish brown) with multi-fissured <0.125in-wide seams (5Y 6/2, light olive gray); Hole 2 sample had abrupt transition to 4/5 GY (Gley 1, dark greenish gray)	Very stiff (3.2)	Grade 1 (non-dispersive)	2 - 10	Strong
S13(26-28)	2.5Y 6/3 (light yellowish brown) with multi-fissured <0.125in-wide seams (5Y 6/2, light olive	Very stiff (2.5)	Grade 1 (non-dispersive)	5 - 10	Very strong

Sample Number (depth interval, ft below surface)	Color, Consistency, and other features	Strength (penetration, tsf)	Crumb Test	Slake Time, minutes	Acid Reaction (Oven-dry sample)
	gray); Hole 2 sample had abrupt transition to 4/5 GY (Gley 1, dark greenish gray); small gypsum crystal inclusions				
S14(28-30)	Abrupt transitions from 4/5 GY (Gley 1, dark greenish gray) to 2.5Y 6/3 (light yellowish brown)	Very stiff (3)	Grade 1 (non-dispersive)	5 - 10	Very strong
S15(30-32)	Abrupt transitions from 4/5 GY (Gley 1, dark greenish gray) to 2.5Y 6/3 (light yellowish brown)	Hard (4)	Grade 1 (non-dispersive)	5 - 10	Strong
S16(32-34)	4/5 GY (Gley 1, dark greenish gray); oxidizes in lab to 5Y 4/1 (dark to olive gray)	Hard (4.2)	Grade 1 (non-dispersive)	6 - 10	Strong

Depth Interval 0 to 6 ft

The grab sample from the ground surface to 6 in depth (**Figure 86**) contained a mixture of dark humus (pine straw, roots, and organic detritus), moist clayey silt, and numerous gravel and ochre inclusions. Below 6 inches the soil became drier, harder, and less friable. At 1.5 ft, there was evidence of a hard fragipan that was difficult to penetrate with a shovel. The Hinds County Soil Survey (USDA 1979) noted this fragipan in the nearby Byram series, but it was not noted in the Grenada series shown under the study site.

The first Shelby tube interval (sample S1, **Figure 87**) began at the 2-ft depth. The next tube went through the hardpan layer. Sample S2 from Hole 1 was not retrieved because it could not be hydraulically extruded,

probably due to its high density. The Hole 2 sample was successfully retrieved (**Figure 88**).



Figure 86. Grab sample containing gravel and limonite ochre nodules from 6 in to 2 ft below ground surface.

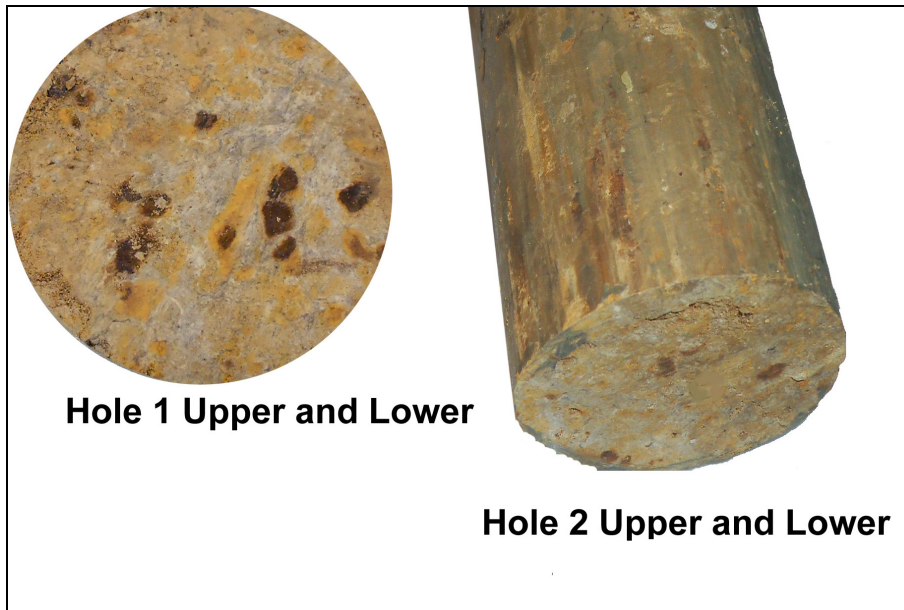


Figure 87. Upper and lower undisturbed samples at depth interval S1 (2ft - 4ft)

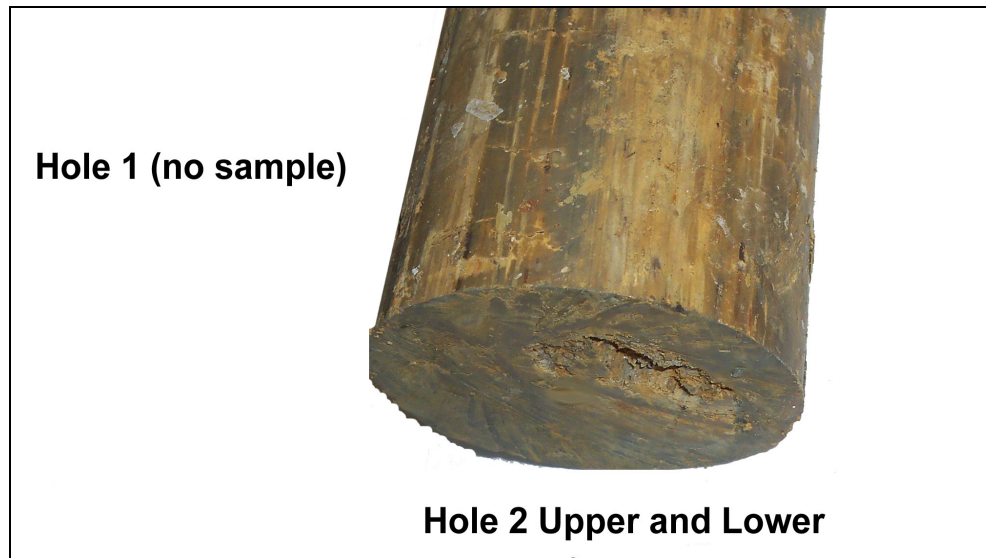


Figure 88. Upper and lower undisturbed samples at depth interval S2 (4ft – 6ft)

Depth Interval 6 to 24 ft

Figures 89 through 97 are representative photographs of the sampled material in the Hole 1 and 2 borehole interval between nominal 6ft to 24 ft depth. The photos were taken inside the lab instead of the drill site, so there may be slight brightness and color variability between photos. The soil samples were photographed at their natural water content state.

The samples from the depth interval 6 to 24 ft (S3 through S11) are traditionally classified as the “weathered” Yazoo clay with its characteristic tan color. At the 24-ft depth the stratigraphy changes between Holes 1 and 2 in that the “unweathered” or blue-green color is revealed in abrupt horizontal and vertical transitions from the tan clay.

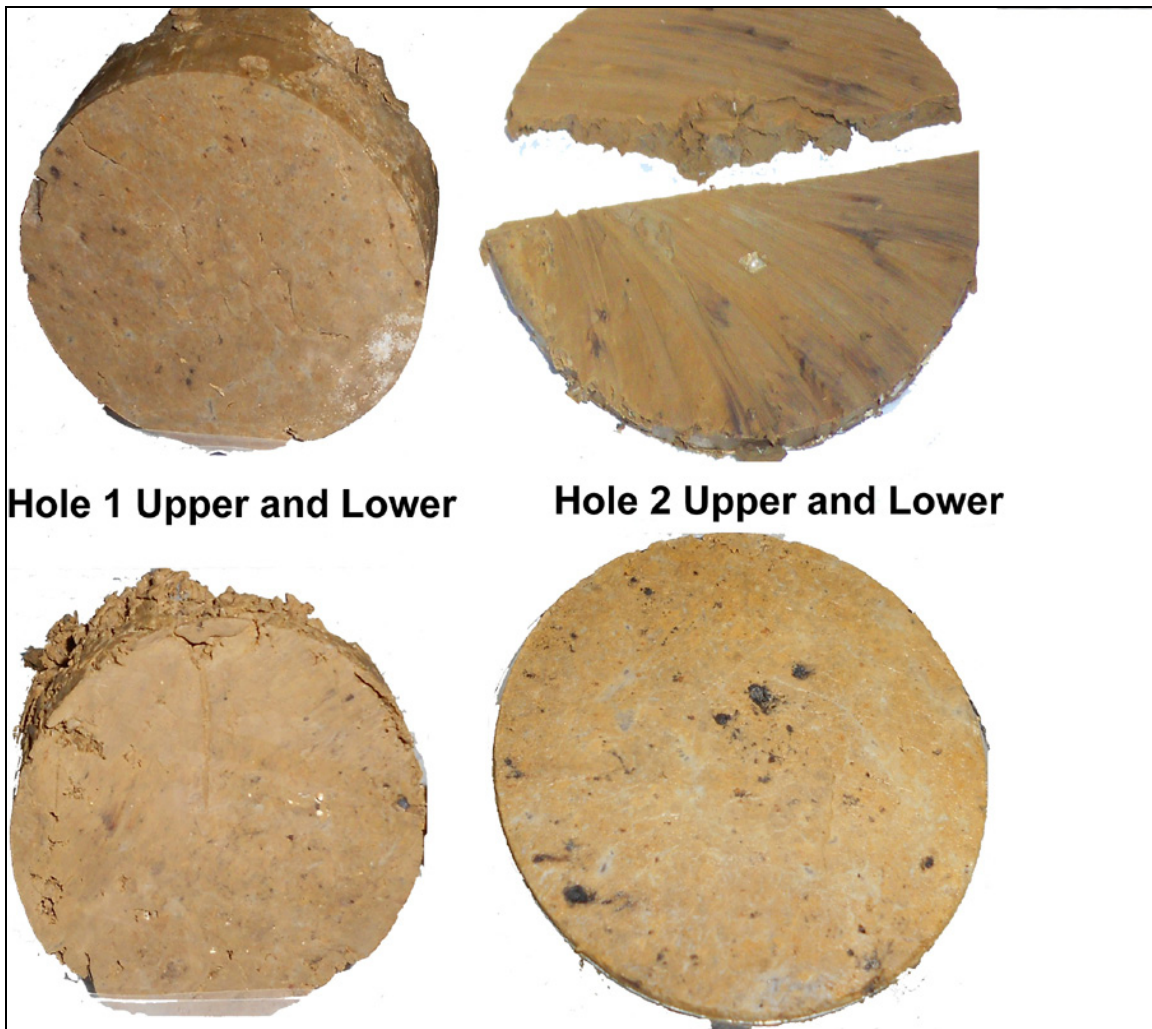


Figure 89. Upper and lower undisturbed samples at depth interval S3 (6ft - 8ft)

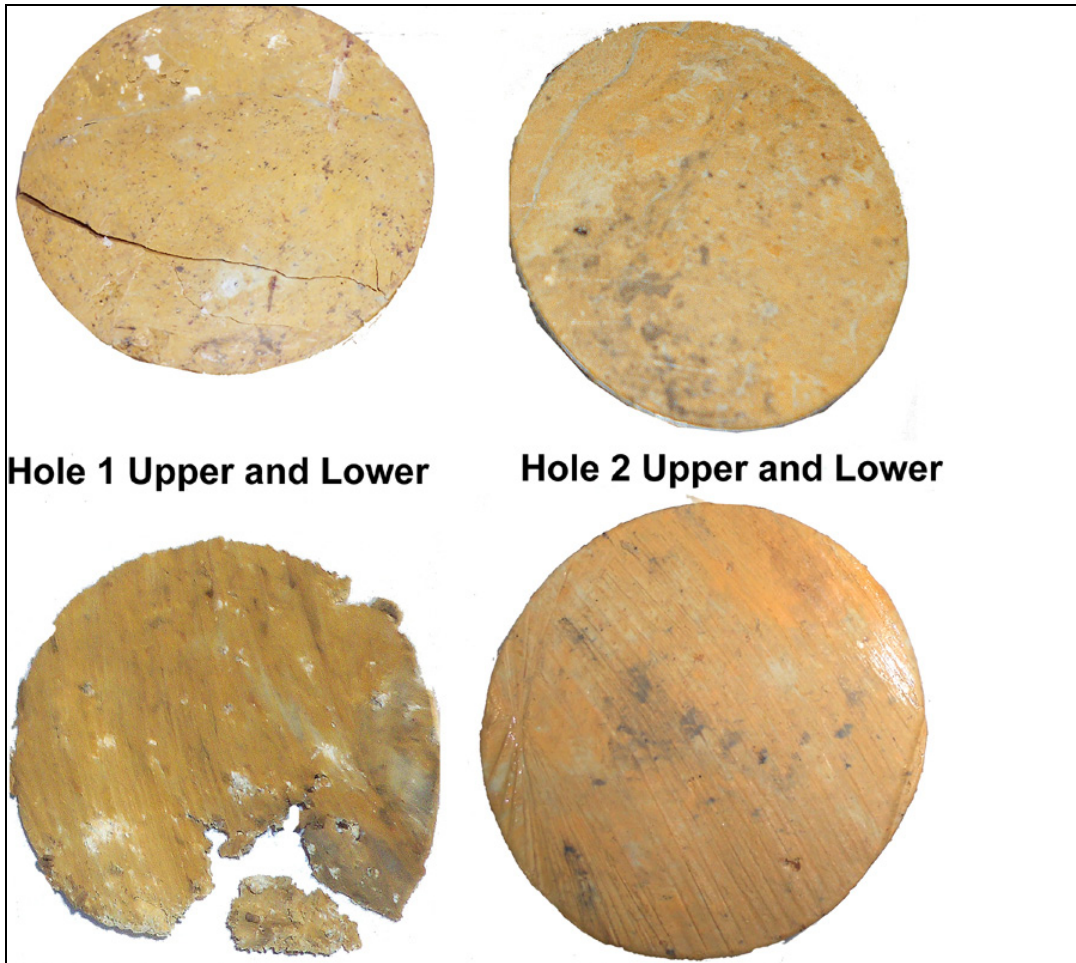


Figure 90. Upper and lower undisturbed samples at depth interval S4 (8ft - 10ft)

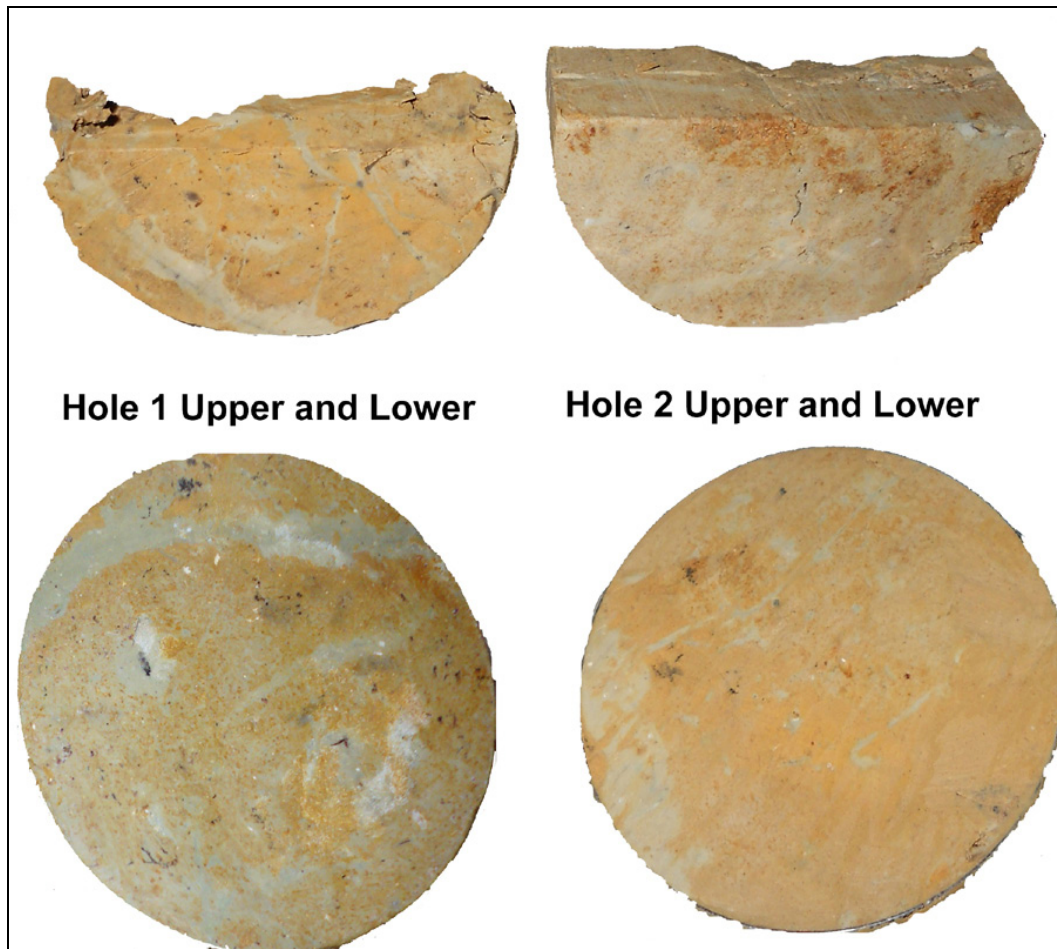


Figure 91. Upper and lower undisturbed samples at depth interval S5 (10ft - 12ft)

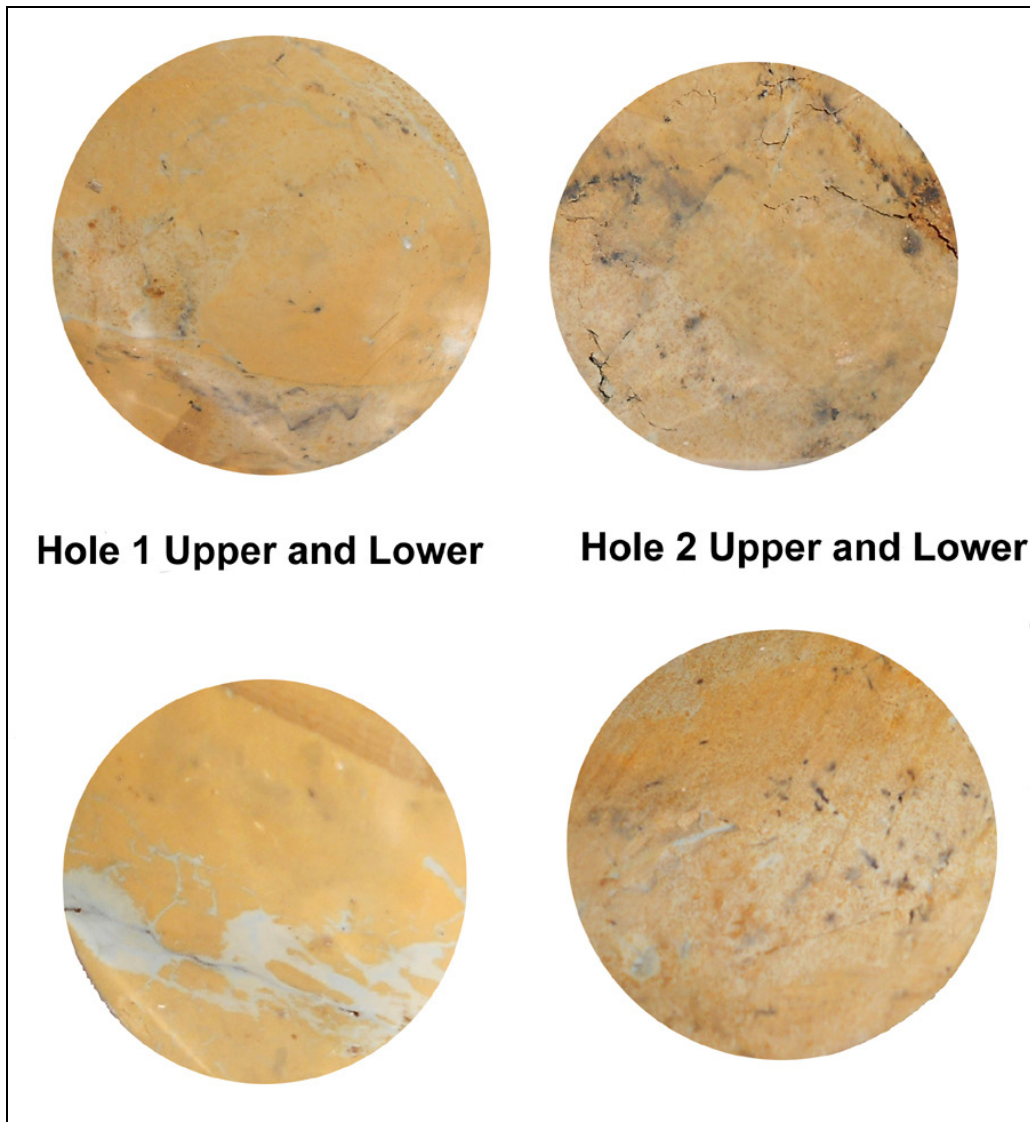


Figure 92. Upper and lower undisturbed samples at depth interval S6 (12ft - 14ft)

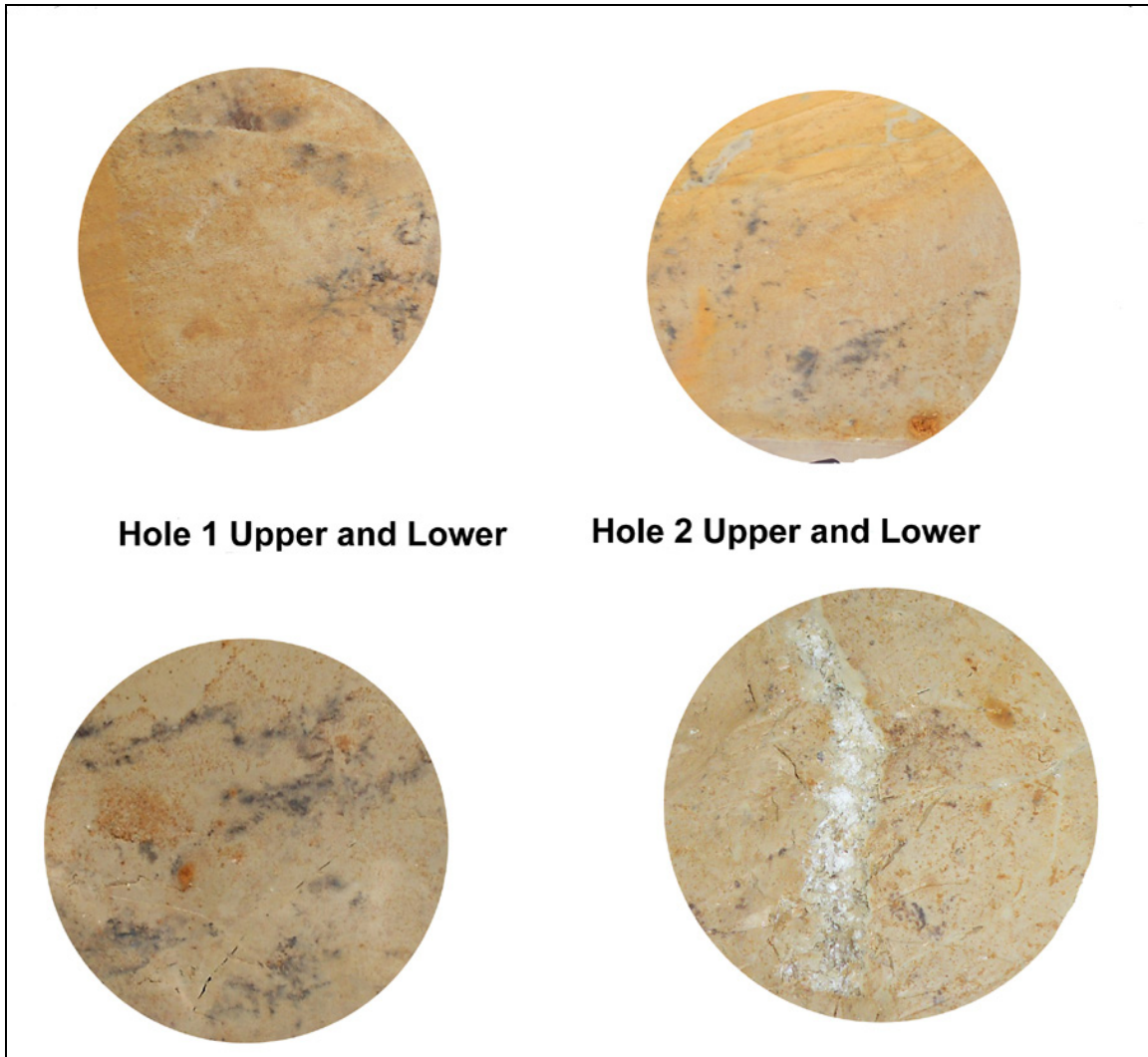


Figure 93. Upper and lower undisturbed samples at depth interval S7 (14ft - 16ft)

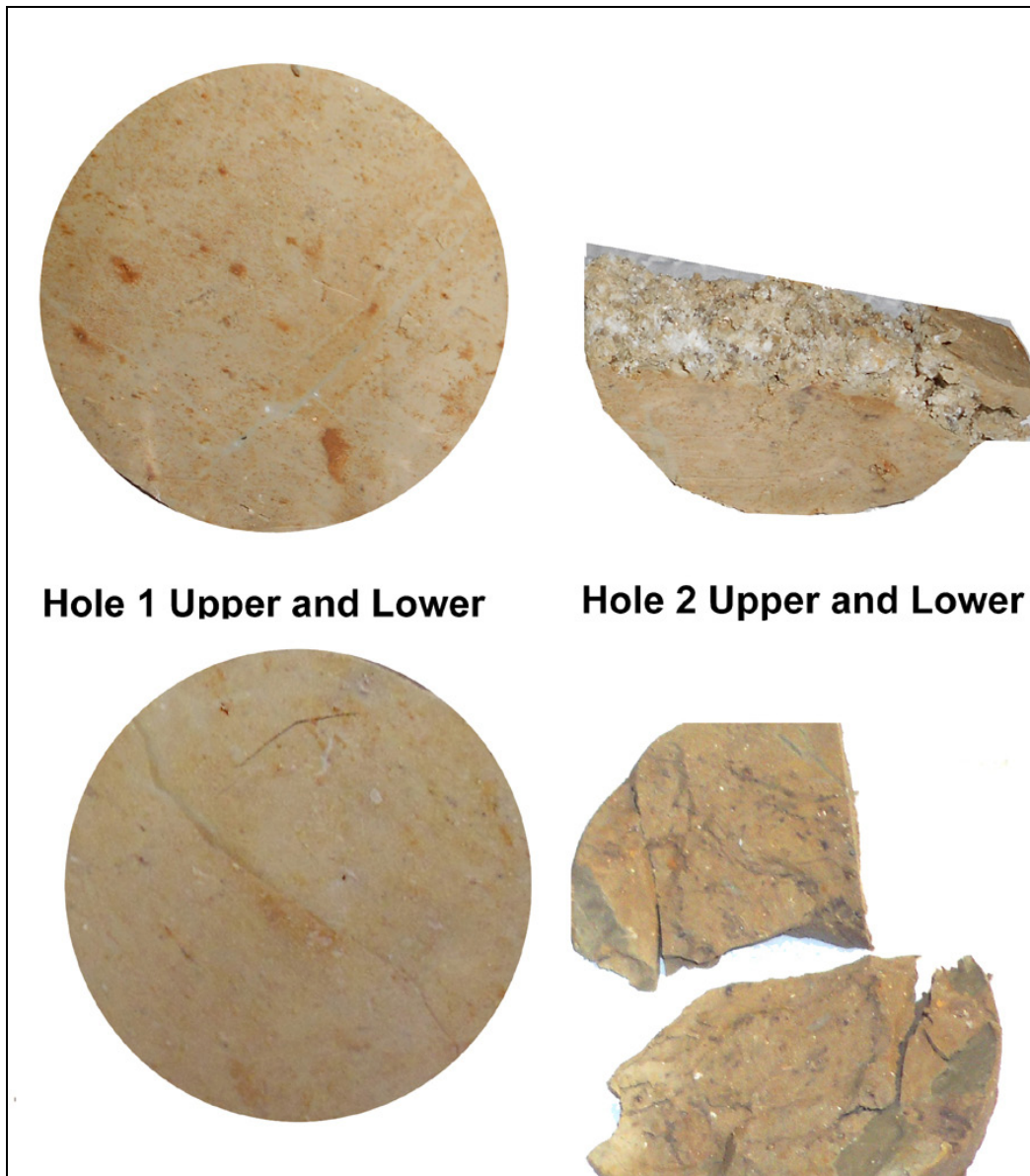


Figure 94. Upper and lower undisturbed samples at depth interval S8 (16ft - 18ft)



Figure 95. Upper and lower undisturbed samples at depth interval S9 (18ft - 20ft)



Figure 96. Upper and lower undisturbed samples at depth interval S10 (20ft - 22ft)



Figure 97. Upper and lower undisturbed samples at depth interval S11 (22ft – 24ft)

Depth Interval 24 to 32 ft

Figures 98 through 101 are representative photographs of the sampled material in the Hole 1 and 2 borehole interval between nominal 24ft to 32 ft depth. The photos were taken inside the lab instead of the drill site, so there may be slight brightness and color variability between photos. The soil samples were photographed at their natural water content state.

The interval between 24ft and 32ft is a transition zone between the two boreholes. The “weathered” and “unweathered” layers exhibit abrupt horizontal and vertical transitions in each borehole.



Figure 98. Upper and lower undisturbed samples at depth interval S12 (24ft - 26ft)

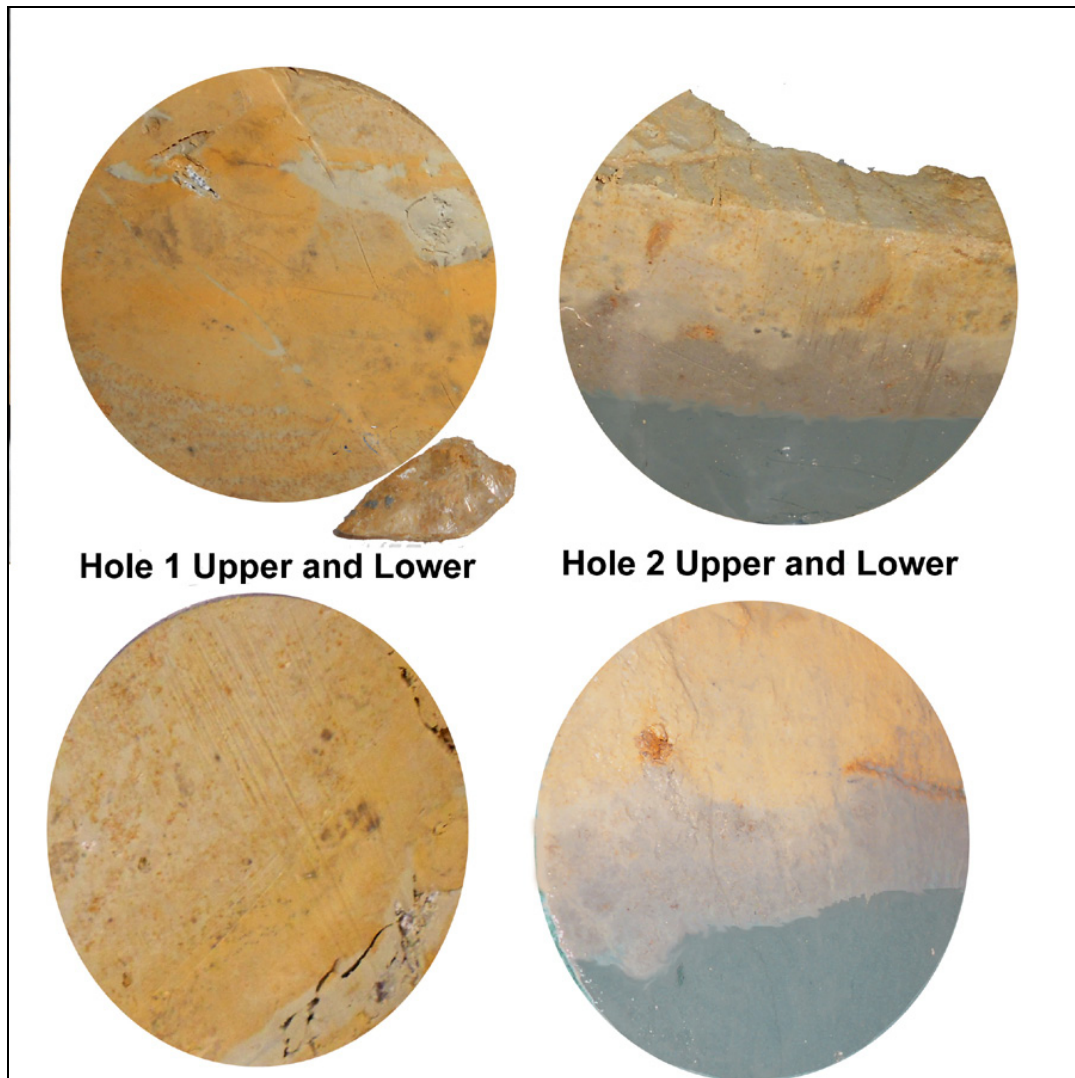


Figure 99. Upper and lower undisturbed samples at depth interval S13 (26ft – 28ft). Hole 1 upper sample contained the gypsum crystal shown above.

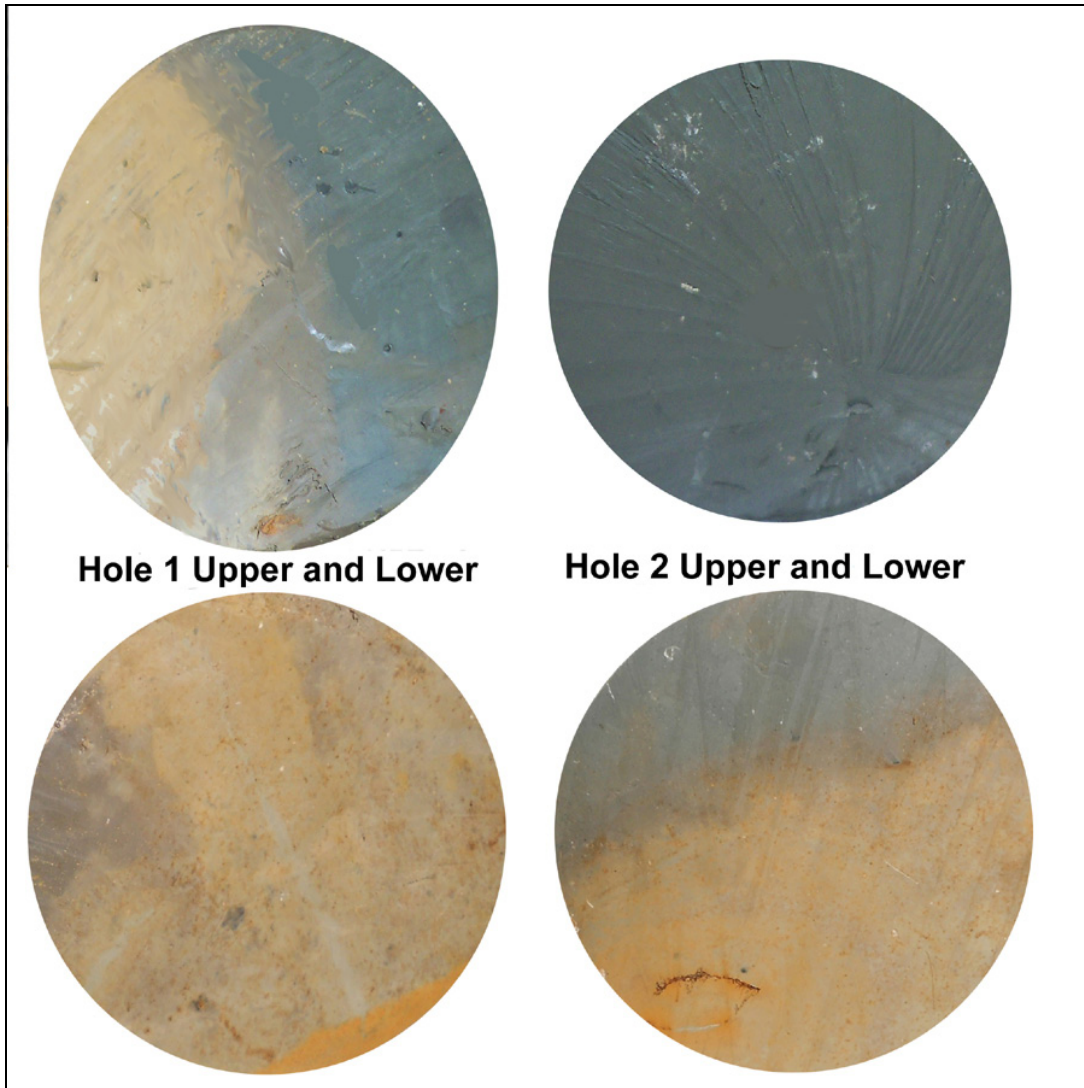


Figure 100. Upper and lower undisturbed samples at depth interval S14 (28ft - 30ft)

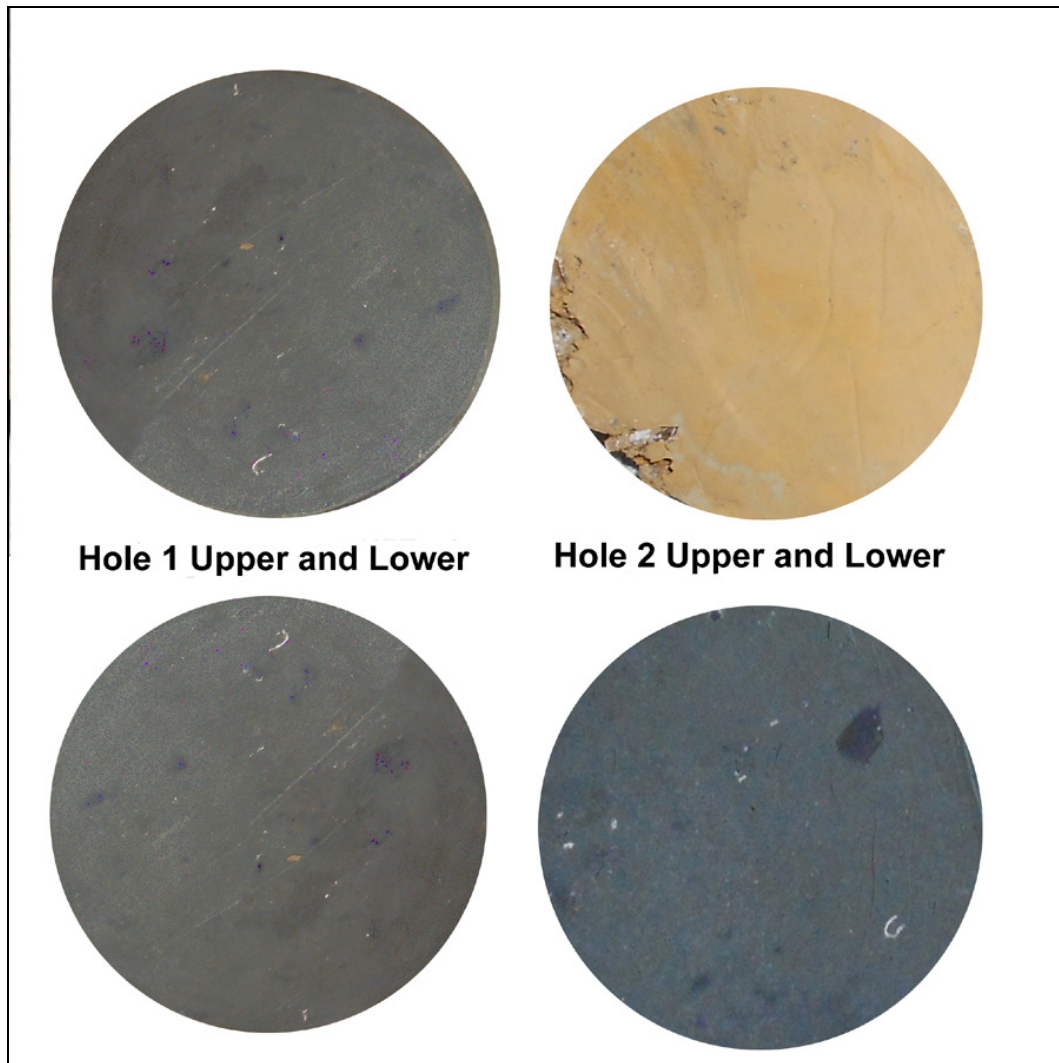


Figure 101. Upper and lower undisturbed samples at depth interval S15 (30ft – 32ft)

Depth Interval 32 to 34 ft

Figure 102 is a representative photograph of the sampled material in the Hole 1 and 2 borehole interval between nominal 32ft to 34 ft depth. The photos were taken inside the lab instead of the drill site, so there may be slight brightness and color variability between photos. The soil samples were photographed at their natural water content state.

This was the termination depth of each borehole, as it captured the solid cores of “unweathered” clay. Nearby borehole logs indicated that this blue-green clay was consistent below the 30-ft depth.

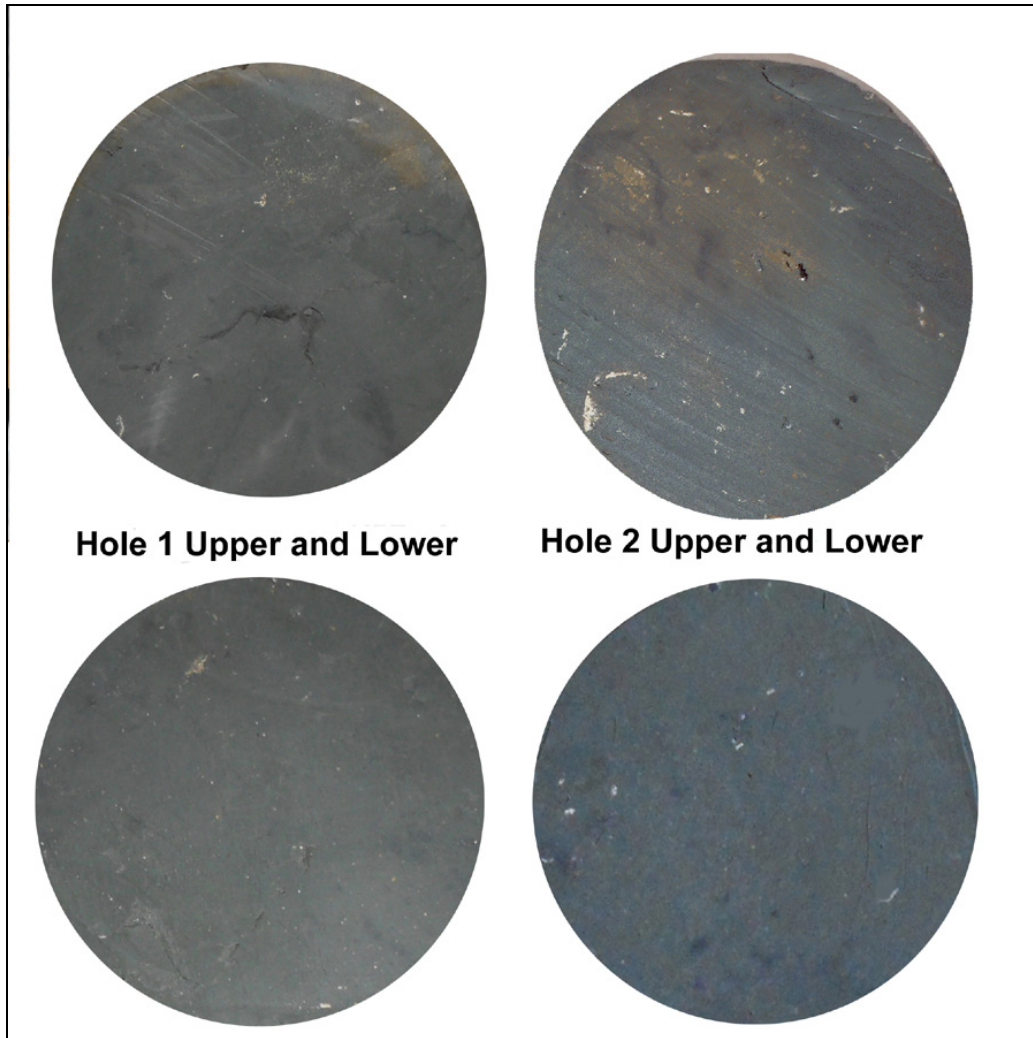


Figure 102. Upper and lower undisturbed samples at depth interval S16 (32ft – 34ft)

Index Properties

Figures 103 and **104** are plots of the Atterberg limits and Volume Change (VC %) results. Note that the LL and its proxies (PI and SI) correlated very well with the VC % results. As expected, PL did not correlate very well.

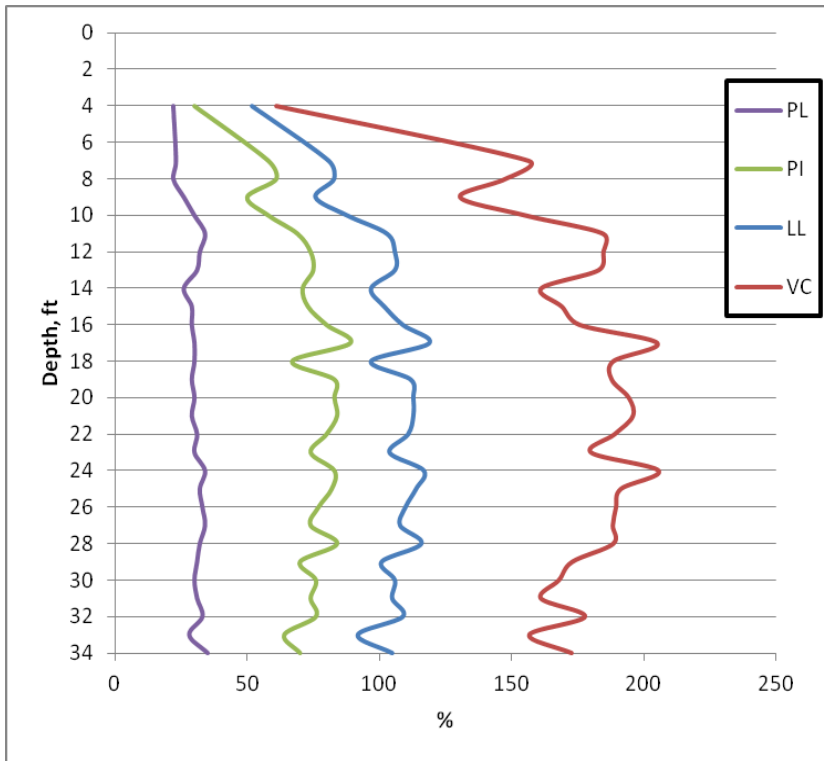


Figure 103. Atterberg Limits (LL and PL) and Volume Change (VC) versus depth

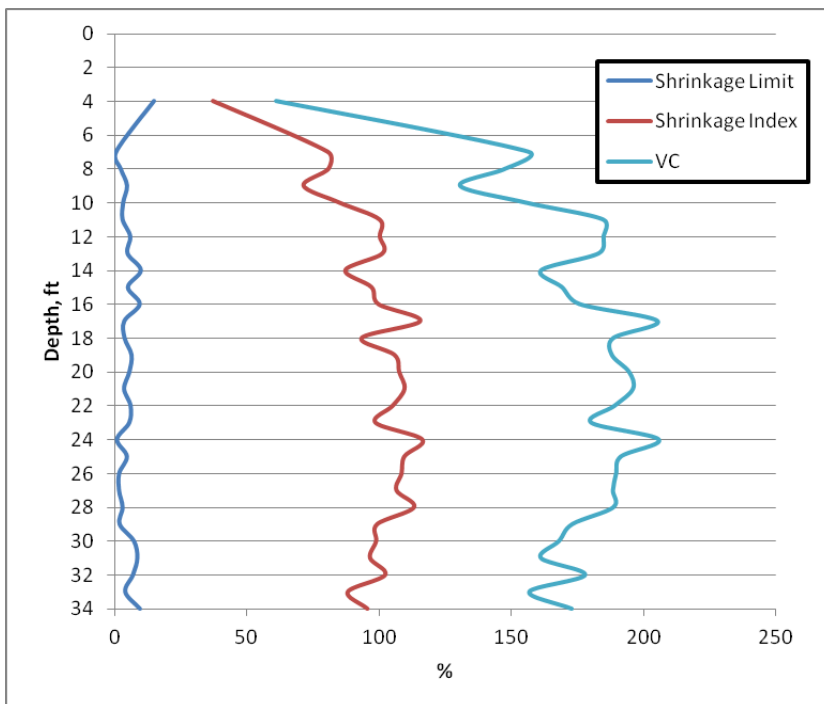


Figure 104. Atterberg Limits (Shrinkage Limit and Index) and Volume Change (VC) versus depth

Remolded (Blenderized) Tests

Comparisons to standard tests

Figure 105 shows small but noticeable differences between the standard and blenderized LL results, as was expected within the Yazoo clay LL range.

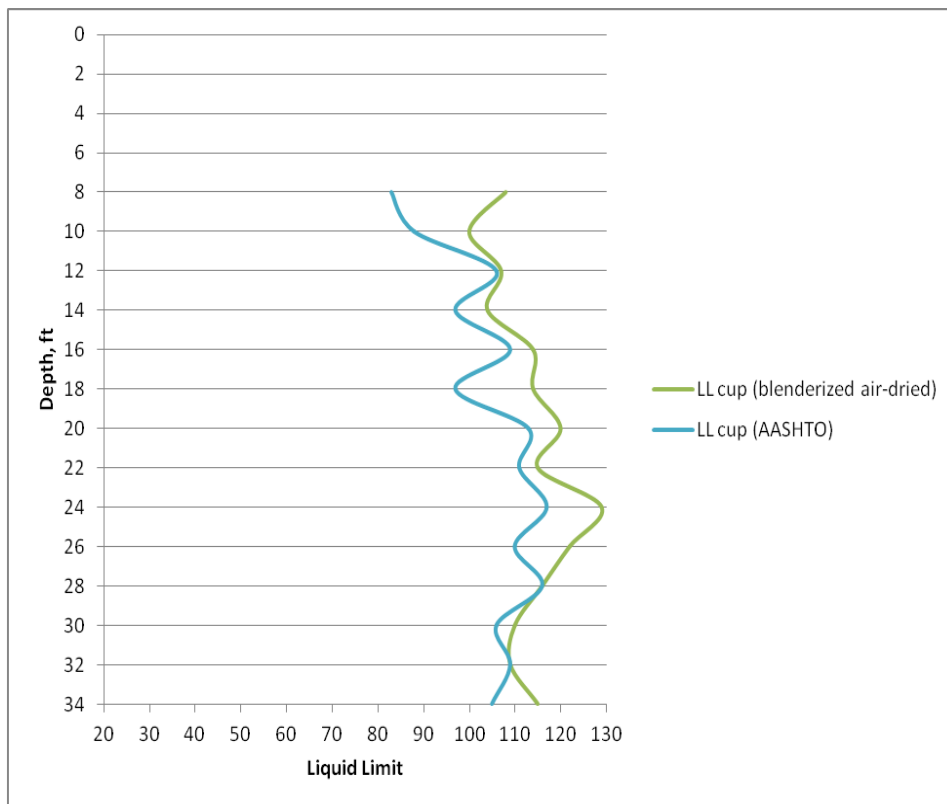


Figure 105. LL results from two different sample preparation methods

Figure 106 shows small but noticeable differences between the standard and blenderized SL results. **Figure 107** shows the much more noticeable differences between the standard and blenderized VC results. **Figure 108** shows that blenderized LL and SI did not correlate with blenderized VC results.

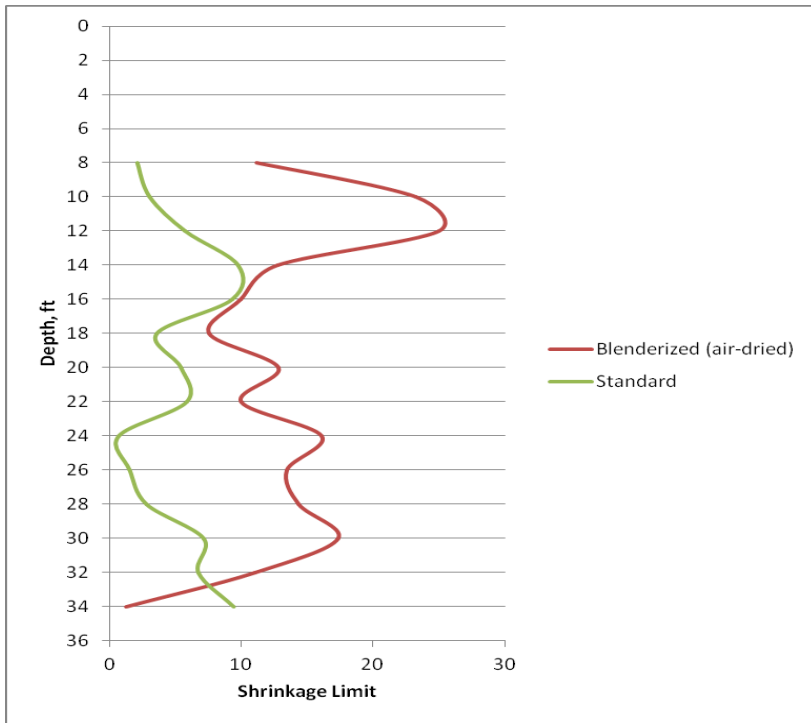


Figure 106. SL results from two different sample preparation methods

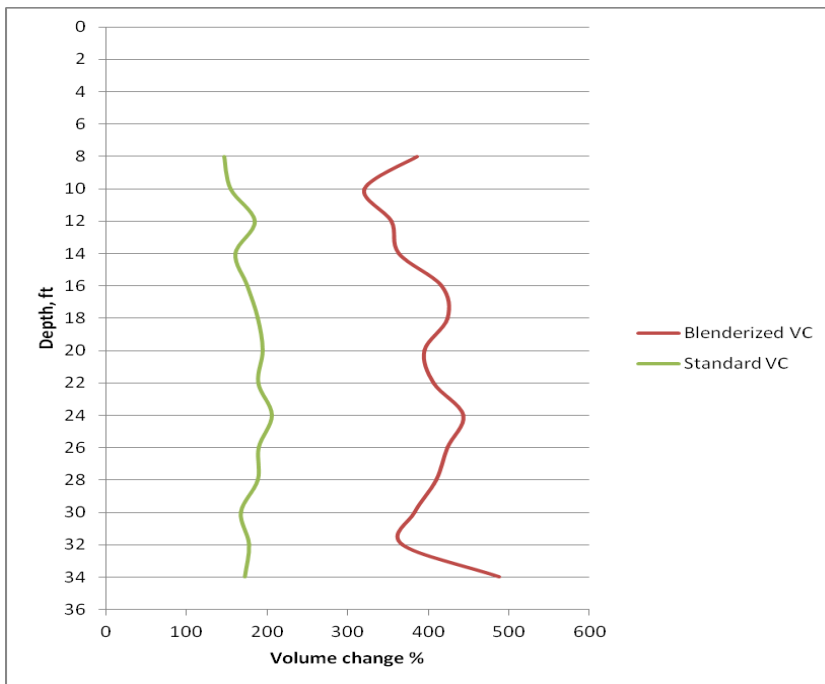


Figure 107. VC results from two different sample preparation methods

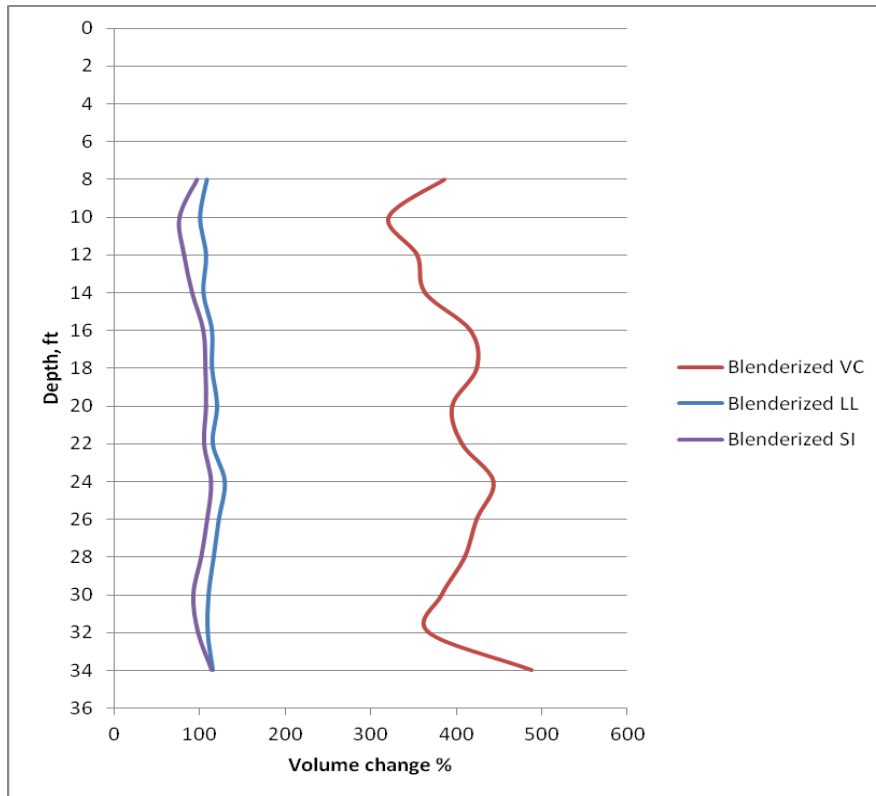


Figure 108. Blenderized LL and VC results did not correlate.

British Fall Cone Tests

Figure 109 shows the undisturbed sample British Fall Cone test results, and **Figure 110** shows the blenderized sample results. The undisturbed samples had a much more limited natural water content range than did the blenderized sample water contents. **Figure 111** shows the LL and PL values predicted from the blenderized Fall Cone results. The undisturbed LL and PL values were selected in a similar fashion, and results are plotted in **Figures 112 and 113**. The regression lines shown in all the plots have R^2 values greater than 0.90.

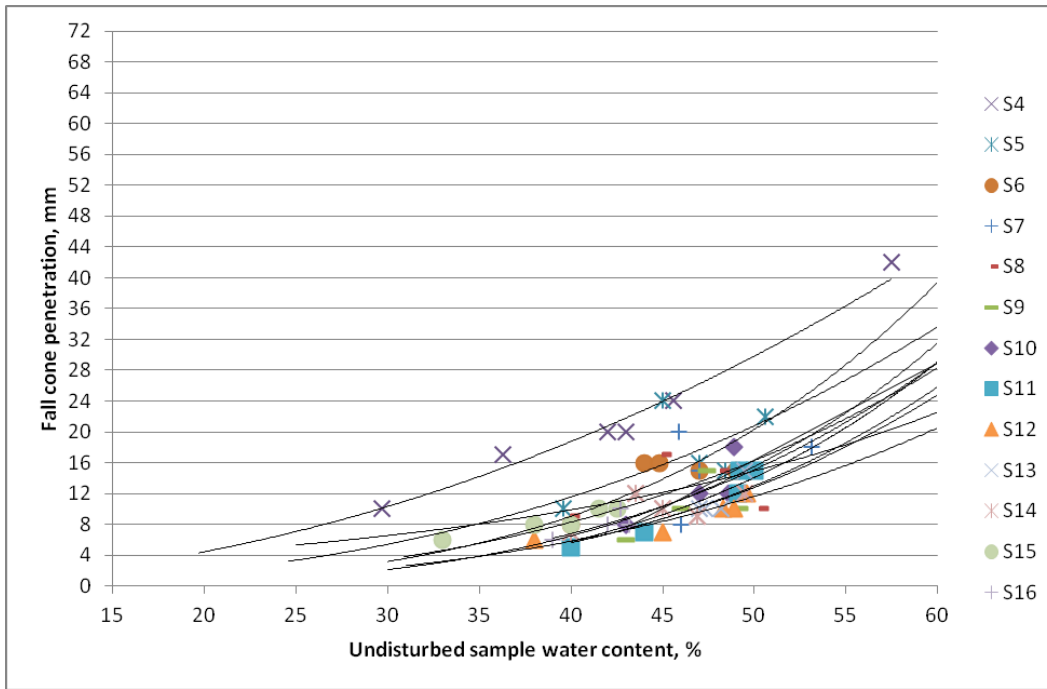


Figure 109. Undisturbed sample Fall Cone results.

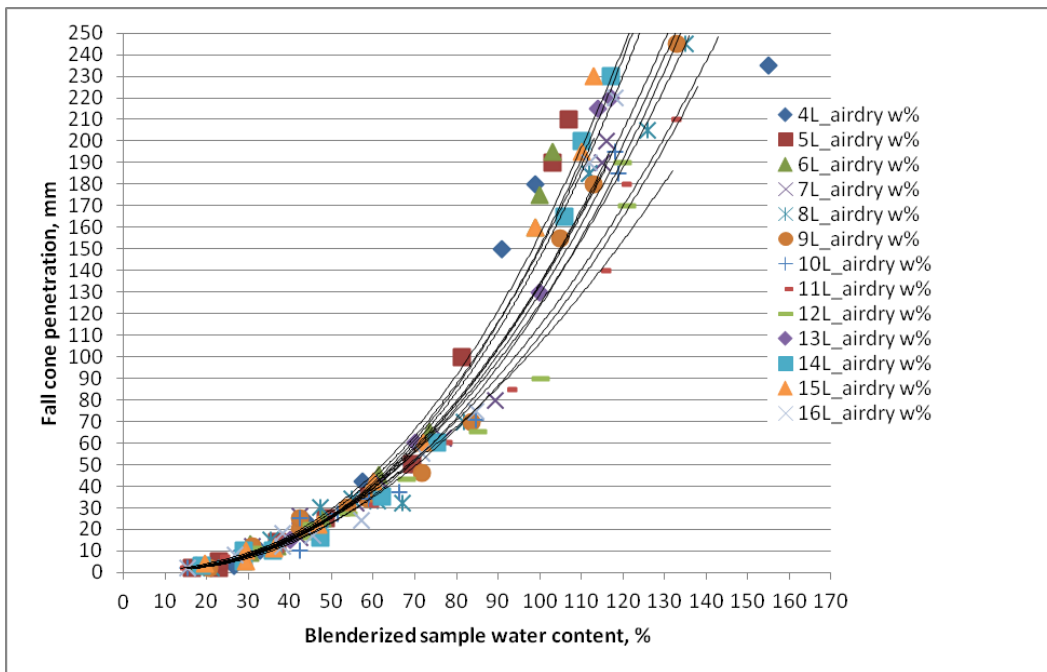


Figure 110. Blenderized sample Fall Cone results.

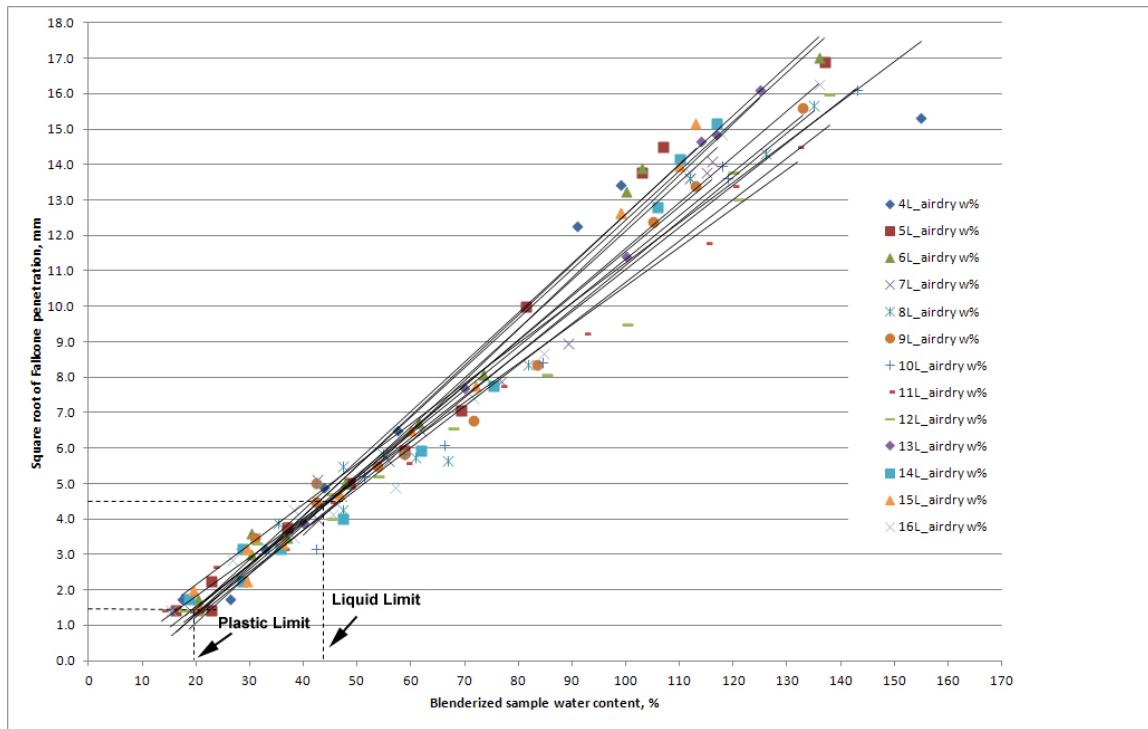


Figure 111. LL and PL values picked from the Fall Cone plot.

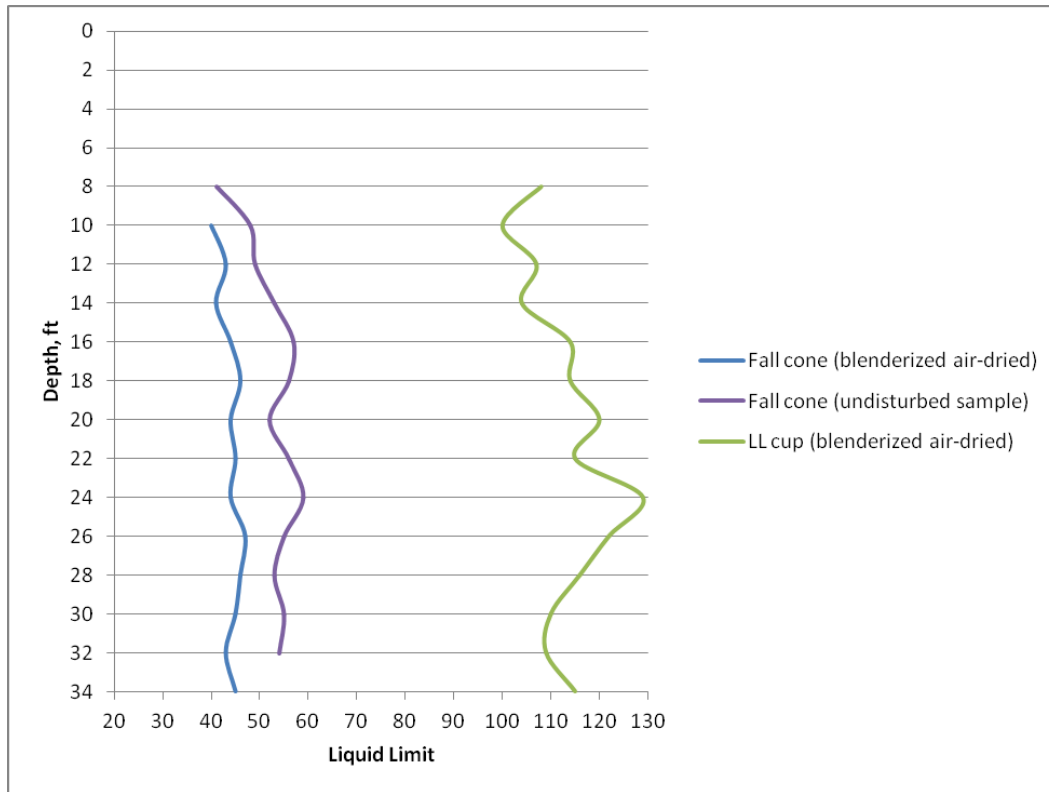


Figure 112. LL values picked from the Fall Cone plot compared to blenderized LL cup values.

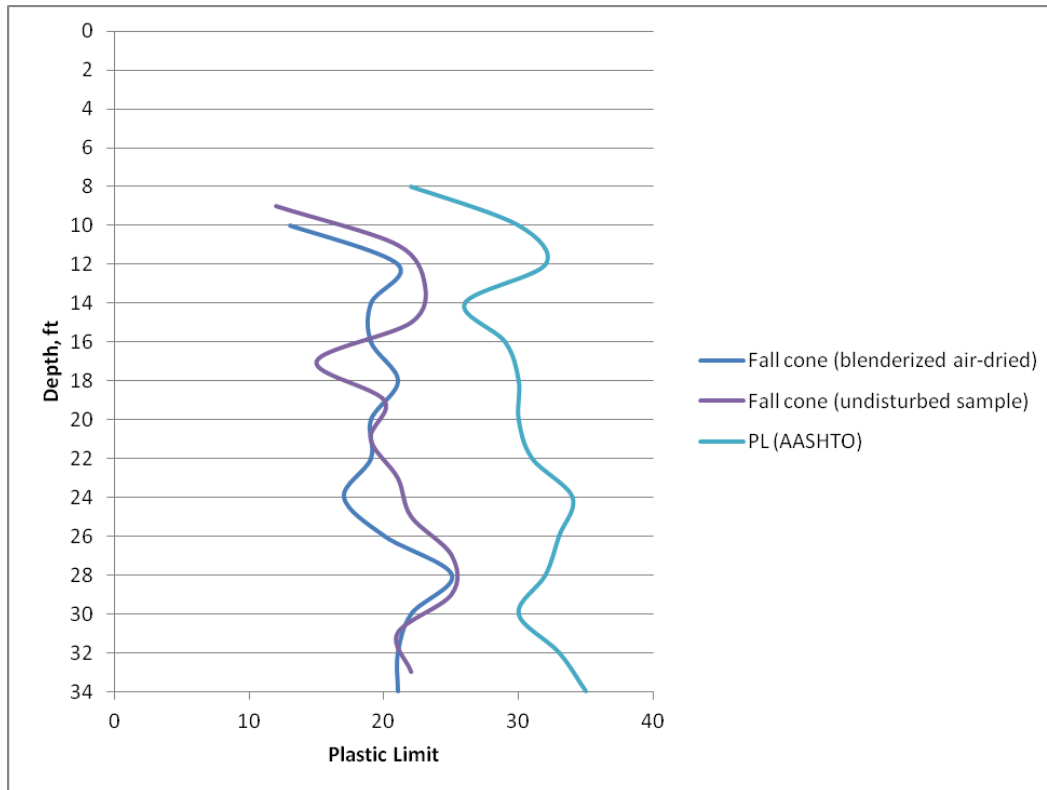


Figure 113. PL values picked from the Fall Cone plot compared to standard PL values.

Shrink-Swell Vertical Strains

The potential vertical swell due to loading or unloading was explored for the purpose of enabling swell strain prediction if a soil under stress at its natural water content is inundated with water. For example, water seepage through a crack will cause swelling strain suppressed by an imposed or in-situ overburden pressure.

Secondly, the potential vertical movement (shrinkage and/or swelling) of a soil with minimal loading was explored. For example, a fresh undercut exposes soil that may either shrink or swell from its natural water content state, depending on drying or wetting conditions.

Development of swell strain versus load curves

Four undisturbed sample slices from each soil layer were individually loaded to develop that sampled interval's swell strain curves as illustrated in **Figure 114**. **Figure 115** shows the curves plotted against sample depth. The regression curves for each sample (sample S7 illustrated in **Figure 116**) were derived from the discrete data points. The curves were

then used for plotting the potential swell strains as continuous functions of normalized stresses at each sample depth (**Figure 117**).

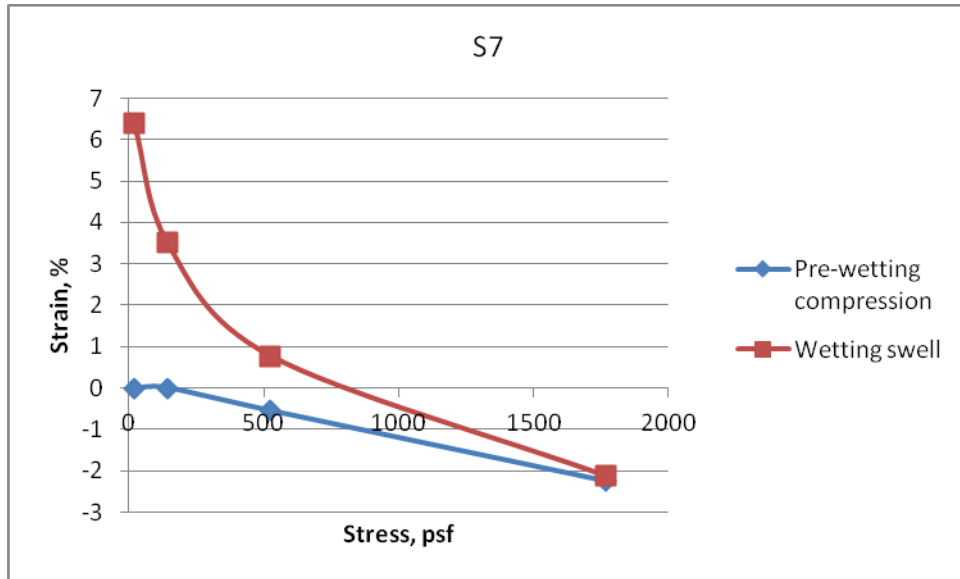


Figure 114. Sample S7 (depth interval 15 – 17 ft) swell strain versus consolidation load curves. The net swell strain at each load increment is the vertical difference between the pre-wetting compression curve and the inundation wetting curve.

Table 19 lists the regression curve equations of the plotted data.

Table 19. Swell strain versus consolidation load

Sample number	Regression curve equations ($R^2 > 0.95$) for Swell % versus Load	
	Undisturbed samples at natural water contents were loaded from 20psf up to overburden stress and allowed to swell during inundation	Undisturbed samples at natural water contents were allowed to swell during inundation. Load normalized to overburden stress.
	Y = swell strain % ; X = load, psf	Y = swell strain %; X = load/overburden
S1	$Y = -2.408 \ln(x) + 15.36$	$Y = -2.408 \ln(x) + 1.2047$
S2	$Y = -3.745 \ln(x) + 25.294$	$Y = -3.745 \ln(x) + 1.2545$
S3	$Y = -2.601 \ln(x) + 19.913$	$Y = -2.601 \ln(x) + 2.3288$
S4	$Y = -2.097 \ln(x) + 16.203$	$Y = -2.097 \ln(x) + 1.5114$
S5	$Y = -325 \ln(x) + 16.755$	$Y = -325 \ln(x) + 0.0386$
S6	$Y = -2.252 \ln(x) + 16.125$	$Y = -2.252 \ln(x) - 0.4189$
S7	$Y = -1.432 \ln(x) + 10.61$	$Y = -1.432 \ln(x) - 0.099$
S8	$Y = -1.104 \ln(x) + 8.239$	$Y = -1.104 \ln(x) - 0.1411$

Sample	Regression curve equations ($R^2 > 0.95$) for Swell % versus Load	
S9	$Y = -2.183 \ln(x) + 17.778$	$Y = -2.183 \ln(x) + 0.9685$
S10	$Y = -1.01 \ln(x) + 8.99$	$Y = -1.01 \ln(x) + 1.1246$
S11	$Y = -0.358 \ln(x) + 3.5$	$Y = -0.358 \ln(x) + 0.6754$
S12	$Y = -1.352 \ln(x) + 10.57$	$Y = -1.352 \ln(x) - 0.1919$
S13	$Y = -0.912 \ln(x) + 7.235$	$Y = -0.912 \ln(x) - 0.0931$
S14	$Y = -0.958 \ln(x) + 8.177$	$Y = -0.958 \ln(x) + 0.4087$
S15	$Y = -0.573 \ln(x) + 4.75$	$Y = -0.573 \ln(x) + 0.0625$
S16	$Y = -0.717 \ln(x) + 6.231$	$Y = -0.717 \ln(x) + 0.3201$

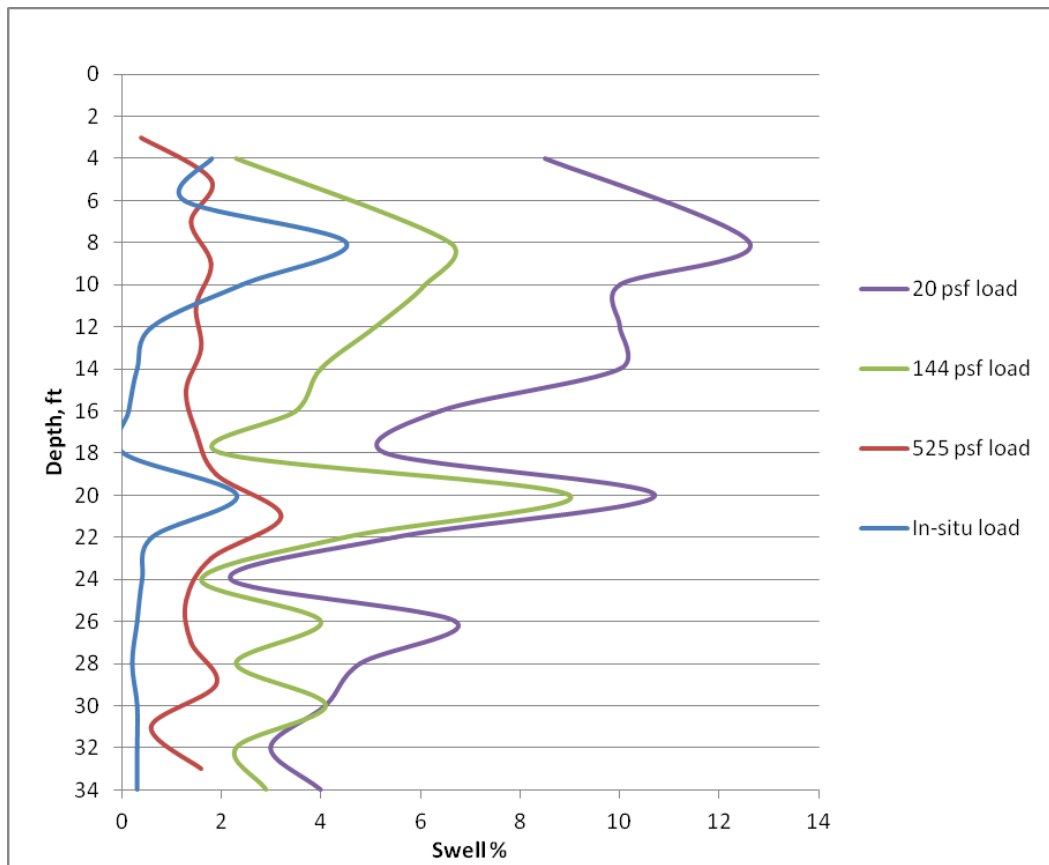


Figure 115. Discrete net swell strain and load increment points plotted at each sample interval depth.

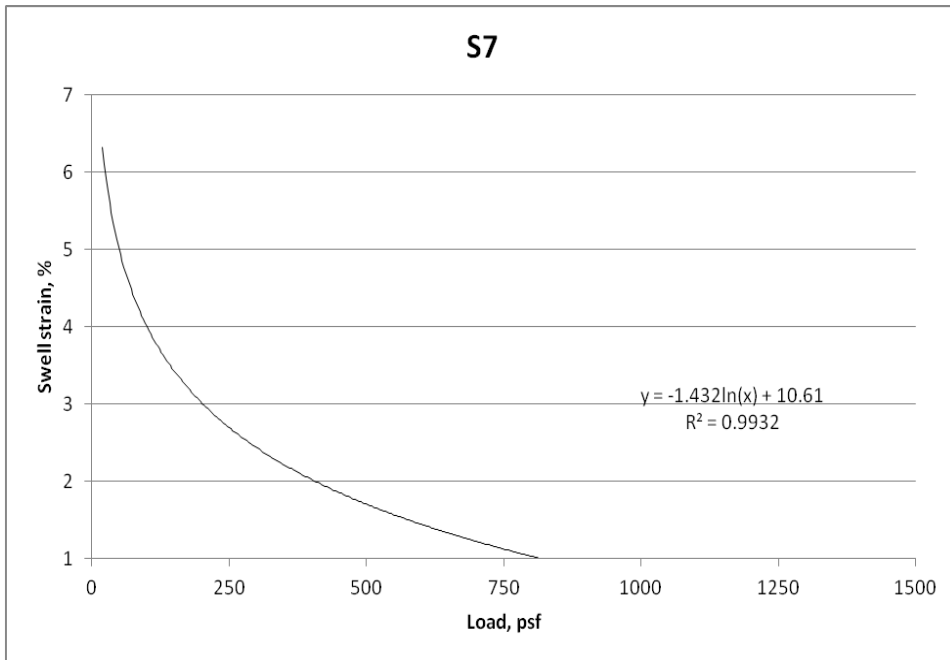


Figure 116. Regression curve for continuous net swell strain and load function, shown for one sample interval (S7).

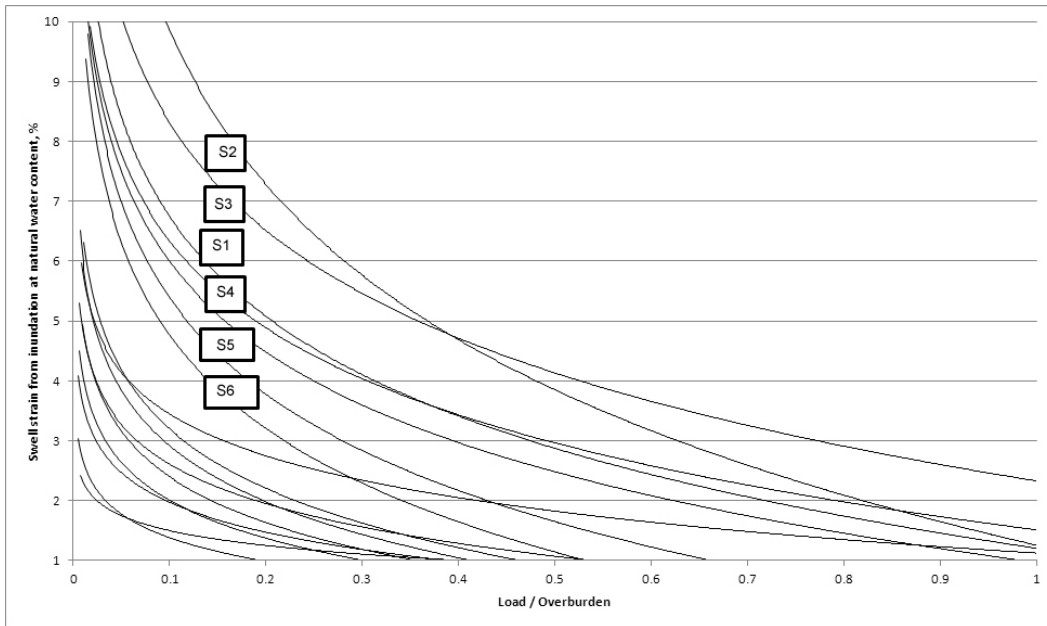


Figure 117. Regression curves for swell strain as a function of normalized loading. The upper-depth samples S1 thru S6 (at their natural water content) exhibited greater swell when their loadings were less than their in-situ (overburden) stresses.

No-load swell strain curves

Swell strain as a function of water content state was developed from samples inundated with water under minimal loading (less than 20 psf). **Figure 118** shows the regression curves.

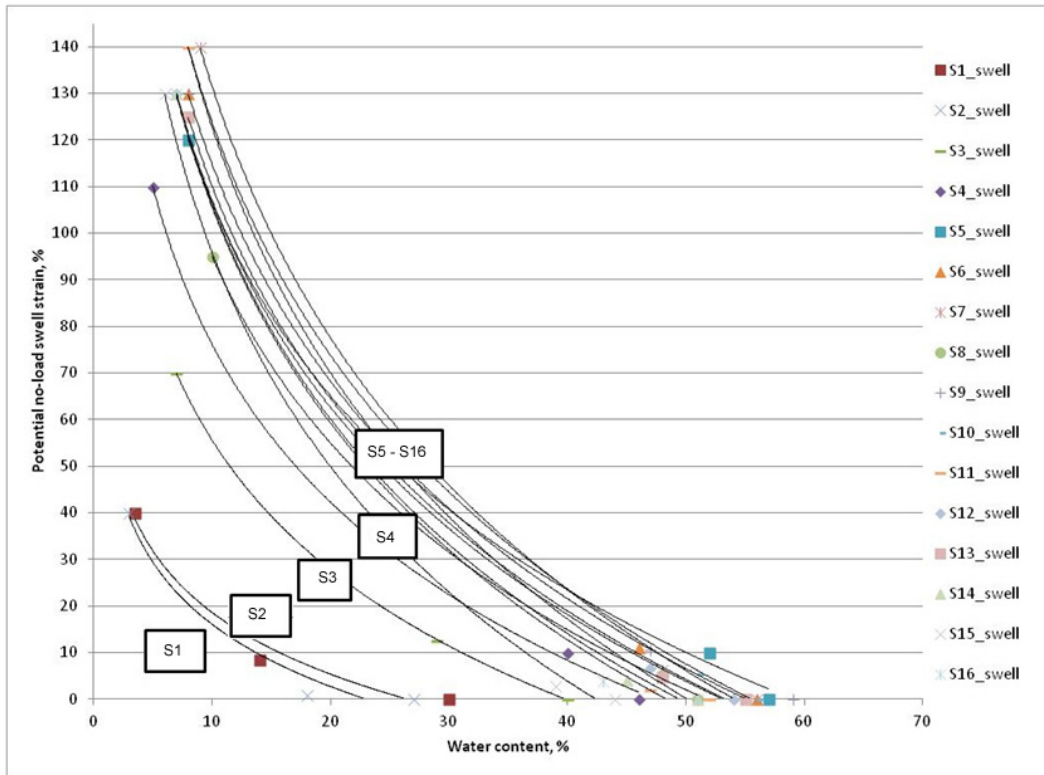


Figure 118. Regression curves for no-load swell strain as a function of water content. The upper-depth samples S1 thru S4 swelled less than lower-depth samples at equal water contents. For all samples, the lower the water content, the higher the swell potential.

No-load shrinkage strain curves

As each sample was dried from its natural water content it exhibited negative strain (i.e. shrinkage). **Figure 119** shows the measured shrinkage strain during air-drying.

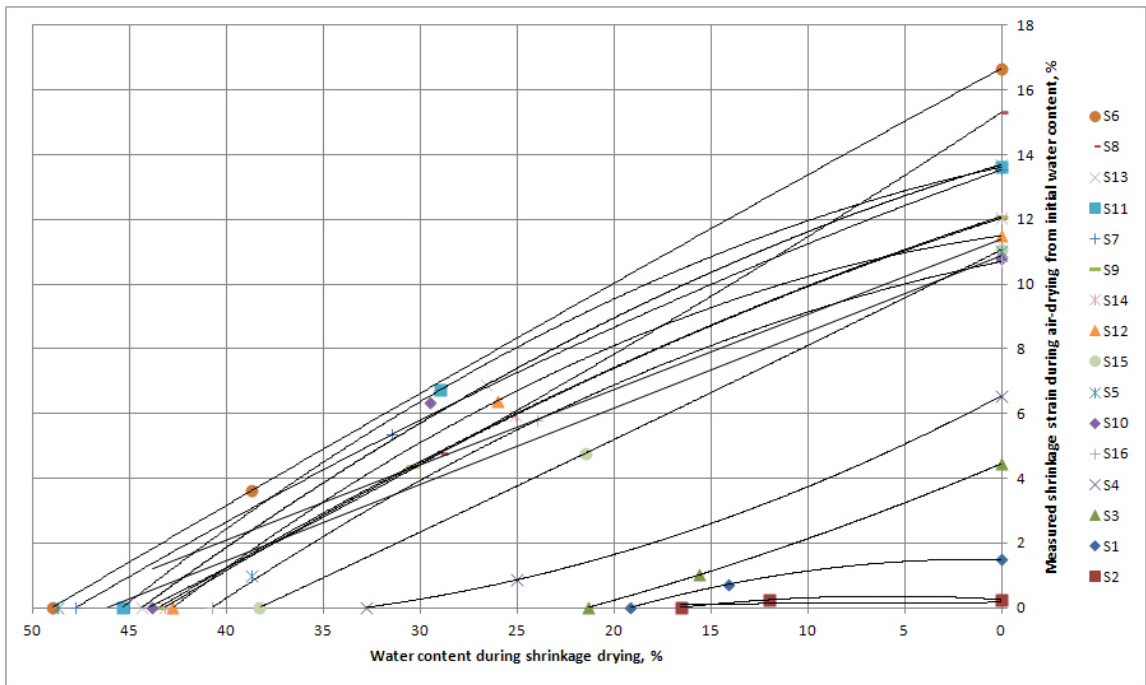


Figure 119. No-load shrinkage strain measured as a function of water content during air-drying

Figure 120 shows the shrinkage potential, which is basically a mirror image of the measured shrinkage regression curves. The shrinkage-water content data showed that the higher the initial water content, the higher the potential for shrinkage during air-drying.

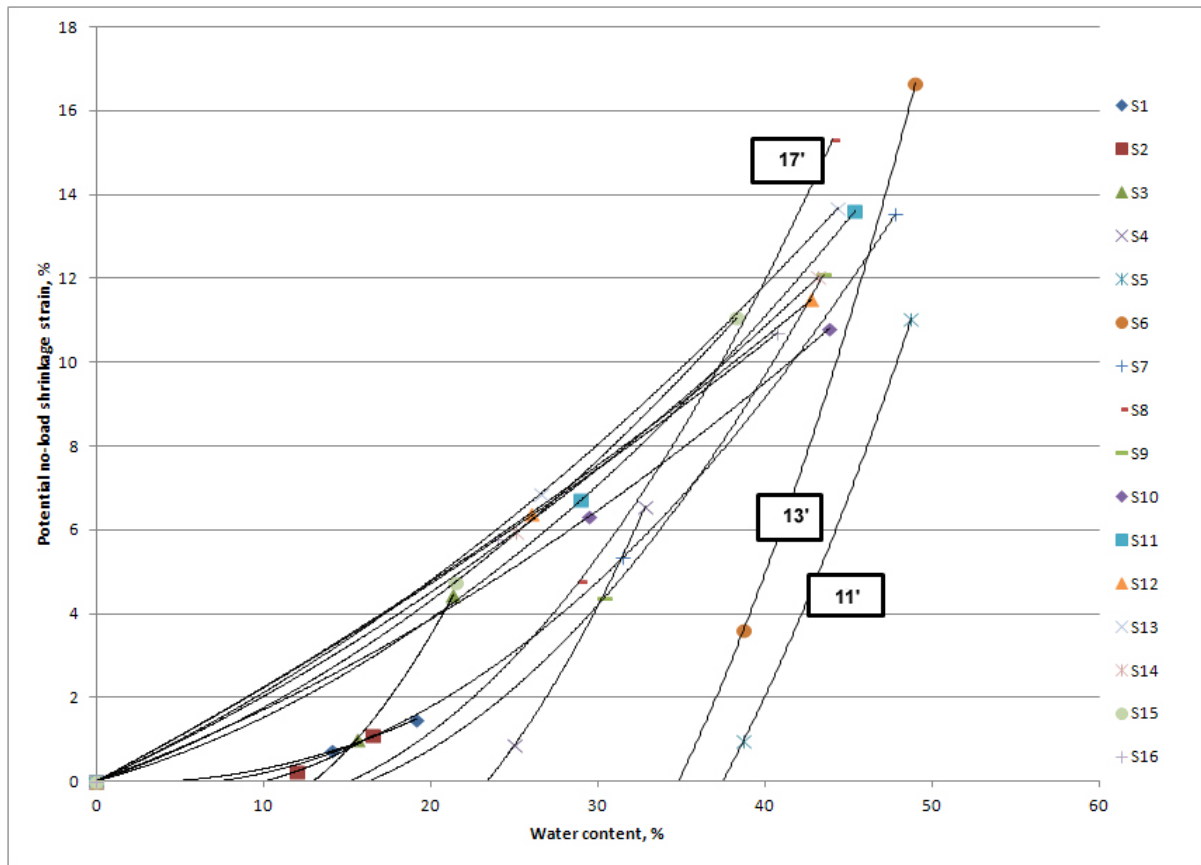


Figure 120. Regression curves for no-load shrinkage potential strain as a function of water content during air-drying; the higher the initial water content, the higher the probability of shrinkage strain if the soil is dried.

Development of no-load combined shrink-swell curves

Applied to a field site, a combined shrink-swell curve would be useful for specifying an optimum water content range during construction on an exposed road embankment excavation. No-load shrink-swell regression curves were plotted together to generate a combined no-load potential shrink-swell relationship as illustrated in **Figure 121**. An example (sample S7) is shown in **Figure 122**. For example, when soil S7 was dried to a water content below about 45%, it developed a swell potential that increased as the water content dropped.

Table 20 lists the regression curve equations from the plotted data.

Table 20. No-load swell and shrinkage strains versus water content

Sample number	Regression curve equations ($R^2 > 0.95$) for No-load Strain % versus Water content %	
	Undisturbed samples at natural water contents minimally loaded (up to 20psf stress) and allowed to swell during inundation	Undisturbed samples at natural water contents allowed to shrink by air-drying (no load stress)
	Y = swell strain % ; X = water content %	Y = shrink strain %; X = water content %
S1	$Y = -19.12 \ln(x) + 62.64$	$Y = 0.0718 (x) - 0.0603$
S2	$Y = -19.28 \ln(x) + 60.49$	$Y = 0.0102 (x^2) - 0.1026 (x) + 0.0011$
S3	$Y = -40.23 \ln(x) + 148.25$	$Y = 0.0249 (x^2) - 0.3237 (x) + 0.0013$
S4	$Y = -48.92 \ln(x) + 188.84$	$Y = 0.0211 (x^2) - 0.4936 (x) + 0.0015$
S5	$Y = -60.05 \ln(x) + 244.98$	$Y = 0.0201 (x^2) - 0.75 (x) + 0.0018$
S6	$Y = -67.29 \ln(x) + 269.81$	$Y = 0.024 (x^2) - 0.8349 (x) + 0.0018$
S7	$Y = 0.0559 (x^2) - 6.61 (x) + 194.97$	$Y = 0.007 (x^2) - 0.0509 (x) + 0.0011$
S8	$Y = -57.79 \ln(x) + 228.1$	$Y = 0.012 (x^2) - 0.1824 (x) + 0.0012$
S9	$Y = -65.94 \ln(x) + 266.86$	$Y = 0.0102 (x^2) - 0.1663 (x) + 0.0012$
S10	$Y = -72.24 \ln(x) + 290.2$	$Y = 0.0022 (x^2) + 0.1484 (x) + 0.0009$
S11	$Y = -76.19 \ln(x) + 298.28$	$Y = 0.0042 (x^2) + 0.1103 (x) + 0.0009$
S12	$Y = -64.11 \ln(x) + 254.68$	$Y = 0.0013 (x^2) + 0.211 (x) + 0.0008$
S13	$Y = -65.8 \ln(x) + 261.67$	$Y = 0.0028 (x^2) + 0.1831 (x) + 0.0008$
S14	$Y = -66.42 \ln(x) + 259.11$	$Y = 0.0023 (x^2) + 0.1792 (x) + 0.0008$
S15	$Y = -66.39 \ln(x) + 248.79$	$Y = 0.004 (x^2) + 0.1353 (x) + 0.0009$
S16	$Y = -67.08 \ln(x) + 260.2$	$Y = 0.0013 (x^2) + 0.2098 (x) + 0.0008$

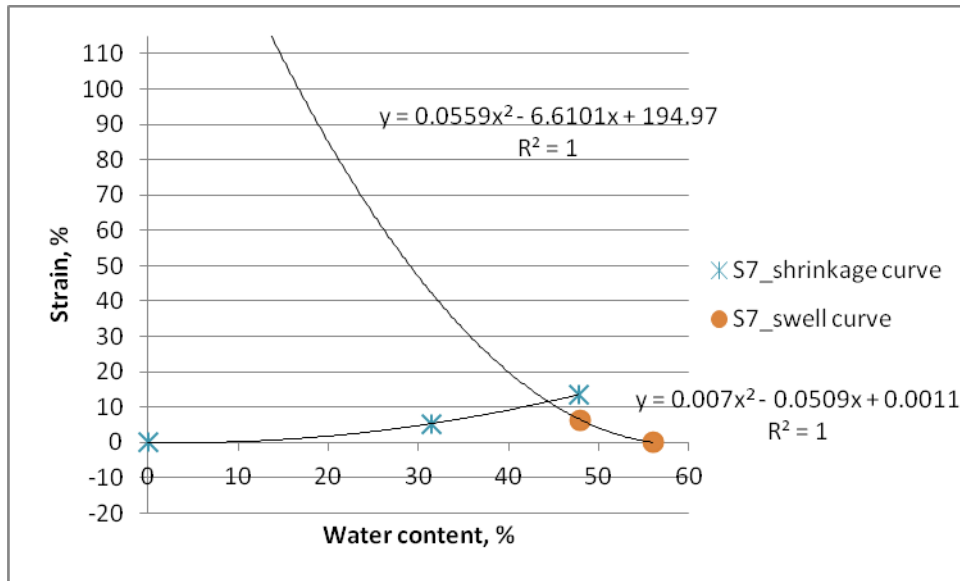


Figure 121. Superimposed no-load shrink-swell strain plotted versus water content for sample S7

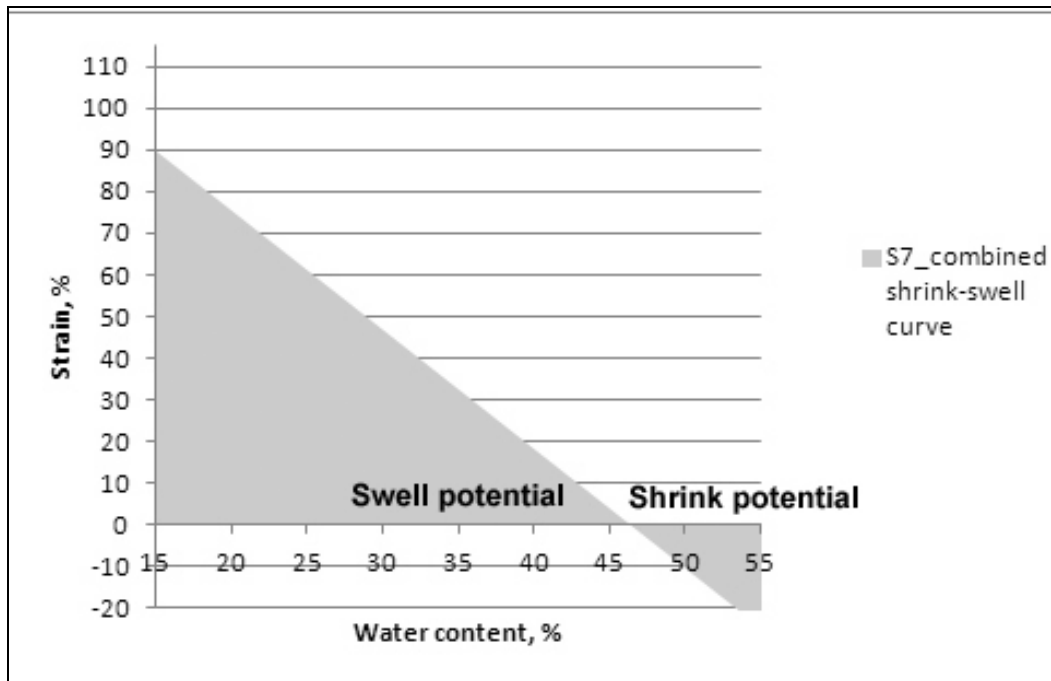


Figure 122. Combined no-load shrink-swell strain plotted versus water content for sample S7

Vertical Swell Pressure

Development of low-strain swell pressure curves

Figure 123 shows the PVC swell pressures normalized to their in-situ overburden pressures and plotted by depth (with regression line shown). The samples were allowed to swell as they exerted pressure on the proving ring but their measured strains were less than about 1%, essentially indicating a no-strain condition.

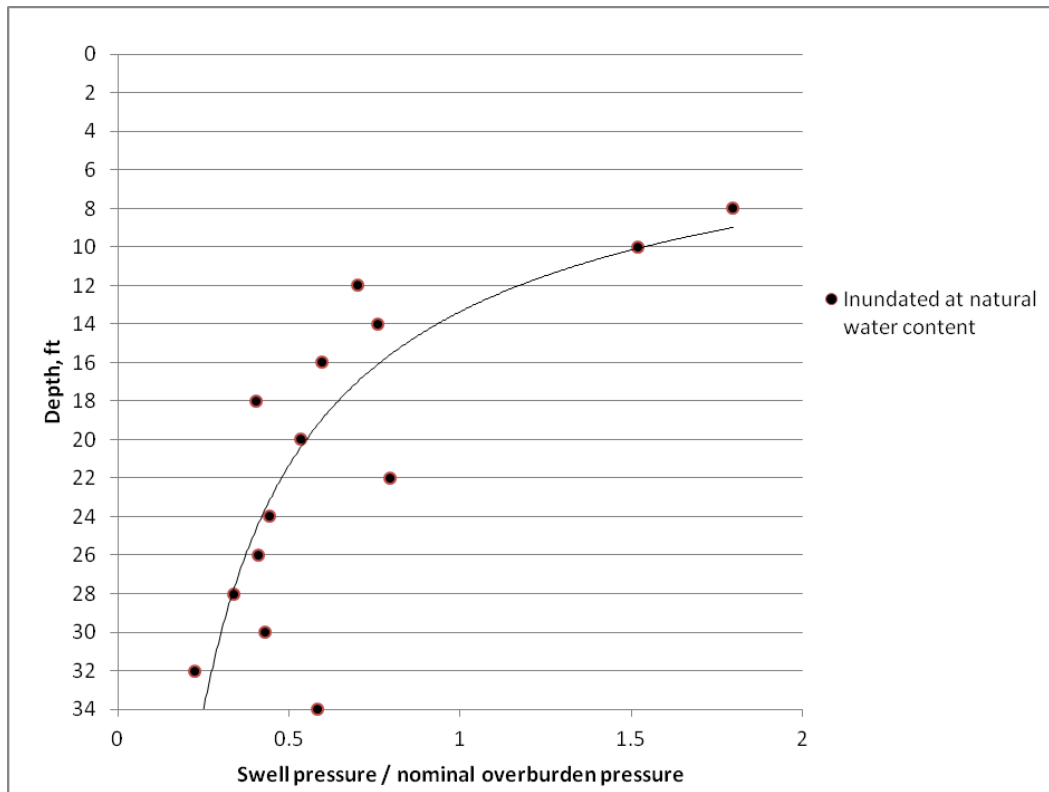


Figure 123. Low-strain (less than 1%) swell pressures normalized to nominal overburden pressures for each sample interval.

Note that the 12 – 14 ft depth interval is where the swell pressures are approximately equal to the in-situ overburden pressures. This agrees with the trend of the consolidation test results shown in above **Figure 117**, where the upper-depth samples have higher swell strains at their overburden pressures when compared to the lower-depth samples.

Figure 124 illustrates the potential sensitivity to water content state, where a drier sample will tend to exert higher swell pressures if given access to free water.

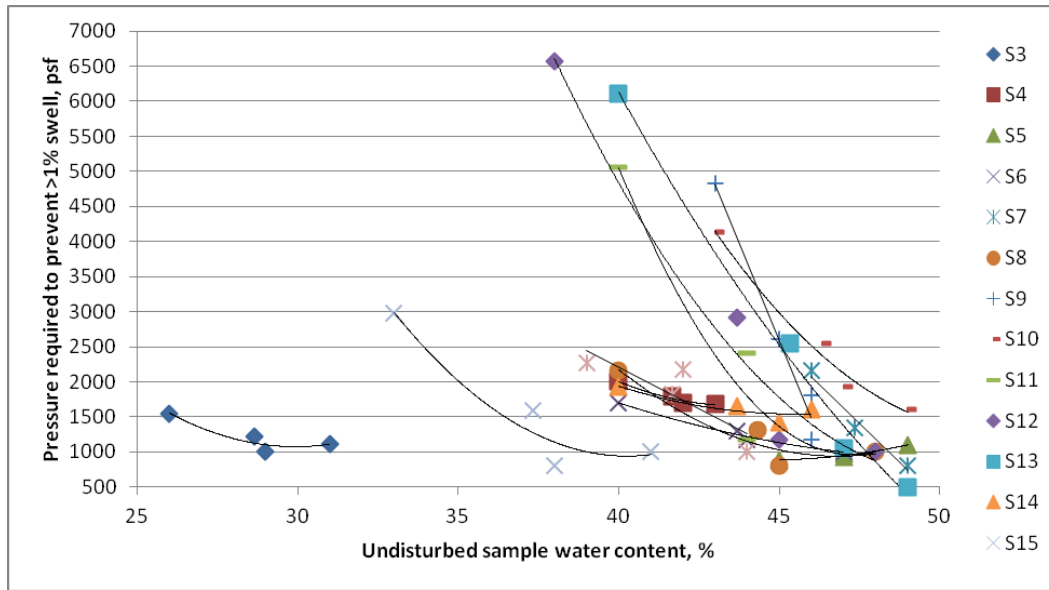


Figure 124. Progressively-drier samples exerted exponentially-higher swell pressures after inundation.

Table 21 lists the regression curve equations from the plotted data.

Table 21. Swell pressure versus water content

Sample number	Regression curve equations ($R^2 > 0.95$) for low-strain Swell Pressure versus Water content %	
	Undisturbed samples at varying initial water contents allowed to exert swell pressure with minimal (< 1%) swell strain during inundation	
	Y = swell pressure, psf ; X = water content %	Applicable water content % range
S1	N/A	N/A
S2	N/A	N/A
S3	$Y = 31.057 (x^2) - 1859.7 (x) + 28914$	$25\% < x < 35\%$
S4	$Y = 25.414 (x^2) - 2219.7 (x) + 50129$	$35\% < x < 45\%$
S5	$Y = 11.15 (x^2) - 994.7 (x) + 23069$	$40\% < x < 50\%$
S6	$Y = 6.6707 (x^2) - 680.6 (x) + 18250$	$40\% < x < 50\%$
S7	$Y = - 448.39 (x) + 22706$	$40\% < x < 50\%$
S8	$Y = 26.393 (x^2) - 2472.6 (x) + 58851$	$40\% < x < 50\%$
S9	$Y = - 1112.9 (x) + 52683$	$40\% < x < 50\%$
S10	$Y = 37.908 (x^2) - 3917.2 (x) + 102493$	$40\% < x < 50\%$
S11	$Y = 77.202 (x^2) - 7302.1 (x) + 173602$	$40\% < x < 50\%$
S12	$Y = 38.9 (x^2) - 3919.1 (x) + 99363$	$40\% < x < 50\%$

Sample number	Regression curve equations ($R^2 > 0.95$) for low-strain Swell Pressure versus Water content %	
	Undisturbed samples at varying initial water contents allowed to exert swell pressure with minimal (< 1%) swell strain during inundation	
	Y = swell pressure, psf ; X = water content %	Applicable water content % range
S13	$Y = 20.613 (x^2) - 2472.1 (x) + 72027$	$35\% < x < 50\%$
S14	$Y = 13.239 (x^2) - 1204 (x) + 28916$	$35\% < x < 50\%$
S15	$Y = 38.983 (x^2) - 3138.6 (x) + 64113$	$30\% < x < 45\%$
S16	$Y = - 237.87 (x) + 11729$	$35\% < x < 50\%$

The swell pressures normalized to a load such as the in-situ overburden may then be plotted using the above equations. For example, **Figure 125** shows the regression line for sample S7 normalized swell pressure as a function of initial water content state.

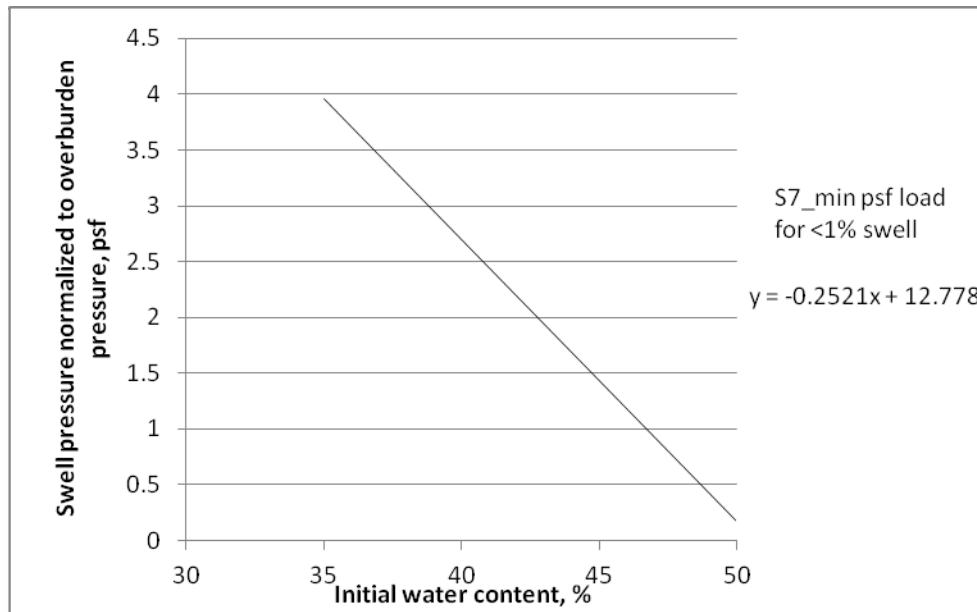


Figure 125. Sample S7 regression line for normalized swell pressures based on initial water contents.

Australian Shrink-Swell Tests

Figure 126 shows the Australian Shrink-Swell and Instability Indices (Iss and Ipt) plotted by depth. The Iss is a good indicator of the active zone depth (about 13 feet below surface), and the Ipt is for calculating the expected vertical displacement of each soil layer. The Ipt assumes that shrinkage strain is a proxy for swelling strain, applies to a no-load condition, and requires an estimate of the potential total suction change within the soil layer.

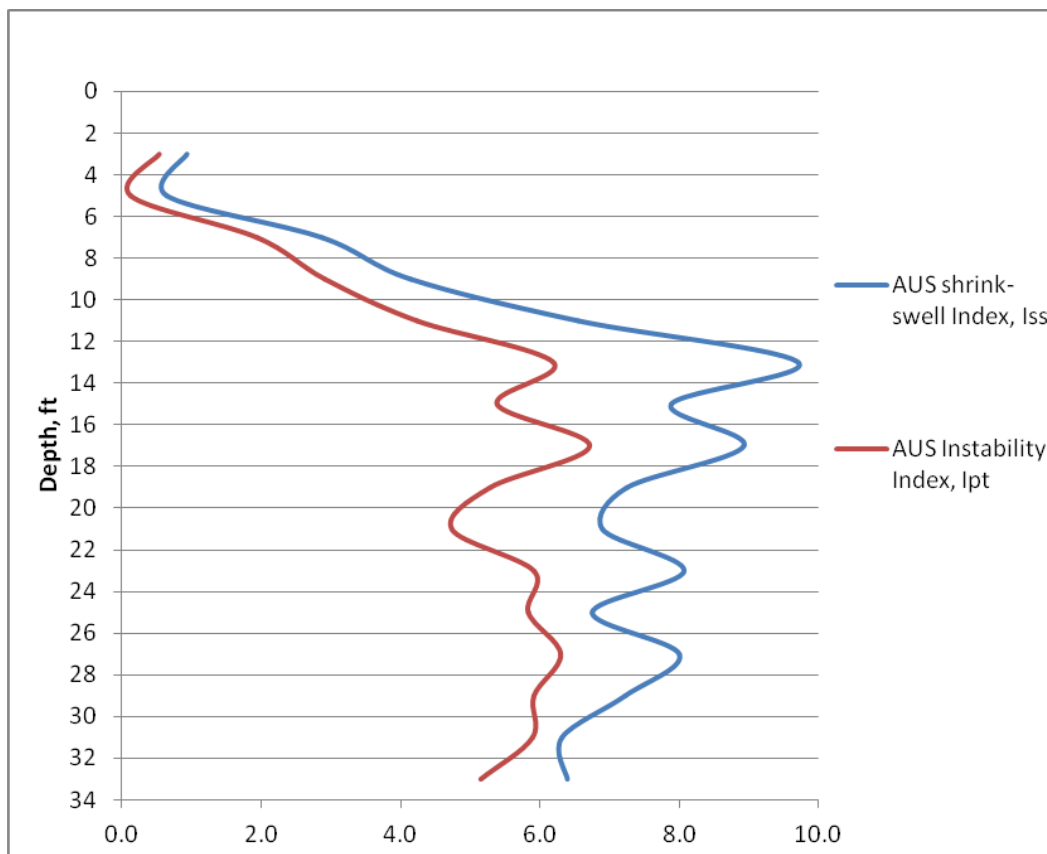


Figure 126. Australian Test Indices

An alternative to the Australian Shrink-Swell Index Test

Figure 127 illustrates an alternate method to the Iss. Instead of requiring a consolidation cell loaded to 525 psf (18 lbs on a 2.5-in dia. sample), a consolidation cell loaded to 144 psf (5 lbs) yields equivalent swell data. Instead of using a 4-in length undisturbed sample for the shrinkage test, a 2- to 3-in sample yields equivalent shrinkage strain data. Note that the depth

to the active zone (13 ft) is easily identified and closely agrees with the Australian test results.

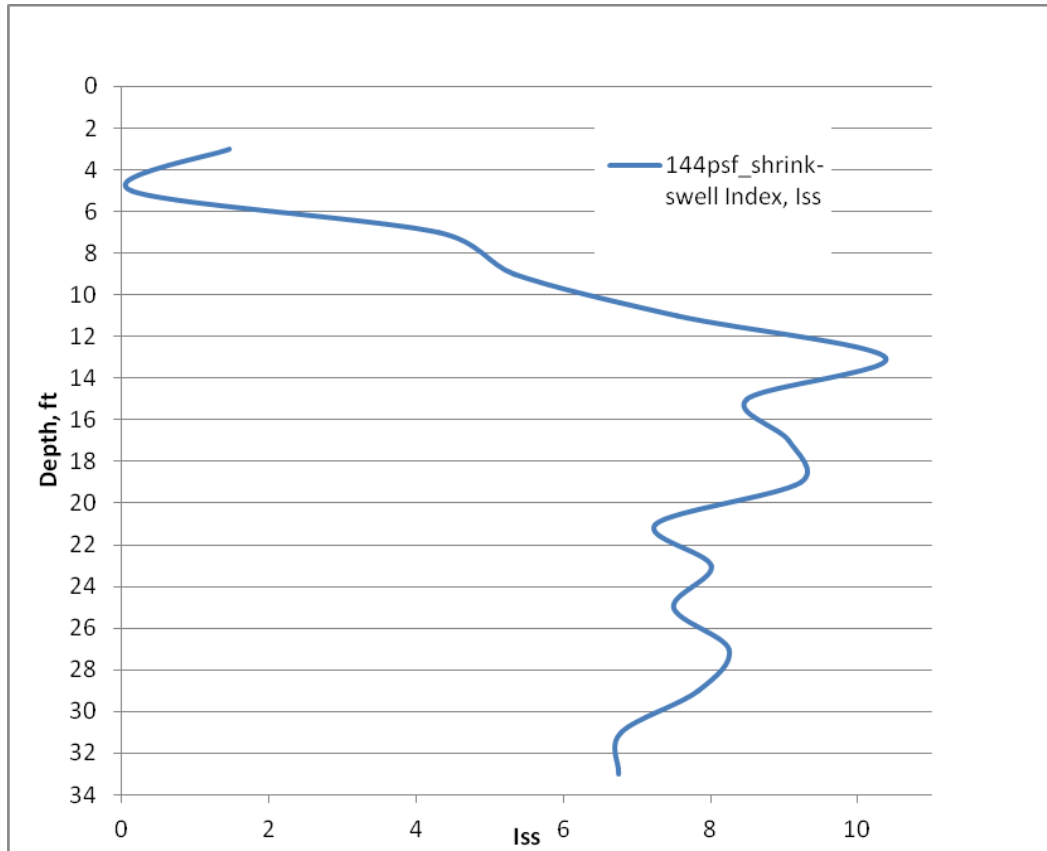


Figure 127. Results of the Alternative Iss Test.

No-load Suction Tests

Figures 128 and 129 are suction-water content plots for the filter paper and iButtons, respectively. At higher soil water contents the filter paper results were more reliable and accurate than the iButtons because the iButton data were not consistent at high (~95%) relative humidities.

The soil suction curves indicate the active zone depth begins between the S4 and S5 sample depths (approximately 13-ft below surface). This active zone depth indication also corresponded to the Australian and PVC test results.

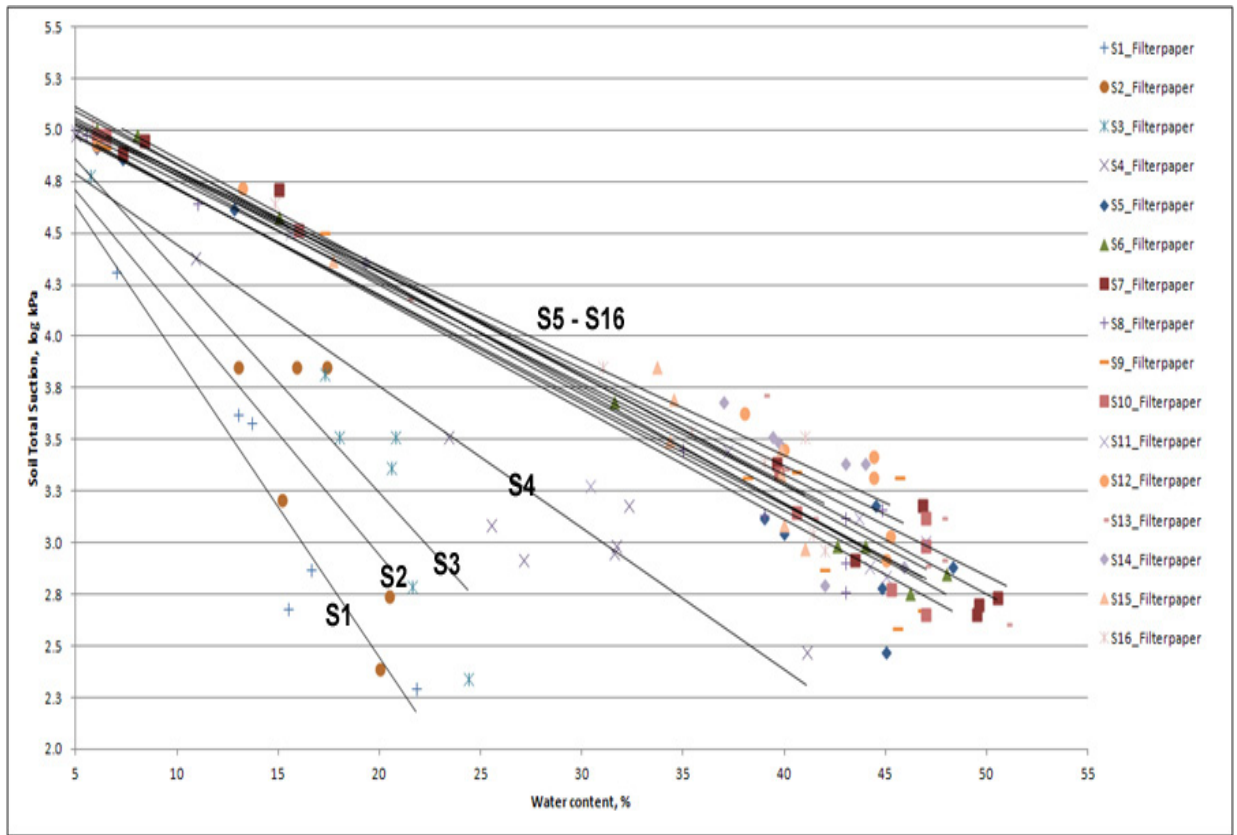


Figure 128. Soil total suction results (filter paper tests)

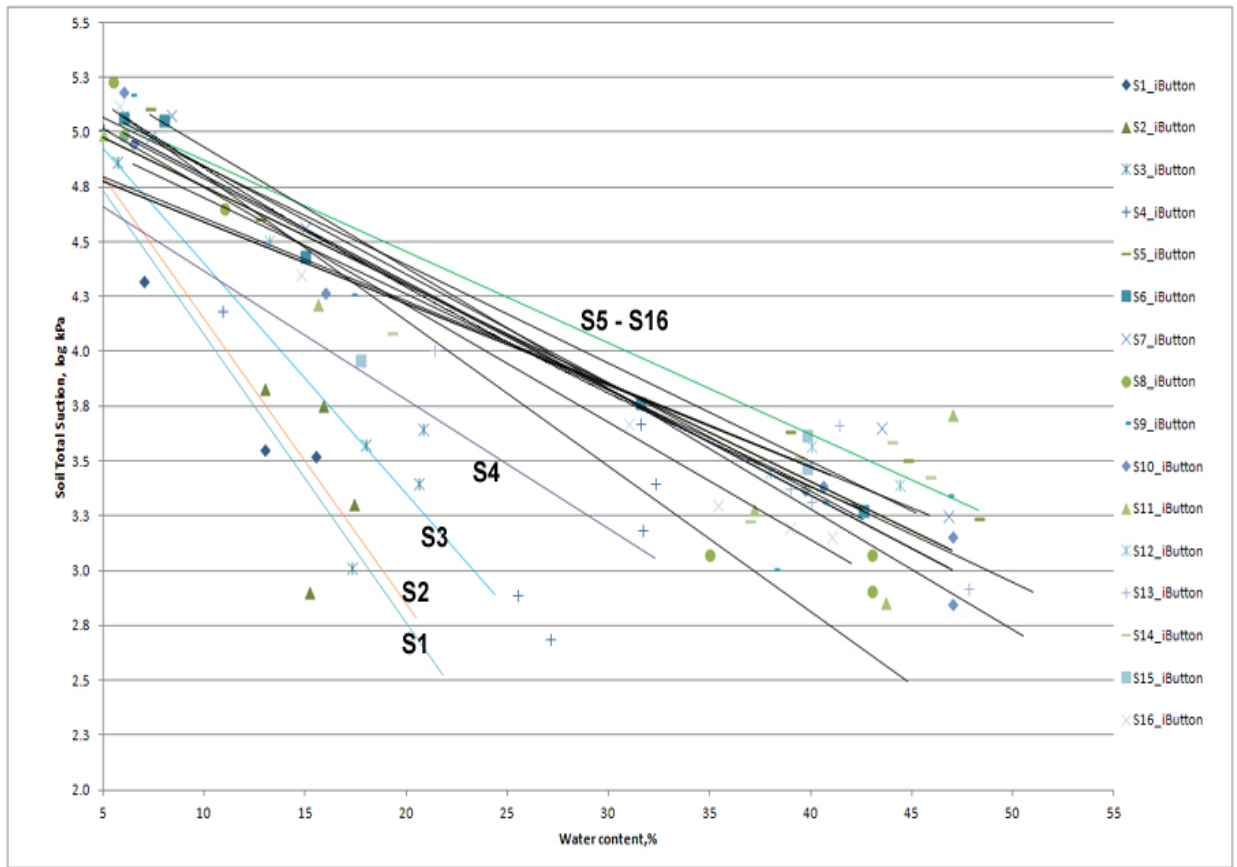


Figure 129. Soil total suction results (iButton tests)

Table 22 lists the regression curve equations for both types of suction sensors.

Table 22. Soil total suction results

Sample number	Regression curve equations ($R^2 > 0.95$) for Soil Total Suction versus Water Content %	
	Soil suction from filter paper	Soil suction from iButton™
S1	$Y = -0.1317(x) + 5.3933$	$Y = -0.1456(x) + 5.3541$
S2	$Y = -0.1297(x) + 5.443$	$Y = -0.1175(x) + 5.2881$
S3	$Y = -0.1051(x) + 5.4545$	$Y = -0.1075(x) + 5.3933$
S4	$Y = -0.0588(x) + 4.9537$	$Y = -0.0685(x) + 5.1282$
S5	$Y = -0.0417(x) + 5.2894$	$Y = -0.0534(x) + 5.2487$
S6	$Y = -0.0494(x) + 5.3401$	$Y = -0.0549(x) + 5.3852$

Sample number	Regression curve equations ($R^2 > 0.95$) for Soil Total Suction versus Water Content %	
	Undisturbed samples at varying initial water contents placed in air-tight jars at constant temperature with (1) filter paper and (2) iButton in headspace. Y = soil total suction, log kPa; X = water content %	
	Soil suction from filter paper	Soil suction from iButton™
S7	$Y = -0.055(x) + 5.4789$	$Y = -0.0527(x) + 5.3876$
S8	$Y = -0.0664(x) + 5.4656$	$Y = -0.0518(x) + 5.2317$
S9	$Y = -0.0482(x) + 5.2714$	$Y = -0.053(x) + 5.3085$
S10	$Y = -0.0485(x) + 5.2854$	$Y = -0.052(x) + 5.3159$
S11	$Y = -0.0448(x) + 5.1972$	$Y = -0.0508(x) + 5.2168$
S12	$Y = -0.0449(x) + 5.2917$	$Y = -0.046(x) + 5.2608$
S13	$Y = -0.0439(x) + 5.1397$	$Y = -0.049(x) + 5.2884$
S14	$Y = -0.0377(x) + 4.9821$	$Y = -0.047(x) + 5.2536$
S15	$Y = -0.0373(x) + 4.9636$	$Y = -0.0491(x) + 5.2463$
S16	$Y = -0.0536(x) + 5.2853$	$Y = -0.0511(x) + 5.3409$

No-load shrinkage results matched to soil suction results

Each sample exhibited increasing total suction as it dried out (i.e. the suction values increased as the shrinkage increased). The water content-strain data were matched to the water content-suction data to develop the shrinkage strain-suction regression lines shown in **Figure 130**.

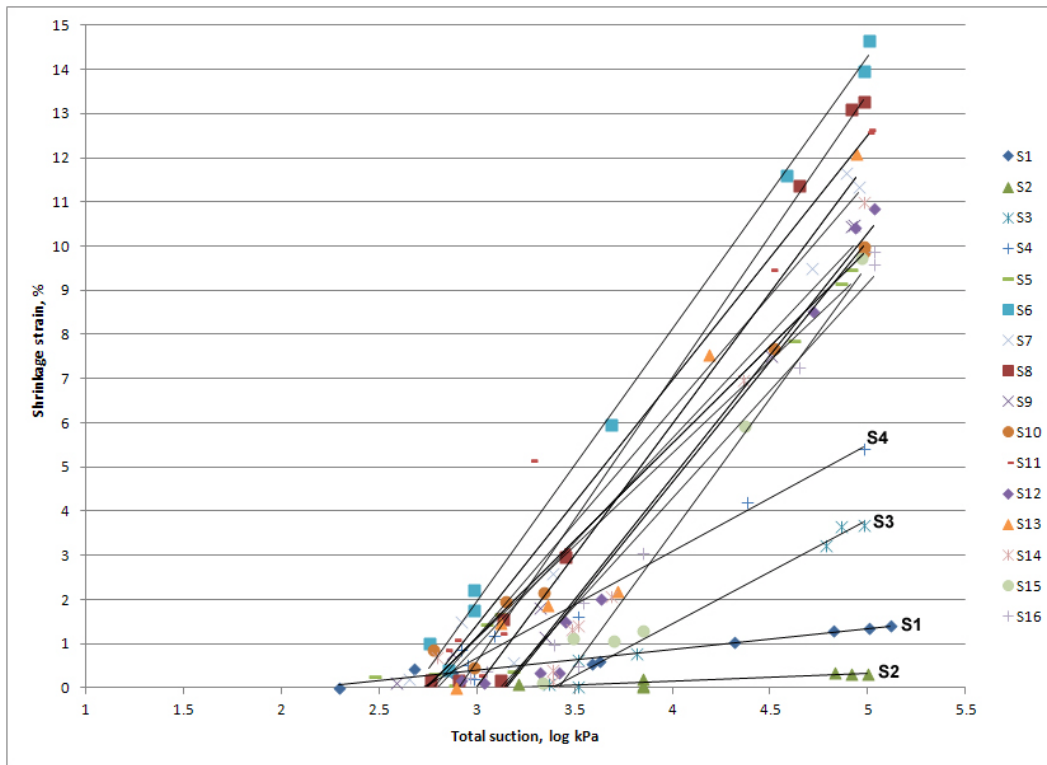


Figure 130. Regression curves for potential no-load shrinkage strain during air-drying as a function of total suction.

Soil suction-shrinkage correlations have been used as proxies for vertical swell strain by numerous researchers. The soil suction-water content curves were matched to the air-dried shrinkage-water content curves to develop soil suction-shrinkage curves. **Table 23** lists the regression curve equations based on the plotted data.

Table 23. Soil suction-shrinkage strain

Sample number	Regression curve equations ($R^2 > 0.95$) for Soil Total Suction versus Shrink Strain %	
	Correlation of soil total suction water contents to air-dried shrinkage strain water contents of undisturbed samples	
	Y = soil total suction, log kPa; X = air-dried shrinkage strain %	
S1	$Y = 2.0425 (x) + 2.2277$	
S2	$Y = 4.385 (x) + 3.4035$	
S3	$Y = 0.4189 (x) + 3.3993$	
S4	$Y = 0.4038 (x) + 2.7403$	
S5	$Y = 0.2305 (x) + 2.7601$	

Sample number	Regression curve equations ($R^2 > 0.95$) for Soil Total Suction versus Shrink Strain %
	Correlation of soil total suction water contents to air-dried shrinkage strain water contents of undisturbed samples
	Y = soil total suction, log kPa; X = air-dried shrinkage strain %
S6	$Y = 0.1617 (x) + 2.6871$
S7	$Y = 0.188 (x) + 2.8103$
S8	$Y = 0.1539 (x) + 2.917$
S9	$Y = 0.2053 (x) + 2.834$
S10	$Y = 0.2251 (x) + 2.7558$
S11	$Y = 0.1736 (x) + 2.7805$
S12	$Y = 0.1751 (x) + 3.1629$
S13	$Y = 0.1587 (x) + 3.0368$
S14	$Y = 0.1633 (x) + 3.2105$
S15	$Y = 0.1576 (x) + 3.4455$
S16	$Y = 0.1977 (x) + 3.1513$

No-load shrink-swell curves matched to soil suction results

Figure 131 illustrates the application of soil suction results to predict vertical movement potential of sample S7. The consolidation test results (potential swell versus water content) and shrinkage results (potential shrinkage versus drying water content) were matched to the soil suction results (water contents versus soil suction) to develop these curves. The filter paper results took about 2 to 3 weeks to obtain, but the iButton results took about 2 to 3 hours to obtain. These curves illustrate the utility of obtaining rapid estimates of potential heave (shrinkage and swelling) based on prior correlations.

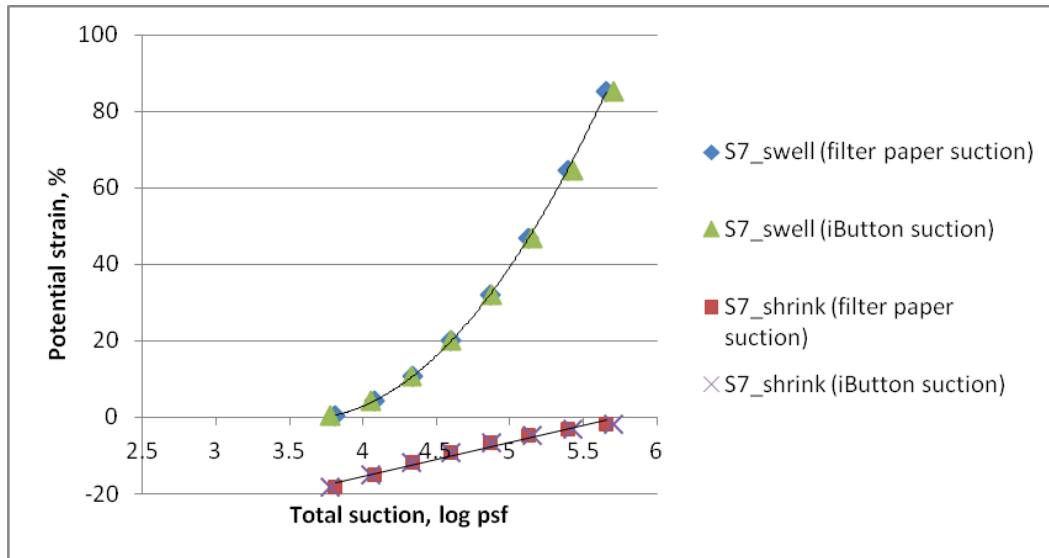


Figure 131. Sample S7 no-load shrink-swell curves matched to soil suction results

Table 24 lists the regression curve equations for potential vertical no-load swell of each soil layer, based on no-load suction results.

Table 24. Soil suction–swell strain

Sample number	Regression curve equations ($R^2 > 0.95$) for potential no-load swell strains estimated from soil suction data (for water contents between 20% and 50%)	
	Correlation of undisturbed sample total suctions to potential no-load swell strain from (1) filter paper and (2) iButton sensors. Y = potential vertical swell strain %; X = soil total suction, log psf; ($3 < \log \text{ psf} < 5.5$)	
	Soil suction from filter paper	Soil suction from iButton™
S1	$Y = 5.86 (x) - 16.7$	$Y = 6.479 (x) - 21.083$
S2	$Y = 7.323 (x) - 28.46$	$Y = 6.634 (x) - 24.94$
S3	$Y = 13.93 (x) - 36.58$	$Y = 13.189 (x) - 35.198$
S4	$Y = 22.93 (x) - 76.52$	$Y = 26.713 (x) - 96.261$
S5	$Y = 31.853 (x) - 115.11$	$Y = 40.791 (x) - 175.5$
S6	$Y = 34.719 (x) - 132.03$	$Y = 38.584 (x) - 156.2$
S7	$Y = 45.873 (x) - 184.4$	$Y = 49.036 (x) - 201.42$
S8	$Y = 33.56 (x) - 133.95$	$Y = 26.185 (x) - 91.701$
S9	$Y = 35.242 (x) - 132.4$	$Y = 38.751 (x) - 154.23$
S10	$Y = 39.351 (x) - 152.42$	$Y = 42.191 (x) - 169.98$
S11	$Y = 45.124 (x) - 184.11$	$Y = 51.167 (x) - 222.62$
S12	$Y = 41.932 (x) - 178.95$	$Y = 42.959 (x) - 187.04$

Sample number	Regression curve equations ($R^2 > 0.95$) for potential no-load swell strains estimated from soil suction data (for water contents between 20% and 50%)	
	Correlation of undisturbed sample total suctions to potential no-load swell strain from (1) filter paper and (2) iButton sensors. Y = potential vertical swell strain %; X = soil total suction, log psf; ($3 < \log \text{psf} < 5.5$)	
	Soil suction from filter paper	Soil suction from iButton™
S13	$Y = 40.402 (x) - 167.16$	$Y = 45.096 (x) - 191.49$
S14	$Y = 42.518 (x) - 183.76$	$Y = 56.567 (x) - 256.98$
S15	$Y = 43.414 (x) - 195.77$	$Y = 61.327 (x) - 291.94$
S16	$Y = 39.495 (x) - 167.86$	$Y = 40.182 (x) - 166.36$

Figure 132 illustrates the application of soil suction results to predict the potential vertical combined movement (shrink-swell strain) of samples S1 thru S16.

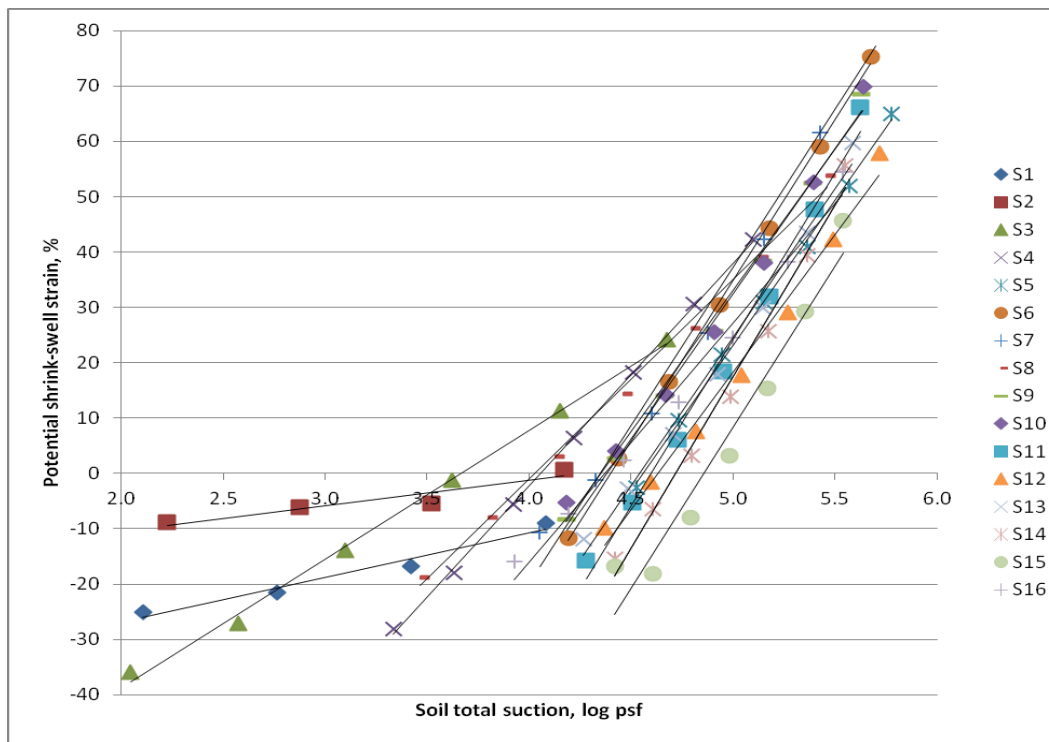


Figure 132. No-load combined shrink-swell curves matched to iButton™ soil suction results

Table 25 lists the regression curve equations from the above figure for potential vertical no-load movement (combined shrink-swell) of each soil layer, based on no-load suction results from the iButton™ sensors.

Table 25. Soil suction–combined shrink-swell strain

Sample number	Regression curve equations ($R^2 > 0.95$) for potential no-load combined shrink-swell strains estimated from iButton™ soil suction data (for water contents between 20% and 50%)
	Correlation of undisturbed sample total suctions to potential no-load combined shrink-swell strain from iButton sensors. Y = combined potential shrink-swell strain %; X = soil total suction, log psf; ($3 < \log \text{psf} < 5.5$)
	Soil suction from iButton™
S1	$Y = 8.06 (x) - 43$
S2	$Y = 4.55 (x) - 19.5$
S3	$Y = 23.3 (x) - 85.3$
S4	$Y = 40.3 (x) - 163.5$
S5	$Y = 52.6 (x) - 240$
S6	$Y = 58.1 (x) - 255.6$
S7	$Y = 57.02 (x) - 247.8$
S8	$Y = 36.1 (x) - 145.4$
S9	$Y = 52.5 (x) - 230$
S10	$Y = 51 (x) - 222.2$
S11	$Y = 60.2 (x) - 276.7$
S12	$Y = 49.7 (x) - 230.1$
S13	$Y = 53.7 (x) - 244.1$
S14	$Y = 62 (x) - 292.6$
S15	$Y = 58.4 (x) - 283.7$
S16	$Y = 43.3 (x) - 189.1$

Low-strain swell pressure curves matched to soil suction results

It is also possible to correlate no-load soil suction to PVC test results. The PVC test results (pressure versus water content) were matched to the soil suction results (water content versus soil suction) to develop these relationships. The filter paper suction results took about 2 to 3 weeks to obtain, but the iButton results took about 2 to 3 hours to obtain. For example, **Figure 133** illustrates the application of soil suction results to predict vertical swell pressure for sample S7. These curves illustrate the utility of obtaining rapid estimates of potential swell pressure based on prior correlations. **Table 26** lists the regression equations.

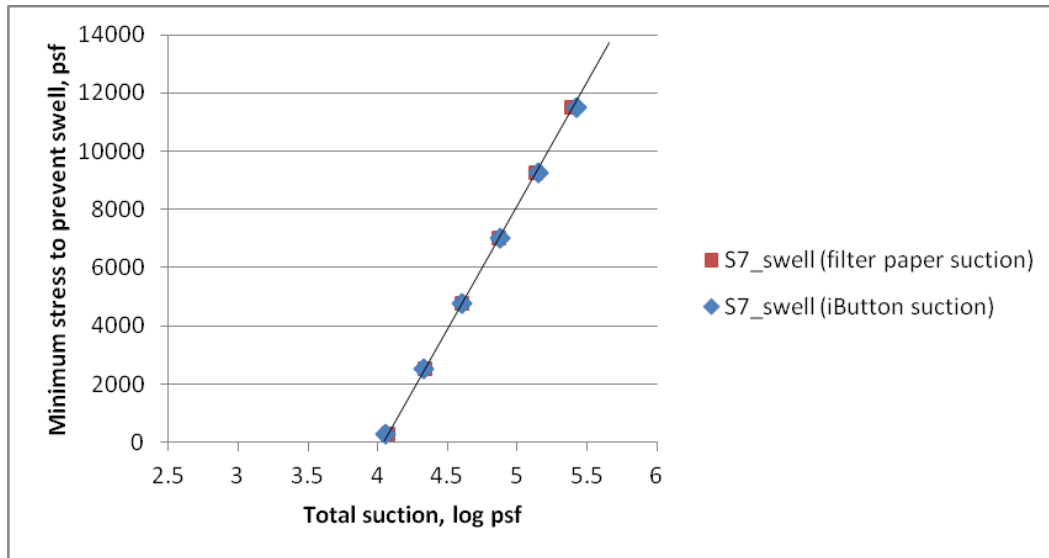


Figure 133. Sample S7 regression line for low-strain swell pressures based on soil suction results

Table 26. Soil total suction results matched to PVC test results

Sample number	Regression curve equations ($R^2 > 0.90$) for Low-strain Swell Pressure versus Soil Suction (for water contents between 25% and 50%)	
	Undisturbed samples at varying initial water contents allowed to exert swell pressure with minimal (< 1%) swell strain during inundation Y = minimum vertical pressure to prevent swell, psf; X = soil total suction, log psf	
	Soil suction from filter paper	Soil suction from iButton™
S1	N/A	N/A
S2	N/A	N/A
S3	$Y = 1055 (x) - 2447$	$Y = 1079 (x) - 2675$
S4	$Y = 7430 (x) - 25612$	$Y = 8656 (x) - 32008$
S5	$Y = 4675 (x) - 19688$	$Y = 5987 (x) - 28551$
S6	$Y = 3284 (x) - 12672$	$Y = 3649 (x) - 14960$
S7	$Y = 8508 (x) - 34383$	$Y = 8152 (x) - 32740$
S8	$Y = 9520 (x) - 39831$	$Y = 8966 (x) - 38418$
S9	$Y = 20998 (x) - 86550$	$Y = 23089 (x) - 99558$
S10	$Y = 20656 (x) - 85166$	$Y = 22146 (x) - 94386$
S11	$Y = 29748 (x) - 123870$	$Y = 33732 (x) - 149261$
S12	$Y = 21774 (x) - 95842$	$Y = 22307 (x) - 100043$
S13	$Y = 18901 (x) - 80401$	$Y = 21096 (x) - 91779$
S14	$Y = 5899 (x) - 25433$	$Y = 7355 (x) - 33006$

Sample number	Regression curve equations ($R^2 > 0.90$) for Low-strain Swell Pressure versus Soil Suction (for water contents between 25% and 50%)	
	Undisturbed samples at varying initial water contents allowed to exert swell pressure with minimal (< 1%) swell strain during inundation Y = minimum vertical pressure to prevent swell, psf; X = soil total suction, log psf	
	Soil suction from filter paper	Soil suction from iButton™
S15	Y = 12316 (x) - 56741	Y = 16212 (x) - 77750
S16	Y = 4655 (x) - 19288	Y = 4438 (x) - 17594

Chemistry Tests

Figures 134 and 135 are plots of soil chemistry changes with depth.

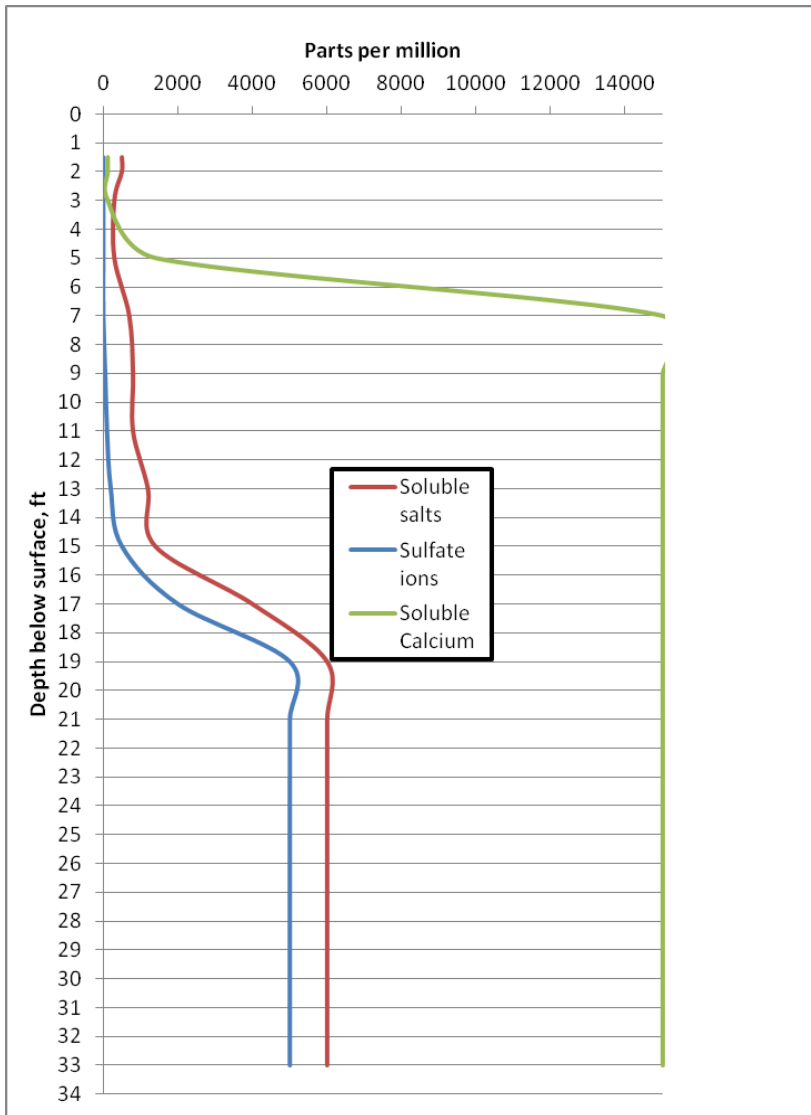


Figure 134. Soluble sulfate and calcium. Note that the calcium concentration is off the chart (greater than 14000 ppm) below about 7-ft depth, and the sulfate concentration increases at the approximate active zone depth (13 ft).

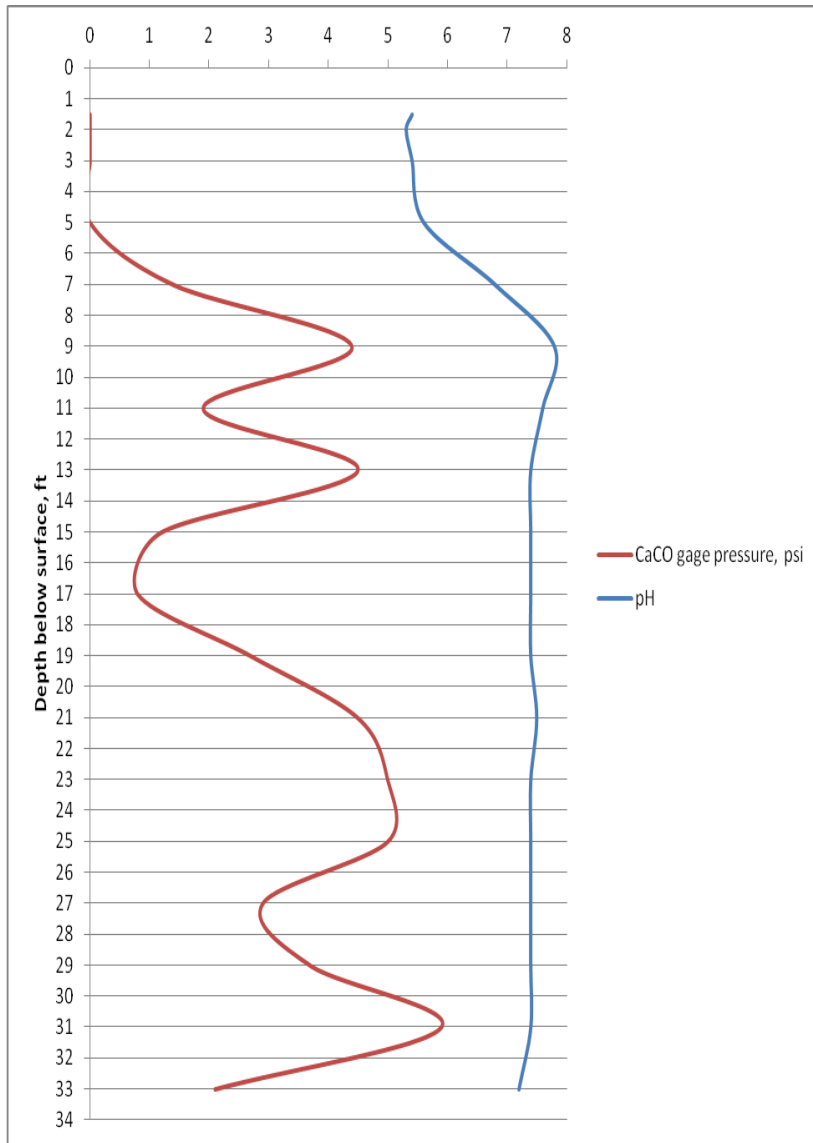


Figure 135. Calcium carbonate and pH test results

Other Tests

Direct shear

Figure 136 is a plot of a direct simple shear test performed on undisturbed sample S16.

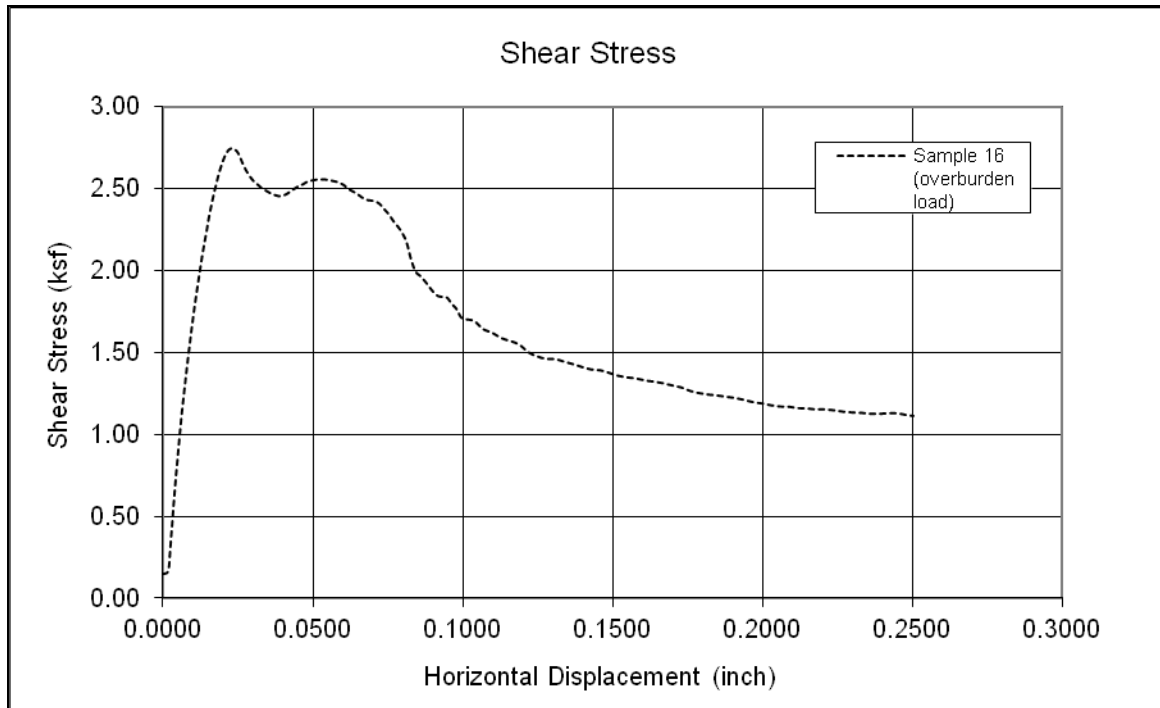


Figure 136. Direct shear test plot for undisturbed sample S16 at natural water content. Overburden load was 4000 psf and handheld Torvane shear was 2000 psf.

Disturbed sample tests

The results of several index-type tests using disturbed (remolded) or completely dis-aggregated (blenderized) materials are shown in **Table 27**.

Table 27. Disturbed sample test results

Sample number (depth, ft)	Δ Liquidity Index	Free Swell Index, %	Free Swell Ratio	Shrink Limit %	VC %	LS % (AASHTO T92)	Bar Linear Shrinkage, %	COLE rod %	ω_{24} hr	ω_{72} hr
S1 (3)	NA	21	1.2						77	37
S2 (5)	NA	22	1.2	13	221	32			100	57
S3 (7)	0.73	48	1.5	11	386	41	21	10	107	69
S4 (9)	1.4	61	1.6	23	321	38	21	26	110	77
S5 (11)	1.1	83	1.8	25	354	39	20	17	140	89
S6 (13)	1.25	78	1.8	13	364	40	23	20	132	97
S7 (15)	1.33	85	1.8	10	417	42	25	26	144	101
S8 (17)	0.74	70	1.7	8	424	42	24	24	132	104
S9 (19)	1.29	70	1.7	13	395	41	20	24	144	109

Sample number (depth, ft)	Δ Liquidity Index	Free Swell Index, %	Free Swell Ratio	Shrink Limit %	VC %	LS % (AASHTO T92)	Bar Linear Shrinkage, %	COLE rod %	ω_{024} hr	ω_{072} hr
S10 (21)	1.11	85	1.8	10	407	42	20	15	147	106
S11 (23)	1.02	71	1.7	16	444	43	23	14	148	108
S12 (25)	1.05	64	1.6	13	424	42	23	14	143	104
S13 (27)	1.15	92	1.9	14	410	42	19	15	143	105
S14 (29)	0.86	77	1.8	17	383	41	17	14	159	112
S15 (31)	0.93	69	1.7	11	368	40	17	15	134	95
S16 (33)	1.43	77	1.8	1	488	44	20	15	146	105

Comparisons to Published Data

Table 28 lists the data from this study and published data previously referenced.

Table 28. Data comparison

Parameter	Published Data	This Study
USCS Class	High-plasticity clay, CH	High-plasticity clay, CH
Consistency	Firm to Stiff	Firm to Hard
Natural Void Ratio	0.6 - 0.9	0.4 - 1.2
Spec. Gravity	2.71 - 2.8	2.4 - 2.65
Dry density, pcf	86 - 105	71 - 106
Natural w%	11 - 35	15 - 50
Optimum Proctor w%	15	NA
Shrinkage Limit (SL)	9 - 11	0.4 - 15
Plastic Limit (PL)	18 - 32	22 - 35
Liquid Limit (LL)	85 - 126	52 - 119
Plasticity Index (PI)	> 50	> 50
< 2 μ m %	60 - 76%	> 60 %
Montmorillonite %	40 - 70%	NA
Vol decrease from shrinkage limit test (VC %)	70 - 235%	>> 60%
"weathered" undrained cohesion, psf	1000 - 3000	NA
"unweathered" undrained cohesion, psf	3000 - 5000	NA
Over-consolidation ratio (OCR)	5 - 10	NA
Unconfined compressive strength, psf	1500 - 6000	2000 - 8000

Swell pressure, psf	< 25000	< 25000
---------------------	---------	---------

Figure 137 shows the present-study natural water contents compared to the adjacent test site’s historic data (Johnson 1973a). Note that the adjacent borehole data classified the upper (1- to 8-ft) layers as lean clay with wetter water contents, and did not consider those layers to be expansive.

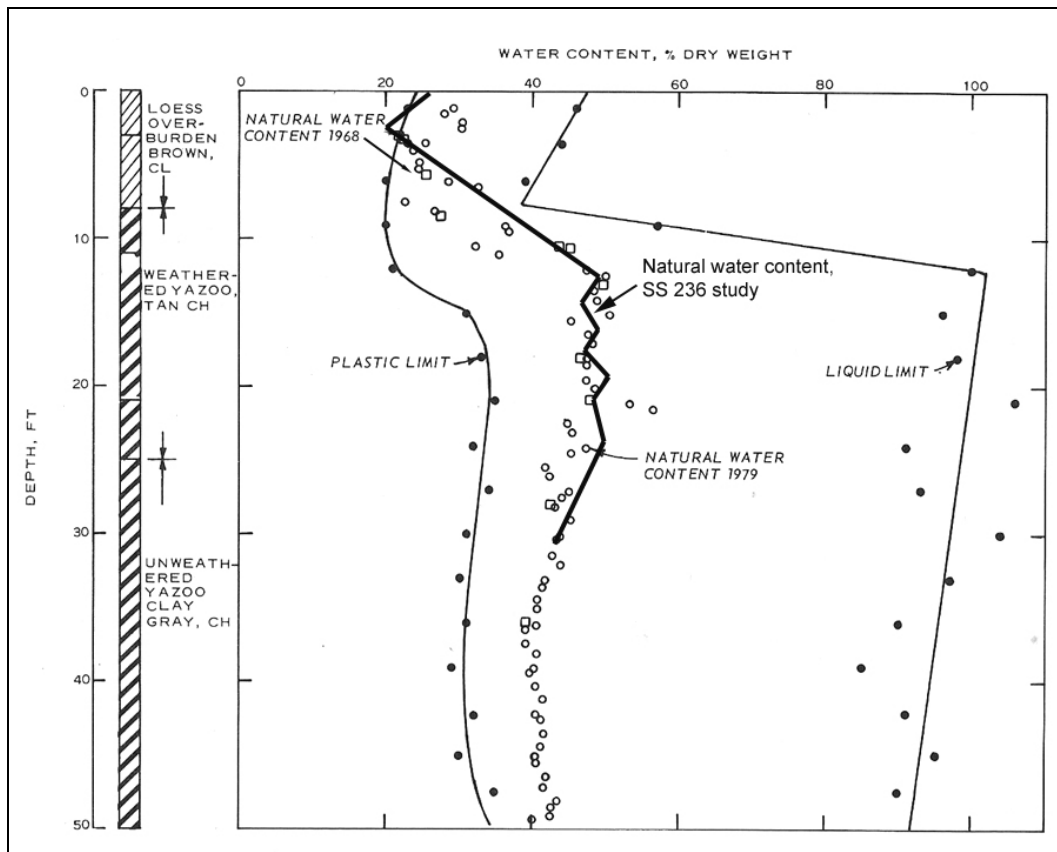


Figure 137. Comparison of adjacent borehole data

Figures 138 and **139** compare the soil suction (filter paper) data for the upper 8 ft and 8 – 24 ft, respectively. The present study indicated that, at a given water content, the soil suction is about 10 times higher than the historic soil suction.

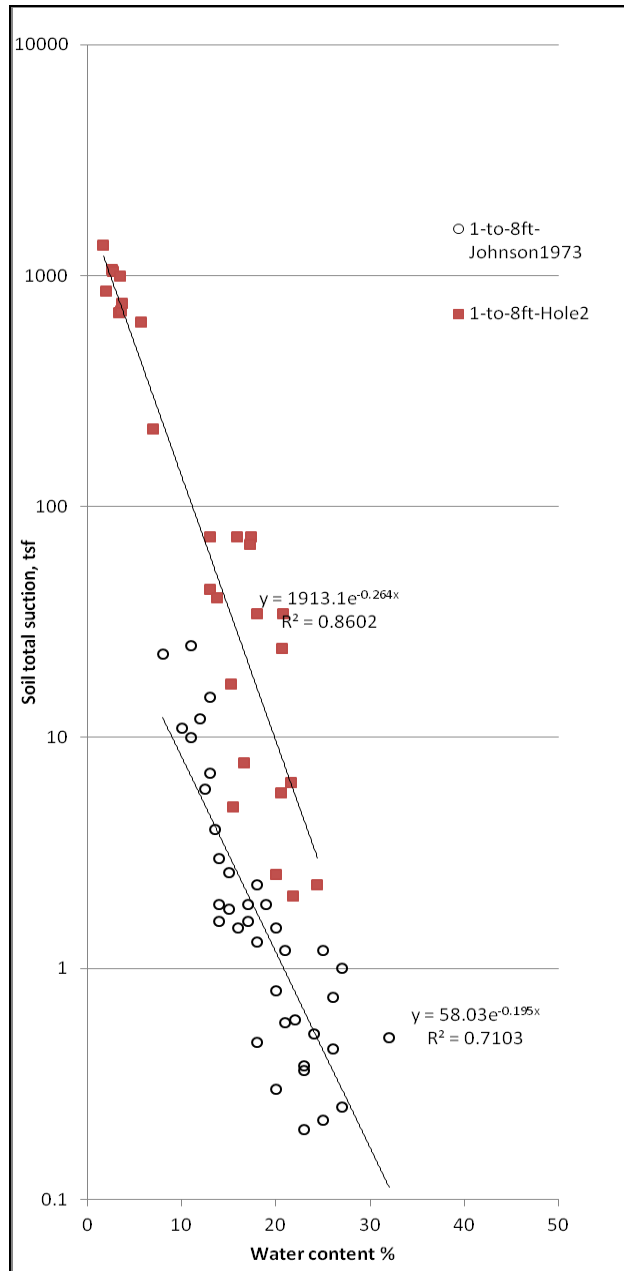


Figure 138. Comparison of adjacent test site soil suction data for the 1- to 8-ft depth interval

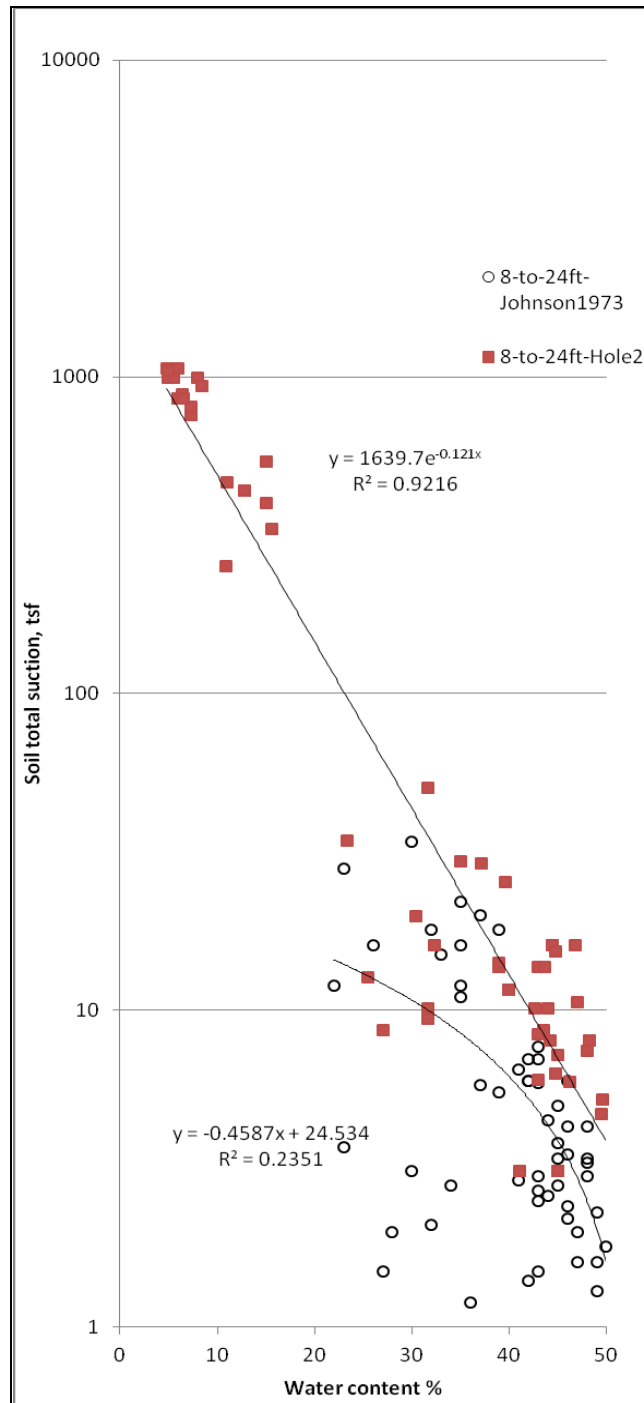


Figure 139. Comparison of adjacent test site soil suction data for the 8- to 24-ft depth interval

The upper 8 ft has a much higher swell potential than previously observed. The 8- to 24-ft layers also exhibit much higher swell potential. In other words, the present study indicated much higher total suctions for equal water contents. This difference between Johnson (1973a) and the present-study data could be due to:

- Spatial heterogeneity (e.g. 1973 data were from boreholes 75 to 200 ft distant)
- Surface conditions (e.g. the surface layers were wetter 40 years ago and no trees were on the site then)
- Geology and subsurface drainage patterns (e.g. 1973 data does not mention the fragipan layer extending to about 6 ft below surface)
- Lab procedures and materials from 40 years ago were probably not duplicated.

Analysis of Test Results

Expansive Soil Indicators

Using the MDoT criteria ($VC > 60\%$), all the samples (S1 through S16) were composed of high volume change (expansive) material. The swell, shrinkage, and other tests performed on the samples also indicated that the soils were expansive.

Comparisons to published literature on expansive soils also indicated the study soils were expansive. **Figure 140** illustrates a comparison plot.

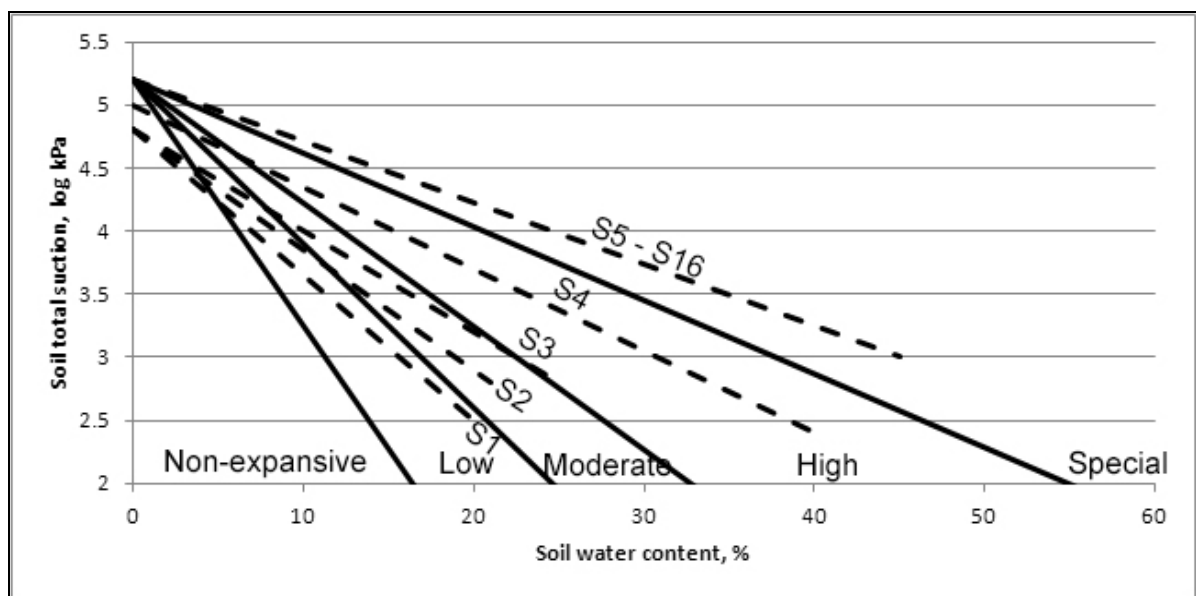


Figure 140. Comparison of expansive soil data (McKeen 1992) to this study.

Paired Data Correlations

Tables 29 and **30** list the best paired correlation coefficients from the data. Any pair with a coefficient less than approximately 0.80 is not shown.

Table 29. Correlation coefficients

	Depth	nat w%	γ_d	w24	w72	FS %	FSI %
Depth, ft	1.00			0.79	0.79		
nat w%		1.00	-0.93	0.84	0.88	0.90	0.92
γ_d			1.00	-0.89	-0.90	-0.93	-0.95
w24				1.00	0.97	0.90	0.88
w72					1.00	0.90	0.88
FS %						1.00	0.91
FSI %							1.00

Table 30. More correlation coefficients

	LL	VC	VC (Blender)	Shrink%	lss	lpt	lss-144
Depth, ft							
nat w%	0.87	0.92		0.88	0.89	0.86	0.91
γ_d	-0.86	-0.81		-0.90	-0.91	-0.91	-0.91
w24	0.94	0.86		0.82	0.83	0.86	0.81
w72	0.93	0.91	0.78	0.88	0.90	0.93	0.88
FS %	0.92	0.83		0.84	0.85	0.86	0.86
FSI %	0.87	0.81		0.87	0.88	0.85	0.88
LL	1.00	0.94			0.78	0.83	0.79
VC		1.00			0.78	0.81	0.80
VC Blend			1.00				
Shrink%				1.00	1.00	0.97	0.98
lss					1.00	0.96	0.98
lpt						1.00	0.93
lss-144							1.00

The following data correlation observations were made:

- Poor quantitative correlations for swell potential and swell pressure versus index-type tests were noted. Qualitative correlations were easily observed (i.e. the higher the LL, the more likely the clay is expansive; the higher the surcharge (load), the lower the swell strain

potential; the drier the soil, the higher the swell strain potential; the higher the suction, the higher the swell strain potential). Quantitative measurement of swell strain or swell pressure should be from individual lab tests, as there appeared to be no correlated surrogates for swell strain or swell pressure. For example, poor correlations were noted between VC and loaded swell strain or swell pressure. This is understandable since VC is a measure of no-load shrinkage strain instead of swell strain.

- The best correlations to no-load swell and shrink strains were from the soil suction tests, as previously tabulated.
- The best correlations to swelling strain versus index-type tests were for the no-load free swell (FS %) and free swell index (FSI %) parameters.
- Good quantitative correlations between index tests (LL, natural water content, and dry density) and shrinkage tests (VC, core shrinkage strain, Iss, Ipt, and Iss-144) were noted.
- The water content tests (natural, 24-hr, and 72-hr) correlated well to index tests, shrinkage tests, and no-load swell tests.

Useful Equations

Site-specific data

The following equations were derived from the lab data from this study site:

If the natural water content % (in the range 25% to 50%) is known,

- Dry density, pcf = $137.19e^{-0.012w\%}$; $e = 2.718$ ($R^2 = 0.85$)
- Free Swell % = $0.9212w\%^{1.2737}$ for ($25\% < w\% < 50\%$); ($R^2 = 0.90$)
- $ISS_{144} = 0.251w\% - 4$ ($R^2 = 0.83$)
- Average total suction below the active zone depth as measured by the iButton, log psf = $-0.079w\% + 6.47$

If the average total suction below the active zone depth as measured by the iButton (log psf units) is known,

- Potential combined shrink-swell vertical movement (strain) % = $51(\log \text{ suction, psf}) - 222$

If the dry density γ_d , pcf is known,

- Free Swell % = $1636.4e^{-0.034 \gamma_d}$ ($R^2 = 0.88$)

If the Free swell % is known,

- $LL = 6.6168FS\%^{0.5741}$ ($R^2 = 0.90$) for ($70\% < FS\% < 140\%$)

If LL is known,

- $VC\% = 0.5665LL^{1.2368}$ ($R^2 = 0.88$) for ($80 < LL < 120$)
- Free swell % = $0.08LL^{1.5754}$ ($R^2 = 0.90$)
- $w_{24hr}\% = 2.5559LL^{0.8571}$ ($R^2 = 0.92$)

If the water content after 24 hours ($w_{24hr}\%$) is known,

- $LL = 0.5344 w_{24hr}\%^{1.0708}$ ($R^2 = 0.92$) for ($100\% < w_{24hr}\% < 150\%$)

Comparisons to other site data

Yazoo clay samples from other MDoT sites were randomly selected and tested for comparison using some of the above equations. The measured and predicted parameters (free swell, dry density, and VC %) are plotted in **Figure 141**. The VC % was the only parameter of the three that did not appear to be predictable when using the above equations. In other words, the above VC % equation applies only to this study site, but the free swell and dry density equations may be applicable at other Yazoo clay sites.

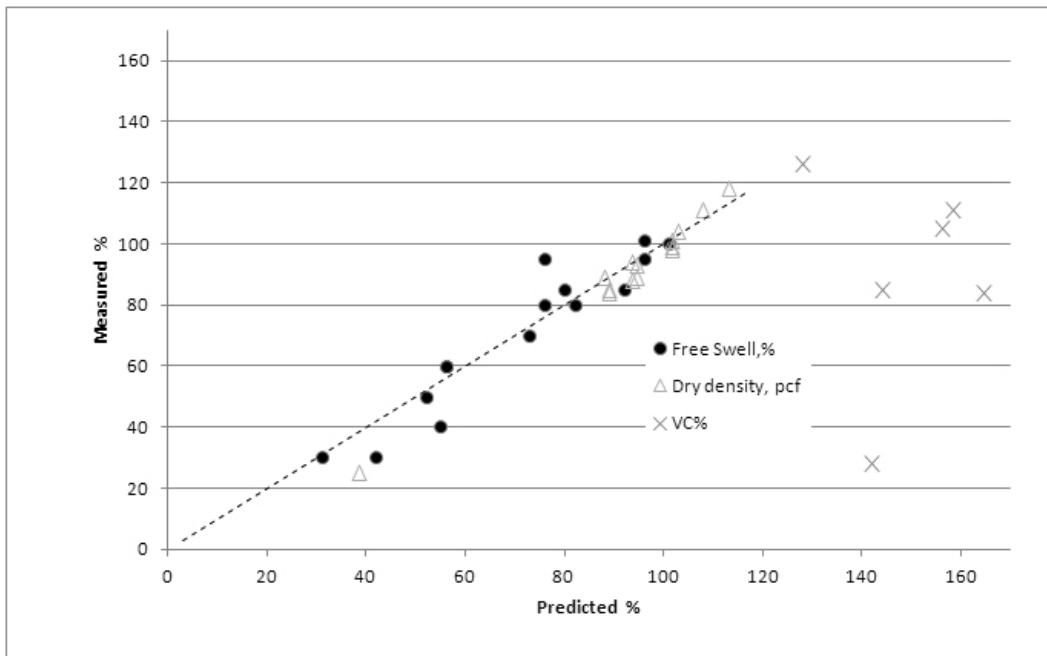


Figure 141. Comparison of measured and predicted values at other Yazoo clay sites

5 Conclusions and Recommendations

General conclusions

Yazoo clay properties were not uniform or linear with depth since it is a spatially-heterogeneous material. Visual and mineralogy descriptors of “weathering” did not generally agree. Kaolinite and quartz contents were generally highest and VC% was generally lowest (indicative of clay weathering) above -15 ft, but there were numerous exceptions at much lower depths in the “unweathered” zone. Relying solely on visual color classification to identify or bracket zones of potential expansive behavior is not recommended. Traditional wisdom separates the Yazoo clay into “weathered” and “unweathered” zones, but based on observations made during this study, these could be two independent geological formations.

The field (in-situ) behavior of Yazoo clay cannot be accurately captured in laboratory tests. Changes in field boundary conditions (climate, drainage, moisture intrusion, irrigation, vegetation, etc.) will cause changes in the shrink-swell behavior. Boundary condition changes may take years or decades to occur before detrimental shrink-swell behavior is realized. Fissures, slickenside structure, and jointing may significantly increase the active zone depth by allowing moisture infiltration below the typical weathered zone.

Specific conclusions

MDoT SOP relies on index tests and shrinkage volume change upon drying from the liquid limit (VC %) to quantify identification of expansive clays. The best correlations between index properties and VC % were observed using site-specific data. Although regional-based index and shrinkage behavior-depth correlations were poor, regional index and mineralogy property correlations were good. As a general observation, LL instead of PL was the best indicator of VC %, and could be used as a proxy for the VC % test.

Swell potential (propensity for volume increase) dramatically increased when the soil was dried below its natural water content and then given free access to water. Conversely, shrinkage potential (propensity for volume decrease) increased at water contents above the natural water content. The swell potential of the overlying soil layers (S1 thru S4) increased if their in-

situ overburden pressure decreased. Removing the overburden from those layers could aggravate swelling even if their water contents did not appreciably change.

Swell pressures increased when soil was inundated from a drier water content state. In other words, the drier the soil was prior to inundation, the higher was the overburden pressure needed to prevent swelling.

Sample preparation standards vary by DoT agencies, and sample preparation makes a difference in test results. Remolding (blenderizing) significantly changes the material index and strength properties, and may be utilized as an indicator that a material is expansive. The more expansive the material, the more the test results will differ if the material is blenderized prior to testing.

This study showed that alternative test methods are available for detecting expansive material and predicting its shrink-swell behavior. Most of these tests are not standardized and are foreign to routine material testing protocols, but they are very useful. The tests most applicable for Yazoo clay were presented heretofore.

Recommendations

Do not assume that fine-grained soil layers overlying Yazoo clay are non-expansive; perform sample testing to verify their shrink-swell behavior. Increased swell potential in those layers could be caused simply by decreasing the overburden pressure while slightly increasing the water content. For example, an excavation final-grade cut into an overburden layer could cause unanticipated heave, especially if exposed to rainfall.

To rapidly identify high volume change soil layers (in conjunction with expert visual observation and qualitative tests such as acid reaction and slaking), conduct a simple free swell test to obtain the FS % or FSI % prior to index testing. Proxies for the free swell test include those listed in above **Tables 29** and **30**.

Conduct soil sampling at closely-spaced intervals if Yazoo clay presence is known or suspected. Concentrate sampling and testing in the interval between the surface and the active zone depth to capture heterogeneous shrink-swell behavior. Non-horizontal clay layers also contribute to long-term strain and lateral movement.

Conduct the Australian test (or its 144 psf alternative) to identify the active zone depth. Proxies for the Australian test include those listed in above **Tables 29** and **30**. Compare those results to shrink-swell test results to best identify the active zone depth and specify excavation limits. The active zone depth is not the same at any given site; in general it is probably deeper than the Jackson-area state-of-practice assumed 8- to 10-ft depth. At this study site it was shown to be around 13 ft below surface. Additionally, the Australian test results can provide an estimate of the potential heave in each layer.

Instead of relying solely on index tests and VC % tests as proxies for expansive (high volume change) behavior, conduct the following tests using undisturbed instead of remolded or compacted samples in order to better estimate in-situ shrink-swell behavior:

- Consolidation (swell) test to determine swell strain potential
- Core shrinkage test to determine shrinkage strain potential
- PVC test to determine swell pressure

Consider soil suction testing using the iButton™ or similar fast-result headspace relative humidity sensors. Soil suction is a very good indicator of shrink-swell behavior, especially for no- or low-load situations such as an undercut or over-excavation.

Consider conducting residual (or fully-softened) shear strength tests to quantify slope stability parameters, instead of relying on the SOP slope angles. Doing so will bracket a more accurate estimate of construction limits, right-of-way acreage, and excavation/fill volumes.

In order to identify any expansive clay materials inadvertently blended into structural fill or backfill, consider including soil shrink-swell QA specs in addition to gradation, PI, and compaction specs. Expansive soils may be mis-identified due to visual similarity to non-expansive materials. Construction contract specifications could also list an allowable water content range for material exposed during construction (e.g. excavations), since shrink-swell behavior is highly dependent on the state of water (moisture) content.

6 References and Expansive Clay Bibliography

- AASHTO (1998). "Standard specifications for transportation materials and methods of sampling and testing: Part I (Specifications) and Part II (Tests)," American Association of State Highway and Transportation Officials, Washington, D.C.
- AASHTO (2007). "Determining water-soluble sulfate ion content in soil," Designation T-290-95. American Association of State Highway and Transportation Officials, Washington, D.C.
- AASHTO (2008a). "Standard method of test for soil suction," Designation T-273-86, American Association of State Highway and Transportation Officials, Washington, D.C.
- AASHTO (2008b). "Standard method of test for determining expansive soils," Designation T-258-81, American Association of State Highway and Transportation Officials, Washington, D.C.
- Abdullah, W.S. (2002). "Bidimensional swell effect on accuracy of footing heave prediction," *Geotechnical Testing Journal* 25(2), ASTM, pp. 177 – 186.
- Abduljauwad, S.N. (1993). "Study on the performance of calcareous expansive clay," *Bulletin of the Association of Engineering Geologists* 30 (4), pp. 481–498.
- Abduljauwad, S.N., Al-Suleimani, G.J. (1993). "Determination of swell potential of Al-Qalif clay," *Geotechnical Testing Journal* 16 (4), pp. 469–484.
- Al-Homoud, A.S., Khoury, H., and Al-Omari, Y.A. (1996). "Mineralogical and engineering properties of problematic expansive clayey beds causing landslides," *Bulletin of the International Association of Engineering Geology* 54, pp.13–31.
- Albrecht, B.A., Benson, C.H., and Beuermann, S. (2003). "Polymer capacitance sensors for measuring soil gas humidity in drier soils," *J. Geotechnical Testing* 26(1), pp. 1 – 9.
- Allbrook, R. (2002). "Relationships between shrinkage indices and soil properties in some New Zealand soils," *Geoderma* 108, pp. 287– 299.
- Allman, M. A., Delaney, M. D., and Smith, D. W. (1998). "A field study of seasonal ground movements in expansive soils," *Proc., 2nd Int. Conf. on Unsaturated Soils*, International Academic Publishers, Beijing, pp. 309–314.
- Al-Rawas, A. A. and Qamaruffin, M. (1998). "Construction problems of engineering structures founded on expansive soils and rocks in northern Oman," *Building and Environment* 33 (2-3), pp. 159-171.
- Al-Rawas, A. A.(1999). "The factors controlling the expansive nature of the soils and rocks of northern Oman," *Engineering Geology* 53, pp. 327-350.

- Al-Shamrani, M.A. (2004). "Influence of lateral restraint on the swelling behavior of expansive soils," *Journal of the Southeast Asia Geotechnical Society*, Dec. pp. 100 – 111.
- Anderson, J. N. and Lade, P. V. (1981). "The Expansion Index Test," *Geotechnical Testing Journal*, Vol. 4, No. 2, pp. 58-67.
- Anon (1971). "Curse of Yazoo clay," *Better Roads*, Vol 41(1), pp. 15 – 17.
- ASTM (1992). "Standard Test Method for Specific Gravity of Soils," ASTM Designation: D854-92, American Society for Testing and Materials, West Conshohoken, Pa
- ASTM (1994). "Standard Test Method for Liquid Limit, Plastic Limit and Plasticity Index Of Soils," ASTM Designation: D4318-93, American Society for Testing and Materials, West Conshohoken, Pa
- ASTM (1994). "Standard Test Method for Particle Size Analysis of Soils," ASTM Designation: D422-63, American Society for Testing and Materials, West Conshohoken, Pa
- ASTM (1995). Standard Test Method for Pore Water Extraction and Determination of the Soluble Salt Content of Soils by Refractometer, ASTM Designation: D 4542 – 95, American Society for Testing and Materials, West Conshohoken, Pa
- ASTM (1996). Standard Test Method for Calcium Carbonate Content of Soils, ASTM Designation: D 4373 – 96, American Society for Testing and Materials, West Conshohoken, Pa
- ASTM (2002). Standard Test Methods for Determination of the Soil Water Characteristic Curve for Desorption Using a Hanging Column, Pressure Extractor, Chilled Mirror Hygrometer, and/or Centrifuge, ASTM Designation: D 6836 – 02, American Society for Testing and Materials, West Conshohoken, Pa
- ASTM (2003). Standard Test Method for Measurement of Collapse Potential of Soils, ASTM Designation: D5333 – 03, American Society for Testing and Materials, West Conshohoken, Pa
- ASTM (2004). Standard Test Methods for One-Dimensional Consolidation Properties of Soils Using Incremental Loading, ASTM Designation: D 2435 – 04, American Society for Testing and Materials, West Conshohoken, Pa
- ASTM (2005). Standard Test Methods for Determining Dispersive Characteristics of Clayey Soils by the Crumb Test, ASTM Designation: D 6572 – 05, American Society for Testing and Materials, West Conshohoken, Pa
- ASTM (2006). Standard Test Method for Swell Index of Clay Mineral Component of Geosynthetic Clay Liners, ASTM Designation: D 5890 – 06, American Society for Testing and Materials, West Conshohoken, Pa
- ASTM (2006). Standard Test Method for Using pH to Estimate the Soil-Lime Proportion Requirement for Soil Stabilization, ASTM Designation: D 6276, American Society for Testing and Materials, West Conshohoken, Pa

- ASTM (2008a). Standard Test Methods for One-Dimensional Swell or Settlement Potential of Cohesive Soils, ASTM Designation: D4546 – 08, American Society for Testing and Materials, West Conshohoken, Pa
- ASTM (2008b). Standard Test Method for Shrinkage Factors of Soils by the Wax Method, ASTM Designation: D4943 – 08, American Society for Testing and Materials, West Conshohoken, Pa
- ASTM (2008c). Standard Test Method for Expansion Index of Soils, ASTM Designation: D4829 – 08, American Society for Testing and Materials, West Conshohoken, Pa
- ASTM (2009a). Standard Test Method for Methylene Blue Index of Clay, ASTM Designation C837 – 09, American Society for Testing and Materials, West Conshohoken, Pa
- ASTM (2009b). Standard Test Methods for Laboratory Determination of Density (Unit Weight) of Soil Specimens, ASTM Designation D7263, American Society for Testing and Materials, West Conshohoken, Pa
- ASTM (2009c). Standard Test Method for Water-soluble Sulfate in Soil, ASTM Designation C1580, American Society for Testing and Materials, West Conshohoken, Pa
- ASTM (2010). Standard Test Method for Density of Soil in Place by the Drive-Cylinder Method, ASTM Designation: D2937 – 10, American Society for Testing and Materials, West Conshohoken, Pa
- ASTM (2010). Standard Test Method for Measurement of Soil Potential (Suction) Using Filter Paper, ASTM Designation: D5298 – 10, American Society for Testing and Materials, West Conshohoken, Pa
- ASTM (2010). Standard Test Method for Measuring the Exchange Complex and Cation Exchange Capacity of Inorganic Fine-Grained Soils, ASTM Designation: D7503 – 10, American Society for Testing and Materials, West Conshohoken, Pa
- Australian Standards (2003). “AS 1289 Test Methods 7.1.1, 7.1.2, 7.1.3: Soil Reactivity Tests,” Standards Assoc. of Australia, Sydney, Australia.
- Attewell, P.B. and Taylor, R.K. (1973). “Geochemical, mineralogical, and geotechnical comparisons between some North American and British clay shales,” Final Report DA-ERO-591-70-G0006 to European Research Office, U.S. Army. 48 pp.
- Attom, M.F. and Barakat, S. (2000). “Investigation of three methods for evaluating swelling pressure of soils,” *Environmental and Engineering Geoscience* 6(3), pp. 293- 299.
- Avsar, E., Ulusay, R., and Erguler, Z.A. (2005). “Swelling properties of Ankara (Turkey) clay with carbonate concentrations,” *Environmental and Engineering Geoscience* 11 (1), pp. 73–93.
- Avsar, E., Ulusay, R., and Sonmez, H. (2009). “Assessments of swelling anisotropy of Ankara clay,” *Engineering Geology* 105, pp. 24–31.

- Azam, S. and Wilson, G.W. (2006). "Volume change behavior of a fissured expansive clay containing anhydrous calcium sulfate," *Proceedings, 4th Intl Conf on Unsaturated Soils*, Carefree, AZ, pp 906 – 915.
- Bandyopadhyay, S.S. (1981). "Prediction of swelling potential for natural soils," *ASCE Journal of Geotechnical Engineering Division*, 107 (1), pp. 658–661.
- Barden, L., Madedor, A. O., and Sides, G. R. (1969). "Volume change characteristics of unsaturated clay," *ASCE Journal Soil Mechanics, Foundation Division*, 95, No. SM1, pp. 33–52.
- Basma, A. A., Al-Homoud, A. S., and Al-Tabari, E. Y. (1994). "Effects of methods of drying on the engineering behavior of clays," *Applied Clay Science* 9, pp.151-164.
- Basma, A.A., Al-Hamoud, A.S., and Husein, A. (1995). "Laboratory assessment of swelling pressure of expansive soils," *Applied Clay Science* 9, pp. 355–368.
- Baughman, W. T., McCutcheon, T.E., Bicker, A.R., Dinkins, T.H., and Shows, T. (1971). "Rankin County geology and Mineral Resources," *Mississippi Geological, Economic, and Topographic Survey Bulletin* 115, 226p.
- Belviso, R., Ciampoli, S., Cotecchia, V., and Federico, A. (1985). "Use of the cone penetrometer to determine consistency limits," *Ground Engineering*, Vol 18, No 5, pp 21-22.
- Berney, E.S. IV and Lee, L.T. (2010). "Operational limitations of polymer-capacitance sensors for measuring relative humidity in compacted soils," submitted for publication in *ASTM Geotechnical Testing Journal*, 23 pp.
- Bergquist, H. R. and McCutcheon, T.E. (1942). "Scott County," *Mississippi State Geological Survey Bulletin* 49, 146p.
- Bishop, A. W. and Blight, G. E. (1963). "Some aspects of effective stress in saturated and unsaturated Soils," *Geotechnique*, Vol. 13, pp. 177–197.
- Blackwell, W.H. and Dukes, G.H. (1981). "Fossil wood from Thompson Creek, Yazoo County, Mississippi," *Mississippi Geology* 2(2), pp. 1 – 6.
- Blackwell, W.H. and Powell, M.J. (1982). "Fossil microalgae (Coccolithophorids) in the Yazoo clay exposures at Thompson Creek, Yazoo County, Mississippi," *Mississippi Geology* 3(2), pp. 1 – 5.
- Bograd, M.B.E. (1996). "Charles Lyell's visit to Mississippi in 1846," *Mississippi Geology*, Vol 17(3), pp. 51 – 55.
- Brackley, J. J. A. (1973). "Swell pressure and free swell in a compact clay," *Proceedings of the 3rd International Conference on Expansive Clays*, Vol. 1, Israel Institute of Technology, Haifa, pp. 169–176.
- Brasher, B.R., Franzmeier, D.P., Valassis, V., and Davidson, S.E. (1966). "Use of saran resin to coat natural soil clods for bulk density and water retention measurements," *Soil Science*, Vol 101, p. 108.

- British Standards Institution (1990). "British Standard methods of test for engineering purposes, BS 1377: Part 2 Classification test," BSI, London.
- Brown, G. and Bridley, G. W. (1980). "X-ray diffraction procedures for clay mineral identification," in Bridley, G. W. and Brown, G., (eds) *Crystal structures of clay minerals and their X-ray identification*. Mineralogical Society Monograph N° 5. London.
- Brunauer, S., Emmett, P.H., and Teller, E. (1938). "Adsorption of gases in multi-molecular layers," *Journal of the American Chemical Society* 60, pp. 309–319.
- Brune, G. (1964). "Anhydrite and gypsum problems in engineering geology," *Annual Meeting of the Assoc. of Engr. Geologists*, Sacramento, CA, pp. 61 – 81.
- Bryson, J.R. and Galicki, S.J. (2003). "An investigation of the origin and extent of a perched wetland, Millsaps College, Jackson, Mississippi," in *Journal of the Mississippi Academy of Sciences* 48(1), pp. 44-45.
- Buck, A. D. (1956). "Mineral composition of the Yazoo clay by X-ray diffraction methods," *Society of Economic Paleontologists and Mineralogists*, Tulsa, OK, pp. 67.
- Bulut, R. and Leong, E.C. (2008). "Indirect measurement of suction," *Geotechnical and Geological Engineering J.*, Vol. 26 (6), pp. 633-644.
- Bulut, R. and Wray, W.K. (2005). "Free energy of water suction in filter papers," *Geotechnical Testing J.*, Vol. 28 (4), pp. 355-364.
- Bulut, R., Aubeny, C.P. and Lytton, R.L. (2005). "Unsaturated soil diffusivity measurements," *International Symposium on Soil Mechanics (EXPERUS 2005)*, Trento, Italy, pp. 281-286.
- Bulut, R., Hineidi, S. M., and Bailey, B., (2002). "Suction measurements- filter paper and chilled-mirror psychrometer," *Proceedings of the Texas Section of the American Society of Civil Engineers Fall 2002 Meeting*, Waco, TX, October 2–5, 2002.
- Bulut, R., Lytton, R. L., and Warren, W. K. (2001). "Soil suction measurement by filter paper," *Expansive Clay Soils and Vegetative Influence on Shallow Foundations, ASCE Geotechnical Special Publication No. 115*. C. Vipulanandan, M. B. Addison and M. Hasen, (Eds.), Houston, TX, pp. 243–261.
- Burland, J.B.(1990). "On the compressibility and shear strength of natural clays," *Geotechnique* 40 (3), pp. 329–378.
- Butler, D.T. and Harris, J.B. (2008). "Shallow shear-wave seismic velocity testing in Jackson, Mississippi," in *Geological Society of America Abstracts with Programs* 40(6), page 562.
- Byerly, G.R., Hazel, J.E., and McCabe, C. (1988). "A new later Eocene micro-spherule layer in central Mississippi," *Mississippi Geology*, Vol 8(4), pp. 1 – 4.
- Cameron, D. A. (1989). "Tests for reactivity and prediction of ground movement," *I. E. Aust. Civ. Eng. Trans*, 3, pp. 121–132.

- Cameron, D. A. (2001). "The extent of soil desiccation near trees in a semi-arid environment," *Geotechnical and Geological Engineering*, Kluwer Academic Publishers, 19(3 and 4), pp. 357–370.
- Cameron, D. A. and Walsh, P. F. (1984a). "Evaluation of soil reactivity: the Instability Index," *Combined Seminar of Institution of Engineers Structural Branch and Geotechnical Society*, Melbourne.
- Cameron, D. A. and Walsh, P. F. (1984b). "The prediction of moisture induced foundation movements using the Instability Index," *Australian Geomechanics*, No. 8.
- Carpenter, K. and Dockery, D.T. (1985). "And the bones came together, bone to his bone (Ezekial 37:7): The making of a state fossil," *Mississippi Geology*, Vol 6(1), pp. 1 – 5.
- Carrier, W.D. and Beckman, J.F. (1984). "Correlations between index tests and the properties of remoulded clays," *Geotechnique* 34(2), pp. 211 – 228.
- Carter, D. L., Heilman, M. D., and Gonzalez, C. L. (1965). "Ethylene glycol monoethyl ether for determining surface area of silicate minerals," *Soil Science*, 100(5), pp. 356–360.
- Carter, D. L., Mortland, M. M., and Kemper, W. D. (1986). "Specific surface. methods of soil analysis," Chapter 16, *Agronomy*, No. 9, Part 1, 2nd Ed., American Society of Agronomy.
- Casagrande, A. (1932). "Research on the Atterberg limits of soil," *Public Roads*, 13(8), pp. 121–136.
- Cerato, A.B. and Lutenegeger, A.J. (2002). "Determination of surface area of fine- grained soils by the ethylene glycol monoethyl ether (EGME) method," *Geotechnical Testing Journal* 25, pp. 1–7.
- Cerato, A.B. and Lutenegeger, A.J. (2004). "Determining intrinsic compressibility of fine grained soils," *Journal of Geotechnical and Geoenvironmental Engineering* 130 (8), pp. 872–877.
- Cerato, A.B. and Lutenegeger, A.J. (2006). "Shrinkage of clays," *Unsaturated Soils 2006*, ASCE, pp. 1097 – 1108.
- Chadwick, C.E. (1965). "An investigation of the volumetric fluctuations of clay soils caused by wetting and drying," Master's Thesis, Mississippi State University, 94 pp.
- Chanasyk, D. S., and Naeth, M. A. (1996). "Field measurement of soil moisture using neutron probe," *Can. J. Soil Sci.*, 76, pp. 317–323.
- Chandler, R. J. and Gutierrez, C. I. (1986). "The filter-paper method of suction measurement," *Geotechnique*, 36(2), pp. 265–268.
- Chaney, R.C., Slonim, S.M., and Slonim, S.S. (1982). "Determination of calcium carbonate content in soils," *Geotechnical Properties, Behavior, and Performance of Calcareous Soils*, ASTM STP 777, K.R. Demars and R.C. Chaney, Eds., American Society for Testing and Materials, pp. 3-15.

- Chapman, H.D. (1965). "Cation exchange capacity," in: Black, J.A. (Ed.), *Methods of Soil Analysis*, American Institution of Agronomy, Madison, Wisconsin, pp. 891–901.
- Chang, S.S., Shau, Y.H., Wang, M.K., Ku, C.T., and Chiang, P.N. (2008). "Mineralogy and occurrence of glauconite in central Taiwan," *Applied Clay Science* Vol 42 (1-2), pp. 74 – 80.
- Chen, F. H. (1988). *Foundations on expansive soils, Developments in Geotechnical Engineering 54*, Elsevier Science Publishers B.V., Amsterdam, 463 pp.
- Chen, G., Pan, J., Han, B., and Yan, H. (1999). "Adsorption of methylene blue on montmorillonite," *Journal of Dispersion Science and Technology* 20 (4), pp. 1179– 1187.
- Chiappone, A., Marello, S., Scavia, C., and Setti, M. (2004). "Clay mineral characterization through the methylene blue test: comparison with other experimental techniques and applications of the method," *Can. Geotech. J.* 41, pp. 1168–1178.
- Churchman, G.J., Burke, C.M., and Parfitt, R.L. (1991). "Comparison of various methods for the determination of specific surfaces of subsoils," *Journal of Soil Science* 42, pp. 449–461.
- Clarion Ledger (1990a). "Yazoo clay: on shaky ground," Newspaper article special series, 28 – 30 October.
- Clarion Ledger (1990b). "Proper drainage will ease problem," Newspaper article, 16 Nov.
- Clarion Ledger (1991a). "Court rules builder is liable for clay damage," Newspaper article, 25 April.
- Clarion Ledger (1994). "Found beneath foundations of 2 Ridgeland schools," Newspaper article, 10 Aug.
- Clark, C.V. (1956). "Engineering problems involving Yazoo clay," Presentation at the Mississippi Academy of Sciences, Millsaps College, MS.
- Clisby, M.B. (1962). "An investigation of the volumetric fluctuations of active clay soils," Ph.D. Dissertation, University of Texas, 125 pp.
- Clisby, M.B. (1967). "Predicting the movement of clays," Presentation to Committee C2, Annual Meeting of the Highway Research Board, printed by Mississippi State University, State College, MS, 35 pp.
- Coffey and Partners Pty. Ltd. (1984). *Specification for Swelling Soil Design Method*, Report to the Builders Licensing Board, Report No. S7032/3-AD, Sydney, Australia.
- Coffey and Partners Pty. Ltd. (1985). *Sydney Swelling Soils Study: Analysis of Data*, Report to the Builders Licensing Board, Report No. S7032/2-AD, Sydney, Australia.
- Cokca, E. (2000). "Measurement of swell pressure," *Quarterly Journal of Engineering Geology and Hydrogeology* 33, pp. 141 – 147.

- Cokca, E. (2002). "Relationship between methylene blue value, initial soil suction and swell percent of expansive soils," *Turk J Eng Environ Sci* 26, pp.521–529.
- Çokca, E. and Birand, A.A. (1993a). "Prediction of swelling potential of Ankara soils by methylene blue test," *Doğa- Turkish Journal of Engineering and Environmental Sciences* 17, pp. 57–63.
- Çokca, E. and Birand, A.A. (1993b). "Determination of cation exchange capacity of clayey soils by the methylene blue test," *Geotechnical Testing Journal* 16 (4), pp. 518–524.
- CDOT, Colorado Dept. of Transportation (2011). Pavement Design Manual, accessed via www.Coloradodot.info/business/designsupport/manuals.pdf
- Coleman, J. D. (1962). "Stress/strain relations for partly saturated soils," *Correspondence, Geotechnique*, Vol. 12, pp. 348–350.
- Coleman, N.J. and Harward, M.E. (1953). "The heats of neutralization of acid clays and cation exchange resins," *Journal of the American Chemical Society* 75, pp. 6045–6046.
- Cooke, C. W. (1939). "Equivalence of the Gosport Sand to the Moodys Marl," *Journal of Paleontology*, 13(3), pp. 337-340.
- Covar, A.P. and Lytton, R.L. (2001). "Estimating soil swelling behavior using soil classification properties," *Geotechnical Special Publication 115, Expansive Clay Soils and Vegetative Influence on Shallow Foundations*, ASCE, pp. 44 – 62.
- Croney, D., Coleman, J. D., and Black, W. P. M. (1958). "Movement and distribution of water in soil in relation to highway design and performance," National Research Council, *Highway Research Board, Special Rep. 40*, Washington, D.C., pp. 226–252.
- Day, R. W. (1994). "Shrink-swell behaviour of compacted clay," *ASCE Journal of Geotechnical Engineering*, 120(3), pp. 618–623.
- Day, R.W. (1998). "Swelling behavior of desiccated clay," *Environmental and Engineering Geoscience IV* (1), pp. 124–129.
- De Bruijn, C. M. A. (1961). "Swelling characteristics of a transported soil profile at Leeuhof Vereeniging (Transvaal)," *Proceedings, 5th International Conference on Soil Mechanics and Foundation Engineering*, Vol. 1, pp. 43–49.
- De Freitas, M.H. and Mannion, W.G. (2007). "A biostratigraphy for the London Clay in London," *Geotechnique* 57(1), pp. 91 – 99.
- Decagon Devices, Inc. (2004). "WP-4 PotentiaMeter Operator's Manual Version 2.2," <http://www.decagon.com/manuals/WP4man22.pdf>.
- Deka, S., Sreedeeep, S., and Kumar, S. (2009). "Re-evaluation of laboratory cone penetration method for high liquid limit based on free swell property of soil," *Geotechnical Testing Journal*, Vol. 32(6)

- Dept of Navy (1971). *Design Manual-Soil Mechanics, Foundations and Earth Structures*, NAVFAC DM-7, Department of Naval Facilities Engineering Command, U.S. Naval Publications and Forms Center.
- Dept. of the Army (1971). "Effect of sample preparation procedures for clay shale on Atterberg limits," Missouri River Division Laboratory Report No. 68/427, Omaha, NE, 7 pp.
- Dept. of the Army (1983). "Foundations on expansive soils," Technical Manual TM 5-818-7, Washington, D.C.
- Dhowian, A. W. (1990). "Heave prediction techniques and design considerations on expansive soils," *Journal of King Saudi University*, 2(2), pp. 355-377.
- Dhowian, A. W. (1990). "Soil suction-potential model," *Journal of Geotechnical Engineering* 118, pp. 521-539.
- Di Maio, C., Santoli, L., and Schiavone, P. (2004). "Volume change behaviour of clays: the influence of mineral composition, pore fluid composition and stress state," *Mechanics of Materials* 36, pp.435-451.
- Diaa, E.A. and Hanafy, E. (1998). "Ring shrinkage test for expansive clays: A suggested simple test method for determining vertical, lateral, and volumetric shrinkage potential," *Geotech Test. J.*, 21(1).
- Dockery, D.T. (1981). "Upper Eocene Carcharodons in Mississippi," *Mississippi Geology* Vol 1(4), p. 6.
- Dockery, D.T. and Siesser, W.G. (1984). "Age of the upper Yazoo Formation in central Mississippi," *Mississippi Geology* 5(1), pp. 1 - 7.
- Dockery, D.T. (1985). "Tar pods from the Yazoo clay (upper Eocene) at Cynthia, Mississippi," *Mississippi Geology* 5(4), pp. 1 - 3.
- Dockery, D.T. and Johnston, J.E. (1986). "Excavation of an archaeocete whale, *Basilosaurus Cetoides* (Owen), from Madison, Mississippi," *Mississippi Geology* 6(3), pp. 1 - 6.
- Dockery, D.T. and Zumwalt, G.S. (1986). "Pteropods (Mollusca: Gastropoda) from the upper Yazoo Formation (Eocene) at Cynthia, Mississippi," *Mississippi Geology* 6(3), pp. 9 - 12.
- Dockery, D.T., Stover, C.W., Weathersby, P., Stover, Jr., C.W., and Ingram, S.L. (1991). "A continuous core through the undifferentiated Yazoo Clay (Late Eocene, Jackson Group) of central Mississippi," *Mississippi Geology*, 12(3 and 4), pp. 21-27.
- Dockery, D.T. (1992). "Jackson Ready Mix Miss-Lite plant and clay pit to close after 34 years of operation," *Mississippi Geology* Vol 13(2), p. 22.
- Dockery, D.T., Starnes, J.E., and Peyton, S. (2003). "A largely complete *Basilosaurus* find in the upper Yazoo clay in Scott County, Mississippi," *Journal of the Mississippi Academy of Sciences*, 67th Annual Meeting Abstracts, Vol 48(1), pp. 42 - 43.

- Dockery, D.T. (2005). "Engineering geologic failures and cost overruns: Examples from Mississippi," in *Geological Society of America, Southeastern Section, 54th Annual Meeting, Abstracts with Programs* 37(2), page 49.
- Dockery, D.T. (2009a). "Engineering geology, the Yazoo clay, and the Saints," *Mississippi Geological Society Bulletin* 58(2), Mississippi Office of Geology. missgeo.com
- Dockery, D.T. (2009b). "Mississippi's giant snakes," *MDEQ Environmental News*, Vol 6(5), p. 5. www.deq.state.ms.us
- Dockery, D.T. (2009c). "The Dogwood Festival slump," *MDEQ Environmental News*, Vol 6(6), pp 6 - 9. www.deq.state.ms.us
- Dockery, D.T. (2010a). "A slope too steep: slumps in the Yazoo clay in central Mississippi," *MDEQ Environmental News*, Vol 7(5), pp 16 - 20. www.deq.state.ms.us
- Dockery, D.T. (2010b). "Holding back the Yazoo clay at the Farmers' Market," *MDEQ Environmental News*, Vol 7(9), pp 14 - 17. www.deq.state.ms.us
- Douglas, S. C., and Dunlap, G. T. (2000). "Light commercial construction on Yazoo clay," *Proc. 2nd Forensic Congress*, San Juan, Puerto Rico, pp. 607-616.
- Easson, G.L., Faraque, F., and Yarbough, L.D. (2005). "Rating the shrink/swell behavior of the Porters Creek Formation," *Environmental & Engineering Geoscience*, Vol. XI (2), pp. 171-176.
- El-Sohby, M. A. and El-Sayed, A. R. (1981). "Some factors affecting swelling of clayey soils," *J. Geotech. Engrg.*, Vol. 12, pp. 19-39.
- Erguler, Z.A. and Ulusay, R. (2003a). "A simple test and predictive models for assessing swell potential of Ankara (Turkey) clay," *Engineering Geology* 67, pp. 331-352.
- Erguler, Z.A. and Ulusay, R. (2003b). "Engineering characteristics and environmental impacts of the expansive Ankara clay, and swelling maps for central and SW parts of the Ankara (Turkey) metropolitan area," *Environmental Geology* 44, pp. 979-992.
- Erzin, Y. and Erol, O. (2004). "Correlations for quick prediction of swell pressures," *The Electronic Journal of Geotechnical Engineering* [serial online], 9(F), Paper No. 0476. www.ejge.com/2004/Ppr0476/Abs0476.htm [accessed 8 June 2011].
- Erzin, Y. and Erol, O. (2007). "Swell pressure prediction by suction methods," *Engineering Geology* 92(3-4), pp.133-145.
- Ewing, R.C. (2010). "Foundation repairs due to expansive soils: Eudora Welty House Jackson, Mississippi," *ASCE Journal of Performance of Constructed Facilities* (accepted for publication 5 July), 26 pages.
- Federal Housing Authority (1974). "Guide to use of the FHA Soil PVC Meter, including results of nationwide soil tests and correlation with climatic factors," FHA 4075.15, U. S. Gov't Printing Office.

- Feng, T. (2004). "Using a small ring and a fall-cone to determine the plastic limit," *ASCE Journal of Geotechnical and Geoenvironmental Engineering*, Vol 130, No 6, pp 630 - 635.
- Fierstine, H. L. and Applegate, S. P. (1974). " *Xiphiorhynchus kimblalocki*, a new billfish from the Eocene of Mississippi with remarks on the systematics of xiphoid fishes," *Bulletin of the Southern California Academy of Sciences*, Vol 73(3), pp. 14 - 22.
- Fierstine, H. L. and Starnes, J.E. (2005). " *Xiphiorhynchus* from the middle Eocene of Mississippi, the first Transatlantic distribution of a species of *Xiphiorhynchus*," *Journal of Vertebrate Paleontology*, Vol 25(2), pp. 280–287
- Fierstine, H. L. and Stringer, G.L. (2007). "Specimens of the Billfish *Xiphiorhynchus* from the Yazoo Clay Formation (Late Eocene), Louisiana," *Journal of Vertebrate Paleontology*, Vol 27(1), pp. 226-231
- Fityus, S. G. (1996). "The effect of initial moisture content and remoulding on the shrink-swell index," *Proceedings of the 7th Australian-New Zealand Conference on Geomechanics*, Institution of Engineers Australia, Adelaide, pp. 388–393.
- Fityus, S. G. (1999). "Transport processes in unsaturated soils," PhD thesis, Univ. of Newcastle, Callaghan, Australia.
- Fityus, S. G. and Delaney, M. D. (1995). "The unique influence of Lower Hunter coal measures on reactive soil phenomena in the Newcastle area," *Proceedings of the 8th Symposium on Advances in the Study of the Sydney Basin*, University of Newcastle, pp. 167–174.
- Fityus, S. G. and Smith, D. W. (2003). "Behaviour of a model footing on expansive clay," *Proceedings of Unsat Asia 2003, the 2nd Asian Unsaturated Soils Conference*, Osaka, pp. 181– 186.
- Fityus, S. G. and Welbourne, J. C. (1996). "Trends in shrink-swell test results in the Newcastle region," *Proceedings of the 7th Australian-New Zealand Conference on Geomechanics*, Institution of Engineers Australia, Adelaide, pp. 394–399.
- Fityus, S. G., Smith, D. W., and Allman, M. A. (2004). "An expansive soil test site near Newcastle," *ASCE Journal of Geotechnical and Geoenvironmental Engineering* 130(7), pp. 686–695.
- Fityus, S. G., Walsh, P. F., and Kleeman, P. W. (1998). "The influence of climate as expressed by the Thornthwaite index on the design depth of moisture change of clay soils in the Hunter Valley," *Conf. on geotechnical engineering and engineering geology in the Hunter Valley*, Conference Publications, Springwood, Australia, pp. 251–265.
- Fityus, S.G., Smith, D.W., and Jennar, A.M. (2000). "Surface area using methylene blue adsorption as a measure of soil expansivity," *GeoEng 2000, An International Conference on Geotechnical and Geological Engineering*, Melbourne, Australia
- Fityus, S.G., Cameron, D.A., and Walsh, P.F. (2005). "The shrink-swell test," *Geotechnical Testing Journal*, 28(1)

- Fluegeman, R. H. (2003). "Paleobathymetry of the Jackson Group (Eocene; Bartonian-Priabonian) of Western Mississippi: Data From Foraminiferal Assemblages," *GSA Abstracts North Central Section Annual Meeting*.
- Franzmeier, D.P. and Ross, S.J. (1968). "Soil swelling: Laboratory measurement and relation to other soil properties," *Soil Sci. Soc. Amer. Journal* 32(4), pp. 573 – 577.
- Frazer, J.C., Taylor, R.K. and Grollman, A. (1928). "Two-phase liquid-vapor isothermal systems, vapor pressure lowering," *International Critical Tables*, Vol 3, p 297.
- Frazier, M.K. (1980). "Archaeocetes: Whale-like mammals from the Eocene of Mississippi," *Mississippi Geology* 1(2), pp. 1 – 3.
- Fredlund, D .G. and Rahardjo, H. (1993). *Soil Mechanics for Unsaturated Soils*, John Wiley & Sons, New York.
- Fredlund, D. G. and Morgenstern, N. R. (1977). "Stress state variables for unsaturated soils," *Journal of Geotechnical Engineering Division*, ASCE, Vol. 103, No. GT5, pp. 447–466.
- Fredlund, D. G., Hasan, J. U., and Filson, H. L. (1980). "The prediction of total heave," *Proceedings of 4th International Conference on Expansive Soils*, ASCE and International Society for Soil Mechanics and Foundation Engineering, Denver, pp. 1–17.
- Freeman, T. J., Burford, D., and Crilly, M. S. (1991). "Seasonal foundation movements in London Clay," *Proceedings, 4th International Conference Ground Movements and Structures*, Cardiff.
- Galicki, S.J. (2008). "Slope failure at Millsaps College, Jackson, Mississippi: There are no simple jobs," *Geological Society of America, Abstracts with Programs* 40(6), page 217.
- Garner, D. N. (2002). "Soil suction for the investigating engineer," *Proceedings of the Texas Section of the American Society of Civil Engineers Fall 2002 Meeting*, Waco, Texas, October 2–5, 2002.
- Gates, C. and Hatano, M. (1967). "Development of a rapid field test for evaluating the expansive potential of clay soils during construction," *Research Report 633139-1*, State of California, Dept. of Public Works, Division of Highways, Materials and Research Dept.
- Gee, G., Campbell, M., Campbell, G., and Campbell, J. (1992). "Rapid measurement of low soil potentials using a water activity meter," *Soil Sci. Soc. Am. J.*, Vol. 56, pp. 1068–1070.
- Gens, A. and Alonso, E. E. (1992). "A framework for the behaviour of unsaturated expansive clays," *Canadian Geotechnical Journal*, Vol. 29, pp. 1013–1032.
- Gibbes, R. W. (1847). "On the fossil genus *Basilosaurus* Harlan (*Zeuglodon*, Owen) with a notice of specimens from the Eocene Green Sand of South Carolina," *Journal of the Academy of Natural Sciences of Philadelphia* 1:2–15.

- Gibbs, H. J. (1973). "Use of a consolidometer for measuring expansion potential of soils," *Proceedings of the Workshop on Expansive Clays and Shales in Highway Design and Construction*, University of Wyoming, Laramie, Vol. 1, pp. 206–213.
- Goetz, A.F.H., Chabrilat, S., and Lu, Z. (2001). "Field reflectance spectrometry for detection of swelling clays at construction sites," *Field Analytical Chemistry and Technology* 5(3) pp. 143 – 155.
- Gourley, C.S. and Schreiner, H.D. (1995). "Field measurement of soil suction," *First International Conference on Unsaturated Soils, UNSAT '95, Paris, 6 - 8 September*.
- Graham, J., and Li, E.C.C. (1985). "Comparison of natural and remolded plastic clay," *Journal of Geotechnical Engineering*, ASCE, 111(7), pp. 865–881.
- Gray, C.W. and Allbrook, R. (2002). "Relationships between shrinkage indices and soil properties in some New Zealand soils," *Geoderma* 108 (3– 4), pp. 287– 299.
- Green, J.W. and Childress, S.C. (1974). "Environmental geology of the Madison, Ridgeland, Jackson, and Jackson SE Quadrangles, Hinds, Madison, and Rankin Counties, Mississippi," *Environmental Geology Series 2, Mississippi Geological, Economic, and Topographical Survey*, Jackson, MS, 64 pp.
- Green, E. (2005). "The science of expansive clays," Internet presentation (accessed Dec 2009), www.slabongrade.net/.../Science_of_Expansive_Clay.pdf
- Greene-Kelly, R. (1974). "Shrinkage of clay soils: A statistical correlation with other soil properties," *Geoderma* 11, pp. 243– 257.
- Grim, R.E. (1968). *Clay Mineralogy*, McGraw-Hill, NY, pp. 185-233.
- Gromko, G.J. (1969). "Planned field testing of expansive clay soil," *Proceedings of 2nd Intl Research and Engineering Conf. on Expansive Clay Soils*, Texas A&M, pp. 235 – 240.
- Gromko, G.J. (1974). "Review of expansive soils," *American Society for Civil Engineering Journal of Geotechnical Engr* 6, pp. 667–687.
- Grossman, R.B., Brasher, B.R., Franzmeier, D.P. and Walker, J.L. (1968). "Linear extensibility as calculated from natural-clod bulk density measurements," *Soil. Sci. Soc. Amer. Journal* 32(4), pp. 570 – 573.
- Haasl, D.M. and Hansen, T.A. (1996). "Timing of latest Eocene molluscan extinction patterns in Mississippi," *Palaios* 11, pp. 487 – 494.
- Hanafy, E. (1991), "Swelling/shrinking characteristic curve of desiccated expansive clays," *Geotechnical Testing Journal*, 14(2), pp. 206–211.
- Hanafy, E. (1998). "Ring shrinkage test for expansive clays: A suggested simple test method for determining vertical, lateral, and volumetric shrinkage potential," *Geotechnical Testing Journal* 21(1), ASTM, pp. 69 – 72.

- Hang, P.T. and Brindley, G.W. (1970). "Methylene blue adsorption by clay minerals: determination of surface areas and cation exchange capacities," *Clays and Clay Minerals* 18, pp. 203–212.
- Hansbo, S. (1957). "A new approach to the determination of the shear strength of clay by the fall-cone test," in *Proceedings of the National Swedish Geotechnical Institute*, No. 14.
- Hardy, R. M. (1965). "Identification and performance of swelling soil types," *Canadian Geotechnical Journal*. Vol. 11, pp. 141-153.
- Harrelson, D.W. (1981). "Igneous rocks of the Jackson Dome, Hinds-Rankin Counties, Mississippi," *Mississippi Geology*, Vol 1(4), pp. 7 – 13.
- Harison, J.A. (1988). "Using the BS cone penetrometer for the determination of the plastic limits of soils," *Geotechnique*, Vol 38 No 3, pp 433 - 438.
- Harrison, B. A., and Blight, G. E. (2000). "A comparison of in situ soil suction measurements," *Unsaturated soils for Asia, Singapore*, H. Rahardo, D. Toll, and E. Leong, eds., Balkema, Rotterdam, The Netherlands, pp. 281–285.
- Hassan, M. and El-Shall, H. (2004). "Glaucconitic clay of El Gidida, Egypt: evaluation and surface modification," *Applied Clay Science* Vol 27(3-4), pp 219 222.
- Heley, W. and MacIver, B.N. (1971). "Engineering properties of clay shales," Report 1, Technical Report S-71-6, 37 pp. plus Appendix A and B, U.S. Army Engineer Waterways Experiment Station, Vicksburg, MS.
- Hight, D.W., Gasparre, A., Nishimura, S., Minh, N.A., Jardine, R.J. and Coop, M.R. (2007). "Characteristics of the London Clay from Terminal 5 site at Heathrow Airport," *Geotechnique* 57(1), pp. 3 – 18.
- Hills, J.F. and Pettifer, G.S. (1985). "The clay mineral content of various rock types compared with the methylene blue value," *Journal of Chemical Technology and Biotechnology* 35, pp. 168–180.
- Holland, J. E., and Lawrence, C. E. (1980). "Seasonal heave of Australia clay soils," *Proc., 4th Int. Conf. on Expansive Soils*, ASCE, New York, pp. 302–321.
- Holland, J. E., and Richards, J. (1982). "Road pavements on expansive clays," *Aust. Road Res.* 12, pp. 173–179.
- Holtz, R. D. and Kovacs, W. D. (1981). *An Introduction to Geotechnical Engineering*, Prentice-Hall, Englewood Cliffs, NJ, 733 pp.
- Holtz, W.G. and Gibbs, H.J. (1954). "Engineering properties of expansive clays," *Proceedings of the American Society of Civil Engineers*, Vol 80, Separate no. 516, October, pp. 1 – 28.
- Holtz, W.G. (1959). "Expansive clays-properties and problems," *Quarterly of the Colorado School of Mines* 54 (4), pp. 89–125.
- Honjo, S. and Berggren, W.A. (1967). "Scanning electron microscope studies of planktonic foraminifera," *Micropaleontology*, Vol 13(4), pp. 393 – 406.

- Hou, J. (1992). "Clay mineralogy of continuous core of upper Yazoo clay, Hinds County, Mississippi," Master's thesis, University of Southern Mississippi, Hattiesburg, MS, 79 pp.
- Houston, S. L., Houston, W. N., and Wagner, A. M. (1994). "Laboratory filter paper suction measurements," *Geotech. Test. J.*, 17(2), pp. 185–194.
- Huff, W.J. (1960). "The Jackson Eocene Ostracoda of Mississippi," PhD thesis, The Rice Institute (Rice University), Houston, TX, 324 pp.
- International Focus Group (IFG) on Rural Road Engineering (2005). "Guidelines for the assessments of soils and gravels," Information Note, website <http://www.ifgworld.org/>
- Indian Standard Code (1977). "Standard methods for testing soils: Determination of free swell index of soils," IS: 2720-part 40, BIS, New Delhi.
- Intl Organization for Standards (ISO) (2004). "Determination of Atterberg limits," TS 17892-12:2004.
- Ito, M. and Azam, S. (2010). "Determination of swelling and shrinkage properties of undisturbed expansive soils," *Geotechnical and Geological Engineering*, Vol 28(4), pp. 413 – 422.
- Jennings, J. E. B. and Knight, K. (1957). "The prediction of total heave from the double oedometer test," *Transactions of the South African Institute of Civil Engineering*, Vol. 7, pp. 285– 291.
- Jennings, J. E. B., Firtu, R. A., Ralph, T. K., and Nagar, N. (1973). "An improved method for predicting heave using the oedometer test," *Proceedings of the 3rd International Conference on Expansive Soils*, Haifa, Israel, Vol. 2, pp. 149–154.
- Jeter, L.W. (2001). "Foundation repair business flourishing in Metro," *Mississippi Business Journal*, October 29.
- Jeter, L.W. (2006). "Weather pattern's impact on Yazoo clay often delayed," *Mississippi Business Journal*, October 2.
- Jiang, H., Liu, Z., and Fang, H.Y. (2002). "Engineering geological characteristics of expansive soils in China," *Engineering Geology* 67 (2002), pp. 63–71.
- Johnson, W.B. and Clark, C.V. (1955). "Hillside multiple slump faulting at Sartartia, MS," presentation to the Mississippi Academy of Sciences, Meridian Municipal College, pp. 101- 103.
- Johnson, L.D. (1969). "Review of literature on expansive clay soils," *Misc. Paper S-69-24*, U.S. Army Engineer Waterways Experiment Station, Vicksburg, Mississippi.
- Johnson, L. D. (1973a). "Properties of expansive clay soils, Jackson field test section study," *Report 1, Misc. Paper S-73-28*, U.S. Army Engineer Waterways Experiment Station, Vicksburg, Mississippi.

- Johnson, L. D. (1973b). "Influence of suction on heave of expansive soils," *Misc. Paper S-73-17*, U.S. Army Engineer Waterways Experiment Station, Vicksburg, Mississippi..
- Johnson, L. D. (1974). "Psychrometric measurement of total suction in a triaxial compression test," *Misc. Paper S-74-19*, U.S. Army Engineer Waterways Experiment Station, Vicksburg, Mississippi.
- Johnson, L. D. (1977). "Evaluation of laboratory suction tests for prediction of heave with time in foundation soils," *Report WES-TR-S-77-7*, U.S. Army Engineer Waterways Experiment Station, Vicksburg, Mississippi.
- Johnson, L. D. (1978). "Predicting potential heave and heave with time in swelling foundation soils," *Technical Report S-78-7*, U.S. Army Engineer Waterways Experiment Station, Vicksburg, Mississippi.
- Johnson, L.D. (1979). "Overview for design of foundations on expansive soils," *Misc. Paper GL-79-21*, U.S. Army Engineer Waterways Experiment Station, Vicksburg, Mississippi.
- Johnson, L. D. and McAnear, C. L. (1973). "Controlled field tests of expansive soils," *Proceedings of the Workshop on Expansive Clays and Shales in Highway Design and Construction*, D.R. Lamb and S.J. Hanna, editors, University of Wyoming, Laramie, Vol. 1, pp. 137–159.
- Johnson, L. D., and Desai, C.S. (1975). " Properties of expansive clay soils; A numerical procedure for predicting heave with time," *Report 2, Misc. Paper S-73-28*, U.S. Army Engineer Waterways Experiment Station, Vicksburg, Mississippi.
- Johnson, L. D., and Stroman, W.R. (1976). "Analysis of behavior of expansive soil foundations," *Technical Report S-76-8*, U.S. Army Engineer Waterways Experiment Station, Vicksburg, Mississippi.
- Johnson, L. D., Sherman, W.C., and McAnear, C. L. (1973). "Field test sections on expansive clays," *Proc. 3rd Intl Conf on Expansive Soils*, Vol 3, pp. 239 – 248.
- Johnson, L.D. and Snethen, D.R. (1978). "Prediction of potential heave of swelling soil," *Geotechnical Testing Journal* 1, pp. 117–124.
- Jones, D. E., and Holtz, W. G. (1973). "Expansive soils—The hidden disaster," *Civ. Eng. (N.Y.)*, 43(8), pp. 49–51.
- Jones, L.D. and Terrington, R. (2011). "Modelling volume change potential in the London Clay," *Quarterly Journal of Engineering Geology and Hydrogeology*, Vol 44, pp. 109 – 122.
- Jong, E. (1999). "Comparison of three methods of measuring surface area of soils," *Canadian Journal of Soil Science* 79, pp. 345–351.
- Kahr, G. and Madsen, F.T. (1995). "Determination of the cation exchange capacity and the surface area of bentonite, illite and kaolinite by methylene blue adsorption," *Applied Clay Science* 9, pp. 327–336.

- Kariuki, P. C. , Van Der Meer, F. and Verhoef, P. N. W.(2003). "Cation exchange capacity (CEC) determination from spectroscopy," *International Journal of Remote Sensing*, 24(1), pp.161-167.
- Kariukia, P.C. and Van der Meer, F. (2004). "A unified swelling potential index for expansive soils," *Engineering Geology* 72, pp. 1–8.
- Kayabali, K. and Demir, S. (2011). "Measurement of swelling pressure: direct method versus indirect methods," *Can Geotech J*, Vol 48, pp. 354 – 364.
- Kipling, J.J. and Wilson, R.B. (1960). "Adsorption of methylene blue in the determination of surface area," *Journal of Applied Chemistry* 10, pp. 109–113.
- Knox, P.R., Kelley, V.A., Vreugdenhil, A., Deeds, N., and Seni, S. (2007). " Structure of the Yegua-Jackson aquifer of the Texas Gulf coastal plain," Texas Water Development Board, contract number 0604830593, 145 p.
- Koester, J.P. (1992). "The influence of test procedure on correlation of Atterberg limits with liquefaction in fine-grained soils," *Geotechnical Testing Journal*, Vol 15, No 4, pp 352 - 361.
- Kovacevic, N., Hight, D.W. and Potts, D.M. (2007). "Predicting the stand-up time of temporary London Clay slopes at Terminal 5, Heathrow Airport," *Geotechnique* 57(1), pp. 63 – 74.
- Kresse, T.W. and Fazio, J.A. (2002). "Pesticides, water quality and geochemical evolution of ground water in the alluvial aquifer, Bayou Bartholomew watershed, Arkansas," Arkansas Department of Environmental Quality Ambient Ground-Water Monitoring Program Report WQ02-05- 1, 87 pp.
- Krohn, I. D. and Slossen, J. E. (1980). "Assessment of expansive soil in the United States," *Proceedings of the 4th International Conference on Expansive Soils*, Denver, pp. 596–608.
- Krosley, L., Likos, W.J. and Lu, N. (2003). "Alternative encasement materials for Clod test," *Geotechnical Testing Journal*, Vol 26(4).
- Laier, J.E. and Lamar, J.H. (1980). "Minimizing foundation swell in Yazoo clay," *Proc. 4th Intl Conference on Expansive Soils*, Denver, CO, Vol. 1, pp. 421 – 437.
- Lambe, T.W. (1960). "The character and identification of expansive soils," *FHA Technical Studies Report 701*, Federal Housing Administration, Washington D.C. , 114 p
- Lambe, T.W. and Whitman, R.V. (1979). *Soil Mechanics*, John Wiley & Sons, Inc., Singapore.
- Lan, T. N. (1979). "A new test for the identification of soils: Methylene blue test," *Bulletin Liaison Laboratoire Ponts et Chaussee* 88, pp. 136–137.
- Lawson, W.D. (2006). "A survey of geotechnical practice for expansive soils in Texas," *Unsaturated Soils 2006*, ASCE, pp. 304 – 314.
- Lee, L.T. (2004). "Method to rapidly assess the index properties of fine-grained dredged materials," *Geotechnical Testing Journal*, Vol 27 No 5, pp 464 - 468.

- Lee, L.T. and Freeman, R.B. (2007). "An alternative method for assessing consistency limits," *Geotechnical Testing Journal*, Vol 30(4), pp. 274 - 281.
- Lee, L.T. and Freeman, R.B. (2009). "Dual-weight fall cone method for simultaneous liquid and plastic limit determination," *ASCE Journal of Geotechnical and Geoenvironmental Engineering* 135(1), pp. 158–161.
- Lee, L.T. (2011). "Investigation of a Mississippi expansive soil (Yazoo clay): Part 1 of 2 (in publication), U.S. Army Engineer Research and Development Center, Vicksburg, Mississippi.
- Leong, E.C., He, L. and Rahardjo, H. (2002). "Factors affecting the filter paper method for total and matric suction measurements." *Geotechnique* 25(3), pp. 322-333.
- Leong, E-C., Tripathy, S., and Rahardjo, H. (2003). "Total suction measurement of unsaturated soils with a device using the chilled-mirror dew-point technique," *Geotechnique*, 53(2), pp. 173–182.
- Leroueil, S. and Le Bihan, J.P. (1996). "Liquid limits and fall cones," *Canadian Geotechnical Journal*, Vol 33, pp 793 - 798.
- Li, J., Smith, D. W., Fityus, S. G., and Sheng, D. C. (2003). "The numerical analysis of neutron moisture probe measurements," *Int. J. Geomech.*, 3, pp. 11–20.
- Likos, W. J. (2008). "Vapor adsorption index for expansive soil classification," *Journal of Geotechnical and Geoenvironmental Engineering* 134(7).
- Likos, W. J. and Lu, N. (2002). "Filter paper technique for measuring total soil suction," *Transportation Research Record: Journal of the Transportation Research Board*, No. 1786, TRB, Washington, DC, pp. 120–128.
- Likos, W. J., Olsen, H. W., Krosley, L., and Lu, N. (2003). "Measured and estimated suction indices for swelling potential classification," *ASCE Journal of Geotechnical and Geoenvironmental Engineering* 129(7), pp. 665–668.
- Likos, W.J., Lu, N. and Sharkey, K.J. (2005). "Laboratory characterization of steeply dipping expansive bedrock in the Rocky Mountain Front Range," *Journal of Geotechnical and Geoenvironmental Engineering* 131(9), pp. 1162 – 1171.
- Lu, N. and Likos, W. J. (2004). *Unsaturated Soil Mechanics*, John Wiley and Sons, NewYork.
- Lucian, C. (2008). "Geotechnical aspects of buildings on expansive soils in Kibaha, Tanzania," Ph.D. Thesis, Division of Soil and Rock Mechanics Department of Civil and Architectural Engineering Royal Institute of Technology Stockholm, Sweden, 196 pp.
- Luper E.E., Angurarohita, R., and Baughman, W.T. (1972). "Smith County Geology and Mineral Resources," *Mississippi Geological, Economic, and Topographic Survey Bulletin* 116, 180p.
- Lytton, R. L. (1994). "Prediction of movement in expansive clays," *ASCE Geotechnical Special Publication No. 40, Volume 2, Vertical and Horizontal Deformations of Foundations and Embankments*, pp. 1827-1844.

- Lytton, R., Aubeny, C., and Bulut, R. (2005). "Design procedure for pavements on expansive soils: Volume 1," *Report No. FHWA/TX-05/O-4518-1*.
- Mabirizi, D. and Bulut, R. (2009). "A comparison of total suction measurements with thermocouple psychrometer, filter paper technique and chilled-mirror device," *Geotechnical Special Publication No. 189, GeoHunan International Conference 2009*.
- Marinho, F.A. M. and Oliveira, O.M. (2006). "The filter paper method revisited," *Geotechnical Testing Journal*, 29(3).
- Martin, R. V. (2007). "Sample, describe, and map Yazoo Clay," Unpublished Report of Mississippi Dept. of Transportation, MDoT Study 151, Jackson, MS.
- Matyas, E. L. and Radhakrishna, H. S. (1968). "Volume change characteristics of partially saturated soils," *Geotechnique*, Vol. 18, pp. 432–448.
- Maxwell, B. (2011a). "The investigation and repair of a 4-story building damaged by Yazoo clay," *ASCE Journal of Performance for Constructed Facilities* Vol 25(1), pp. 18 – 23.
- Maxwell, B. (2011b). "Field measurements of Yazoo clay reveals expansive soil design issues," *ASCE Journal of Performance for Constructed Facilities* Vol 25(1), pp. 45 – 49.
- McCook, D. K., and Shanklin, D. W. (2000). "NRCS experience with field density test methods including the sand-cone, nuclear gage, rubber balloon, drive-cylinder, and clod test," *Constructing and Controlling Compaction of Earth Fills, ASTM STP 1384*, D. W. Shanklin, K. R. Rademacher, and J. R. Talbot, Eds., American Society for Testing and Materials, West Conshohocken, PA.
- McDowell, C. (1959). "The relation of laboratory testing to design for pavements and structures on expansive soils," *Quarterly of the Colorado School of Mines*, 54(4), pp. 127 – 153.
- McKeen, R. G. (1981). "Design of airport pavements on expansive soils," *DOT/FAA/RD-81/25*, Systems Research and Development Service, Federal Aviation Administration, Washington, DC.
- McKeen, R. G. (1985). "Validation of procedures for pavement design on expansive soils," *DOT/FAA/PM-85/15*, Program Engineering and Maintenance Service, Federal Aviation Administration, Washington, DC.
- McKeen, R. G. and Johnson, L. D. (1990). "Climate-controlled soil design parameters for mat foundations," *Journal of Geotechnical Engineering*, ASCE, 116(7), pp. 1073-1094.
- McKeen, R. G. and Nielsen, J. P. (1978). "Characterization of expansive soils for airport pavement design," U.S. Department of Transportation, Federal Aviation Administration, *Report No. FAA-120-78-59*.

- McKeen, R.G. (1992). "A model for predicting expansive soil behaviour," *Proceedings of the 7th International Conference on Expansive Soils*, Dallas, Tex., 3–5 August 1992. American Society of Civil Engineers, New York. Texas Tech University Press, Lubbock. Vol. 1, pp. 1–6.
- McKeen, R.G., and Hamberg, D.J. (1981). "Characterization of expansive soils," *Transportation Research Record*, vol. 790. Transportation Research Board, USA, pp. 73–78.
- McKeen, R.G. (2001). "Investigating field behavior of expansive clay soils," *Geotechnical Special Publication 115, Expansive Clay Soils and Vegetative Influences*, pp. 82 – 94.
- Mendoza, M.J. and Orozco, M. (2001). "Quick and reliable procedure for liquid limit determination of fine-grained soils," *Geotechnical Testing Journal*, Vol 24, No 1, pp 103 - 108.
- Meisina, C. (2007). "Relationship between the residual shear strength and the methylene blue value in weathered clay soils," *Geophysical Research Abstract* 9.
- Meisina, C.(2000). "Predicting swelling/shrinkage potential using the methylene blue method: some examples from Italian clayey soils," *Geoeng 2000*, Melbourne, Australia.
- Mellen, F. F. (1940). "Yazoo County Mineral Resources," *Mississippi State Geological Survey*, Bulletin 39
- Mesri, G. and Shahien, M. (2003). "Residual shear strength mobilized in first-time slope failures." *Journal of Geotechnical and Geoenvironmental Engineering*, ASCE, Vol 129, No. 1, pp 12-31.
- Mississippi Business Journal (2001). "Foundation repair business flourishing in metro," October 29, 3 pp.
- Mississippi Business Journal (2004). "That pesky Yazoo clay," November 22, 2 pp.
- Mississippi Business Journal (2006a). "Tackling troublesome Yazoo clay," March 20, 2 pp.
- Mississippi Business Journal (2006b). "Weather pattern's impact on Yazoo clay often delayed," October 2, 2 pp.
- Mississippi Business Journal (2008). "Yazoo clay: Old problem getting new look from researchers," June 16, 2 pp.
- Mississippi Business Journal (2009). "Making the most of shifty developments," June 15, 2 pp.
- Mississippi Business Journal (2010). "Dry as dust," Nov 14, 2 pp.
- Mississippi Business Journal (2011). "Yazoo clay can be a dirty word," June 5, 2 pp.
- Mitchell, J. K. (1993). *Fundamentals of Soil Behavior*, 3rd ed., John Wiley, New York.

- Mitchell, P. W. and Avalue, D. L. (1984). "A technique to predict expansive soil movements," *Proceedings of the 5th International Conference on Expansive Soils*, Adelaide, South Australia, pp. 124-130.
- Monroe, W.H. (1954). "Geology of the Jackson area, Mississippi," *U.S. Geol. Survey Bull.* 986, pp. 57 - 59.
- Moore, W. H. (1973). *Mississippi Geological, Economic and Topographical Survey*, Mississippi Geology Survey Information, Bulletin 118, Jackson, Mississippi.
- Moore, W. H., Bicker Jr., A.R., McCutcheon, T.E., and Parks, W.S. (1965). "Hinds County Geology and Mineral Resources," *Mississippi Geological, Economic, and Topographic Survey Bulletin* 105, 244p.
- Mulla, D. J., Low, P. F., and Roth, C. B. (1985). "Measurement of the specific surface area of clays by internal reflectance spectroscopy," *Clays and Clay Minerals*, 33(5), pp. 391-396.
- Murphy, W.L. and Albertson, P.E. (1996). "Engineering geological geographical information system of the Waterways Experiment Station," *Mississippi Geology* 17(2), pp. 1 - 39.
- Nagaraj, H.B., Munnas, M.M., and Sridharan, A. (2009). "Critical evaluation of determining swelling pressure by swell-load method and constant volume method," *Geotechnical Testing Journal*, 32(4).
- Nagaraj, T.S. and Murthy, B.R.S. (1985). "Rational approach to predict swelling soil behavior," *Transportation Research Record* 1032, *Evaluation and Control of Expansive Soils*, TRB, pp. 1 - 7.
- Nelson, J. D. and Miller, D. J. (1992). *Expansive Soils - Problems and Practice in Foundation and Pavement Engineering*, John Wiley & Sons, New York, New York, 259 pp.
- Nelson, J.D., Overton, D.D., and Durkee, D.B. (2001). "Depth of wetting and the active zone," *Geotechnical Special Publication 115, Expansive Clay Soils and Vegetative Influence on Shallow Foundations*, ASCE, pp. 95 - 109.
- Nevins, M.J. and Weintritt, D.J. (1967). "Determination of cation exchange capacity by methylene blue adsorption," *Ceramic Bulletin* 46 (6), pp. 587-592.
- Newman, A.C.D. (1983). "The specific surface area of soils determined by water sorption," *Journal of Soil Science* 34, pp. 23-32.
- Nikol'shii, N.N. (1959). *Practical Soil Science*, translated from Russian by Israel Program for Scientific Translations, Jerusalem. Available from U.S. Dept of Commerce Office of Technical Services, Washington, D.C.
- Nishimura, T. and Fredlund, D.G. (1999). "Unconfined compression shear strength of an unsaturated silty soil subjected to high total suctions," in *Proceedings of the International Symposium on Slope Stability Engineering, IS-Shikoku'99*, Japan. pp. 757- 762.

- Nobel, C. A. (1966). "Swelling measurements and prediction of heave for a lacustrine clay," *Canadian Geotechnical Journal*, Vol. 3, pp. 32–41.
- Northway, W. (2008). "Yazoo clay: Old problem getting new look from researchers," *Mississippi Business Journal*, June 16, 2008.
- Obradovich, J.D., Dockery, D.T., and Swisher, C.C. (1993). "Argon ages of bentonite beds in the upper part of the Yazoo Formation (upper Eocene), west-central Mississippi," *Mississippi Geology* 14(1), pp. 1 – 9.
- Patrick, D.M. and Snethen, D.R. (1976). "An occurrence and distribution survey of expansive materials in the United States by physiographic areas," Federal Highway Administration Report FHWA-RD-76-82, 11 pp.
- Patrick, P.K., Olsen, H.W., and Higgins, J.D. (2007). "Comparison of chilled-mirror measurements and filter paper estimates of total soil suction," *Geotechnical Testing Journal* 30(5).
- Petry, T. M. and Bryant, J. T. (2002). "Evaluation and use of the Decagon WP4 Dewpoint Potentiometer," *Proceedings of the Texas Section of the American Society of Civil Engineers Fall 2002 Meeting*, Waco, TX, October 2–5.
- Phelps, G.W. and Harris, D.L. (1968). "Specific surface and dry strength by methylene blue adsorption," *Ceramic Bulletin* 47 (12), pp. 1146–1150.
- Pitalo, A.T., Lynch, F.L., Martin, R.V., and Schmitz, D.W. (2004). "The South shall rise (and shrink) again; Mineralogy and engineering properties of the expansive Yazoo clay in central Mississippi," in *Geological Society of America, Abstracts with Programs* 36(5), page 372.
- Poor, A.R. (1978). "Experimental residential foundation designs on expansive clay soils," *Contract Final Report H-2240R*, U.S. Dept of Housing and Urban Development, Wash D.C.
- Popescu, M.E. (1979). "Engineering problems associated with expansive clays from Romania," *Engineering Geology* 14, pp. 43–53.
- Power, K.C. and Vanapalli, S.K. (2010). "Modified null pressure plate apparatus for measurement of matric suction," *Geotechnical Testing Journal* 33(4).
- Power, K.C., Vanapalli, S.K., and Garga, V.K. (2008). "A revised contact filter paper method," *Geotechnical Testing Journal* 31(6).
- Prakash, K. and Sridharan, A. (2002). "Determination of liquid limit from equilibrium sediment volume," *Geotechnique*, Vol 52, No 9, pp 693 - 696.
- Prakash, K. and Sridharan, A. (2004). "Free swell ratio and clay mineralogy of fine-grained soils," *Geotechnical Testing Journal* 27(2), pp. 220–225.
- Priddy, R. R. (1960). "Madison County Geology," *Mississippi State Geological Survey Bulletin* 88, 123 p.

- Puppala, A.J., Enayatpour, S., Vanapalli, S.K., and Intharasombat, N. (2004). "Review of current methods for swell characterization of subsoils for transportation infrastructure design," *GeoTrans 2004*, pp. 1105 – 1114.
- Rao, A.S. Phanikumar, B.R. and Sharma, R.S. (2004). "Prediction of swelling characteristics of remoulded and compacted expansive soils using free swell index," *Quarterly Journal of Engineering Geology and Hydrogeology*, 37, pp.217–226.
- Rao, B.H., Venkataramana, K. and Singh, D.N. (2011). "Studies on the determination of swelling properties of soils from suction measurements," *Can Geotech J*, Vol 48, pp. 375 – 387.
- Rani, C.S., Reddy, P.V.S., and Rao, K.M. (2010). "SIVACS: Knowledge based system developed for soil identification and assessment of volume change characteristics," *EJGE* 15, pp. 995 – 1009.
- Redus, J. F. (1962). "Experiences with expansive clay in Jackson, Miss.," *Moisture, Density, Swelling and Swell Pressure Relationships*, Highway Research Board Bulletin No. 313, pp 40 - 46.
- Richards, B. G. (1966). "The significance of moisture flow and equilibria in unsaturated soils in relation to the design of engineering structures built on shallow foundations in Australia," *Symposium on Permeability and Capillarity, ASTM STP 417*, ASTM International, West Conshohocken, PA, pp. 4–34..
- Richards, B. G., Peter, P., and Emerson, W. W. (1983). "The effects of vegetation on the swelling and shrinking of soils in Australia," *Geotechnique*, 33, pp.127–139.
- Ristori, G.G., Sparvoli, E., Landi, L., and Martelloni, C. (1989). "Measurement of specific surface areas of soils by p-Nitrophenol adsorption," *Applied Clay Science* 4, pp. 521–532.
- Rogers, J.A. (1936). "Foraminifera from the Yazoo clay of the Jackson Formation near Shubuta, Mississippi," Thesis Presented to the Faculty of the Graduate Division of the Texas Technological College in Partial Fulfillment of the Requirements For the Degree of Master of Arts Houston, Texas.
- Ross, G.J. (1978). "Relationships of specific surface areas and clay content to shrink–swell potential of soils having different clay mineralogical compositions," *Can. J. Soil Sci.* 58, pp.159-166.
- Sabtani, A. A. (2005). "Geotechnical properties of expansive clay shale in Tabuk, Saudi Arabia," *Journal of Asian Earth Sciences* 25, pp.747–757.
- Santamarina, J.C., Klein, K.A., Wang, Y.H., and Prencke, E.(2002). "Specific surface: Determination and relevance," *Canadian Geotechnical Journal* 39, pp. 233–241.
- Scanlon, B. R., Andraski, B. J., and Bilskie, J.(2002). "Miscellaneous methods for measuring matric or water potential," *Methods of Soil Analysis, Part 4, Physical Properties* J. H. Dane and G. C. Topp, Eds., Soil Science Society of America, Inc., Madison, Wisconsin, pp. 643–670.

- Schafer, W.M. and Singer, M.J. (1976). "A new method of measuring shrink– swell potential using soil pastes," *Soil Sci. Soc. Am. J.* 40, pp. 805– 806.
- Schneider, G.L. and Poor, A.R. (1974). "The prediction of soil heave and swell pressures developed by an expansive clay," *Research Report TR-9-74*, Nov 1974, Construction Research Center, Univ of Texas, Arlington.
- Scholtes, R.M. (1964). "An investigation of the swelling mechanism of Yazoo clay," Ph.D. Dissertation, Georgia Institute of Technology, GA, 139 pp.
- Sedano, I., Vanapalli, J.A., and Garga, V. K. (2007). "Modified ring shear apparatus for unsaturated soils testing," *Geotech. Test. J.*, Vol. 30, pp. 39–47.
- Seed, B., Woodward, R.J., and Lundgren, R. (1962). "Prediction of swelling potential for compacted clays," *Journal of the Soil Mechanics and Foundations Division*, Proceedings of the American Society of Civil Engineers, 88(3), pp. 53–87.
- Seed, B., Woodward, R.J., and Lundgren, R. (1964). "Clay mineralogical aspects of the Atterberg Limits," *Journal of the Soil Mechanics and Foundations Division*, Proceedings of the American Society of Civil Engineers, 90(4), pp. 107 - 131.
- Seed, B., Woodward, R.J., and Lundgren, R. (1964). "Fundamental aspects of the Atterberg Limits," *Journal of the Soil Mechanics and Foundations Division*, Proceedings of the American Society of Civil Engineers, 90(6), pp. 75 - 105.
- Sheffield, J.P. (1987). "A study of active clays as related to highway design," *Final Report MSHD-RD-84-045*, Mississippi State Highway Dept., Jackson, MS, 40 pp.
- Shepherd, K.D. and Markus, G.W. (2002). "Development of reflectance spectral libraries for characterization of soil properties," *Soil Sci. Soc. Am. J.* 66, pp. 988– 998.
- Shi, B., Jiang, H., Liu, Z., and Fang, H.Y. (2002). "Engineering geological characteristics of expansive soils in China," *Engineering Geology* 67, pp. 63 – 71.
- Sibley, J. W. and Williams, D. J. (1990). "A new filter material for measuring soil suction," *Geotechnical Testing Journal* 13(4), pp. 381-384.
- Simon, J.J, Oosterhuis, L. and Reneau, R.B. (1987). "Comparison of shrink-swell potential of seven ultisols and one alfisol using two different COLE techniques," *Soil Science* 143, pp. 50 – 55.
- Simunek, J., Wendroth, O., and van Genuchten, M.T. (1998). "Parameter estimation analysis of the evaporation method for determining soil hydraulic properties," *Soil Sci. Soc. Am. J.* 62, pp.894-905.
- Sivapullaiah, P.V., Sitharam, T.G., and Rao, K.S.S. (1987). "Modified free swell index for clays," *Geotechnical Testing Journal* 10(2), pp. 80–85.
- Sivapullaiah, P.V., Sridharan, A., and Ramesh, H.N. (2000). "Strength behavior of lime-treated soils in the presence of sulfate," *Canadian Geotechnical Journal* 37, pp. 1358–1367.
- Skempton, A.W. (1964). "Long-term Stability of Clay Slopes", *Geotechnique*, Vol 14(2), pp 77-101.

- Skempton, A.W. (1970). "First Time Slides in Overconsolidated Clays", *Geotechnique*, Vol 20, pp 320-324.
- Skempton, A.W. and Northey, R.D. (1953). "The sensitivity of clays," *Geotechnique*, Vol 3, No. 1, pp 30-53.
- Smith, S.M. and Zumwalt, G.S. (1987). "Gravity flow introduction of shallow water micro fauna into deep water depositional environments," *Mississippi Geology*, Vol 8(2), pp. 1 – 7.
- Snethen, D.R., Townsend, F.C., Johnson, L.D., Patrick, D.M., and Vedros, P.J. (1975). "A review of engineering experiences with expansive soils in highway subgrades," Federal Highway Administration Report FHWA-RD-75-48, 137 pp.
- Snethen, D. R. (1979). "Technical guidelines for expansive soils in highway subgrades," *Report No. FHWA-RD-79-51*, U.S. Dept of Transportation, Federal Highway Administration, Washington D.C.
- Snethen, D. R. (1980). "Characterization of expansive soils using soil suction data," *Proceedings, Fourth International Conference on Expansive Soils*, Vol. 1, Denver, CO, pp. 54-75.
- Snethen, D. R. (1984). "Evaluation of expedient methods for identification and classification of potentially expansive soils," *Proceedings, Fifth International Conference on Expansive Soils*, Institution of Engineers, Adelaide, South Australia, pp. 22-26.
- Snethen, D. R. and Johnson, L. D. (1980). "Evaluation of soil suction from filter paper," *Miscellaneous Paper No. GL-80-4*, Geotechnical Laboratory, U.S. Army Corps of Engineers Waterways Experiment Station, Vicksburg, MS.
- Snethen, D. R., and Johnson, L.D. (1977). "Characterization of expansive soil subgrades using soil suction data," *Proceedings, Moisture Influence on Pavement Materials Characterization and Performance Conference session of Transportation Research Board Committee A2L06 "Environmental Factors Except Frost*, 31 pp.
- Snethen, D.R., Johnson, L.D., and Patrick, D.M. (1977a). "An evaluation of expedient methodology for identification of potentially expansive soils," *U.S. Federal Highway Administration Interim Report FHWA-RD-77- 94*, Soil and Pavements Laboratory, U.S. Army Eng. Waterway Exp. Sta., Vicksburg, MS, 48 pp.
- Snethen, D.R., Johnson, L.D., and Patrick, D.M. (1977b). "An investigation of the natural microscale mechanisms that cause volume change in expansive clays," *U.S. Federal Highway Administration Interim Report FHWA-RD-77- 75*, Soil and Pavements Laboratory, U.S. Army Eng. Waterway Exp. Sta., Vicksburg, MS, 48 pp.
- Snowden, J. O. and Priddy, R. R. (1968). "Loess investigations in Mississippi," *Mississippi Geological, Economic and Topographical Survey, Bulletin 111*, Jackson, Mississippi.
- Soon, Y.K. (1988). "A rapid method for cation exchange capacity estimation of mineral soils using methylene blue adsorption," *Canadian Journal of Soil Science* 68, pp.165–169.

- Sposito, G. (1989). *The Chemistry of Soils*, Oxford University Press, Oxford, page 35.
- Springer, E. (1962). "Active clay subjected to dynamic forces," Master's Thesis, Mississippi State University, 51 pp.
- Sreedeeep, S. and Singh, D.H. (2006). "Methodology for determination of osmotic suction of soils," *Geotechnical and Geological Engineering* 24, pp. 1469–1479.
- Sreedeeep, S. and Singh, D.N. (2003). "Laboratory measurement of soil suction," *Indian Geotechnical Journal*, 33(3), pp. 279–290.
- Sreedeeep, S. and Singh, D.N. (2005). "A study to investigate influence of soil properties on its suction," *Journal of Testing and Evaluation*, ASTM, 33(1), pp. 579–584.
- Sridharan, A., Rao, S. M., and Murthy, N. S. (1986). "Liquid limit of montmorillonite soils," *Geotechnical Testing Journal* 9(3), ASTM, pp. 156 – 159.
- Sridharan, A. (1991). "Engineering behaviour of fine grained soils—A fundamental approach," *Indian Geotechnical Journal* 21(1), pp. 1–13.
- Sridharan, A. and Prakash, K. (1999a). "Influence of clay mineralogy and pore medium chemistry on clay sediment formation," *Canadian Geotechnical Journal*, 36(5), pp. 961– 966.
- Sridharan, A. and Prakash, K. (1999b). "Mechanisms controlling the undrained shear strength behaviour of clays," *Canadian Geotechnical Journal* 36(6), pp. 1030–1038.
- Sridharan, A. and Prakash, K. (2000). "Classification procedures for expansive soils," *Proc. Instn Civ. Engrs Geotech. Engng* 143, pp. 235-240.
- Sridharan, A. and Rao, S. M. (1988). "A scientific basis for the use of index tests in identification of expansive soils," *Geotechnical Testing Journal*, ASTM, 11(3), pp. 208-212.
- Sridharan, A., Rao, S. M., and Joshi, S.(1990). "Classification of expansive soils by sediment volume method," *Geotechnical Testing Journal* 13(4), pp. 375–380.
- Sridharan, A., Rao, S. M., and Murthy, N. S. (1985). "Free swell index of soils: A need for redefinition," *Indian Geotechnical Journal* 15(2), pp. 94–99.
- Sridharan, A., Rao, S. M., and Murthy, N. S. (1986). "A rapid method to identify clay type in soils by the free-swell technique," *Geotechnical Testing Journal*, ASTM, 9(4), pp. 193-203.
- Sridharan, A., Rao, S.M., and Sivapullaiah, P. V.(1986). "Swelling pressure of clays," *Geotech. Test. J.* 9(1), pp. 24–33.
- Sridharan, A. and Gurtag, Y. (2004). "Swelling behaviour of compacted fine-grained soils," *Engineering Geology* 72(1-2), pp. 9 – 18.
- Standards Assoc. of Australia (1992). "Methods for testing soils for engineering purposes: Method 7.1.1: Determination of the shrinkage index of a soil; shrink swell index," AS 1289.7.1.1, Sydney, Australia.

- Stapel, E.E. and Verhoef, P.N.W. (1989). "The use of methylene blue adsorption test in assessing the quality of basaltic tuff rock aggregate," *Eng Geol* 26(3), pp.233–246.
- Stark, T.D. and Eid, H.T. (1994). "Drained Residual Strength of Cohesive Soils", *Journal of Geotechnical Engineering*, ASCE, Vol 120, No. 5, May, pp 856-871.
- Stark, T.D. and Eid, H.T. (1997). "Slope stability analyses in stiff fissured clays", *Journal of Geotechnical and Geoenvironmental Engineering*, ASCE, Vol 123, No. 4, Apr., pp 335-343.
- Starnes, J.E. and Peyton, S. (2003). "Preliminary osteology of a *Basilosaurus cetoides* from the upper Yazoo clay in Scott County, Mississippi," *Journal of the Mississippi Academy of Sciences*, 67th Annual Meeting Abstracts, Vol 48(1), p. 43.
- Starnes, J.E. and Berry, T. (2010). "Excavation of a partial skeleton of a juvenile *Zygorhiza Kochi* in the lower Yazoo clay, Yazoo county, Mississippi," *MDEQ Environmental News*, Vol 7(2), pp. 6 – 7. www.deq.state.ms.us
- Stephens, I.J., Olsen, R.S., Manning, A.R., Galan-comas, G., Ahue, W.K., Pearson, M.L, Coffing, L.R., and Lee, L.T. (2011, in publication). "Trinity River, Dallas, TX, Floodway System: Fully-softened shear strength testing program," ERDC Technical Report __, U.S. Army Engineer Research and Development Center, Vicksburg, MS.
- Stover, C. W., Williams, R. D. and Peel, C. O. (1988). "Yazoo clay: Engineering aspects and environmental geology of an expansive clay," *Circular 1*, Mississippi Department of Natural Resources, Bureau of Geology, Jackson, Mississippi, pp.1-11.
- Strohm, W.E., Bragg, G.H., and Ziegler, T.W. (1978). "Design and construction of compacted shale embankments: Volume 5, Technical Guidelines," FHWA-RD-78-141, U.S. Army Engineer Waterways Experiment Station, Vicksburg, MS.
- Stroman, W.R. and Feese, A.H. (1984). "Engineering properties of clay shales," Report 5, Technical Report S-71-6, 52 pp. plus Appendix A and B, U.S. Army Engineer Waterways Experiment Station, Vicksburg, MS.
- Sullivan, R. A. and McClelland, B.(1969). "Predicting heave of buildings on unsaturated clay," *Proceedings, 2nd International Research and Engineering Conference on Expansive Soils*, Texas A&M Univ. Press, College Station, TX, pp. 404– 420.
- Taylor, A.C. (2005). "Mineralogy and engineering properties of the Yazoo clay formation, Jackson Group," Thesis for Degree of Master of Science in Geology in the Department of Geosciences, Mississippi State University.
- Taylor, R.K. (1985). "Cation exchange in clays and mudrocks by methylene blue," *Journal of Chemical Technology and Biotechnology* 35, pp. 195–207.
- Teng, T. C. P. and Clisby, M. B. (1975). "Experimental work for active clays in Mississippi," *Transp. Engrg. J.* 101, pp. 77–95.

- Teng, T. C. P., Mattox, R. M., and Clisby, M. B. (1972a). "A study of active clays as related to highway design (phase one)," *Final Report MSHDRD-72-045*, Research and Development Division, Mississippi State Highway Department, Engineering and Industrial Research Station, Mississippi State University.
- Teng, T. C. P., Mattox, R. M., and Clisby, M. B. (1972b). "A study of active clays as related to highway design (phase one)," *Appendices to Final Report MSHDRD-72-045*, Research and Development Division, Mississippi State Highway Department, Engineering and Industrial Research Station, Mississippi State University.
- Teng, T. C. P., Mattox, R. M., and Clisby, M. B. (1973). "Mississippi's experimental work on active clays," *Proceedings of the Workshop on Expansive Clays and Shales in Highway Design and Construction*, University of Wyoming, Laramie, pp. 1–17.
- Texas Dept of Transportation (TxDOT) (2005). "Soils and aggregates test procedure 107-E; Determining the bar linear shrinkage of soils," Texas State Department of Transportation website <http://manuals.dot.state.tx.us/dynaweb/colmates/>
- Texas Dept of Transportation (TxDOT) (2010). "Test procedure for preparing soil and flexible base materials for testing," TxDOT Designation Tex-101-E.
- Thakur, V.K.S. and Singh, D.N. (2005). "Rapid determination of swelling pressure of clay minerals," *ASTM Journal of Testing and Evaluation* 33(4), pp. 239 - 245.
- Thakur, V.K.S., Sreedeeep, S., and Singh, D.N. (2006). "Laboratory investigations on extremely high suction measurements for fine-grained soils," *Geotechnical and Geological Engineering* 24, pp. 565 – 578.
- Theng, B.K.G., Ristori, G.G., Santi, C.A., and Percival, H.J. (1999). "An improved method for the determining the specific surface areas of topsoils with varied organic matter content, texture and clay mineral composition," *European Journal of Soil Science* 50, pp. 309–316.
- Thomas, P.J., Baker, J.C., and Zelazny, L.W. (2000). "An expansive soil index for predicting shrink– swell potential," *Soil Sci. Soc. Am. J.* 64, pp. 268– 274.
- Thompson, R. W. and McKeen, R. G. (1995). "Heave prediction using soil suction: A case history," *ASCE Geotechnical Special Publication No. 48, Soil Suction Applications in Geotechnical Engineering Practice*, W. K. Wray and S. L. Houston, Eds., ASCE National Convention, San Diego, CA, October 1995, pp. 1–13.
- Thompson, R.W., Perko, H. A., and Rethamel, W. D. (2006). "Comparison of constant volume swell pressure and oedometer load back pressure," *Proceedings of the 4th International Conference on Unsaturated Soils*, Geotechnical Special Publication No. 147, Vol. 2, ASCE, Reston, VA, pp. 1787–1798.
- Thornthwaite, C. W. (1948). "An approach toward a rational classification of climate," *Geogr. Rev.* 38(1), pp. 54–94.
- Townsend, F.C. and Gilbert, P.A. (1974). "Engineering properties of clay shales," Report 2, Technical Report S-71-6, 71 pp. plus Appendices A, B, and C.

- Tripathy, S., Subba Rao, K., and Fredlund, D. (2002). "Water content-void ratio swell-shrink paths of compacted expansive soils," *Canadian Geotechnical Journal* 39(4), pp. 938–959.
- U.S. Army Engineer Waterways Experiment Station (1960). "The Unified Soil Classification System, Appendix A and B," *Geotechnical Laboratory Technical Memorandum 3-357*, 30 pp.
- U.S. Army Corps of Engineers (1961). "Engineering and design: Procedures for foundation design of buildings and other structures (except hydraulic structures)," *Engineer Manual EM 110-345*, Department of the Army, Washington, DC.
- U.S. Army Corps of Engineers (1970). "Laboratory soils manual," *Engineer Manual EM 1100-2-1906*, 30 Nov (with changes), Department of the Army, Washington, DC.
- USDA (1979). "Soil survey of Hinds County, Mississippi," National Cooperative Soil Survey, Washington, D.C.
- USDA-NRCS (2006). "Soil properties and qualities," NSSH Part 618, pp. 23 - 41
- Van Der Merwe, D. H. (1964). "The prediction of heave from the plasticity index and percentage clay fraction of soils," *Civil Engineer in South Africa* 6(6), pp. 103-107.
- Vaught, R., Brye, K.R. and Miller, D.M. (2006). "Relationships among coefficient of linear extensibility and clay fractions in expansive stony soils," *Soil Sci. Soc. Am. J.* 70, pp. 1983–1990
- Vijayvergiya, V.N. and Ghazzally, O.I. (1973). "Prediction of swelling potential of natural clays," *Proc 3rd Intl Conf on Expansive Clays*, Haifa, Israel, 30 July – 1 August 1973. Academic Press, Jerusalem, Israel, pp. 227 – 234.
- Vu, H.Q. and Fredlund, D.G. (2004). "The prediction of one-, two-, and three-dimensional heave in expansive soils," *Canadian Geotechnical Journal* 41, pp. 713 – 737.
- Wang, M.K., Wang, S.L., and Wang, W.M. (1996). "Rapid estimation of cation exchange capacities of soils and clays with methylene blue exchange," *Soil Science Society of America Journal* 60, pp. 138–141.
- Watkins, N.A. (1965). "A study of the relationships between the suction, swelling, consolidation, and strength characteristics of clay soils," Master's Thesis, Mississippi State University, 87 pp.
- Wheeler, R.L. and Crone, A.J. (2001). "Known and suggested quaternary faulting in the mid-continent U.S.," *Engineering Geology* Vol 62, pp. 51 – 78.
- White, D. J. and Bergeson, K. L. (2002). "Empirical performance classification for cohesive embankment soils," *Geotechnical Testing Journal* 25(1) pp. 70–77.
- Williams, A.B. and Donaldson, G.W. (1980). "Building on expansive soils in South Africa: 1973 – 1980," *Proc 4th Intl Conf on Expansive Clays*, Denver, CO, pp. 834 – 844.

- Wikipedia (2010). www.wikipedia.com
- Wong, H. Y. and Yong, R. M. (1973). "A study of swelling and swelling force during unsaturated flow in expansive soils," *Proceedings, 3rd International Conference on Expansive Soils*, Haifa, Israel, Vol. 1, pp. 143–151.
- Wood, D.M. and Wroth, C.P. (1978). "The use of the cone penetrometer to determine the plastic limit of soils," *Ground Engineering*, Vol 11, No 3, pg 37.
- Woodburn J.A., Holden J.C., and Peter, P. (1993). "The transistor psychrometer: a new instrument for measuring soil suction," *Unsaturated soils, ASCE geotechnical special publication no. 39*, Houston S.L. and Wray, W.K. (eds), Dallas, Texas, pp. 91–102.
- Wray, W. K. (1995). "So your home is built on expansive soils," *Shallow Foundations Committee of the Geotechnical Division of the American Society of Civil Engineers*, Reston, VA, pp. 2 -3.
- Wray, W. K. (1998). "Mass transfer in unsaturated soils: A review of theory and practices," *Proceedings of the 2nd International Conference on Unsaturated Soils*, Beijing, China, pp. 99– 155.
- Wroth, C.P. (1979). "Correlations of some engineering properties of soils," *2nd Intl Conf on Behaviour of Offshore Structures (BOSS'79)*, London, England, pp. 121 – 132.
- Xin, J. Z. and Ling, Q. X. (1992). "A new method for calculating lateral swelling pressure in expansive soil," *Proceedings of the 7th International Conference on Expansive Soils*, 3–5 Aug., Dallas, TX.
- Yao, H.L., Yang, Y. and Cheng, P. (2004). "Standard moisture absorption water content of soil and its testing method," *Rock and Soil Mechanics* 25(6), pp. 856-859.
- Yevnin, A. and Zaslavsky, D. (1970). "Some factors affecting compacted clay swelling," *Can. Geotech. J.* 7(1), pp. 79– 89.
- Yilmaz, I. (2000). "Evaluation of shear strength of clayey soils by using their liquidity index," *Bulletin of Engineering Geology and the Environment* 59, pp. 227 – 229.
- Yilmaz, I. (2004). "Relationships between liquid limit, cation exchange capacity, and swelling potentials of clayey soils," *Eurasian Soil Science* 37, pp. 506 – 512.
- Yilmaz, I. (2006). "Indirect estimation of the swelling percent and a new classification of soils depending on liquid limit and cation exchange capacity," *Engineering Geology* 85, pp. 295 – 301.
- Yilmaz, I. (2009). "Swell potential and shear strength estimation of clays," *Applied Clay Science* 46, pp. 376 – 384.
- Yitagesu, F. A., Van der Meer, F., Van der Werff, H., and Zigterman, W. (2009). "Quantifying engineering parameters of expansive soils from their reflectance spectra," *Engineering Geology* 105, pp.151–160.

- Yool, A.I.G., Lees, T.P., and Fried, A. (1998). "Improvements to the methylene blue dye test for harmful clay in aggregates for concrete and mortar," *Cement and Concrete Research* 28 (10), pp. 1417–1428.
- Young, J. F. (1967). "Humidity control in the laboratory using salt solutions—A review." *J. Appl. Chem.* 17, pp. 241–245.
- Yu, Z. (1992). "Clay mineralogy of continuous core of lower Yazoo clay, Hinds County, Mississippi," Master's thesis, University of Southern Mississippi, Hattiesburg, MS, 79 pp.
- Yukselen, Y. and Kaya, A. (2006). "Comparison of methods for determining specific surface area of soils," *Journal of Geotechnical and Geoenvironmental Engineering*, ASCE 132 (7), pp. 931–936.
- Yukselen, Y. and Kaya, A. (2006). "Prediction of cation exchange capacity from soil index properties," *Clay Minerals* 41, pp. 827 –837.
- Yukselen, Y., Kaya, A., and Oren, A.H. (2008). "Seawater effect on consistency limits and compressibility characteristics of clays," *Engineering Geology* 102, pp. 54–61.
- Yukselen, Y. and Kaya, A. (2008). "Suitability of the methylene blue test for surface area, cation exchange capacity and swell potential determination of clayey soils," *Engineering Geology* 102, pp.38–45.
- Yule, D.F. and Ritchie, J.T. (1980). "Soil shrinkage relationships of Texas vertisols: Small cores," *Soil Science Society of America Journal* 44, pp.1285– 1291.
- Zachos, L.G. and Molineux, A. (2003). "Eocene Echinoids of Texas," *J. Paleontology* 77(3), pp. 491 – 508.
- Zemenu, G., Martine, A. and Roger, C. (2009). "Analysis of the behaviour of a natural expansive soil under cyclic drying and wetting," *Bull Eng Geol Environ*, Vol 68, pp. 421 – 436.
- Zhang, X. and Briaud, J.L. (2006). "Coupled water content method for shrink and swell predictions," Transportation Research Board, 2006 Annual Meeting CD-ROM, TRB, Washington, D.C., 22 pp.
- Zheng, J.L., Zhang, R. and Yang, H.P. (2008). "Validation of a swelling potential index for expansive soils," in *Unsaturated Soils: Advances in Geo-Engineering*, Toll et al. (eds), Taylor and Francis Group, London
- Zohar, Y.R., Banin, A., and Chen, Y. (1983). "Oven drying as a pretreatment for surface-area determinations of soils and clays," *Soil Science Society of America Journal* 47, pp. 1056–1058.

7 Appendix A: State Study 151 Data

1	A	B	C	D	E	F	G	H	I	J	K	L	M	N	O	P	Q	R	S	T	U
	County	Site	Hole No.	Hole Elev msl	Sample Number	Dry Density	Wet Density	Percent Moisture	LL	PL	PI	% VC	Depth	Elev msl	Yellow/Blue	clay %	qtz %	Calcite %	% Smec	% Illite	% Kaol
2	61	1202	3		6	89	119	34	73	33	40	125	-30		Yellow						
3	61	1202	4		8	84	116	38	84	37	47	117	-40		Yellow						
4	61	1203	11		6	84	115	37	82	39	43	111	-30		Blue						
5	61	1203	6		5	82	115	40	85	45	40	118	-30		Yellow						
6	61	1203	14		8	83	114	37	96	45	51	141	-40		Blue						
7	61	1203	10		9	84	115	37	84	41	42	120	-45		Blue						
8	61	1203	16		10	92	120	30	84	41	43	117	-50		Blue						
9	61	1203	17		13	85	116	37	84	41	43	126	-70		Blue						
10	61	1204	5	267	9			37	74	28	46	100	-45	222	Blue						
11	61	1204	6		9			43	90	39	51	127	-30		Blue						
12	61	1204	8		6			33	62	34	28	81	-30		Blue						
13	61	1204	1		6			40	85	40	45	114	-30		Yellow						
14	61	1204	4		8			36	78	39	39	104	-40		Blue						
15	61	1205	6	273	9	81	114	41					-45	228	Blue						
16	61	1205	6	273	10	87	118	36					-50	223	Blue						
17	61	1205	10		5			34	79	36	43	99	-25		Yellow						
18	61	1205	3		6			32	65	31	34	82	-30		Blue						
19	61	1205	7		11	82	113	38					-35		Blue						
20	61	1205	8		7	83	115	39					-35		Blue						
21	61	1205	9		7			35	79	40	39	96	-35		yellow						
22	61	1205	12		10			33	35			100	-40		Blue						
23	61	1205	7		12			40	90	47	43	109	-40		Yellow						
24	61	1205	8		8	94	123	31					-40		yellow						
25	61	1205	9		8	87	34						-40		Yellow						
26	61	1205	7		13	84	115	37					-45		Blue						
27	61	1206	1	267	6			32	73	32	41	127	-30	237	Yellow						
28	61	1206	5	267	14			28	61	29	32	81	-45	222	Blue						
29	61	1206	4	264	6			37	82	39	43	104	-30	234	yellow						
30	61	1207	8	279	11			39	93	43	50	117	-55	224	Blue						
31	61	1207	2	269	8			31	67	35	32	100	-41	228	Blue						
32	61	1207	7	266	9			36	110	41	69	116	-45	221	Blue						
33	61	1207	3	265	9			30	78	37	41	60	-45	220	blue						
34	61	1207	1	264	8			37	79	37	42	100	-35	229	Blue						
35	61	1207	5	264	7			33	72	38	34	51	-35	229	Yellow						
36	61	1207	4	264	11			35	83	40	43	105	-55	209	Blue						
37	61	1207	10	262	6			33	74	38	36	105	-30	232	Blue						
38	45	1823	12	293	4	78	112	43	98	38	60		-20	273	yellow						
39	45	1823	12	293	6	87	117	34	71	28	43		-30	263	Yellow						
40	45	1823	12	293	8	90	120	33	74	33	41		-40	253	Blue						
41	45	1823	13	289	4	82	112	37	98	68	30		-20	269	Yellow						
42	45	1823	13	289	6	80	113	41	97	30	67		-30	259	Yellow						
43	45	1823	13	289	8	85	116	36	88	32	56		-40	249	yellow						
44	45	1824	1	282	5				107	27	80	158	-25	257	Yellow						
45	45	1824	1	282	6			92	26	66	137		-30	252	Yellow						
46	45	1824	1	282	7			84	25	59	117		-35	247	Yellow						
47	45	1824	1	282	8	84	115	37	88	59	29	115	-40	242	Blue						
48	45	1824	1	282	9	103	127	23	87	26	61	107	-45	237	Blue						
49	45	1824	1	282	10			79	37	42	117		-50	232	Blue						
50	45	1824	1	282	11	86	117	36	78	34	44	111	-55	227	blue						
51	45	1824	1	282	12			75	35	40	103		-60	222	blue						
52	45	1824	1	282	13	84	115	37	88	41	47	140	-70	212	blue						
53	45	1824	1	282	14			79	39	40	141		-80	202	blue						
54	25	1831	1	294	6	87	118	35	77	36	41	104	-30	264	yellow						
55	25	1831	1	294	7			90	39	51	127		-35	259	Blue						
56	25	1831	1	294	8	82	115	40	97	44	53	157	-40	254	Blue						
57	25	1831	1	294	9	67	105	56	86	64	22	83	-45	249	blue						
58	25	1831	1	294	10	80	114	42	98	41	57	151	-50	244	blue						
59	25	1831	1	294	11	82	114	39	94	45	49	139	-55	239	Blue						
60	25	1831	1	294	12	87	119	37	96	37	59	125	-60	234	Blue						
61	25	1831	1	294	13	84	116	38	92	45	47	130	-70	224	Blue						
62	25	1831	1	294	14			94	47	47	139		-80	214	Blue						
63	25	1831	4	293	12	82	116	41	93	37	56	140	-30	263	Yellow	66	10	6	45	15	40
64	25	1831	4	293	13	74	102	38	86	35	51	131	-35	258	Yellow	68	11	15	44	7	49
65	25	1831	4	293	14			88	35	53	130		-40	253	Blue	64	9	24	52	9	39
66	25	1831	4	293	15	87	118	35	80	33	47	117	-45	248	yellow	60	27	10	63	6	31
67	25	1831	4	293	16	81	113	40	92	40	52	136	-50	243	Blue	75	15	7	55	7	38

1	A	B	C	D	E	F	G	H	I	J	K	L	M	N	O	P	Q	R	S	T	U
	County	Site	Hole No.	Hole Elev msl	Sample Number	DRY Density	Wet Density Percent	Moisture	LL	PL	PI	% VC	Depth	Elev msl	Yellow/Blue	clay %	qtz %	Calcite %	% Smec	% Illite	% Kaol
68	25	1831	4	293	17	79	113	43	96	37	59	185	-55	238	Blue						
69	25	1831	4	293	18	82	115	40	96	38	58	122	-60	233	Blue						
70	25	1831	4	293	19	85	118	39	79	35	44	78	-70	223	Blue						
71	25	1831	4	293	20	85	117	38	97	42	52	153	-80	213	Blue						
72	25	1831	3	292	5	76	106	40	109	45	64	114	-25	267	Yellow						
73	25	1831	2	292	6	80	112	40	99	42	57	157	-30	262	Yellow						
74	25	1831	3	292	6	75	107	43	94	36	58	89	-30	262	Yellow						
75	25	1831	3	292	7	87	117	34	90	37	53	123	-35	257	Blue						
76	25	1831	2	292	7	83	15	39	101	42	59	34	-35	257	Yellow						
77	25	1831	2	292	8	82	115	40	96	42	54	147	-40	252	yellow						
78	25	1831	3	292	8	88	116	32	98	40	58	88	-40	252	Yellow						
79	25	1831	2	292	9	85	116	36	89	38	51	121	-45	247	Blue						
80	25	1831	3	292	9				75	30	45	101	-45	247	Blue						
81	25	1831	2	292	10	82	114	39	98	42	56	101	-50	242	Blue						
82	25	1831	3	292	10	83	115	39	97	39	58	90	-50	242	blue						
83	25	1831	2	292	11	72	107	48	113	49	64	115	-55	237	Blue						
84	25	1831	3	292	11	81	113	40	90	33	57	145	-55	237	Blue						
85	25	1831	2	292	12	84	116	38	83	36	47	105	-60	232	Blue						
86	25	1831	3	292	12	83	115	38	90	31	59	107	-60	232	Blue						
87	25	1831	2	292	13	84	113	35	101	40	61	138	-70	222	Blue						
88	25	1831	3	292	13	80	112	40	95	42	53	80	-70	222	Blue						
89	25	1831	2	292	14	87	118	35	90	39	51	120	-80	212	Blue						
90	25	1831	3	292	14				91	39	52	130	-80	212	Blue						
91	25	1832	10	369	5	93	119	28	97	25	72	120	-25	344	Yellow						
92	25	1832	17	369	5	88	116	32	99	35	64	152	-25	344	Yellow						
93	25	1832	10	369	7	83	115	38	92	31	61	162	-35	334	Blue						
94	25	1832	17	369	7		0		87	30	57	129	-35	334	Yellow						
95	25	1832	17	369	8	76	111	46	113	29	84	157	-40	329	Blue						
96	25	1832	10	369	9	79	112	42	95	32	63	148	-45	324	blue						
97	25	1832	17	369	9				109	39	70	160	-45	324	Blue						
98	25	1832	17	369	10	83	115	39	94	37	57	131	-50	319	Blue						
99	25	1832	10	369	11	84	114	36	107	36	71	164	-55	314	Blue						
100	25	1832	10	369	12	85	116	37	102	37	65	148	-60	309	Blue						
101	25	1832	08	368	3	91	117	29	75	34	41	123	-15	353	yellow						
102	25	1832	08	368	5				97	25	72	157	-25	343	Yellow						
103	25	1832	09	368	5	90	118	31	76	38	38	122	-25	343	yellow						
104	25	1832	08	368	7	78	111	42	107	48	59	174	-35	333	Blue						
105	25	1832	09	368	7	78	111	42	98	29	69	155	-35	333	Yellow						
106	25	1832	08	368	8	86	114	33	93	34	59	148	-40	328	blue						
107	25	1832	09	368	8				106	33	73	137	-40	328	Blue						
108	25	1832	8	368	10				77	30	47	103	-50	318	Blue						
109	25	1832	9	368	10	86	118	37	64	33	31	140	-50	318	Blue						
110	25	1832	8	368	11	85	116	36	94	35	59	132	-55	313	Blue						
111	25	1832	9	368	11	105	128	22	74	29	45	112	-55	313	Blue						
112	25	1832	06	367	2	100	125	25	98	32	66	157	-10	357	Blue						
113	25	1832	18	367	3	87	115	32	81	40	41	124	-15	352	Yellow						
114	25	1832	29	367	3	91	118	30	103	33	70	167	-15	352	Yellow						
115	25	1832	32	367	3	112	131	17	90	34	56	135	-15	352	Yellow						
116	25	1832	06	367	4	79	111	41	103	35	68	167	-20	347	Yellow						
117	25	1832	18	367	5	72	107	48	122	28	94	189	-25	342	Yellow						
118	25	1832	29	367	5	76	109	44	114	35	79	171	-25	342	Yellow						
119	25	1832	06	367	6	84	115	37	80	30	50	123	-30	337	yellow						
120	25	1832	32	367	6	86	113	31	85	31	54	131	-30	337	yellow						
121	25	1832	18	367	7	77	111	44	112	49	63	157	-35	332	Blue						
122	25	1832	29	367	7	88	118	34	103	39	64	147	-35	332	blue						
123	25	1832	6	367	7	75	108	44	104	41	63	157	-35	332	blue						
124	25	1832	32	367	7	100	127	27	77	29	48	141	-35	332	Yellow						
125	25	1832	18	367	8	83	114	37	90	39	51	133	-40	327	blue						
126	25	1832	29	367	8	85	116	36	99	36	63	148	-40	327	blue						
127	25	1832	32	367	8	77	111	44	114	40	74	165	-40	327	blue						
128	25	1832	6	367	9	83	116	40	96	37	59	138	-45	322	Blue						
129	25	1832	18	367	10				73	27	46	97	-50	317	Blue						
130	25	1832	29	367	10				58	23	35	85	-50	317	Blue						
131	25	1832	32	367	10	88	116	32	99	41	58	140	-50	317	Blue						
132	25	1832	05	365	2	78	110	41	106	35	71	161	-10	355	Yellow						
133	25	1832	07	365	2	84	114	36	85	26	59	148	-10	355	Yellow						

1	A	B	C	D	E	F	G	H	I	J	K	L	M	N	O	P	Q	R	S	T	U
	County	Site	Hole No.	Hole Elev msl	Sample Number	Dry Density	Wet Density	Percent Moisture	LL	PL	PI	% VC	Depth	Elev msl	Yellow/Blue	clay %	qtz %	Calcite %	% Smec	% Illite	% Kaol
134	25	1832	14	365	4	95	122	28	76	27	49	90	-20	###	Yellow						
135	25	1832	05	365	4	78	111	42	105	33	72	177	-20	345	Yellow						
136	25	1832	07	365	4	85	112	32	87	33	54	139	-20	345	Yellow						
137	25	1832	07	365	6	83	114	37	91	30	61	148	-30	335	Blue						
138	25	1832	5	365	6	81	113	39	109	48	61	162	-30	335	Blue						
139	25	1832	14	365	6	74	108	46	96	38	58	134	-30	335	Yellow						
140	25	1832	7	365	7	82	112	37	104	39	65	148	-35	330	Yellow						
141	25	1832	14	365	8	80	114	43	89	35	54	138	-40	325	Blue						
142	25	1832	5	365	8	80	114	42	105	39	66	155	-40	325	Yellow						
143	25	1832	14	365	9	81	113	40	83	37	46	78	-45	320	Blue						
144	25	1832	7	365	9	83	111	34	102	41	61	148	-45	320	blue						
145	25	1832	14	365	10	87	118	36	76	34	42	97	-50	315	Blue						
146	25	1832	5	365	10	88	119	35	93	34	59	126	-50	315	Blue						
147	25	1832	04	364	2	84	113	35	82	30	52	133	-10	354	Blue						
148	25	1832	37	364	2	82	113	38	104	38	66	164	-10	354	Yellow						
149	25	1832	13	364	4				75	29	46	67	-20	344	Yellow						
150	25	1832	33	364	4	85	114	34	94	34	60	138	-20	344	Yellow						
151	25	1832	37	364	4	84	122	45	111	36	75	142	-20	344	Yellow						
152	25	1832	04	364	5	80	112	40	104	35	69	172	-25	339	Yellow						
153	25	1832	13	364	6	77	109	42	92	35	57	93	-30	334	Blue						
154	25	1832	4	364	6				106	39	67	147	-30	334	Blue						
155	25	1832	33	364	6	77	110	43	105	42	63	95	-30	334	yellow						
156	25	1832	37	364	6	78	111	42	97	41	56	141	-30	334	yellow						
157	25	1832	37	364	7	80	113	41	113	45	68	236	-35	329	yellow						
158	25	1832	13	364	8	87	118	36	88	31	57	108	-40	324	Blue						
159	25	1832	33	364	8	83	115	38	90	40	50	121	-40	324	Blue						
160	25	1832	4	364	8	89	121	36	101	38	63	147	-40	324	Blue						
161	25	1832	13	364	9	87	117	35	84	35	49	111	-45	319	Blue						
162	25	1832	37	364	9	81	113	40	100	43	57	143	-45	319	Blue						
163	25	1832	13	364	10	87	118	36	83	33	50	103	-50	314	Blue						
164	25	1832	33	364	10	86	117	36	69	29	40	79	-50	314	Blue						
165	25	1832	4	364	10	103	127	23	87	31	56	117	-50	314	Blue						
166	25	1832	38	363	2	87	116	33	93	32	61	141	-10	353	Yellow						
167	25	1832	19	363	4	85	115	35	112	71	41	163	-20	343	Yellow						
168	25	1832	38	363	4	83	115	38	92	33	59	118	-20	343	yellow						
169	25	1832	19	363	6	76	110	45	96	43	53	147	-30	333	Blue						
170	25	1832	19	363	7	90	118	31	102	39	63	162	-35	328	yellow						
171	25	1832	38	363	7	82	112	37	106	48	58	150	-35	328	Yellow						
172	25	1832	19	363	9	80	114	42	95	41	54	137	-45	318	blue						
173	25	1832	38	363	9	88	117	33	98	39	59	134	-45	318	blue						
174	25	1832	36	362	2	87	117	34	102	40	62	163	-10	352	Yellow						
175	25	1832	36	362	4	84	115	37	97	35	62	152	-20	342	Yellow						
176	25	1832	12	362	5	88	117	33	78	32	46	117	-25	337	Yellow						
177	25	1832	36	362	6	78	112	44	106	43	63	141	-30	332	yellow						
178	25	1832	12	362	7	81	114	41	86	35	51	127	-35	327	Yellow						
179	25	1832	12	362	8	82	116	41	92	39	53	125	-40	322	yellow						
180	25	1832	36	362	8	83	115	38	98	41	57	141	-40	322	Yellow						
181	25	1832	12	362	10	98	125	28	85	36	49	104	-50	312	Blue						
182	25	1832	36	362	10	89	119	34	85	33	52	117	-50	312	Blue						
183	25	1832	34	361	4	86	116	35	62	24	38	86	-20	341	Yellow						
184	25	1832	40	361	4	40	72	80	107	36	71	150	-20	341	Yellow						
185	25	1832	34	361	6	82	111	35	88	34	54	143	-30	331	Yellow						
186	25	1832	40	361	6	22	46	107	66	26	40	94	-30	331	Yellow						
187	25	1832	40	361	8	106	130	23	71	25	46	99	-40	321	blue						
188	25	1832	34	361	9	104	129	24	38	20	18	52	-45	316	Blue						
189	25	1832	34	361	10	87	117	35	84	34	50	100	-50	311	Blue						
190	25	1832	40	361	10	85	116	37	93	41	52	121	-50	311	Blue						
191	25	1832	11	360	4	93	118	27	59	24	35	87	-20	340	yellow						
192	25	1832	20	360	4	75	108	44	114	37	77	148	-20	340	Yellow						
193	25	1832	11	360	6	78	110	41	82	33	49	100	-30	330	Yellow						
194	25	1832	20	360	6	76	109	43	103	40	63	153	-30	330	Yellow						
195	25	1832	11	360	8	82	114	39	80	39	41	99	-40	320	Blue						
196	25	1832	20	360	8	85	116	36	81	36	45	111	-40	320	Yellow						
197	25	1832	20	360	9	91	118	30	64	28	36	85	-45	315	blue						
198	25	1832	11	360	10	87	120	38	84	37	47	60	-50	310	Blue						
199	25	1832	20	360	10	93	116	25	95	36	59	125	-50	310	Blue						

1	A	B	C	D	E	F	G	H	I	J	K	L	M	N	O	P	Q	R	S	T	U	
	County	Site	Hole No.	Hole Elev msl	Sample Number	Dry Density	Wet Density	Moisture Percent	LL	PL	PI	% VC	Depth	Elev msl	Yellow/Blue	clay %	qtz %	Calcite %	% Smec	% Illite	% Kaol	
200	25	1832	31	358	3	84	113	35	89	33	56	148	-15	343	Yellow							
201	25	1832	31	358	5	77	109	42	107	38	69	192	-25	333	Yellow							
202	25	1832	31	358	8	87	117	34	94	32	62		-40	318	Yellow							
203	25	1832	31	358	10	88	119	35	104	41	63		-50	308	Blue							
204	25	1832	03	357	1	85	114	34	93	29	64	162	-5	352	Yellow							
205	25	1832	03	357	3	82	112	37	108	40	68	171	-15	342	Yellow							
206	25	1832	15	357	3	101	123	22	73	27	46	83	-15	342	Yellow							
207	25	1832	03	357	5	80	112	40	91	30	61	153	-25	332	Yellow							
208	25	1832	15	357	5	79	111	41	89	38	51	95	-25	332	yellow							
209	25	1832	3	357	6	81	112	38	96	36	60	132	-30	327	Yellow							
210	25	1832	15	357	7	77	109	42	86	42	44	124	-35	322	Blue							
211	25	1832	15	357	8	82	115	40	81	35	46	114	-40	317	Blue							
212	25	1832	3	357	8	111	128	15	56	24	32	105	-40	317	Blue							
213	25	1832	15	357	10				87	35	52	121	-50	307	blue							
214	25	1832	3	357	10	87	117	34	91	34	57	120	-50	307	Blue							
215	25	1832	3	357	13	88	119	35	86	31	55	125	-70	287	Blue							
216	25	1832	39	356	3	77	111	44	127	42	85	153	-15	341	Yellow							
217	25	1832	39	356	5	40	72	81	99	38	61	144	-25	331	Blue							
218	25	1832	39	356	7	94	129	37	95	33	62	124	-35	321	Yellow							
219	25	1832	39	356	9	97	125	29	89	35	54	124	-45	311	Yellow							
220	25	1832	35	354	3	88	117	33	61	25	36	97	-15	339	Yellow							
221	25	1832	35	354	5	75	110	46	109	45	64	157	-25	329	yellow							
222	25	1832	35	354	6	79	112	42	93	37	56	131	-30	324	Blue							
223	25	1832	35	354	8	88	119	35	80	35	45	104	-40	314	Blue							
224	25	1832	35	354	10	91	121	33	78	33	45	105	-50	304	Blue							
225	25	1832	01	353	3	87	114	31	69	27	42	88	-15	338	Yellow							
226	25	1832	01	353	5	79	110	39	90	35	55	88	-25	328	Yellow							
227	25	1832	01	353	7	95	116	22	69	35	34	46	-35	318	Blue							
228	25	1832	1	353	8				89	33	56	25	-40	313	Blue							
229	25	1832	1	353	10	83	115	38	75	31	44	83	-50	303	blue							
230	25	1832	1	353	12	110	132	20	50	21	29	57	-60	293	Blue							
231	25	1832	1	353	14	109	131	20	59	24	35	49	-80	273	Blue							
232	25	1832	02	350	3	75	108	44	110	24	86	165	-15	335	Yellow							
233	25	1832	02	350	5	78	111	42	97	37	60	141	-25	325	Yellow							
234	25	1832	2	350	7	104	129	24	71	28	43	97	-35	315	Yellow							
235	25	1832	2	350	9	87	116	33	81	33	48	110	-45	305	Blue							
236	25	1832	2	350	11	108	131	21	63	26	37	95	-55	295	Blue							
237	25	1832	2	350	13	91	120	32	89	34	55	121	-70	280	Blue							
238	25	1832	23		2	86	112	30	79	30	49	132	-10		Blue							
239	25	1832	24		2	82	112	36	93	34	59	133	-10		Yellow							
240	25	1832	22		3	83	114	37	99	39	60	151	-15		yellow							
241	25	1832	26		3	90	117	30	70	26	44	114	-15		yellow							
242	25	1832	27		3	91	118	30	100	35	65	164	-15		Yellow							
243	25	1832	28		3	91	117	29	84	27	57	148	-15		Yellow							
244	25	1832	30		3	89	118	33	89	30	59	133	-15		Yellow							
245	25	1832	16		4	87	116	33	87	42	45	105	-20		Yellow							
246	25	1832	21		4	84	113	35	63	23	40	103	-20		yellow							
247	25	1832	23		4	77	109	42	95	37	58	139	-20		Yellow							
248	25	1832	25		4	76	109	43	83	36	47	130	-20		yellow							
249	25	1832	22		5	86	116	35	85	32	53	133	-25		yellow							
250	25	1832	26		5	82	113	38	106	34	72	148	-25		Yellow							
251	25	1832	27		5	86	116	35	96	35	61	161	-25		yellow							
252	25	1832	28		5	80	110	38	93	35	58	157	-25		Yellow							
253	25	1832	30		5	84	114	36	73	28	45	112	-25		yellow							
254	25	1832	16		6	78	111	42	94	39	55	192	-30		Blue							
255	25	1832	21		6	80	111	39	87	32	55	131	-30		Blue							
256	25	1832	23		6	84	113	35	93	33	60	137	-30		Blue							
257	25	1832	24		6	78	112	44	99	42	57	68	-30		Yellow							
258	25	1832	25		6	77	109	42	104	39	65	157	-30		Yellow							
259	25	1832	21		7	76	109	44	106	37	69	165	-35		Blue							
260	25	1832	22		7	81	108	33	89	35	54	138	-35		Blue							
261	25	1832	27		7	74	108	46	116	44	72	177	-35		Blue							
262	25	1832	28		7	84	114	36	77	32	45	121	-35		Blue							
263	25	1832	23		7	81	113	39	95	39	56	112	-35		Yellow							
264	25	1832	30		7	84	113	35	104	40	64	153	-35		Yellow							
265	25	1832	16		8	80	112	40	90	37	53	175	-40		Blue							

	A	B	C	D	E	F	G	H	I	J	K	L	M	N	O	P	Q	R	S	T	U
1	County	Site	Hole No.	Hole Elev msl	Sample Number	Dry Density	Wet Density	Percent Moisture	LL	PL	PI	% VC	Depth	Elev msl	Yellow/Blue	clay %	qtz %	Calcite %	% Smec	% Illite	% Kaol
266	25	1832	22		8	85	115	35	102	38	64	115	-40		Blue						
267	25	1832	24		8	84	115	37	100	36	64	71	-40		Blue						
268	25	1832	25		8	80	113	41	99	39	60	66	-40		Blue						
269	25	1832	26		8	85	116	37	104	37	67	166	-40		Blue						
270	25	1832	27		8	81	113	40	101	42	59	154	-40		Blue						
271	25	1832	28		8	79	113	43	105	37	68	171	-40		Blue						
272	25	1832	30		8	82	115	40	104	39	65	164	-40		Blue						
273	25	1832	16		9	83	114	37	79	30	49	100	-45		Blue						
274	25	1832	21		9	83	114	37	66	27	39	93	-45		Blue						
275	25	1832	23		9	83	115	38	92	36	56	65	-45		Blue						
276	25	1832	16		10	103	128	24	50	22	28	53	-50		Blue						
277	25	1832	21		10	82	116	41	104	44	60	149	-50		blue						
278	25	1832	22		10	88	117	33	83	36	47	115	-50		blue						
279	25	1832	24		10	99	126	27	54	24	30	33	-50		Blue						
280	25	1832	25		10	82	115	40	88	38	50	185	-50		Blue						
281	25	1832	26		10	85	117	38	89	35	54	132	-50		Blue						
282	25	1832	27		10	86	116	35	93	36	57	138	-50		Blue						
283	25	1832	28		10	84	116	38	90	33	57	115	-50		Blue						
284	25	1832	30		10	86	117	36	92	34	58	131	-50		Blue						
285	45	1837	2	229	1								-5	224	Y	24	61	1	13	62	25
286	45	1837	2	229	2								-10	219	Y	39	46	9	46	9	44
287	45	1837	2	229	3								-15	214	Y	51	12	37	46	6	49
288	45	1837	2	229	4								-20	209	Y	45	11	44	48	7	45
289	45	1837	2	229	5								-25	204	Y	64	10	25	41	7	53
290	45	1837	2	229	6								-30	199	B	58	10	32	47	8	45
291	45	1837	2	229	7								-35	194	B	50	9	41	39	7	54
292	45	1837	2	229	8								-40	189	B	33	4	63	52	6	42
293	45	1837	2	229	9								-45	184	B	47	6	47	42	7	50
294	45	1837	2	229	10								-50	179	B	51	7	42	48	8	44
295	45	1837	2	229	11								-55	174	B	55	8	36	43	7	50
296	45	1837	2	229	12								-60	169	B	49	5	44	50	7	43
297	45	1837	1	228	1								-5	223	Y	15	76	0	0	50	50
298	45	1837	1	228	2								-10	218	Y	28	59	T	0	67	33
299	45	1837	1	228	3								-15	213	Y	34	61	T	30	16	54
300	45	1837	1	228	4								-20	208	Y	45	17	T	56	5	39
301	45	1837	1	228	5								-25	203	Y	47	19	29	34	10	56
302	45	1837	1	228	6								-30	198	Y	49	8	41	54	7	39
303	45	1837	1	228	7								-35	193	B	60	7	33	52	8	40
304	45	1837	1	228	8								-40	188	B	45	5	50	49	9	42
305	45	1837	1	228	9								-45	183	B	56	8	37	46	11	44
306	45	1837	1	228	10								-50	178	B	63	8	30	46	8	46
307	45	1837	1	228	11								-55	173	B	49	7	44	51	8	41
308	45	1837	1	228	12								-60	168	b	55	5	40	35	10	55
309	45	1838	3	272	3								-15	257	Y	58	10	31	49	8	43
310	45	1838	3	272	4								-20	252	Y	69	13	18	49	9	42
311	45	1838	3	272	5								-25	247	B	60	11	28	38	8	54
312	45	1838	3	272	6								-30	242	Y	63	12	24	43	9	49
313	45	1838	3	272	7								-35	237	B	57	10	31	48	7	45
314	45	1838	3	272	8								-40	232	B	34	11	55	37	9	55
315	45	1838	3	272	9								-45	227	B	71	4	24	44	7	49
316	45	1838	3	272	10								-50	222	B	52	13	33	40	10	50
317	45	1838	3	272	11								-55	217	B	58	11	29	51	6	43
318	45	1838	3	272	12								-60	212	B	46	9	44	33	9	59
319	25	1864	1	395	1	84	113	35	110	48	62	168	-5	390	Blue						
320	25	1864	1	395	2	83	114	37	111	37	74	127	-10	385	Blue						
321	25	1864	1	395	3	85	114	34	91	35	56	125	-15	380	Yellow						
322	25	1864	1	395	4	78	111	42	102	38	64	148	-20	375	Yellow						
323	25	1864	1	395	5	81	113	40	114	38	76	164	-25	370	Yellow						
324	25	1864	1	395	6	83	116	40	100	34	66	139	-30	365	Yellow						
325	25	1864	1	395	7	79	112	42	110	40	70	174	-35	360	Blue						
326	25	1864	1	395	8	79	111	41	106	39	67	160	-40	355	blue						
327	25	1864	1	395	9	81	114	41	108	38	70	170	-45	350	Blue	84	13	3	46	10	44
328	25	1864	1	395	10				100	35	65	145	-50	345	Blue						
329	25	1864	1	395	11	81	114	41	111	38	73	181	-55	340	blue						
330	25	1864	1	395	12	82	114	39	112	35	77	192	-60	335	blue						
331	25	1864	1	395	13	81	113	40	107	40	67	162	-70	325	blue						

1	A	B	C	D	E	F	G	H	I	J	K	L	M	N	O	P	Q	R	S	T	U
	County	Site	Hole No.	Hole Elev msl	Sample Number	Dry Density	Wet Density	Moisture Percent	LL	PL	PI	% VC	Depth	Elev msl	Yellow/Blue	clay %	qtz %	Calcite %	% Smec	% Illite	% Kaol
332	25	1864	1	395	14	82	112	36	107	46	61	172	-80	315	blue						
333	25	1864	2	355	1	76	108	42	101	34	67	177	-5	350	Blue						
334	25	1864	2	355	2	78	111	42	111	83	28	240	-10	345	Yellow						
335	25	1864	2	355	4	79	113	43	114	43	71	188	-20	335	Yellow						
336	25	1864	2	355	5	78	112	44	107	58	49	135	-25	330	Yellow						
337	25	1864	2	355	6	74	109	47	98	44	54	130	-30	325	yellow						
338	25	1864	2	355	7				123	53	70	172	-35	320	Blue						
339	25	1864	2	355	8	78	112	43	101	51	50	159	-40	315	Yellow						
340	25	1864	2	355	9	76	109	44	102	59	43	153	-45	310	Blue						
341	25	1864	2	355	10	77	110	43	118	39	79	177	-50	305	Blue						
342	25	1864	2	355	11	76	110	45	101	52	49	127	-55	300	blue						
343	25	1864	2	355	12	80	114	42	90	27	63	129	-60	295	blue						
344	25	1864	2	355	13	83	115	39	90	48	42	185	-70	285	blue						
345	25	1864	2	355	14	83	114	37					-80	275	blue						
346	25	1864	3	342	4	72	107	49	125	45	80	196	-20	322	yellow						
347	25	1864	3	342	5	68	106	56	121	42	79	171	-25	317	Yellow						
348	25	1864	3	342	6				115	19	96	167	-30	312	Yellow						
349	25	1864	3	342	7	68	105	54	126	53	73	204	-35	307	Blue						
350	25	1864	3	342	8	74	110	49	100	43	57	153	-40	302	Yellow						
351	25	1864	3	342	9	75	112	49	114	47	67	164	-45	297	Blue						
352	25	1864	3	342	10	76	112	47	112	60	52	171	-50	292	Blue						
353	25	1864	3	342	11	77	112	46	118	47	71	206	-55	287	blue						
354	25	1864	3	342	12	78	112	44	106	40	66	156	-60	282	blue						
355	25	1864	3	342	13	81	115	42	100	38	62	162	-70	272	blue						
356	25	1864	3	342	14	90	124	38	109	46	63	202	-80	262	blue						
357	25	1864	4	296	3	71	106	49	112	55	57	177	-15	281	Yellow						
358	25	1864	4	296	4	71	108	52	113	47	66	140	-20	276	yellow						
359	25	1864	4	296	5	73	109	49	106	57	49	161	-25	271	Yellow						
360	25	1864	4	296	6	69	108	57	118	60	58	202	-30	266	Blue						
361	25	1864	4	296	7	72	109	52	112	47	65	155	-35	261	Blue						
362	25	1864	4	296	8	76	110	45	110	42	68	148	-40	256	Blue						
363	25	1864	4	296	9	77	111	44	102	41	61	152	-45	251	blue						
364	25	1864	4	296	10	82	116	41	72	38	34	127	-50	246	Blue						
365	25	1864	4	296	11	81	115	42	108	47	61	136	-55	241	blue						
366	25	1864	4	296	12	82	116	42	110	40	70	158	-60	236	blue						
367	25	1864	4	296	13	82	115	40	109	38	71	168	-70	226	blue						
368	25	1864	4	296	14	81	113	40	100	44	56	171	-80	216	blue						
369	82	1888	1	236	6	111	133	20	39	16	23	34	-30	206	Blue						
370	82	1888	1	236	7	118	137	16	48	19	29	37	-35	201	Blue						
371	82	1888	1	236	8	96	122	27	108	34	74	60	-40	196	Blue						
372	82	1888	1	236	9	84	114	36	94	34	60	105	-45	191	Blue						
373	82	1888	1	236	10	89	122	37	98	34	64	84	-50	186	Blue						
374	82	1888	1	236	11	85	116	36	95	35	60	111	-55	181	blue						
375	82	1888	1	236	12	88	119	35	99	36	63	72	-60	176	blue						
376	82	1888	1	236	13	89	117	31	87	35	52	28	-70	166	blue						
377	82	1888	1	236	14	100	125	25	51	27	24		-80	156	blue						
378	82	1889	1		6			26	52	20	32	74	-30		Blue						
379	82	1889	1		7	84	117	39	93	28	65		-35		yellow	43	6	51	40	9	51
380	82	1889	1		8	79	113	43	107	32	75	157	-40		Yellow	64	8	28	38	12	49
381	82	1889	1		9	89	119	34	80	25	55	138	-45		Blue						
382	82	1889	1		10	89	121	36	76	23	53	93	-50		Blue						
383	82	1889	1		11	95	124	30	89	31	58	91	-55		blue	42	6	49	54	5	40
384	82	1889	1		12	100	117	17	85	29	56	93	-60		blue	44	6	45	65	6	29
385	82	1890	1	225	6	82	111	35	151	35	116	161	-30	195	Yellow						
386	82	1890	1	225	7	88	116	32	82	45	37	63	-35	190	yellow						
387	82	1891	1		1			23	36	24	12	21	-5		Yellow						
388	82	1891	1		2			27	31	22	9	23	-10		Blue						
389	82	1891	1		3			23	32	19	13	31	-15		Yellow						
390	82	1891	1		4	99	124	25	51	21	30	73	-20		Yellow						
391	82	1891	1		5				80	18	62	126	-25		Yellow						
392	82	1891	1		6				30	33		139	-30		yellow						
393	82	1891	1		7	99	126	27	80	29	51	128	-35		Blue	43	6	51	40	9	51
394	82	1891	1		8	85	117	37	94	30	64	97	-40		Yellow	64	8	28	38	12	49
395	82	1891	1		9	25	52	106	86	28	58	85	-45		Blue						
396	82	1891	1		10	24	49	104	64	24	40	71	-50		blue						
397	82	1891	1		11	25	50	98	62	24	38	75	-55		blue						

	A	B	C	D	E	F	G	H	I	J	K	L	M	N	O	P	Q	R	S	T	U
1	County	Site	Hole No.	Hole Elev msl	Sample Number	Dry Density	Wet Density Percent	Moisture	LL	PL	PI	% VC	Depth	Elev msl	Yellow/Blue	clay %	qtz %	Calcite %	% Smec	% Illite	% Kaol
398	82	1891	1		12				70	30	40	54	-60		blue						
399	82	1892	1	218	4	93	122	31	53	27	26	107	-25	193	yellow						
400	82	1892	1	218	5	101	126	25	57	24	33	85	-30	188	blue						
401	82	1892	1	218	6	94	124	32	56	32	24	127	-35	183	yellow						
402	82	1892	1	218	7	101	128	27	70	31	39	90	-40	178	Blue						
403	82	1892	1	218	8	88	116	32	47	30	17	60	-45	173	Blue						
404	82	1892	1	218	9	93	124	33	53	45	8	76	-50	168	blue						
405	82	1892	1	218	10	90	115	28	61	41	20	54	-55	163	blue						
406	45	1894	1	331	1								-5	326	Yellow	33	58	0	54	21	25
407	45	1894	1	331	2								-10	321	Yellow	40	54	0	50	9	42
408	45	1894	1	331	3	84	114	36	105	34	71		-15	316	Yellow	74	12	15	42	10	48
409	45	1894	1	331	4	77	110	43	108	35	73	221	-20	311	Yellow	74	13	12	54	7	39
410	45	1894	1	331	5	76	107	41					-25	306	yellow	48	12	39	25	19	56
411	45	1894	1	331	6	71	107	50	102	37	65		-30	301	yellow	62	14	25	30	18	52
412	45	1894	1	331	7	106	130	23					-35	296	Blue	43	4	51	72	6	23
413	45	1894	1	331	8	84	114	36					-40	291	Blue	71	12	17	40	11	49
414	45	1894	1	331	9	79	114	44	27	16	11	21	-45	286	Blue	83	11	6	37	17	46
415	45	1894	1	331	10	82	115	40					-50	281	Blue	74	15	10	42	13	45
416	45	1894	1	331	11	82	116	41	125	27	98		-55	276	Blue	79	15	5	43	12	45
417	45	1894	1	331	12		0						-60	271	Blue	59	31	10	42	12	46
418	45	1894	1	331	13	84	114	36	99	33	66	157	-70	261	Blue	71	12	17	42	11	47
419	45	1894	1	331	14								-80	251	Blue	75	15	10	41	14	45
420	45	1894	3		2	85	114	34	99	30	69	139	-10		Blue						
421	45	1894	7		5	108	131	21	102	30	72	165	-10		Blue						
422	45	1894	2		2	74	107	44	102	35	67	214	-10		Yellow						
423	45	1894	5		5	90	118	31	87	31	56		-10		Yellow						
424	45	1894	5		6	83	114	37					-12		Blue						
425	45	1894	5		7	74	108	46	104	35	69	168	-14		Yellow						
426	45	1894	7		7	82	112	37	103	29	74		-14		Yellow						
427	45	1894	8		7	76	109	43					-14		Yellow						
428	45	1894	12		3	91	118	30	91	28	63		-15		Blue						
429	45	1894	6		3	83	113	36					-15		Blue						
430	45	1894	2		3	81	113	40					-15		yellow						
431	45	1894	3		3								-15		yellow						
432	45	1894	4		3	80	113	41					-15		Yellow						
433	45	1894	5		8	81	113	40	93	30	63		-16		Yellow						
434	45	1894	8		9	79	111	40	10	35			-18		Yellow						
435	45	1894	5		9	78	108	39					-18		Yellow						
436	45	1894	7		9	81	113	39					-18		Yellow						
437	45	1894	8		10	79	111	41	110	38	72	166	-20		yellow						
438	45	1894	9		4	83	114	37	103	21	82	155	-20		yellow						
439	45	1894	11		4	104	127	22	99	34	65	136	-20		Yellow						
440	45	1894	12		4	89	119	34	69	27	42	132	-20		Yellow						
441	45	1894	2		4	77	111	44	101	33	68		-20		Yellow						
442	45	1894	4		4				104	37	67	175	-20		Yellow						
443	45	1894	5		10	77	99	28	100	33	67	157	-20		Yellow						
444	45	1894	6		4	75	107	43	97	32	65	159	-20		Yellow						
445	45	1894	2		5	76	110	45					-25		Yellow						
446	45	1894	4		5	83	115	38					-25		yellow						
447	45	1894	8		11	75	109	45					-25		Yellow						
448	45	1894	9		5	81	113	40					-25		Yellow						
449	45	1894	11		5	78	111	42					-25		yellow						
450	45	1894	12		5	90	117	30					-25		Yellow						
451	45	1894	3		5	104	127	22	103	33	70	152	-25		Yellow						
452	45	1894	5		11	80	112	40	78	28	50		-25		Yellow						
453	45	1894	6		5	74	110	48	105	40	65		-25		Yellow						
454	45	1894	7		11	80	112	40	105	31	74	168	-25		Yellow						
455	45	1894	3		6	108	131	21					-30		Yellow						
456	45	1894	4		6	81	114	41					-30		yellow						
457	45	1894	5		12	76	112	48	98	34	64		-30		Yellow						
458	45	1894	8		12	87	117	35	113	36	77		-30		Yellow						
459	45	1894	9		7	89	117	32	103	34	69		-30		Yellow						
460	45	1894	10		6	83	112	35					-30		Yellow						
461	45	1894	11		6	84	116	38	121	34	87		-30		Yellow						
462	45	1894	12		6	81	109	34	123	41	82	198	-30		yellow						
463	45	1894	6		6	77	112	45					-30		Yellow						

1	A	B	C	D	E	F	G	H	I	J	K	L	M	N	O	P	Q	R	S	T	U	
	County	Site	Hole No.	Hole Elev msl	Sample Number	Dry Density	Wet Density percent	Moisture	LL	PL	PI	% VC	Depth	Elev msl	Yellow/Blue	clay %	qtz %	Calcite %	% Smec	% Illite	% Kaol	
464	45	1894	7		12	79	111	40	103	35	68		-30		Yellow							
465	45	1894	3		7	84	114	36	95	33	62	148	-35		blue							
466	45	1894	10		7	79	111	40	108	35	73		-35		Blue							
467	45	1894	11		7	84	113	35					-35		Blue							
468	45	1894	12		7	83	114	37					-35		Blue							
469	45	1894	8		13	75	110	46					-35		Blue							
470	45	1894	5		13	80	114	42					-35		Yellow							
471	45	1894	6		7	80	114	43					-35		Yellow							
472	45	1894	7		13	92	121	32					-35		Yellow							
473	45	1894	9		8	81	113	40	128	41	87	198	-35		yellow							
474	45	1894	12		8	84	117	39	117	35	82	176	-40		Blue							
475	45	1894	5		14	81	114	41	101	36	65		-40		Blue							
476	45	1894	6		8	85	117	38					-40		Blue							
477	45	1894	8		14	97	112	15					-40		blue							
478	45	1894	9		9	94	116	23					-40		Blue							
479	45	1894	10		8	82	114	39					-40		yellow							
480	45	1894	12		9	84	117	39	110	34	76		-45		blue							
481	45	1894	5		15	89	113	27					-45		blue							
482	45	1894	6		9	81	115	42	106	36	70	175	-45		Blue							
483	45	1894	7		15				113	37	76	181	-45		yellow							
484	45	1894	12		10	83	116	40					-50		Blue							
485	45	1894	5		16	86	118	37					-50		Blue							
486	45	1894	6		10								-50		blue							
487	45	1894	7		16								-50		Blue							
488	45	1894	12		11	81	115	42					-55		Blue							
489	45	1894	5		17	81	113	40	103	36	67	171	-55		Blue							
490	45	1894	6		11	80	113	41					-55		Blue							
491	45	1894	7		17	97	114	18					-55		Blue							
492	45	1894	12		12	81	115	42					-60		Blue							
493	45	1894	5		18	86	117	36					-60		Blue							
494	45	1894	6		12	85	116	37					-60		Blue							
495	45	1894	7		18								-60		Blue							
496	45	1894	5		19	84	114	36					-70		Blue							
497	45	1894	6		13	86	117	36	99	39	60		-70		Blue							
498	45	1894	7		19	82	114	39	108	39	69	178	-70		Blue							
499	45	1894	5		20	82	116	41					-80		Blue							
500	45	1894	6		14	89	111	25					-80		Blue							
501	45	1894	7		20	84	117	39	110	35	75		-80		Blue							
502	61	1921	2	349	5	60	100	67	128	53	75	219	-25	324	Blue							
503	61	1921	2	349	6	76	110	45	95	35	60	148	-30	319	Blue							
504	61	1921	1	349	10	73	107	46	113	38	75	187	-35	314	Blue							
505	61	1921	2	349	7	77	110	43	110	36	74	165	-35	314	Blue							
506	61	1921	1	349	11	77	110	43	111	51	60	150	-40	309	Blue							
507	61	1921	2	349	8	76	110	45	98	34	64	154	-40	309	Blue							
508	61	1921	1	349	12	80	111	39	120	58	62	208	-45	304	Blue							
509	61	1921	2	349	9	80	113	41	107	37	70	165	-45	304	Blue							
510	61	1921	1	349	13	79	114	44	109	44	65	179	-50	299	Blue							
511	61	1921	2	349	10	80	113	41	108	36	72	167	-50	299	Blue							
512	61	1921	1	349	14	80	114	42	114	48	66	200	-55	294	Blue							
513	61	1921	2	349	11	81	113	40	97	38	59	152	-55	294	Blue							
514	61	1921	1	349	15	78	110	41	94	40	54	138	-60	289	Blue							
515	61	1921	2	349	12	76	110	45	100	36	64	155	-60	289	Blue							
516	61	1921	1	349	16	81	113	40	97	40	57	134	-70	279	Blue							
517	61	1921	2	349	13	72	107	49	107	43	64	162	-70	279	Blue							
518	61	1922	1	345	6	77	112	45	116	48	68	181	-30	315	Blue							
519	61	1922	1	345	7	77	112	45	109	39	70	180	-35	310	Blue							
520	61	1922	1	345	8	78	109	40	110	54	56	192	-40	305	Blue							
521	61	1922	1	345	9	75	110	47	112	62	50	183	-45	300	Blue							
522	61	1922	1	345	10	73	110	50	113	60	53	184	-50	295	Blue							
523	61	1922	1	345	11	68	106	56	109	58	51	171	-55	290	Blue							
524	61	1922	1	345	12	68	106	56	116	63	53	206	-60	285	Blue							
525	61	1922	1	345	13	72	108	50					-70	275	Blue							
526	61	1922	3	342	7	69	102	48	107	42	65	168	-25	317	Blue							
527	61	1922	3	342	8	76	110	45	99	40	59	159	-30	312	Blue							
528	61	1922	3	342	9	76	110	45	108	40	68	172	-35	307	Blue							
529	61	1922	3	342	10	76	110	45	110	40	70	180	-40	302	Blue							

1	A	B	C	D	E	F	G	H	I	J	K	L	M	N	O	P	Q	R	S	T	U
	County	Site	Hole No.	Hole Elev msl	Sample Number	Dry Density	Wet Density Percent	Moisture	LL	PL	PI	% VC	Depth	Elev msl	Yellow/Blue	clay %	qtz %	Calcite %	% Smec	% Illite	% Kaol
530	61	1922	3	342	11				107	41	66	171	-45	297	Blue						
531	61	1922	3	342	12	72	106	47	105	41	64	155	-50	292	Blue						
532	61	1922	3	342	13	71	107	50	107	45	62	164	-55	287	Blue						
533	61	1922	3	342	14	72	108	50	106	46	60	157	-60	282	Blue						
534	61	1922	3	342	15				109	45	64	173	-70	272	Blue						
535	61	1922	2	337	4	76	113	48	104	40	64	183	-20	317	Blue						
536	61	1922	2	337	5	78	114	46	106	40	66	171	-25	312	Blue						
537	61	1922	2	337	6	77	112	46	114	42	72	185	-30	307	Blue						
538	61	1922	2	337	7	74	108	46	113	46	67	183	-35	302	Blue						
539	61	1922	2	337	8	69	106	54	117	52	65	188	-40	297	Blue						
540	61	1922	2	337	9	70	107	53	111	52	59	97	-45	292	Blue						
541	61	1922	2	337	10	72	109	52	104	52	52	166	-50	287	Blue						
542	61	1922	2	337	11	74	110	48	111	47	64	165	-55	282	Blue						
543	61	1922	2	337	12	71	107	50	113	48	65	168	-60	277	Blue						
544	61	1922	2	337	13	73	110	51					-70	267	Blue						
545	61	1926	1	351	13	74	104	41	93	36	57	130	-40	311	Blue						
546	61	1926	1	351	14	80	112	40	99	35	64	138	-45	306	Blue						
547	61	1926	1	351	15	79	111	40	105	38	67	155	-50	301	Blue						
548	61	1926	1	351	16	82	115	40	105	39	66	150	-55	296	Blue						
549	61	1926	1	351	17	79	111	41	108	39	69	173	-60	291	Blue						
550	61	1926	1	351	18	77	110	43	106	41	65	153	-70	281	Blue						
551	61	1926	2	350	7	75	110	46	107	40	67	169	-35	315	Blue						
552	61	1926	2	350	8	76	109	44	101	33	68	161	-40	310	Blue						
553	61	1926	2	350	9	76	110	45	113	38	75	166	-45	305	Blue						
554	61	1926	2	350	10	71	106	49	108	38	70	147	-50	300	Blue						
555	61	1926	2	350	11	76	108	42	118	38	80	167	-55	295	Blue						
556	61	1926	2	350	12	78	111	42	104	37	67	143	-60	290	Blue						
557	61	1926	2	350	13	79	112	42	110	36	74	178	-70	280	Blue						
558	61	1927	2	351	9	79	111	40	104	39	65	147	-25	326	Yellow						
559	61	1927	2	351	10	74	108	46	109	44	65	147	-30	321	Yellow						
560	61	1927	2	351	11	78	111	42	93	36	57	169	-35	316	Blue						
561	61	1927	2	351	12	80	113	41	105	42	63	164	-40	311	Blue						
562	61	1927	2	351	13	80	113	41	95	37	58	194	-45	306	Blue						
563	61	1927	2	351	14	82	116	41	105	37	68	157	-50	301	Blue						
564	61	1927	2	351	15	81	114	41	107	38	69	168	-55	296	Blue						
565	61	1927	2	351	16				106	36	70	161	-60	291	Blue						
566	61	1927	2	351	17	83	116	40	100	39	61	152	-70	281	Blue						
567	61	1927	1	350	9	77	110	43	110	39	71	173	-40	310	Blue						
568	61	1927	1	350	10	74	109	47	107	39	68	150	-45	305	Blue						
569	61	1927	1	350	11	81	112	38	104	40	64	166	-50	300	Blue						
570	61	1927	1	350	12	77	109	42	104	40	64	153	-55	295	Blue						
571	61	1927	1	350	13	81	113	40	103	38	65	145	-60	290	Blue						
572	61	1927	1	350	14	73	107	46	99	43	56	155	-70	280	Blue						
573	61	1928	5	420	3	75	107	42	81	43	38	131	-15	405	Yellow						
574	61	1928	5	420	4	75	107	43	88	34	54	137	-20	400	Yellow						
575	61	1928	5	420	5	71	104	47	103	38	65	160	-25	395	Yellow						
576	61	1928	5	420	6	81	113	39	103	37	66	171	-30	390	Yellow						
577	61	1928	5	420	7	76	109	43	97	37	60	159	-35	385	Yellow						
578	61	1928	5	420	8				69	29	40	108	-40	380	Yellow						
579	61	1928	5	420	9	81	113	40	96	37	59	139	-45	375	Blue						
580	61	1928	5	420	10	74	103	39	84	32	52	130	-50	370	Blue						
581	61	1928	5	420	11	79	111	41	97	38	59	135	-55	365	Blue						
582	61	1928	5	420	12	80	111	39	97	36	61	138	-60	360	Blue	72	11	17	47	12	41
583	61	1928	5	420	13	83	114	37	58	23	35	80	-70	350	Blue						
584	61	1928	4	419	4	73	105	44	91	35	56	124	-8	411	Yellow						
585	61	1928	4	419	5	78	110	41	111	39	72	194	-10	409	Yellow						
586	61	1928	4	419	6	78	112	43	90	36	54	154	-12	407	Yellow						
587	61	1928	4	419	7	75	108	44	101	38	63	171	-14	405	Yellow						
588	61	1928	4	419	8	82	110	34	104	41	63	206	-16	403	Yellow						
589	61	1928	4	419	9	80	111	39	89	36	53	134	-18	401	Yellow						
590	61	1928	4	419	10				97	38	59	165	-20	399	Yellow						
591	61	1928	4	419	11	82	113	38	74	29	45	107	-25	394	Yellow						
592	61	1928	4	419	12	100	124	24	59	24	35	79	-30	389	Blue						
593	61	1928	4	419	13				89	34	55	142	-35	384	Blue	73	12	13	45	8	47
594	61	1928	4	419	15				93	34	59	155	-45	374	Blue	74	8	15	45	11	44
595	61	1928	4	419	16	81	113	39	98	37	61	132	-50	369	Blue						

1	A	B	C	D	E	F	G	H	I	J	K	L	M	N	O	P	Q	R	S	T	U	
	County	Site	Hole No.	Hole Elev msl	Sample Number	Dry Density	Wet Density Percent	Moisture	LL	PL	PI	% VC	Depth	Elev msl	Yellow/Blue	clay %	qtz %	Calcite %	% Smec	% Illite	% Kaol	
596	61	1928	4	419	17				99	38	61	141	-55	364	Blue							
597	61	1928	4	419	18	83	112	35	90	34	56	137	-60	359	Blue							
598	61	1928	4	419	19	81	112	38	97	35	62	126	-70	349	Blue							
599	61	1929	1	373	9	105	127	21	51	16	35	79	-18	355	Yellow							
600	61	1929	1	373	10	116	130	12	50	16	34	92	-20	353	Yellow							
601	61	1929	1	373	11	75	108	44	110	39	71	182	-25	348	Yellow							
602	61	1929	1	373	12	75	110	47	110	43	67	189	-30	343	Yellow							
603	61	1929	2	373	6	76	110	45	104	41	63	169	-30	343	Yellow							
604	61	1929	2	373	7	80	112	40	92	36	56	138	-35	338	Blue							
605	61	1929	1	373	13	76	110	45	98	37	61	157	-35	338	Yellow							
606	61	1929	1	373	14	78	112	44	109	39	70	180	-40	333	Blue							
607	61	1929	2	373	8	76	110	45	107	36	71	166	-40	333	Blue							
608	61	1929	1	373	15	80	115	4	108	36	72	190	-45	328	Blue							
609	61	1929	2	373	9	77	111	44	108	40	68	162	-45	328	Blue							
610	61	1929	1	373	16	78	112	44	113	37	76	180	-50	323	Blue							
611	61	1929	2	373	10	78	112	44	98	39	59	141	-50	323	Blue							
612	61	1929	1	373	17	83	117	41	96	32	64	139	-55	318	Blue							
613	61	1929	2	373	11	81	116	43	100	38	62	148	-55	318	Blue							
614	61	1929	1	373	18	79	113	43	104	37	67	168	-60	313	Blue							
615	61	1929	2	373	12	82	115	40	103	36	67	148	-60	313	Blue							
616	61	1929	1	373	19	83	115	38	97	37	60	152	-70	303	Blue							
617	61	1929	2	373	13	83	116	40	97	36	61	192	-70	303	Blue							
618	62	1930	1	378	2								-10	368	Yellow	51	48	1	60	8	31	
619	62	1930	1	378	3	90	118	31	70	25	45	100	-15	363	yellow	43	4	53	49	8	44	
620	62	1930	1	378	4								-20	358	yellow	53	6	39	49	9	42	
621	62	1930	1	378	5								-25	353	yellow	19	2	75	50	9	41	
622	62	1930	1	378	6								-30	348	Blue	41	11	40	36	7	57	
623	62	1931	1	479	1								-5	474	Yellow	48	48	0	39	8	53	
624	62	1931	1	479	2	92	124	35	86	33	53	148	-10	469	Yellow	70	12	18	39	12	49	
625	62	1931	1	479	3	78	110	41	51	43	8	161	-15	464	yellow	68	13	16	57	10	34	
626	62	1931	1	479	4	79	108	37	100	33	67	37	-20	459	Yellow	75	14	2	53	12	35	
627	62	1931	1	479	5	76	109	43	105	39	66	42	-25	454	Yellow	71	10	18	47	9	44	
628	62	1931	1	479	6	74	111	50	109	40	69	42	-30	449	Blue	77	15	7	60	7	33	
629	62	1931	1	479	7	77	110	43	94	37	57	28	-35	444	Blue	65	10	25	42	10	49	
630	62	1931	1	479	8	76	111	46	110	38	72	187	-40	439	Blue	77	14	9	46	9	45	
631	62	1931	1	479	9	82	110	34	97	38	59	166	-45	434	Blue	73	12	14	46	10	44	
632	62	1931	1	479	10	77	112	45	108	35	73	182	-50	429	Blue	72	10	15	50	8	42	
633	62	1931	1	479	11	77	111	44	108	38	70	177	-55	424	blue	70	17	12	51	9	40	
634	62	1931	1	479	12	74	109	47	113	43	70	189	-60	419	blue	74	10	15	52	8	40	
635	62	1931	1	479	13	75	110	46	111	43	68	182	-70	409	blue	75	8	15	55	7	38	
636	62	1931	1	479	14	74	109	47	112	51	61	178	-80	399	blue	74	10	16	49	6	45	
637	62	1932	1	497	1				22	67	22	45	120	-5	492	Blue	60	36	0	45	8	46
638	62	1932	1	497	2	85	113	33	91	28	63	145	-10	487	Blue	69	12	17	54	6	40	
639	62	1932	1	497	3	77	109	41	99	32	67	171	-15	482	yellow	68	13	17	49	8	43	
640	62	1932	1	497	4				100	32	68	159	-20	477	Yellow	35	5	58	54	7	39	
641	62	1932	1	497	5	83	114	37	88	29	58	173	-25	472	Yellow	58	9	25	50	7	43	
642	62	1932	1	497	6	79	97	23	98	35	63	148	-30	467	Yellow	67	9	22	44	9	47	
643	62	1932	1	497	7	79	112	42	71	27	44	100	-35	462	Yellow	59	8	27	35	12	53	
644	62	1932	1	497	8	78	110	41	98	37	61	164	-40	457	Blue	74	12	12	28	11	61	
645	62	1932	1	497	9	80	112	40	107	33	74	163	-45	452	Blue	74	15	10	45	11	44	
646	62	1932	1	497	10	81	113	40	100	33	67	196	-50	447	Blue	74	13	12	43	12	45	
647	62	1932	1	497	11	83	115	38	100	30	70	151	-55	442	blue	65	14	20	48	9	42	
648	62	1932	1	497	12	85	117	38	106	34	72	171	-60	437	blue	75	16	6	48	8	43	
649	62	1932	1	497	13	80	113	41	104	35	69	185	-70	427	blue	71	14	8	46	9	45	
650	62	1932	1	497	14	86	115	34	107	37	70	162	-80	417	blue	67	10	21	47	9	44	
651	62	1933	1	452	7				91	37	54	144	-35	417	Yellow	64	8	27	41	8	51	
652	62	1933	1	452	8	77	109	42	97	38	59	164	-40	412	blue	66	9	7	47	9	44	
653	62	1933	1	452	9	77	109	42	98	56	42	159	-45	407	Blue	72	14	11	41	12	47	
654	62	1933	1	452	10	73	105	44	99	38	61	153	-50	402	blue	72	16	11	39	9	52	
655	62	1933	1	452	11	80	112	40	95	35	60	151	-55	397	Blue	73	13	14	40	10	49	
656	62	1933	1	452	12	77	109	42	94	64	30	144	-60	392	Blue	74	12	14	43	9	48	
657	62	1933	1	452	13	77	111	44					-70	382	Blue	80	13	7	51	9	39	
658	62	1933	1	452	14	79	111	41	104	38	66	147	-80	372	Blue	72	11	15	51	8	41	
659	61	1936	1	375	1								-5	370	y	63	34	0	42	12	46	
660	61	1936	1	375	2								-10	365	Y	71	14	12	51	10	39	

1	A	B	C	D	E	F	G	H	I	J	K	L	M	N	O	P	Q	R	S	T	U
	County	Site	Hole No.	Hole Elev msl	Sample Number	Dry Density	Wet Density Percent	Moisture	LL	PL	PI	% VC	Depth	Elev msl	Yellow/Blue	clay %	qtz %	Calcite %	% Smec	% Illite	% Kaol
661	61	1936	1	375	3								-15	360	Y	69	15	17	58	10	33
662	61	1936	1	375	4								-20	355	Y	68	12	20	55	10	35
663	61	1936	1	375	5								-25	350	Y	65	9	25	54	10	37
664	61	1936	1	375	6								-30	345	Y	60	9	32	51	9	40
665	61	1936	1	375	7								-35	340	B	77	13	10	51	13	36
666	61	1936	1	375	8								-40	335	B	62	15	18	46	6	48
667	61	1936	1	375	9								-45	330	B	76	11	13	56	8	36
668	61	1936	1	375	10								-50	325	B	71	11	17	55	10	35
669	61	1936	1	375	11								-55	320	B	73	17	9	44	8	48
670	61	1936	1	375	12								-60	315	B	77	12	9	51	9	40
671	61	1937	1	369	2	73	106	45	112	39	73	176	-10	359	Yellow	75	11	13	45	6	49
672	61	1937	1	369	3	72	106	47	114	32	82	172	-15	354	Yellow	77	12	12	48	8	44
673	61	1937	1	369	4	72	105	46	109	40	69	178	-20	349	Yellow	82	13	5	51	9	39
674	61	1937	1	369	5	62	89	43	118	36	82	185	-25	344	Yellow	77	13	8	59	9	32
675	61	1937	1	369	6	70	104	48	114	43	71	170	-30	339	Yellow	72	13	13	62	7	31
676	61	1937	1	369	7	71	105	48	126	46	80	185	-35	334	Blue	75	12	13	66	6	28
677	61	1937	1	369	8	73	109	49	116	43	73	139	-40	329	Blue	72	9	18	65	11	24
678	61	1937	1	369	9	70	102	46	128	45	83	181	-45	324	Blue	73	11	13	61	14	25
679	61	1937	1	369	10	71	105	48	123	44	79	177	-50	319	Blue	80	10	8	72	9	19
680	61	1937	1	369	11	71	104	46	119	44	75	171	-55	314	Blue	72	10	16	63	10	26
681	61	1937	1	369	12	72	106	47	122	47	75	173	-60	309	Blue	79	13	8	65	12	22
682	61	1937	1	369	13	70	105	50	116	42	74	164	-70	299	Blue	72	10	10	66	6	28
683	61	1937	1	369	14	79	111	40	119	38	81	184	-80	289	Blue	71	13	13	57	8	34
684	61	1938	1		1								-5		y	24	72	0	69	8	24
685	61	1938	1		2								-10		Y	50	48	0	78	3	19
686	61	1938	1		3								-15		Y	79	14	8	78	5	17
687	61	1938	1		4								-20		Y	84	11	6	72	6	22
688	61	1938	1		5								-25		Y	77	10	9	84	5	11
689	61	1938	1		6								-30		B	66	12	16	76	6	18
690	61	1938	1		7								-35		B	71	12	14	56	8	36
691	61	1938	1		8								-40		b	69	15	16	62	6	33
692	61	1938	1		9								-45		b	70	12	18	60	7	34
693	61	1938	1		10								-50		B	52	8	37	47	8	45
694	61	1938	1		11								-55		B	74	11	15	62	7	31
695	61	1938	1		12								-60		b	66	7	24	61	8	31
696	25	2379	2	355	8	85	114	34	100	36	64	168	-20	335	yellow						
697	25	2379	2	355	10	91	111	37	94	33	61	68	-30	325	yellow						
698	25	2379	2	355	11	82	120	30	80	31	49	111	-35	320	Blue						
699	25	2379	2	355	12				86	35	51	107	-45	310	Blue						
700	25	2379	1	348	4	86	114	33	94	31	63	137	-8	340	yellow						
701	25	2379	9	348	5	85	112	32	90	28	62	151	-10	338	Yellow						
702	25	2379	1	348	6	81	111	37	60	21	39	95	-12	336	yellow						
703	25	2379	9	348	7	98	123	25	78	23	55	132	-14	334	Yellow						
704	25	2379	9	348	10	91	117	29	75	28	47	118	-20	328	Yellow						
705	25	2379	1	348	8	80	110	37	99	31	68	144	-20	328	yellow						
706	25	2379	1	348	10	91	18	30					-30	318	Blue						
707	25	2379	9	348	12	80	110	38	92	23	69	137	-30	318	Yellow						
708	25	2379	9	348	13	93	120	29	86	28	58	120	-35	313	blue						
709	25	2379	1	348	11	86	114	33	92	35	57	119	-35	313	Blue						
710	25	2379	10	346	6	87	114	31	87	28	59	141	-12	334	yellow						
711	25	2379	10	346	10	93	119	28	86	28	56	131	-20	326	yellow						
712	25	2379	10	346	12	87	113	30	86	27	59	133	-30	316	yellow						
713	25	2379	10	346	14	85	116	36	110	32	78	131	-40	306	blue						
714	25	2379	10	346	15	86	117	36	98	34	64	142	-45	301	blue						
715	25	2379	11	343	4	102	124	22	79	25	54	119	-8	335	yellow						
716	25	2379	11	343	7	78	108	39	97	30	67	145	-20	323	yellow						
717	25	2379	11	343	9	87	116	33	102	30	72	144	-30	313	blue						
718	25	2379	11	343	10	85	116	36	94	31	63	144	-35	308	blue						
719	25	2379	3	340	3	85	113	33	79	30	49	156	-15	325	yellow						
720	25	2379	3	340	5	91	117	29					-25	315	Blue						
721	25	2379	3	340	6	86	115	34	89	36	53	153	-30	310	Blue						
722	25	2379	8	338	3	98	123	25	75	21		165	-6	332	Yellow						
723	25	2379	8	338	4	84	111	32	92	27		151	-8	330	Yellow						
724	25	2379	8	338	5	90	117	30	81	22	59	138	-10	328	Yellow						
725	25	2379	7	337	4	85	114	34	99	28	71	153	-8	329	Yellow						
726	25	2379	7	337	6	83	113	36	107	29	78	171	-15	322	Yellow						

1	A	B	C	D	E	F	G	H	I	J	K	L	M	N	O	P	Q	R	S	T	U
	County	Site	Hole No.	Hole Elev msl	Sample Number	Dry Density	Wet Density Percent	Moisture	LL	PL	PI	% VC	Depth	Elev msl	Yellow/Blue	clay %	qtz %	Calcite %	% Smec	% Illite	% Kaol
727	25	2379	7	337	8	76	108	42	111	33	78	172	-25	312	Yellow						
728	25	2379	7	337	9	98	124	26	90	30	60	116	-30	307	Blue						
729	25	2379	7	337	10	87	116	33					-35	302	Blue						
730	25	2379	4	335	3	101	123	22	65	20	45	114	-6	329	yellow						
731	25	2379	4	335	6	79	108	37	93	32	61	165	-15	320	yellow						
732	25	2379	4	335	7	86	115	34					-20	315	yellow						
733	25	2379	4	335	8	84	113	35	90	32	58	123	-25	310	Blue						
734	25	2379	4	335	9	101	125	24					-30	305	Blue						
735	25	2379	5	334	3	107	127	19	51	14	37	80	-6	328	yellow						
736	25	2379	5	334	4	94	120	28	79	27	52	120	-8	326	yellow						
737	25	2379	6	334	5	82	112	37	85	28	57	128	-10	324	yellow						
738	25	2379	5	334	6	84	114	34	83	27	56	123	-15	319	yellow						
739	25	2379	6	334	7	84	113	35	107	41	66	165	-20	314	yellow						
740	25	2379	5	334	8	83	114	37	91	33	58	122	-25	309	Blue						
741	25	2379	5	334	9	84	116	38					-30	304	Blue						
742	25	2379	6	334	9	78	109	40	108	41	67	160	-30	304	yellow						
743	25	2379	6	334	10	91	120	32	95	32	63	138	-35	299	Blue						
744	25	2379	6	334	11	102	127	24					-40	294	Blue						
745	25	2531	2	352	1	83	115	38	114	35	79	181	-5	347	Blue						
746	25	2531	1	352	2	89	120	35	104	32	72	141	-10	342	Yellow	63	34	0	57	7	35
747	25	2531	2	352	2	77	109	42	117	35	82	176	-10	342	Yellow						
748	25	2531	1	352	3	68	106	56	138	42	96	166	-15	337	Yellow	76	24	0	54	8	38
749	25	2531	2	352	3				121	38	83	210	-15	337	yellow						
750	25	2531	1	352	4	71	108	52	139	44	95	208	-20	332	yellow	85	15	0	66	6	29
751	25	2531	2	352	4	74	110	48	121	35	86	192	-20	332	Yellow						
752	25	2531	1	352	5	72	107	49	131	45	86	206	-25	327	Yellow	81	16	2	69	5	26
753	25	2531	2	352	5	75	110	47	108	38	70	141	-25	327	Yellow						
754	25	2531	1	352	6	76	112	47	123	39	84	171	-30	322	Yellow	80	16	4	64	5	31
755	25	2531	2	352	6				106	40	66	168	-30	322	yellow						
756	25	2531	1	352	7				112	33	79	175	-35	317	Yellow	78	17	5	50	11	39
757	25	2531	2	352	7	69	104	51	111	53	58	153	-35	317	Yellow						
758	25	2531	1	352	8	81	114	41	107	35	72	167	-40	312	Blue	84	0	0	46	11	43
759	25	2531	2	352	8	77	111	44	101	38	63	157	-40	312	Blue						
760	25	2531	1	352	9	85	120	41	97	33	64	157	-45	307	Blue	71	15	13	42	11	48
761	25	2531	2	352	9	77	110	43	103	48	55	147	-45	307	Blue						
762	25	2531	1	352	10	93	123	32	89	30	59	142	-50	302	Blue	61	12	26	38	10	52
763	25	2531	2	352	10	77	112	45	107	41	66	160	-50	302	Blue						
764	25	2531	1	352	11	83	116	40	96	35	61	143	-55	297	Blue	68	11	20	45	10	45
765	25	2531	2	352	11	71	104	46	108	42	66	166	-55	297	Blue						
766	25	2531	1	352	12	80	114	43	98	36	62	143	-60	292	Blue	72	12	13	49	11	40
767	25	2531	2	352	12	76	111	46	112	7	105	178	-60	292	Blue						
768	25	2531	1	352	13	79	112	42	104	36	68	155	-70	282	Blue						
769	25	2531	2	352	13	79	111	41	98	36	62	148	-70	282	Blue						
770	25	2531	1	352	14	84	117	39	93	35	58	138	-80	272	Blue						
771	25	2531	2	352	14	81	114	41	101	36	65	155	-80	272	Blue						
772	82	2550	1	211	13				79	24	55	136	-70	141	blue						
773	82	2550	1	211	14	80	111	39	108	32	76	141	-80	131	blue						
774	45	2551	2	190	3	92	117	27	35	24	11		-15	175	Yellow						
775	45	2551	2	190	4	98	119	21	32	20	12		-20	170	Yellow						
776	45	2551	2	190	5	69	104	50	103	34	69		-25	165	Yellow						
777	45	2551	2	190	6	74	107	44	92	30	62		-30	160	Yellow						
778	45	2551	2	190	7	72	107	48	101	36	65		-35	155	Yellow						
779	45	2551	2	190	8	74	109	47	111	40	71		-40	150	Yellow						
780	45	2551	2	190	9	80	113	41	105	37	68		-45	145	Blue						
781	45	2551	2	190	10	78	110	41	115	38	77		-50	140	Blue						
782	45	2551	2	190	11				110	38	72		-55	135	Blue						
783	45	2551	2	190	12	78	109	40	118	26	92		-60	130	Blue						
784	45	2551	2	190	13	79	105	33					-70	120	Blue						
785	45	2551	2	190	14								-80	110	Blue						
786	25	2552	1	266	2	70	105	50	51	22	29	80	-10	256	Yellow						
787	25	2552	1	266	3	77	109	42	110	42	68	206	-15	251	yellow						
788	25	2552	1	266	4	81	113	39	112	41	71	212	-20	246	yellow						
789	25	2552	1	266	5	79	112	42	107	42	65	201	-25	241	blue						
790	25	2552	1	266	6	85	116	36	99	32	67	185	-30	236	blue						
791	25	2552	1	266	7	92	121	31	77	28	49	121	-35	231	blue						
792	25	2552	1	266	8	84	115	37	95	35	60	170	-40	226	blue						

1	A	B	C	D	E	F	G	H	I	J	K	L	M	N	O	P	Q	R	S	T	U
	County	Site	Hole No.	Hole Elev msl	Sample Number	Dry Density	Wet Density Percent	Moisture	LL	PL	PI	% VC	Depth	Elev msl	Yellow/Blue	clay %	qtz %	Calcite %	% Smec	% Illite	% Kaol
793	25	2552	1	266	9	84	117	39	95	33	62	164	-45	221	blue						
794	25	2552	1	266	10	86	118	37	96	31	65	173	-50	216	blue						
795	25	2552	1	266	11	83	116	40	77	30	40	112	-55	211	blue						
796	25	2552	1	266	12	89	120	35	103	33	70	165	-60	206	blue						
797	25	2552	1	266	13	85	117	37	92	31	61	144	-70	196	blue						
798	25	2552	1	266	14	88	119	35	89	31	58	143	-80	186	blue						
799	25	2553	1	274	2	79	110	39	86	28	58	76	-10	264	Yellow						
800	25	2553	1	274	3	79	111	41	78	25	53	70	-15	259	Yellow						
801	25	2553	1	274	4	78	110	41	112	32	80	95	-20	254	Yellow						
802	25	2553	1	274	5	77	110	43	100	33	67	86	-25	249	Yellow						
803	25	2553	1	274	6	72	108	50	118	34	84	95	-30	244	Yellow						
804	25	2553	1	274	7	86	116	35	80	30	50	57	-35	239	Blue						
805	25	2553	1	274	8	103	128	24	84	27	57	66	-40	234	Blue						
806	25	2553	1	274	9	85	117	37	93	30	63	76	-45	229	Blue						
807	25	2553	1	274	10	85	116	36	102	30	72	85	-50	224	Blue						
808	25	2553	1	274	11	84	114	36	88	28	60	75	-55	219	Blue						
809	25	2553	1	274	12	85	115	35	106	28	78	84	-60	214	Blue						
810	25	2553	1	274	13	86	116	35	104	33	71	83	-70	204	Blue						
811	25	2553	1	274	14	85	114	34	55	32	23	88	-80	194	Blue						
812	25	2554	1	361	3	109	129	18	55	11	44	62	-15	346	Yellow						
813	25	2554	1	361	4	84	113	35	72	20	52	122	-20	341	Yellow						
814	25	2554	1	361	5	82	112	37	71	20	51	128	-25	336	Yellow						
815	25	2554	1	361	6	76	109	44	96	32	64	171	-30	331	Yellow						
816	25	2554	1	361	7	74	110	48	87	29	58	147	-35	326	Yellow						
817	25	2554	1	361	8	83	116	40	80	26	54	137	-40	321	Blue						
818	25	2554	1	361	9	83	115	38	71	22	49	114	-45	316	Blue						
819	25	2554	1	361	10	90	119	32	80	29	51	95	-50	311	Blue						
820	25	2554	1	361	11	79	112	42	112	33	79	175	-55	306	Blue						
821	25	2554	1	361	12	82	115	40	94	31	63	82	-60	301	Blue						
822	25	2554	1	361	13	86	116	35	85	31	54	137	-70	291	Blue						
823	25	2554	1	361	14	90	120	33	80	30	50	127	-80	281	Blue						
824	25	2555	1	325	2				114	39	75	185	-10	315	Yellow						
825	25	2555	1	325	3				122	36	86	204	-15	310	Yellow						
826	25	2555	1	325	4				127	38	89	206	-20	305	Yellow						
827	25	2555	1	325	5				115	36	79	183	-25	300	Yellow						
828	25	2555	1	325	6				91	31	60	167	-30	295	Yellow						
829	25	2555	1	325	7				91	30	61	125	-35	290	yellow						
830	25	2555	1	325	8				106	35	71	162	-40	285	Blue						
831	25	2555	1	325	9				108	35	73	159	-45	280	Blue						
832	25	2555	1	325	10				100	29	71	138	-50	275	Blue						
833	25	2555	1	325	11				92	35	57	196	-55	270	Blue						
834	25	2555	1	325	12				97	37	60	192	-60	265	Blue						
835	25	2555	1	325	13				80	32	48	108	-70	255	Blue						
836	25	2555	1	325	14				91	35	56	126	-80	245	Blue						
837	82	2556	1	286	8	75	109	45	98	41	57	148	-40	246	yellow	72	23	3	62	5	33
838	82	2556	1	286	9	80	111	39	90	30	60	154	-45	241	yellow	63	16	19	47	8	45
839	82	2556	1	286	10	98	125	27	91	31	60	133	-50	236	yellow	58	12	29	35	7	58
840	82	2556	1	286	11	84	113	35	87	47	40	115	-55	231	blue	58	21	22	48	7	45
841	82	2556	1	286	12	98	103	5	74	47	27	166	-60	226	Blue	51	23	24	43	8	50
842	82	2557	1		1								-5		B	32	60	0	23	52	25
843	82	2557	1		2								-10		Y	21	61	0	30	55	15
844	82	2557	1		3								-15		Y	24	68	0	35	50	15
845	82	2557	1		4								-20		b	19	70	0	0	59	41
846	82	2557	1		5								-25		B	22	63	0	0	67	33
847	82	2557	1		6								-30		b	33	56	1	0	60	40
848	82	2557	1		7								-35		B	40	56	0	0	43	57
849	82	2557	1		8								-45		B	27	54	1	0	43	57
850	82	2557	1		9								-50		y	18	70	0	36	18	46
851	45	2558	1	251	1								-5	246	Yellow	35	60	0	0	66	34
852	45	2558	1	251	2								-10	241	Yellow	27	61	0	25	52	23
853	45	2558	1	251	3								-15	236	Yellow	20	64	0	0	52	48
854	45	2558	1	251	4	93	121	30	68	25	43	114	-20	231	Yellow	41	54	0	50	10	40
855	45	2558	1	251	5	80	110	38	89	29	60	147	-25	226	Blue	56	11	31	58	7	36
856	45	2558	1	251	6				110	38	72	181	-30	221	Yellow	77	11	10	51	5	44
857	45	2558	1	251	7				101	39	62	165	-35	216	Blue	84	12	4	51	7	42
858	45	2558	1	251	8	78	114	46	105	38	67	176	-40	211	blue	82	13	4	45	9	46

	A	B	C	D	E	F	G	H	I	J	K	L	M	N	O	P	Q	R	S	T	U
1	County	Site	Hole No.	Hole Elev msl	Sample Number	Dry Density	Wet Density Percent	Moisture	LL	PL	PI	% VC	Depth	Elev msl	Yellow/Blue	clay %	qtz %	Calcite %	% Smecc	% Illite	% Kaol
859	45	2558	1	251	9	80	114	43	103	38	65	168	-45	206	Blue	80	15	5	50	8	42
860	45	2558	1	251	10	81	112	38	101	36	65	163	-50	201	blue	80	15	5	50	9	41
861	45	2558	1	251	11	85	116	36	107	33	74	164	-55	196	Blue	67	16	17	47	12	41
862	45	2558	1	251	12	82	116	41	107	37	70	171	-60	191	Blue	84	13	3	52	10	38
863	45	2558	1	251	13	86	118	37	108	37	71	170	-70	181	Blue	72	14	14	47	8	45
864	45	2558	1	251	14	87	118	35	101	36	65	166	-80	171	Blue	70	16	13	55	7	38
865	45	2559	1	203	1								-5	198	Y	17	72	0	32	27	41
866	45	2559	1	203	2								-10	193	Y	30	58	0	34	42	24
867	45	2559	1	203	3								-15	188	Y	20	62	0	27	58	16
868	45	2559	1	203	4								-20	183	Y	23	75	0	12	20	68
869	45	2559	1	203	5								-25	178	Y	27	66	0	47	7	47
870	45	2559	1	203	6								-30	173	Y	67	22	9	50	9	41
871	45	2559	1	203	7								-35	168	B	78	17	5	40	11	50
872	45	2559	1	203	8								-40	163	Y	79	15	5	50	8	42
873	45	2559	1	203	9								-45	158	B	80	16	3	53	7	40
874	45	2559	1	203	10								-50	153	B	75	16	9	53	8	39
875	45	2559	1	203	11								-55	148	B	70	15	15	51	8	41
876	45	2559	1	203	12								-60	143	B	75	16	7	43	11	45
877	45	2560	1	282	1								-5	277	y	15	70	0	19	58	23
878	45	2560	2	282	1								-5	277	y	27	60	T	34	45	21
879	45	2560	1	282	2								-10	272	y	12	83	0	0	65	35
880	45	2560	2	282	2								-10	272	y	25	71	0	0	58	42
881	45	2560	1	282	3								-15	267	y	10	86	0	30	15	55
882	45	2560	2	282	3								-15	267	y	29	71	0	27	8	65
883	45	2560	1	282	4								-20	262	y	26	74	0	60	6	35
884	45	2560	2	282	4								-20	262	y	31	69	0	45	7	48
885	45	2560	2	282	5								-25	257	y	43	57	0	60	8	32
886	45	2560	1	282	5	80	112	40	96	44	52	170	-25	257	Yellow	57	43	0	69	6	25
887	45	2560	1	282	6	71	108	52	123	43	80	201	-30	252	Yellow	59	41	0	58	8	34
888	45	2560	2	282	6				116	46	70	216	-30	252	Yellow	84	16	0	62	7	31
889	45	2560	1	282	7	68	105	54	116	45	71	183	-35	247	Blue	69	31	0	60	8	32
890	45	2560	2	282	7	80	114	42	106	41	65	185	-35	247	yellow	74	15	11	57	8	35
891	45	2560	1	282	8	73	110	50	100	40	60	169	-40	242	Blue	79	16	5	71	6	23
892	45	2560	2	282	8	87	120	38	94	35	59	149	-40	242	blue	67	14	18	59	6	35
893	45	2560	1	282	9	83	117	41	99	59	40	184	-45	237	Blue	73	15	9	60	6	34
894	45	2560	2	282	9	77	109	41	102	39	63	154	-45	237	blue	77	15	8	63	6	32
895	45	2560	1	282	10	83	117	41	102	59	43	196	-50	232	Blue	72	17	9	59	6	35
896	45	2560	2	282	10	85	118	39	87	32	55	134	-50	232	blue	53	14	33	48	7	45
897	45	2560	1	282	11	82	113	38	99	57	42	190	-55	227	Blue	79	15	7	57	7	36
898	45	2560	2	282	11	89	121	36	100	36	64	170	-55	227	Blue	67	13	20	58	5	37
899	45	2560	1	282	12	84	116	38	100	36	64	169	-60	222	Blue	70	14	16	47	9	44
900	45	2560	2	282	12	82	116	41	103	38	65	170	-60	222	Blue	45	16	38	49	8	44
901	45	2560	1	282	13	90	120	33	84	31	53	129	-70	212	Blue	49	12	31	52	7	41
902	45	2560	2	282	13	85	117	38	105	35	70	167	-70	212	Blue	65	13	22	55	10	35
903	45	2560	1	282	14	88	118	34	94	36	58	143	-80	202	Blue	54	18	26	40	7	52
904	45	2560	2	282	14	89	120	35	86	30	56	124	-80	202	Blue	53	14	29	54	8	38

ERDC (hole 2) results		Jar Fall Cone										MDOT (hole 1) results									
Iteration%	Avg γd	Avg w%	Sample	Depth	nat w%	80g	152g	LL	PL	PI	lc	LI	SL	SI	VC%	γd	nat w%	Gs	Avg Satrn%		
				1																	
98				2																	
108			IU	3	17	5	10														
99	15		1L	4				52	22	30	1.22	-0.22	14.7	37	061	106	15	2.65	73		
	18		2U	5	13	2	5														
93	19		2L	6																	
84			3U	7	28	7	16	81	23	58	0.88	0.12	0.4	81	156	92	30	2.62	100		
80	29		3L	8				83	22	61	0.88	0.12	2.1	81	148	92	29	2.6	100		
			4U	9	30	10	20	76	26	50	0.88	0.12	4.5	71	130	90	32	2.43	114		
73	41		4L	10				88	30	58	0.90	0.10	3.1	85	155	86	36	2.42	115		
72	49		5U	11	40	10	20	103	34	69	0.86	0.14	2.8	100	185	77	44	2.39	110		
77	48		5L	12				106	32	74	0.86	0.14	5.7	100	185	80	42	2.4	117		
71	48		6U	13	45	18	25	106	31	75	0.80	0.20	4.7	101	183	77	46	2.48	113		
			6L	14				97	26	71	0.76	0.24	9.8	87	161	78	43	2.59	104		
75	51		7U	15	46	20	30	102	29	73	0.76	0.24	4.9	97	169	76	47	2.55	110		
75	48		7L	16				109	29	80	0.75	0.25	9.3	100	176	73	49	2.55	107		
74	47		8U	17	50	10	20	119	30	89	0.77	0.23	3.5	116	205	72	51	2.48	110		
75	46		8L	18				97	30	67	0.70	0.30	3.6	93	189	72	50	2.45	109		
75	47		9U	19	49	10	22	112	29	83	0.78	0.22	6.2	106	188	76	47	2.5	110		
74	45		9L	20				113	30	83	0.81	0.19	5.4	108	194	77	46	2.51	110		
74	47		10U	21	49	12	22	113	29	84	0.75	0.25	3.4	110	196	73	50	2.48	110		
76	47		10L	22				111	31	80	0.78	0.22	5.9	105	189	73	48	2.51	105		
74	48		11U	23	49	12	20	104	30	74	0.73	0.27	5.4	99	180	71	50	2.55	103		
76	46		11L	24				117	34	83	0.80	0.20	0.7	116	206	72	51	2.53	107		
74	47		12U	25	50	12	25	114	32	82	0.80	0.20	4.5	110	191	73	48	2.54	105		
74	45		12L	26				110	33	77	0.79	0.21	1.5	108	190	73	49	2.54	105		
76	47		13U	27	50	15	25	108	34	74	0.80	0.20	1.5	107	188	73	49	2.56	105		
75	47		13L	28				116	32	84	0.81	0.19	2.8	113	189	75	48	2.59	106		
80	45		14U	29	50	12	20	101	31	70	0.78	0.22	1.7	99	173	75	46	2.55	104		
82	45		14L	30	44	10	15	106	30	76	0.80	0.20	7.1	99	168	77	45	2.58	107		
78	41		15U	31	42	10	15	105	31	74	0.75	0.25	8.4	97	161	75	50	2.51	114		
77	39		15L	32				109	33	76	0.89	0.11	6.7	102	178	80	42	2.53	107		
			16U	33				92	28	64	0.78	0.22	3.9	88	157	80	42	2.55	109		
			16L	34				105	35	70	0.88	0.12	9.4	96	173	80	43	2.56	111		

e	0 psf Free swell			144 psf swell slice			Hole 1 Shrink-Swell			Depth	Δ LiqInd	Ic	FSI %	FSR	Mdot VC
	w%	ε %	γd	w%	ε %	γd	w%	shrinkε %	Iss						
	3	10								S1	3		21	1.2	61
	3	18								S2	5		22	1.2	
	4	40								S3	7	0.73	48	1.5	156
	3	50								S4	9	1.4	61	1.6	130
	9	100					30.9	8.1		S5	11	1.1	83	1.8	185
	10	130					43.2	2.0		S6	13	1.25	78	1.8	183
	9	150					42.8	17.3		S7	15	1.33	85	1.8	169
	9	130	43	78	92		46.2	17.5	12.3	S8	17	0.74	70	1.7	205
	9	135	48	74	2.8		50.4	19.4	11.6	S9	19	1.29	70	1.7	188
	9	125	51	70	4.1		47.7	15.9	10.0	S10	21	1.11	85	1.8	196
	8	145	45	74	9		49.1	15.5	11.1	S11	23	1.02	71	1.7	180
	9	115	48	72	4		50	14	8.9	S12	25	1.05	64	1.6	191
	9	135	52	69	2.3		46.7	13.9	8.4	S13	27	1.15	92	1.9	188
	10	130	47	73	3.5		50.5	18.7	11.4	S14	29	0.86	77	1.8	173
	8	130	48	72	4		47.2	17.3	10.7	S15	31	0.93	69	1.7	161
	8	130	44	77	7.8		43.2	12.2	8.9	S16	33	1.43	77	1.8	157
	7	130	39	82	1		42	12.9	7.4						

BlendVC	LS%	LSblend%	BartLS%	ColeR%	w24 oven	w72 oven	w24/w72 ratio air	w24/w72 ratio oven	CalciumCarbonate Test, psi Hole1_U	CalciumCarbonate Test, psi Hole2
	14.5				77	37	2.1	19.25		
221		31.9			100	57	1.75	33.3		
386	26.7	40.7	21	10	107	69	1.55	10.7	0	1.4
321	24.0	37.8	21	26	110	77	1.42	5.78	6.1	4.4
354	29.2	39.3	20	17	140	89	1.57	4.11	1	1.9
364	29.1	39.7	23	20	132	97	1.36	4.71	4.3	4.5
417	27.9	41.9	25	26	144	101	1.42	4.36	1.5	1.2
424	30.8	42.1	24	24	132	104	1.27	9.43	1.9	0.8
395	29.5	41.0	20	24	144	109	1.32	9	2.5	2.7
407	30.1	41.5	20	15	147	106	1.38	3.97	4.5	4.5
444	28.8	42.8	23	14	148	108	1.37	5.69	6	5
424	29.7	42.1	23	14	143	104	1.37	3.18	2.2	5
410	29.5	41.6	19	15	143	105	1.36	3.04	1.5	2.9
383	28.2	40.5	17	14	159	112	1.42	3.78	3.7	3.7
368	27.1	39.9	17	15	134	95	1.41	12.18	5	5.9
488	26.8	44.3	20	15	146	105	1.4	4.05	4.2	2.1